Advances in Clinical and Experimental Medicine

MONTHLY ISSN 1899-5276 (PRINT) ISSN 2451-2680 (ONLINE) www.advances.umed.wroc.pl

2019, Vol. 28, No. 6 (June)

Impact Factor (IF) – 1.262
Ministry of Science and Higher Education – 15 pts.
Index Copernicus (ICV) – 155.19 pts.

Wroclaw Medical University

Advances
in Clinical and Experimental
Medicine

Advances
in Clinical and Experimental Medicine

ISSN 1899-5276 (PRINT) ISSN 2451-2680 (ONLINE) www.advances.umed.wroc.pl

MONTHLY 2019
Vol. 28, No. 6
(June)

Advances in Clinical and Experimental Medicine is a peer-reviewed open access journal published by Wroclaw Medical University. Its abbreviated title is Adv Clin Exp Med. Journal publishes original papers and reviews encompassing all aspects of medicine, including molecular biology, biochemistry, genetics, biotechnology, and other areas. It is published monthly, one volume per year.

Editorial Office
ul. Marcinkowskiego 2–6
50-368 Wrocław, Poland
Tel.: +48 71 784 11 36
E-mail: redakcja@umed.wroc.pl

Publisher
Wroclaw Medical University
Wybrzeże L. Pasteura 1
50-367 Wrocław, Poland

Online edition is the original version of the journal

Editorial Policy

Advances in Clinical and Experimental Medicine (Adv Clin Exp Med) is an independent multidisciplinary forum for exchange of scientific and clinical information, publishing original research and news encompassing all aspects of medicine, including molecular biology, biochemistry, genetics, biotechnology and other areas. During the review process, the Editorial Board conforms to the "Uniform Requirements for Manuscripts Submitted to Biomedical Journals: Writing and Editing for Biomedical Publication" approved by the International Committee of Medical Journal Editors (www.ICMJE.org/). The journal publishes (in English only) original papers and reviews. Short works considered original, novel and significant are given priority. Experimental studies must include a statement that the experimental protocol and informed consent procedure were in compliance with the Helsinki Convention and were approved by an ethics committee.

For all subscription-related queries please contact our Editorial Office:
redakcja@umed.wroc.pl

For more information visit the journal's website:
www.advances.umed.wroc.pl

Pursuant to the ordinance No. 134/XV R/2017 of the Rector of Wroclaw Medical University (as of December 28, 2017) from January 1, 2018 authors are required to pay a fee amounting to 700 euros for each manuscript accepted for publication in the journal Advances in Clinical and Experimental Medicine.

„Podniesienie poziomu naukowego i poziomu umiędzynarodowienia wydawanych czasopism naukowych oraz upowszechniania informacji o wynikach badań naukowych lub prac rozwojowych – zadanie finansowane w ramach umowy 784/p-DUN/2017 ze środków Ministra Nauki i Szkolnictwa Wyższego przeznaczonych na działalność upowszechniającą naukę".

Indexed in: MEDLINE, Science Citation Index Expanded, Journal Citation Reports/Science Edition, Scopus,
EMBASE/Excerpta Medica, Ulrich's™ International Periodicals Directory, Index Copernicus

Typographic design: Monika Kolęda, Piotr Gil
DTP: Wydawnictwo UMW
Cover: Monika Kolęda
Printing and binding: EXDRUK

Advances
in Clinical and Experimental Medicine

MONTHLY 2019, Vol. 28, No. 6 (June)

ISSN 1899-5276 (PRINT)
ISSN 2451-2680 (ONLINE)
www.advances.umed.wroc.pl

Contents

Original papers

Reviews

MicroRNA-124 represses wound healing by targeting *SERP1* and inhibiting the Wnt/β-catenin pathway

Guohui Zhang[1,B,D,F], Kunxiu Song[2,C,D,F], Hongshan Yan[3,A,D–F]

[1] Department of Burn and Plastic Surgery, Binzhou Medical University Hospital, China
[2] Department of Hand and Microsurgery, Binzhou Medical University Hospital, China
[3] Jiangsu Liyang Zhimeixing Medical Cosmetic Clinic, China

A – research concept and design; B – collection and/or assembly of data; C – data analysis and interpretation; D – writing the article; E – critical revision of the article; F – final approval of the article

Advances in Clinical and Experimental Medicine, ISSN 1899–5276 (print), ISSN 2451–2680 (online) *Adv Clin Exp Med*. 2019;28(6):711–718

Address for correspondence
Hongshan Yan
E-mail: yanhongshan123@126.com

Funding sources
None declared

Conflict of interest
None declared

Received on March 9, 2017
Reviewed on June 7, 2017
Accepted on August 9, 2018

Published online on February 8, 2019

Abstract

Background. Wound healing is a complex process which restores cellular structures and tissue layers after their destruction. Accumulating evidence has proven that microRNAs (miRs) are involved in wound healing.

Objectives. The aim of the study was to research the role of miR-124 in wound healing.

Material and methods. Keratinocytes were respectively transfected with miR-124 mimic, scrambled miRNA (a negative control of miR-124 mimic: mimic NC), antisense oligonucleotides against miR-124 (ASO-miR-124), or a negative control of ASO-miR-124 (ASO-NC), and then cell viability, colony formation, cell cycle, expression of cell cycle-associated proteins, and collagen content were all evaluated. The target gene of miR-124 was predicted using TargetScan and verified with luciferase assay. Subsequently, the effects of target gene overexpression on cell viability, colony formation and collagen synthesis were all evaluated. Finally, the expression levels of key kinases in the Wnt/β-catenin pathway were detected using western blot analysis.

Results. Cell viability, colony formation, expression levels of cell cycle-associated proteins, and collagen content were all significantly reduced by miR-124 overexpression. As predicted using bioinformatics and validated with luciferase assay, stress-associated endoplasmic reticulum protein 1 (*SERP1*) is a target gene of miR-124. Meanwhile, the miR-124 mimic-induced decrease in cell viability, colony formation and collagen synthesis was reversed by *SERP1* overexpression. Furthermore, the miR-124 mimic obviously upregulated glycogen synthase kinase 3β (GSK-3β) while downregulating β-catenin, T cell transcription factor 4 (TCF-4) and leukemia enhancer factor 1 (LEF-1). Additionally, all the effects of ASO-miR-124 were the opposite of those of the miR-124 mimic.

Conclusions. We found that miR-124 inhibited keratinocyte proliferation, collagen biosynthesis and activation of Wnt/β-catenin by targeting *SERP1*.

Key words: wound healing, collagen biosynthesis, Wnt/β-catenin pathway, miR-124, keratinocyte proliferation

Cite as
Zhang G, Song K, Yan H. MicroRNA-124 represses wound healing by targeting *SERP1* and inhibiting the Wnt/β-catenin pathway. *Adv Clin Exp Med*. 2019;28(6):711–718. doi:10.17219/acem/94163

DOI
10.17219/acem/94163

Wound healing is a complex biological process in which cellular structures and tissue layers are restored after their destruction.[1] Approximately 1–1.5% of the population in the developed world suffers from chronic wounds and the costs of their treatment account for 2–4% of the healthcare budget.[2] The process of wound healing consists of 4 distinct but overlapping phases: hemostasis, inflammation, proliferation, and tissue remodeling.[3] These 4 phases must be orchestrated in a precise and regulated manner; otherwise, wound healing can be delayed or even prevented.[4] Scars are usually formed by excessive non-functioning disorganized deposition of extracellular matrix (ECM) components during normal wound healing.[5] However, keloids and hypertrophic scars, which are formed by prolonged and aberrant ECM accumulation during burns, surgery and wounds, can cause functional disability, cosmetic deformities, psychological stress, and a huge socioeconomic burden.[6] Due to the deficiencies of current therapeutic approaches, it is urgent to explore novel targets that could promote wound healing and help avoid keloids or hypertrophic scars.

MicroRNAs (miRs) are a category of highly conserved small non-coding RNAs 18–22 nt in length.[7] Recently, increasing numbers of miRs have been reported as participating in wound healing through recognizing and binding complementarily to the 3'-untranslated region (3'UTR) of target genes, resulting in degradation of mRNA or repression of translation.[8] For example, miR-27b accelerates wound healing in type 2 diabetes mellitus.[9] Another report showed that miR-21 regulates wound contraction and collagen deposition by targeting various aspects of the healing process.[10] In addition, miR-1908 plays a positive role in scar formation by suppressing Ski-mediated inflammation in vitro and in vivo.[11] The functional role of miR-124 has been widely investigated in various cancers, including ovarian cancer,[12] non-small-cell lung cancer,[13] esophageal cancer,[14] and breast cancer.[15] However, the specific role of miR-124 in wound healing remains unclear.

The process of wound healing involves various types of cells, including inflammatory cells, keratinocyte, fibroblasts, and endothelial cells.[4] As the major cell type in the epidermal layer, keratinocytes migrate to cover the lesion and restore the barrier function of the skin during wound healing. When the wound area is totally covered, the keratinocytes are differentiated to a basal phenotype by contact inhibition.[16] Considering the essential roles of keratinocyte in wound healing, we chose keratinocytes to explore the effects of miR-124 on wound healing and the underlying mechanisms. Furthermore, the possible target gene of miR-124 was also investigated.

Material and methods

Cell culture and transfection

Primary human epidermal keratinocytes were purchased from the American Type Culture Collection (ATCC, Manassas, USA). The keratinocytes were maintained in Dermal Cell Basal Medium (ATCC) supplemented with a Keratinocyte Growth Kit (ATCC) at 37°C with 5% CO_2. To obtain non-physiological expression of miR-124, the keratinocytes were transfected with miR-124 mimic, scrambled miRNA (a negative control of miR-124 mimic: mimic NC), antisense oligonucleotides against miR-124 (ASO-miR-124), or a negative control of ASO-miR-124 (ASO-NC) (all from GenePharma, Shanghai, China). To overexpress stress-associated endoplasmic reticulum protein 1 (SERP1), complete SERP1 sequences were cloned into a pcDNA3.1/Zeo vector (Invitrogen, San Diego, USA) to generate pcDNA3.1/SERP1 (pc-SERP1); the recombined plasmid was then transfected into keratinocytes. The keratinocytes were seeded with a density of 1×10^5 cells/well and were maintained to 30–50% confluence. Cell transfection was then performed using Lipofectamine 2000 transfection reagent (Invitrogen) according to manufacturer's instructions. The keratinocytes were divided into 4 groups (mimic NC, miR-124 mimic, ASO-miR-124, and ASO-NC) or 3 groups (mimic NC, miR-124 mimic and miR-124 mimic + pc-SERP1) through cell transfection. Each group included 3 replicate wells.

Cell viability and cell cycle

Cell viability was measured with MTS assay using the CellTiter 96 AQueous One Solution Cell Proliferation Assay (Promega Corp., Madison, USA). Briefly, keratinocytes were seeded into a 96-well plate. At 24 h, 48 h and 72 h after transfection, 20 µL of AQueous One Solution Reagent (Promega Corp.) was added to each well and the keratinocytes were incubated at 37°C for additional 4 h. The absorbance was detected with a microplate reader (Bio-Rad Laboratories Inc., Hercules, USA) at 490 nm. To determine the cell cycle, keratinocytes were collected at 48 h post-transfection and washed in phosphate-buffered saline (PBS; Beyotime, Shanghai, China). The keratinocytes were then fixed in cold 70% ethanol at 4°C overnight. The fixed keratinocytes were washed in PBS until the ethanol was thoroughly decanted. Afterwards, the keratinocytes were incubated in propidium iodide solution (PI, 50 µg/mL; Sigma-Aldrich, St. Louis, USA) at 37°C for 30 min in the dark. The fluorescence intensity of the stained keratinocytes was detected on a FACSCalibur flow cytometer (BD Biosciences, San Jose, USA) and the data was analyzed using FlowJo software (Tree Star Inc., San Carlos, USA).

Colony formation assay

Twenty-four hours after transfection keratinocytes were plated into a 12-well plate at a density of 300 cells/well. The keratinocytes were then cultured at 37°C for 14 days; the culture medium was changed every 3 days. After being stained with 2% crystal violet, the colonies that included more than 50 cells were counted.

RNA isolation and qRT-PCR

The total RNA of transfected keratinocytes was extracted with TRIzol reagent (Invitrogen) according to the manufacturer's instructions, and reverse transcription of 1 μg RNA was performed using an mRNA Selective PCR kit (Takara, Dalian, China). Using cDNA as a template (50 ng), quantitative real-time polymerase chain reaction (qRT-PCR) was performed by means of the Power SYBR Green PCR Master Mix with the 7500 Fast Real-Time PCR system (Applied Biosystems, Foster City, USA). The primers were designed and synthesized by Sangon (Shanghai, China). The relative expression fold was calculated according to the $2^{-\Delta\Delta Ct}$ method.[17] *GAPDH* acted as the housekeeping gene.

Protein extraction and western blot analysis

Transfected keratinocytes were lysed in ice-cold RIPA buffer (Beyotime) containing a protease inhibitor cocktail (Roche Diagnostics GmbH, Mannheim, Germany). After quantification with a bicinchoninic acid (BCA) assay kit (Pierce Biotechnology, Rockford, USA), lysates containing approx. 30 μg of proteins were separated using sodium dodecyl sulfate polyacrylamide gel electrophoresis (SDS-PAGE), and the proteins in the SDS-PAGE gels were further transferred onto polyvinylidene fluoride (PVDF) membranes (EMD Millipore, Billerica, USA). After blocking and incubation with primary antibodies against cyclin B1 (ab32053), cyclin D1 (ab137875), cyclin-dependent kinase 2 (CDK2, ab32147), collagen I (ab34710), SERP1 (ab130974), β-catenin (ab6302), glycogen synthase kinase 3β (GSK-3β, ab131356), T-cell transcription factor 4 (TCF-4, ab185736), leukemia enhancer factor 1 (LEF-1, ab52017), or GAPDH (ab128915) (all from Abcam, Cambridge, UK), the blots were detected using appropriate secondary horseradish peroxidase-conjugated secondary antibodies (Abcam) and visualized using enhanced chemiluminescence (Pierce Biotechnology). The intensity of the bands was detected using Image Lab software (Bio-Rad Laboratories Inc.) and quantified using Image J software (National Institutes of Health, Bethesda, USA).

Collagen assay

The quantity of fibrillar collagens (type I to V) was assayed using the Sircol Soluble Collagen Assay Kit (Biocolor Ltd., Carrickfergus, UK) according to the manufacturer's protocol. Briefly, the cell culture medium was collected at 48 h post-transfection and mixed with Sircol dye reagent, which specially binds to the Gly-X-Y fragment in the helical structure. The serum concentration of the culture medium must be no more than 5% at this point. After incubation for 30 min at room temperature, the mixture was centrifuged and the precipitate was mixed with ice-cold acid-salt washing reagent, followed by another centrifugation. The precipitate was dissolved in Alka reagent for approx. 5 min and the absorbance was detected under 555 nm.

Luciferase reporter assay

Putative target genes of miR-124 were predicted using a TargetScan algorithm. A wild-type (WT) 3'UTR fragment containing a putative binding site for miR-124 and mutant (Mut) 3'UTR with site-mutagenesis at the binding site were inserted into a pmirGLO Vector (Promega Corp.). The mutant was constructed using the Directed Mutagenesis System (Invitrogen) with the sequence of SERP1 at the position between 188 and 194 as well as the position between 1645 and 1652. For the luciferase reporter assays, keratinocytes were seeded in a 24-well plate (1×10^5 cells/well) and maintained for 24 h before transfection. The 3'UTR reporter plasmids (WT or Mut) and miR-124 mimic, mimic NC, ASO-miR-124, or ASO-NC were co-transfected into the keratinocytes using Lipofectamine 2000 reagent (Invitrogen). The transfected keratinocytes were harvested 24 h later and assayed using the Dual-Luciferase Reporter Assay System (Promega Corp.) according to the manufacturer's protocol. Firefly luciferase activity was normalized to renilla luciferase activity for each well.

Statistical analysis

All the experiments were repeated 3 times. The results are presented as means ± standard deviation (SD). The statistical analysis was performed using GraphPad Prism 5 software (GraphPad Software Inc., San Diego, USA). The p-values were calculated using the unpaired two-tailed t-test or one-way analysis of variance (ANOVA) with Bonferroni's correction. A p-value less than 0.05 (marked by *) was considered statistically significant.

Results

MicroRNA-124 is non-physiologically expressed in keratinocytes

Mimic NC, miR-124 mimic, ASO-NC, and ASO-miR-124 were transfected into keratinocytes. The results in Fig. 1 showed that the miR-124 level was significantly upregulated after transfection with miR-124 mimic compared to the mimic NC group ($p < 0.01$), but was markedly downregulated after transfection with ASO-miR-124 compared to the ASO-NC group ($p < 0.01$). This data indicates that miR-124 was non-physiologically expressed in keratinocytes after cell transfection.

MicroRNA-124 inhibits keratinocyte proliferation

To investigate the effects of miR-124 on keratinocytes, cell proliferation, cell viability, colony formation, the cell

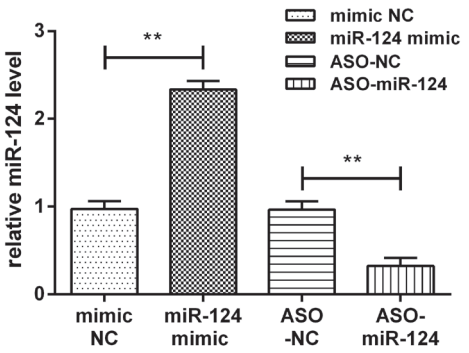

Fig. 1. MicroRNA miR-124 is non-physiologically expressed in keratinocytes after cell transfection. Keratinocytes were transfected with miR-124 mimic, mimic NC, ASO-miR-124, or ASO-NC. The level of miR-124 was measured using quantitative real-time polymerase chain reaction (qRT-PCR). The data presented is the means of at least 3 independent experiments. Error bars indicate the standard deviation (SD)

** $p < 0.01$.

cycle, and expressions of cell cycle-associated proteins were all assessed in transfected keratinocytes. In Fig. 2A, cell viability was markedly reduced by miR-124 mimic compared with the mimic NC group at 24 h ($p < 0.05$), 48 h ($p < 0.01$) and 72 h ($p < 0.01$) after transfection. Meanwhile, the number of colonies formed in keratinocytes overexpressing miR-124 was obviously lower than in the mimic NC group ($p < 0.05$, Fig. 2B). The fluorescence-activated cell sorting (FACS) results in Fig. 2C show that miR-124 overexpression reduced the number of keratinocytes in the S phase, while it increased the number in G_0/G_1 phase, accompanied by nearly unchanged numbers in the G_2/M phase when compared with the mimic NC group. In addition, mRNA and protein expression levels of cyclinB1, cyclinD1 and CDK2 were all significantly decreased by miR-124 overexpression in comparison with the mimic NC group ($p < 0.05$ or $p < 0.01$, Fig. 2D–E). Also, the effects of ASO-miR-124 on keratinocytes were the opposite to those of miR-124

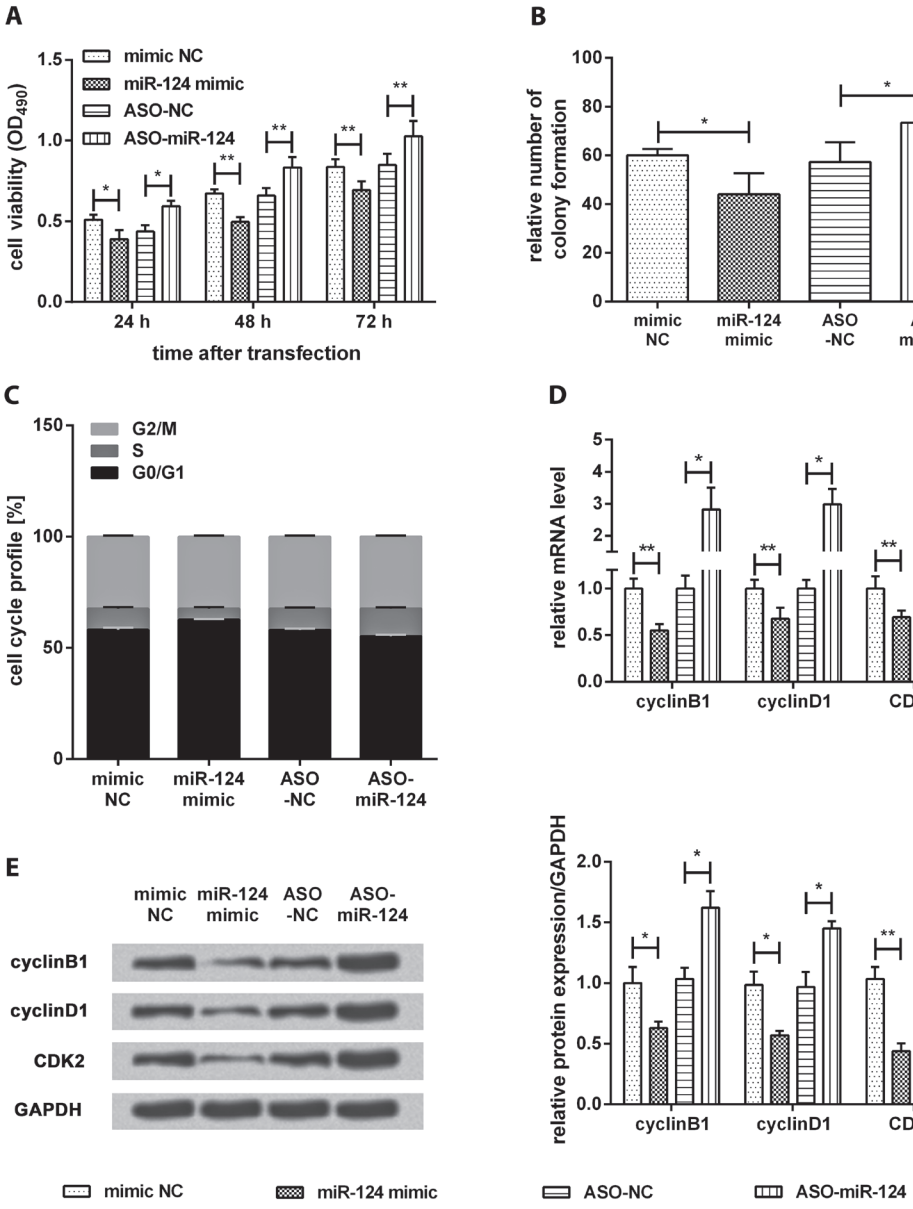

Fig. 2. MicroRNA miR-124 inhibits keratinocyte proliferation. Keratinocytes were transfected with miR-124 mimic, mimic NC, ASO-miR-124, or ASO-NC. A) cell viability by MTS assay; B) colony formation rate; C) cell cycle by fluorescence-activated cell sorting (FACS) assay; D) mRNA expression levels of cell cycle-associated proteins measured using quantitative real-time polymerase chain reaction (qRT-PCR); E) protein expression levels of cell cycle-associated proteins measured using western blot analysis. The data presented is the means of at least 3 independent experiments. Error bars indicate the standard deviation (SD)

* $p < 0.05$; ** $p < 0.01$; CDK2 – cyclin-dependent kinase 2.

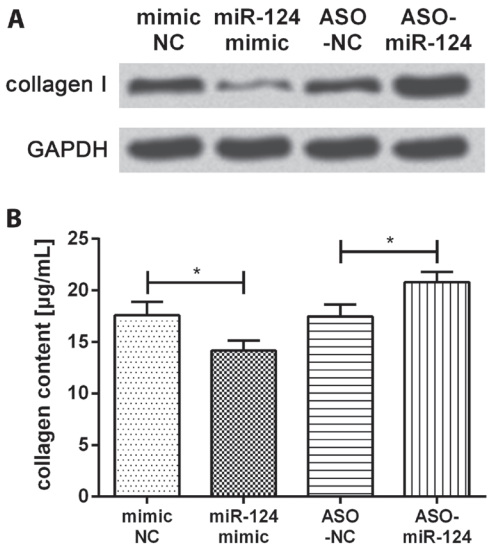

Fig. 3. MicroRNA miR-124 inhibits collagen biosynthesis. Keratinocytes were transfected with miR-124 mimic, mimic NC, ASO-miR-124, or ASO-NC. A) expression of collagen I measured using western blot analysis; B) collagen content in the culture medium measured using collagen assay. The data presented is the means of at least 3 independent experiments. Error bars indicate the standard deviation (SD)

* $p < 0.05$.

mimic. Taking all this together, we concluded that miR-124 inhibited the cell proliferation of keratinocytes.

MicroRNA-124 inhibits collagen biosynthesis

To assess the effects of miR-124 on collagen biosynthesis, intracellular collagen and collagen in a culture medium were both evaluated. In Fig. 3A, intracellular collagen I was markedly downregulated by miR-124 mimic, while it was upregulated by ASO-miR-124. Likewise, the content of collagens in the culture medium of keratinocytes overexpressing miR-124 was lower than in the mimic NC group ($p < 0.05$, Fig. 3B). The effect of ASO-miR-124 was just the opposite. This demonstrates that miR-124 inhibited collagen biosynthesis in keratinocytes.

SERP1 is a target gene of miR-124

After screening with a TargetScan algorithm, *SERP1* was identified as a putative target gene of miR-124. The complement sequence is shown in Fig. 4A. To identify whether

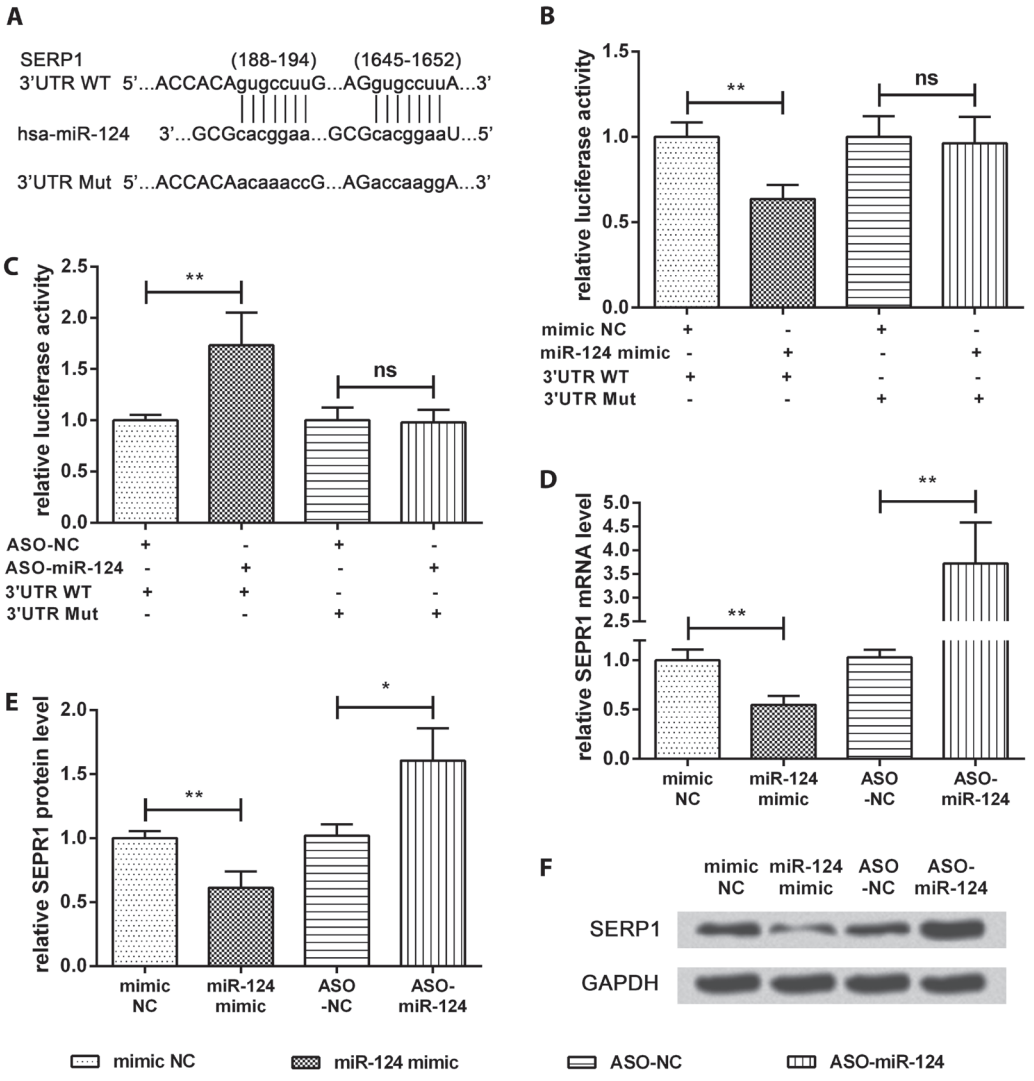

Fig. 4. *SERP1* is a target gene of microRNA (miR)-124. A) sequence complementarity between miR-124 and the seed region in the SERP1 3'-untranslated region (3'UTR) reporter plasmids (WT or Mut); short vertical lines indicate complementary nucleotides; B) relative luciferase activity in keratinocytes after co-transfection with miR-124 mimic or mimic NC and SERP1 3'UTR plasmid (WT or Mut); C) relative luciferase activity in keratinocytes after co--transfection with ASO-miR-124 or ASO-NC and *SERP1* 3'UTR plasmid (WT or Mut); D) relative SERP1 mRNA; E–F) protein expression levels after transfection with mimic NC, miR-124 mimics, ASO-NC, or ASO-miR-124. The data presented is the means of at least 3 independent experiments. Error bars indicate the standard deviation (SD)

ns: $p > 0.05$; * $p < 0.05$; ** $p < 0.01$; WT – wild-type; Mut – mutant.

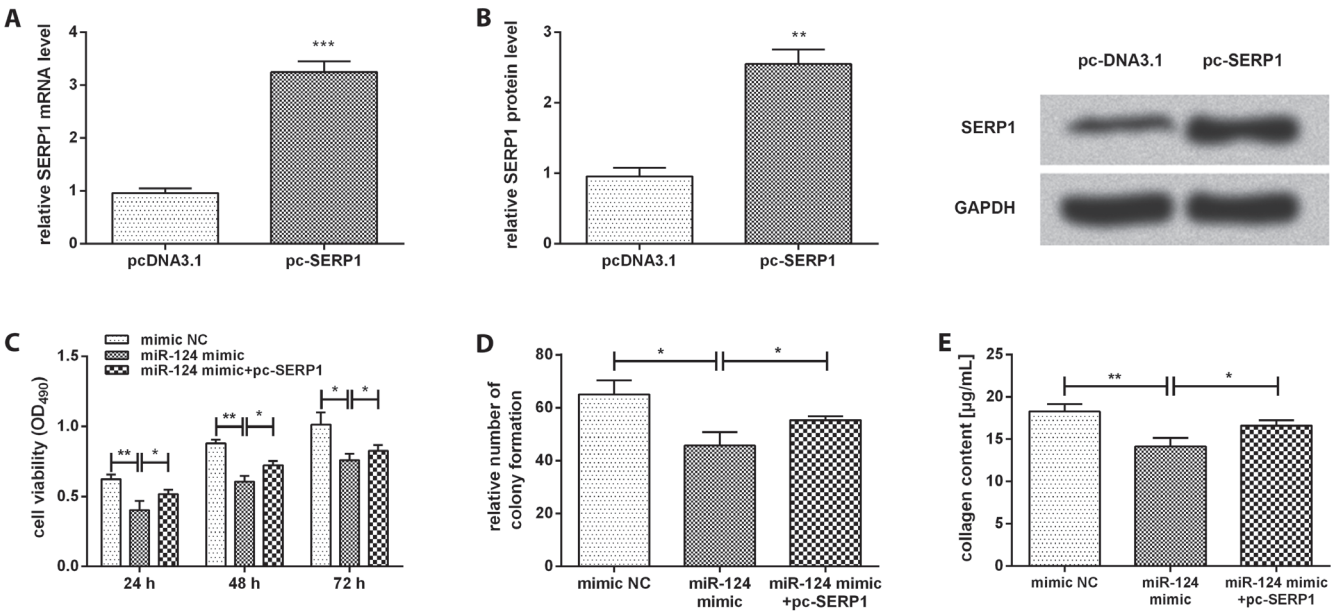

Fig. 5. *SERP1* reverses the inhibitory effects of miR-124 on keratinocytes. Keratinocytes were transfected with pcDNA3.1 or pcDNA3.1/SERP1 (pc-SERP1), followed by (A) quantitative real-time polymerase chain reaction (qRT-PCR) assessing the mRNA levels of SERP1 and (B) western blot analysis for assessing the protein levels of SERP1. Keratinocytes were transfected with mimic NC, miR-124 mimic alone or accompanied by pc-SERP1; C) cell viability measured using MTS assay; D) colony formation rate; E) collagen content in the culture medium measured using collagen assay. The data presented is the means of at least 3 independent experiments. Error bars indicate the standard deviation (SD)

* $p < 0.05$; ** $p < 0.01$; *** $p < 0.001$.

miR-124 directly targets *SERP1*, luciferase activity was assessed after co-transfection. As shown in Fig. 4B, miR-124 mimic markedly decreased the luciferase activity of keratinocytes transfected with plasmid containing WT 3'UTR but not Mut 3'UTR ($p < 0.01$). Meanwhile, ASO-miR-124 significantly increased the luciferase activity of keratinocytes transfected with plasmid containing WT 3'UTR but not Mut 3'UTR reporter ($p < 0.01$), as shown in Fig. 4C. In Fig. 4D–F, the mRNA and protein expression levels of *SERP1* were both reduced in keratinocytes overexpressing miR-124 compared with the mimic NC group ($p < 0.01$). At the same time, the expression levels of *SERP1* were elevated in keratinocytes with ASO-miR-124 compared with the ASO-NC group ($p < 0.05$ or $p < 0.01$). All these results suggest that *SERP1* is a target gene of miR-124 and its expression was negatively regulated by miR-124.

SERP1 overexpression rescues inhibitory effects of miR-124 on keratinocytes

After pcDNA3.1 or pc-SERP1 was transfected into keratinocytes, mRNA and protein expression levels of *SERP1* were assessed. As shown in Fig. 5A–B, both mRNA and protein expression levels of *SERP1* were significantly upregulated after transfection with pc-SERP1 compared to the pcDNA3.1 groups ($p < 0.01$ or $p < 0.001$). Cell viability, which was decreased by miR-124 overexpression, was obviously increased by *SERP1* overexpression when compared to the miR-124 mimic group at 24 h, 48 h and 72 h (all $p < 0.05$, Fig. 5C) after transfection. Analogically, the colony formation rate and collagen content, which were reduced by miR-124 overexpression, were both enhanced by *SERP1* overexpression when compared to the corresponding miR-124 mimic group ($p < 0.05$, Fig. 5D–E). These results imply that *SERP1* overexpression could reverse the effects of miR-124 overexpression on keratinocytes.

MicroRNA-124 represses activation of the Wnt/β-catenin pathway

To reveal the underlying mechanisms of miR-124 modulations, the expression of key kinases involved in the Wnt/β-catenin pathway was assessed with western blot analysis in transfected keratinocytes. The results presented in Fig. 6A showed that miR-124 mimic obviously downregulated β-catenin but upregulated GSK-3β. Further results suggested that TCF-4 and LEF-1 expression were both downregulated by miR-124 mimic (Fig. 6B). Not surprisingly, the effects of ASO-miR-124 on the expressions of these kinases were just the opposite. All these results indicate that miR-124 repressed activation of the Wnt/β-catenin pathway in keratinocytes.

Discussion

Considering the deficiencies of current therapeutic treatments for the effective reduction of skin scar formation, it is an unmet challenge for clinicians to explore novel therapeutic targets. In this study, we found that miR-124

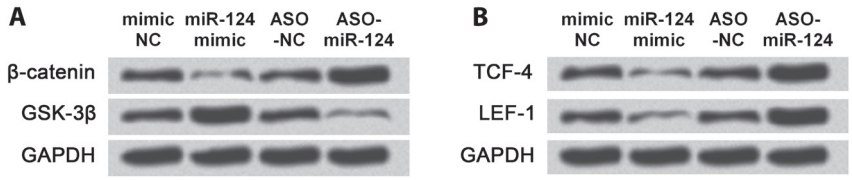

Fig. 6. MicroRNA miR-124 represses activation of the Wnt/β-catenin signaling pathway. Keratinocytes were transfected with miR-124 mimic, mimic NC, ASO-miR-124, or ASO-NC. A) protein expressions of β-catenin and glycogen synthase kinase 3β (GSK-3β) measured using western blot analysis; B) protein expressions of TCF-4 and LEF-1 measured using western blot analysis

significantly reduced cell viability, lowered the colony formation rate and downregulated expressions of cell cycle-associated proteins as well as collagens. Additionally, miR-124 overexpression induced G_0/G_1 phase arrest in keratinocytes. The effects of miR-124 silence on keratinocytes were just the opposite. Afterwards, using the online TargetScan software, *SERP1* was hypothesized to be a target gene of miR-124, and the subsequent luciferase assay verified the hypothesis. Meanwhile, *SERP1* overexpression could reverse the effects of miR-124 overexpression, also validating this hypothesis. The final western blot analysis suggested that miR-124 deactivated the Wnt/β-catenin signaling pathway.

During the course of wound healing, re-epithelialization is pivotal to optimal wound closure due to its role in wound contraction.[18] The process of re-epithelialization is partially mediated by keratinocyte proliferation.[19] At the wound margin, keratinocytes begin to proliferate behind the migrating cells and thereby feed the migrating sheets.[20] Thus, cell proliferation of keratinocytes plays an essential role in wound healing. A previous study reported that Smad4 inhibits wound healing by inhibiting keratinocyte proliferation.[21] Another study also reported that dermatopontin has a profound role in wound healing by promoting keratinocyte proliferation.[19] In our study, miR-124 overexpression significantly inhibited keratinocyte proliferation, while miR-124 silence markedly promoted keratinocyte proliferation, indicating that miR-124 might inhibit wound healing. The inhibitory effect of miR-124 on cell proliferation was also consistent with previous studies performed in cancer cells.[22,23] To our knowledge, it is the first time the role of miR-124 in wound healing has been explored.

In order to close a wound opening, maturing ECM is recruited.[24] As collagen is a major component of ECM, collagen biosynthesis is critical to both normal and pathological skin wound healing and can greatly affect the quality and outcome of healing.[25] Zhou et al. demonstrated that the rate of collagen synthesis was increased during wound healing in muscle.[26] Wang et al. also illustrated that calcium alginate accelerated the process of wound healing by improving type I collagen synthesis.[27] Therefore, we also explored alterations of collagen biosynthesis in keratinocytes with ectopic miR-124 expression. Our results showed that collagen synthesis was markedly decreased by miR-124 overexpression, while it was increased by miR-124 silence, indicating the potential inhibitory effect of miR-124 on wound healing.

MicroRNAs usually function by binding to the 3'UTR of target genes, so we further explored the possible target gene of miR-124. TargetScan algorithms predicted more than 2,000 genes as possible target genes of miR-124. SERP1, also termed ribosome-associated membrane protein 4 (RAMP4), is implicated in the stabilization of newly synthesized membrane proteins and in N-linked glycosylation.[28] Previous studies have reported that heat shock protein (Hsp47), which localizes in the endoplasmic reticulum, is a collagen-specific molecular chaperone, and that miR-29b reduces collagen biosynthesis by inhibiting Hsp47.[29,30] We therefore hypothesized that *SERP1* might be a target gene of miR-124. The subsequent luciferase assay and the changes in *SERP1* expression induced by ectopic expression of miR-124 verified this hypothesis. Additionally, we also evaluated the cell viability, colony formation and collagen content in keratinocytes transfected with miR-124 alone or accompanied by *SERP1* overexpression. The results once again verified that SERP-1 is a target gene of miR-124.

The Wnt/β-catenin signaling pathway has been widely explored; it is involved not only in cell proliferation and the cell cycle, but also in wound healing.[31,32] Moreover, the Wnt/β-catenin pathway has been proven to regulate the proliferation and apoptosis of keratinocytes in psoriasis lesions.[33] Hence, we studied the expressions of key kinases involved in the Wnt/β-catenin signaling pathway. In the canonical Wnt/β-catenin pathway, Wnt activates the "destruction complex", which is composed of axin, adenomatous polyposis coli (APC) and GSK-3β, and prevents the phosphorylation and ubiquitination of β-catenin.[34] When the β-catenin in cytoplasm is accumulated and translocates to the nucleus, β-catenin binds with TCF/LEF-1 transcription factors and then activates the transcription of downstream target genes, including cyclinB1, cyclinD1 and CDK2.[35,36] In the present study, miR-124 obviously upregulated GSK-3β expression, suggesting upregulation of the destruction complex. As might be expected, the expression of β-catenin was downregulated, and downstream TCF-4 and LEF-1 were also markedly downregulated. As a consequence, cell cycle-associated proteins, including cyclin B1, cyclin D1 and CDK2, were all downregulated by miR-124. Hence, we came to the conclusion that miR-124 might affect keratinocyte proliferation and the cell cycle by deactivating the Wnt/β-catenin pathway.

Finally,, we have shown that miR-124 significantly inhibited cell proliferation and collagen synthesis in keratinocytes. *SERP1* is a target gene of miR-124 and its

overexpression could attenuate the effects of miR-124 on keratinocytes. Moreover, miR-124 significantly deactivates the Wnt/β-catenin pathway. These findings imply that miR-124 silence in wounds might be an effective strategy for healing and that miR-124 is a potential therapeutic target for wound healing.

References

1. Velnar T, Bailey T, Smrkolj V. The wound healing process: An overview of the cellular and molecular mechanisms. *J Int Med Res*. 2009;37(5): 1528–1542.
2. Gottrup F. A specialized wound-healing center concept: Importance of a multidisciplinary department structure and surgical treatment facilities in the treatment of chronic wounds. *Am J Surg*. 2004;187(5A): 38s–43s.
3. Gosain A, DiPietro LA. Aging and wound healing. *World J Surg*. 2004; 28(3):321–326.
4. Guo S, DiPietro LA. Factors affecting wound healing. *J Dent Res*. 2010; 89(3):219–229.
5. Takeo M, Lee W, Ito M. Wound healing and skin regeneration. *Cold Spring Har Perspect Med*. 2015;5(1):a023267.
6. Huang C, Akaishi S, Hyakusoku H, Ogawa R. Are keloid and hypertrophic scar different forms of the same disorder? A fibroproliferative skin disorder hypothesis based on keloid findings. *Int Wound J*. 2014;11(5):517–522.
7. Ameres SL, Zamore PD. Diversifying microRNA sequence and function. *Nat Rev Mol Cell Biol*. 2013;14(8):475–488.
8. Banerjee J, Chan YC, Sen CK. MicroRNAs in skin and wound healing. *Physiol Genomics*. 2011;43(10):543–546.
9. Wang JM, Tao J, Chen DD, et al. MicroRNA miR-27b rescues bone marrow-derived angiogenic cell function and accelerates wound healing in type 2 diabetes mellitus. *Arterioscler Thromb Vasc Biol*. 2014; 34(1):99–109.
10. Wang T, Feng Y, Sun H, et al. miR-21 Regulates skin wound healing by targeting multiple aspects of the healing process. *Am J Pathol*. 2012;181(6):1911–1920.
11. Xie C, Shi K, Zhang X, Zhao J, Yu J. MiR-1908 promotes scar formation post-burn wound healing by suppressing Ski-mediated inflammation and fibroblast proliferation. *Cell Tissue Res*. 2016;366(2):1–10.
12. Zhang H, Wang Q, Zhao Q, Di W. MiR-124 inhibits the migration and invasion of ovarian cancer cells by targeting SphK1. *J Ovarian Res*. 2013;6(1):84.
13. Zhenhua LI, Huang J, Zhenhong HU, Gao S. Effect of miR-124 on migration and invasion of non-small-cell lung cancer cells. *Shandong Medical Journal*. 2016;56:18–20.
14. Zhang YH, Wang QQ, Li H, Ye T, Gao F, Liu YC. miR-124 radiosensitizes human esophageal cancer cell TE-1 by targeting CDK4. *Genet Mol Res*. 2016;15(2). doi:10.4238/gmr.15027893
15. Li L, Luo J, Wang B, et al. MicroRNA-124 targets flotillin-1 to regulate proliferation and migration in breast cancer. *Mol Cancer*. 2013;12:163.
16. Walter MN, Wright KT, Fuller HR, MacNeil S, Johnson WE. Mesenchymal stem cell-conditioned medium accelerates skin wound healing: An in vitro study of fibroblast and keratinocyte scratch assays. *Exp Cell Res*. 2010;316(7):1271–1281.
17. Livak KJ, Schmittgen TD. Analysis of relative gene expression data using real-time quantitative PCR and the 2(-Delta Delta C(T)) Method. *Methods*. 2001;25(4):402–408.
18. Shibata S, Tada Y, Asano Y, et al. Adiponectin regulates cutaneous wound healing by promoting keratinocyte proliferation and migration via the ERK signaling pathway. *J Immunol*. 2012;189(6):3231–3241.
19. Krishnaswamy VR. Role of dermatopontin in re-epithelialization: Implications on keratinocyte migration and proliferation. *Sci Rep*. 2014;4:7385.
20. Santoro MM, Gaudino G. Cellular and molecular facets of keratinocyte reepithelization during wound healing. *Exp Cell Res*. 2005;304(1): 274–286.
21. Yang L, Li W, Wang S, et al. Smad4 disruption accelerates keratinocyte re-epithelialization in murine cutaneous wound repair. *Histochem Cell Biol*. 2012;138(4):573–582.
22. Sun Y, Ai X, Shen S, Lu S. NF-κB-mediated miR-124 suppresses metastasis of non-small-cell lung cancer by targeting MYO10. *Oncotarget*. 2015;6(10):8244.
23. Li X, Yu Z, Li Y, et al. The tumor suppressor miR-124 inhibits cell proliferation by targeting STAT3 and functions as a prognostic marker for postoperative NSCLC patients. *Int J Oncol*. 2015;46(2):798–808.
24. Kondo T, Ishida Y. Molecular pathology of wound healing. *Forensic Sci Int*. 2010;203(1–3):93–98.
25. Xue M, Jackson CJ. Extracellular matrix reorganization during wound healing and its impact on abnormal scarring. *Adv Wound Care (New Rochelle)*. 2015;4(3):119–136.
26. Zhou S, Salisbury J, Preedy VR, Emery PW. Increased collagen synthesis rate during wound healing in muscle. *PLoS One*. 2013;8(3):e58324.
27. Wang T, Gu Q, Zhao J, et al. Calcium alginate enhances wound healing by up-regulating the ratio of collagen types I/III in diabetic rats. *Int J Clin Exp Pathol*. 2015;8(6):6636–6645.
28. Pool MR. A trans-membrane segment inside the ribosome exit tunnel triggers RAMP4 recruitment to the Sec61p translocase. *J Cell Biol*. 2009;185(5):889–902.
29. Ito S, Nagata K. Biology of Hsp47 (Serpin H1), a collagen-specific molecular chaperone. *Semin Cell Dev Biol*. 2016;62:142–151.
30. Zhu Y, Li Z, Wang Y, et al. Overexpression of miR-29b reduces collagen biosynthesis by inhibiting heat shock protein 47 during skin wound healing. *Transl Res*. 2016;178:38–53.e36.
31. Yang HL, Tsai YC, Korivi M, Chang CT, Hseu YC. Lucidone promotes the cutaneous wound healing process via activation of the PI3K/AKT, Wnt/β-catenin and NF-κB signaling pathways. *Biochim Biophys Acta Mol Cell Res*. 2016;1864(4):151–168.
32. Lu T, Bao Z, Wang Y, et al. Karyopherin β1 regulates proliferation of human glioma cells via Wnt/β-catenin pathway. *Biochem Biophys Res Commun*. 2016;478(3):1189–1197.
33. Zhang Y, Tu C, Zhang D, et al. Wnt/β-catenin and Wnt5a/$Ca2^+$ pathways regulate proliferation and apoptosis of keratinocytes in psoriasis lesions. *Cell Physiol Biochem*. 2015;36(5):1890–1902.
34. Klaus A, Birchmeier W. Wnt signalling and its impact on development and cancer. *Nat Rev Cancer*. 2008;8(5):387–398.
35. Jamieson C, Sharma M, Henderson BR. Targeting the β-catenin nuclear transport pathway in cancer. *Semin Cancer Biol*. 2014;27:20–29.
36. Ashihara E, Takada T, Maekawa T. Targeting the canonical Wnt/β-catenin pathway in hematological malignancies. *Cancer Sci*. 2015; 106(6):665–671.

Knockdown of long noncoding RNA Malat1 aggravates hypoxia-induced cardiomyocyte injury by targeting miR-217

Yuan Yao*[1,B–D,F], Xiaoying Fan*[1,B–D,F], Bo Yu[1,B,D,F], Tianfa Li[2,C,D,F], Yao Zhang[1,A,D–F]

[1] Department of Cardiovascular Medicine, The 2nd Affiliated Hospital of Harbin Medical University, China
[2] Department of Cardiovascular Medicine, The Affiliated Hospital of Hainan Medical College, Haikou, China

A – research concept and design; B – collection and/or assembly of data; C – data analysis and interpretation;
D – writing the article; E – critical revision of the article; F – final approval of the article

Advances in Clinical and Experimental Medicine, ISSN 1899–5276 (print), ISSN 2451–2680 (online) *Adv Clin Exp Med*. 2019;28(6):719–728

Address for correspondence
Yao Zhang
E-mail: zhangyao0612@126.com

Funding sources
None declared

Conflict of interest
None declared

* These authors contributed equally to this work.

Received on May 5, 2017
Reviewed on June 30, 2017
Accepted on August 1, 2018

Published online on March 7, 2019

Abstract

Background. Expression of long noncoding (lncRNA) Malat1 can be increased by hypoxia in cardiomyocyte. Downregulation of Malat1 contributes to the reduction of cardiomyocyte apoptosis. However, the function of Malat1 in myocardial ischemia is unclear.

Objectives. This study investigated the functional role of lncRNA Malat1 in hypoxia-induced H9c2 cell injury.

Material and methods. H9c2 cells were exposed to hypoxia treatment. Cell proliferation, migration, invasion, and apoptosis were detected using trypan blue exclusion assay, two-chamber migration/invasion assay, annexin V-FITC/PI staining, and western blotting, respectively. Quantitative real-time polymerase chain reaction (qRT-PCR) was performed to analyze the expression levels of Malat1. The effects of Malat1 knockdown on cell proliferation, migration, invasion, and apoptosis were also measured. The interaction between Malat1 and microRNA-217 (miR-217) as well as miR-217 and sirtuin 1 (Sirt1) were analyzed using a dual luciferase reporter assay and qRT-PCR. Effects of miR-217 and Sirt1 on hypoxia-induced H9c2 cell growth were assessed.

Results. Hypoxia induced H9c2 cell injury by inhibiting cell proliferation, migration and invasion, and by promoting apoptosis. Hypoxia significantly enhanced the expression of Malat1. Malat1 bound to miR-217 and Sirt1 was a direct target of miR-217. Knockdown of Malat1 aggravated hypoxia-induced H9c2 cell injury by overexpression of miR-217. Overexpression of Sirt1 alleviated H9c2 cell injury by activating phosphatidylinositol 3-kinase/protein kinase 3 (PI3K/AKT) and Notch signaling pathways.

Conclusions. These findings suggest that Malat1 exerted important roles in hypoxia-induced cardiomyocyte injury by regulating miR-217-mediated Sirt1 and downstream PI3K/AKT and Notch signaling pathways.

Key words: myocardial ischemia, Malat1, hypoxia-induced cell injury, microRNA-217, sirtuin 1

Cite as
Yao Y, Fan X, Yu B, Li T, Zhang Y. Knockdown of long noncoding RNA Malat1 aggravates hypoxia-induced cardiomyocyte injury by targeting miR-217. *Adv Clin Exp Med*. 2019;28(6):719–728. doi:10.17219/acem/93878

DOI
10.17219/acem/93878

Background

Myocardial ischemia is a heart condition caused by the reduction of blood flow to the heart, which prevents the heart from receiving enough oxygen.[1] It has become one of the leading causes of death all over the world and a serious threat to human health.[2] Myocardial ischemia is the main factor contributing to cardiomyocyte impairment.[3] The main clinical symptoms of myocardial ischemia are severe persistent chest pain, dyspnea, fever, and syncope.[4,5] Hypoxia in varying degrees threatens the function and survival of cardiomyocytes,[6,7] although numerous adaptive countermeasures can be activated in the cardiomyocytes in response to the hypoxic condition.[8,9]

Recently, researchers have demonstrated that numerous noncoding transcripts were involved in the physiological and pathological regulation of many diseases, including myocardial ischemia.[10,11] Long noncoding RNAs (lncRNAs) are noncoding RNA molecules longer than 200 nucleotides that are not translated into proteins, but regulate the transcription of genes that are involved in different cellular processes, including differentiation, cancer initiation and progression.[12] Metastasis-associated lung adenocarcinoma transcript 1 (Malat1), an lncRNA, is expressed in the nucleus and participates in many cellular processes.[13] Several studies have confirmed that Malat1 is responsible for cancer.[14–16] Zhao et al. proved that Malat1 functions as a mediator in the cardioprotective effects of fentanyl on myocardial ischemia-reperfusion injury.[17] More research is still needed to further explore the effects of Malat1 on myocardial ischemia.

Several lncRNAs or microRNAs (miRNAs) are functionally involved in acute myocardial infarction (e.g., ANRIL, KCNQ1OT1, Malat1, miR-499, and miR-214), mitochondrial function and apoptosis of cardiomyocytes (e.g., CHRF, miR-145 and miR-22).[18–24] Although lncRNAs have not been extensively researched in myocardial ischemic injury, recent studies are increasingly focusing on the possible contribution of lncRNAs in ischemia.[25,26] Michalik et al. demonstrated that Malat1 regulates the endothelial cell function and vessel growth.[27] Interestingly, a negative correlation exists between Malat1 and miR-217.[13] Moreover, researchers found that miR-217 targets and regulates sirtuin 1 (Sirt1) expression.[28] However, involvement and the functional mechanism of miR-217 and Malat1 in myocardial ischemic injury remains uncertain. The present study established an in vitro myocardial cell model of hypoxia and investigated the effects of Malat1, miR-217 and Sirt1 on the hypoxia-induced cardiomyocyte injury.

Material and methods

Cell culture and treatment

The cardiomyocytes cell line H9c2 was purchased from Sigma-Aldrich (St. Louis, USA) and cultured in Dulbecco's Modified Eagle Medium (DMEM; Life Technologies Corp., Carlsbad, USA) supplemented with 10% fetal bovine serum (FBS), 1% penicillin/streptomycin (100 U/mL:100 mg/mL) and 1% GlutaMAX (Life Technologies), at 37°C under 5% CO_2. Culture medium was changed every other day. H9c2 cells were cultured in a hypoxic incubator with 3% O_2 concentration for 24 h to induce injury.

Quantitative real-time polymerase chain reaction

After relevant treatment, total RNA was extracted from cells using Trizol reagent (Life Technologies) according to the manufacturer's instructions. Quantitative real-time polymerase chain reaction analysis was performed using One Step SYBR PrimeScript PLUS RT-RNA PCR Kit (TaKaRa Biotechnology, Dalian, China) to assess the expression levels of Malat1 according to the protocol instructions. Taqman MicroRNA Reverse Transcription Kit and Taqman Universal Master Mix II with the TaqMan MicroRNA Assay of miR-217 and U6 (Applied Biosystems, Foster City, USA) were used to test the expression levels of miR-217 in cells. RNA PCR Kit (AMV) v. 3.0 (TaKaRa Biotechnology) was used to assess the expression of Sirt1. *GAPDH* or U6 was used as an internal control. The relative expressions were calculated using $2^{-\Delta\Delta Ct}$ method. Sequences of primers were as follows: Malat1 forward primer: 5'-AGCGGAAGAACGAATGTAAC-'3, reverse primer: 5'-GAACAGAAGGAAGAGCCAAG-'3; miR-217 forward primer: 5'-TACTGCATCAGGAACTGACTGGA-'3, reverse primer: 5'-GTGCAGGGTC CGAGGT-'3; Sirt1 forward primer: 5'-AGGAGACTTGCCTGGTGAAA-'3, reverse primer: 5'-CAGGGGTGGTTATTGCATCT-'3; GAPDH forward primer: 5'-GCACCGTCAAGGCTGAGAAC-'3, reverse primer: 5'-TGGTGAAGACGC CAGTGGA-'3; U6 forward primer: 5'-CTCGCTTCGGCAGCACATATACT-'3, reverse primer: 5'-ACGCTTCACGAATTTGCGTGTC-'3.

Transfection and generation of stably transfected cell lines

Short-hairpin RNA directed against lncRNA Malat1 was ligated into the U6/GFP/Neo plasmid (GenePharma, Shanghai, China) and this was referred to as sh-Malat1. The following target regions were chosen: Malat1#1, 5'-GGGAGTTACTTGCCAACTTG-'3; Malat1#2, 5'-CCAGGCTGGTTATG ACTCAG-'3. For the analysis of Sirt1 functions, full-length *Sirt1* sequences and short-hairpin RNA directed against *Sirt1* were constructed in pEX-2 and U6/GFP/Neo plasmids (GenePharma), respectively. These were referred to as pEX-Sirt1 and sh-Sirt1. The sequence of pEX-Sirt1 was 5'-ACUUUGCUGUAACCCUGUA-'3. The forward sequence of sh-Sirt1 was 5'-CACCACACCAGATTCTTCAGTGAT TGTCATCTCTGACAATCACTGAAGAATCTGGTGG-'3 and the reverse sequence of sh-Sirt1 was 5'-AAAACCAGATTCTTCAGTG

ATTGTCAGAGATGA CAATCACTGAACCTGGTGG-'3. The plasmid carrying a non-targeting sequence was used as a negative control (NC) that was referred to as sh-NC. miR-217 mimics, inhibitors and their respective NCs were synthesized by Life Technologies and were transfected into the cells in line with the manufacturer's instruction. The sequences used were: pEX-miR-217, 5'-UACUGCAUCAGGAACUGAUUGGA-'3; si-miR-217, 5'-UACUGCAUCAGG AACUGAUUGGA-'3. Cell transfection was performed using lipofectamine 3000 reagent (Life Technologies) according to the manufacturer's instructions. The stably transfected cells were selected by the culture medium containing 0.5 mg/mL of G418 (Sigma-Aldrich). After approx. 4 weeks, G418-resistant cell clones were established. The highest transfection efficiency occurred at 48 h, and thus 72 h post-transfection was considered as the harvest time in the subsequent experiments.

Cell proliferation assays

For cell proliferation assay, 1×10^5 cells were seeded in duplicate in 60-millimeter dishes. After normoxia or hypoxia treatment for 24 h, cells were washed and the live cell numbers were determined using trypan blue exclusion assay.

Apoptosis assay

Cell apoptosis assay was performed using propidium iodide (PI) and fluorescein isothiocynate (FITC)-conjugated annexin V staining. Briefly, 1×10^5 cells were seeded in duplicate in 60-millimeter dishes. After normoxia or hypoxia treatment for 24 h, the cells were washed in phosphate buffered saline (PBS) and fixed in 70% ethanol. Fixed cells were then washed twice in PBS and stained with PI/FITC-annexin V in the presence of 50 µg/mL RNase A (Sigma-Aldrich), and then were incubated for 1 h at room temperature in the dark. The rate of apoptotic cells was recorded using Flow cytometer (Beckman Coulter, Fullerton, USA). The data was analyzed using FlowJo software (www.flowjo.com).

Migration and invasion assay

Cell migration was determined using a modified two-chamber migration assay with a pore size of 8 mm. After normoxia or hypoxia treatment for 24 h, 5.0×10^4 H9c2 cells were seeded into the upper compartment of 24-well transwell culture chamber supplemented with 200 mL of serum-free medium, while 600 mL of complete medium was added into the lower compartment. After incubation at 37°C for 48 h, the cells were fixed with methanol. After that, non-traversed cells were carefully removed from the upper surface of the filter with a cotton swab, while traversed cells on the lower side of the filter were stained with crystal violet and then counted.

The invasive behavior of the cells was determined using 24-well Millicell Hanging Cell Culture inserts with 8 mm PET membranes (Merck Millipore, Bedford, USA). In brief, after normoxia or hypoxia treatment for 24 h, 5.0×10^4 H9c2 cells in 200 µL serum-free DMEM medium were plated onto BD BioCoat Matrigel Invasion Chambers (8 µM pore size polycarbonate filters; BD Biosciences, Franklin Lakes, USA), while a complete medium containing 10% FBS was added to the lower chamber. After processing the invasion chambers for 48 h (37°C, 5% CO_2 or 37°C, 3% CO_2) in accordance with the manufacturer's protocol, the non-invading cells were removed with a cotton swab. The invading cells were fixed in 100% methanol and then stained with crystal violet solution and counted microscopically. The data is presented as the average number of cells attached to the bottom surface from 5 randomly chosen fields.

Reporter vector constructs and luciferase reporter assay

The Malat1 fragment containing the predicted miR-217 binding site was amplified using PCR and then cloned into pmirGlO Dual-Luciferase miRNA Target Expression Vector (Promega, Madison, USA) to form the reporter vector Malat1-wild-type (Malat1-Wt). To mutate the putative binding site of miR-217 in the Malat1, the sequence of putative binding site was replaced and named as Malat1-mutated-type (Malat1-Mt). Then the vectors and miR-217 mimics were co-transfected into HEK293 cells and the Dual-Luciferase Reporter Assay System (Promega) was performed to test the luciferase activity.

The construction process of Sirt1-wt and Sirt1-mt reporter vectors was similar to the Malat1-wt and Malat1-mt. After that, Sirt1-wt and Sirt1-mt reporter vectors and miR-217 mimic were co-transfected into HEK293 cells, and the relative luciferase activities were measured with Dual-Luciferase Reporter Assay System.

Western blotting

The protein used for western blotting was extracted using the RIPA lysis buffer (Beyotime Biotechnology, Shanghai, China) that was supplemented with protease inhibitors (Roche Diagnostics, Basel, Switzerland). The proteins were then quantified using the BCA Protein Assay Kit (Pierce, Appleton, USA) accordingly. The western blotting system was established using a Bio-Rad Bis-Tris Gel system (Bio-Rad Laboratories, Hercules, USA), according to the manufacturer's instructions. Protein samples were electrophoresed using western blot system and transferred into polyvinylidene difluoride (PVDF) membranes (Merck Millipore). After being blocked with 5% bovine serum albumin (BSA; Sigma-Aldrich) for 1 h, the membrane was incubated with primary antibodies at 4°C overnight. The following primary antibodies were used in this study: anti-Bcl-2 antibody (ab59348), anti-Bax antibody (ab182733), anti-p-PI3K antibody (ab191606), anti-PI3K antibody (ab109006),

anti-p-AKT antibody (ab81283), anti-AKT antibody (ab8805), and anti-Notch 3 (ab23426); all of the above were obtained from Abcam Biotechnology (Cambridge, UK). Anti-caspase 3 antibody (#9662), anti-caspase 9 antibody (#9508), anti-Notch 1 antibody (#3608), anti-Notch 2 antibody (#5732), and anti-GAPDH antibody (#5174) were purchased from Cell Signaling Technology (Danvers, USA). After that, membranes were washed and incubated with secondary antibody (ab6788, ab6721; Abcam Biotechnology) for 1 h at room temperature. The protein signals were measured using Bio-Rad ChemiDoc XRS system (Bio-Rad), which was supplemented with 200 µL of Immobilon Western Chemiluminescent HRP Substrate (Merck Millipore).

Statistical analysis

All experiments were repeated 3 times. The results of multiple experiments are presented as mean ± standard deviation (SD). Statistical analyses were performed using Graphpad v. 6.0 statistical software (Graphpad Software, San Diego, USA). The p-values were calculated using one-way analysis of variance (ANOVA) with Sidak post-hoc test. A p-value <0.05 was considered to indicate a statistically significant result.

Results

Hypoxia induces H9c2 cell injury

Hypoxic treatment significantly downregulated the H9c2 cell viability (Fig. 1A, $p < 0.05$), migration (Fig. 1B, $p < 0.05$) and invasion (Fig. 1C, $p < 0.05$), while increasing cell apoptosis (Fig. 1D, $p < 0.005$) as compared to the normoxia treatment. Similar results were obtained from western blotting analysis (Fig. 1E), which presented that the expression levels of Bax, cleaved-caspase 3 and cleaved-caspase 9 were all enhanced after hypoxia treatment. These results suggest that hypoxia induces H9c2 cell injury by inhibiting cell viability, migration and invasion, and promoting cell apoptosis.

Hypoxia promotes the expression of Malat1

The qRT-PCR was performed to analyze the expression level of Malat1 after hypoxia treatment. Results showed that the relative expression of Malat1 was significantly increased in the hypoxic condition compared to the control (Fig. 2, $p < 0.01$).

Suppression of Malat1 aggravates hypoxia-induced H9c2 cell injury

Either sh-Malat1#1 or sh-Malat1#2 were transfected into H9c2 cells to decrease the expression level of Malat1. As shown in Fig. 3A, the relative expression of Malat1 was significantly decreased in H9c2 cells after transfection with sh-Malat1#1 ($p < 0.005$) and sh-Malat1#2 ($p < 0.01$). Considering that sh-Malat1#1 had more significant inhibition, sh-Malat#1 was used in further experiments. Hypoxia-induced cell injury was significantly exacerbated by Malat 1 suppression, as evidenced by cell viability (Fig. 3B, $p < 0.05$), migration (Fig. 3C, $p < 0.05$) and invasion (Fig. 3D, $p < 0.05$) decreases, and by cell apoptosis increase (Fig. 3E, $p < 0.01$) after sh-Malat1#1 transfection. The apoptosis results were further confirmed with western blotting (Fig. 3F), which indicted that the expressions of Bax, cleaved-caspase 3 and cleaved-caspase 9 were further upregulated after Hypoxia+sh-Malat1#1 treatment. The expression of Bcl-2 was downregulated after Hypoxia+sh-Malat1#1 treatment. These results suggest that knockdown of Malat1 expression aggravates hypoxia-induced H9c2 cell injury.

Malat1 negatively regulates the level of miR-217 in H9c2 cells

The qRT-PCR was performed to detect the expression of miR-217 in H9c2 cells after hypoxia treatment and sh-Malat1#1 transfection. As shown in Fig. 4A, the expression of miR-217 was significantly decreased after hypoxia treatment ($p < 0.01$). Knockdown of Malat1 markedly increased the miR-217 expression ($p < 0.005$), which suggests that Malat1 bind to miR-217 in H9c2 cells. This hypothesis was further confirmed by dual luciferase activity assay, which pointed out co-transfection with miR-217 and Malat1-wt notably reduced the relative luciferase activity (Fig. 4B, $p < 0.05$). This data indicates that Malat1 negatively regulates the expression level of miR-217 in H9c2 cells.

Knockdown of Malat1 aggravates hypoxia-induced H9c2 cell injury by upregulating of miR-217

The effects of Malat1 and miR-217 on viabilities, migration, invasion, and apoptosis of H9c2 cells were then investigated. The expression level of miR-217 was significantly increased after miR-217 mimic transfection (Fig. 5A, $p < 0.005$) and remarkably decreased after si-miR-217 transfection ($p < 0.01$). The si-miR-217 single transfection obviously reversed the hypoxia-induced cell viability, migration and invasion inhibition (Fig. 5B–D, $p < 0.05$) as well as the cell apoptosis enhancement (Fig. 5E, $p < 0.01$). Moreover, compared to hypoxia+sh-Malat1#1+siNC treatment group, the cell viability, migration and invasion were all increased in hypoxia+sh-Malat1#1+si-miR-217 treatment group (Fig. 5B–D, $p < 0.01$). The cell apoptosis was dramatically decreased after hypoxia+sh-Malat1#1+si-miR-217 treatment (Fig. 5E, $p < 0.005$). This data suggests that knockdown of Malat1 aggravates hypoxia-induced H9c2 cell injury by overexpression of miR-217.

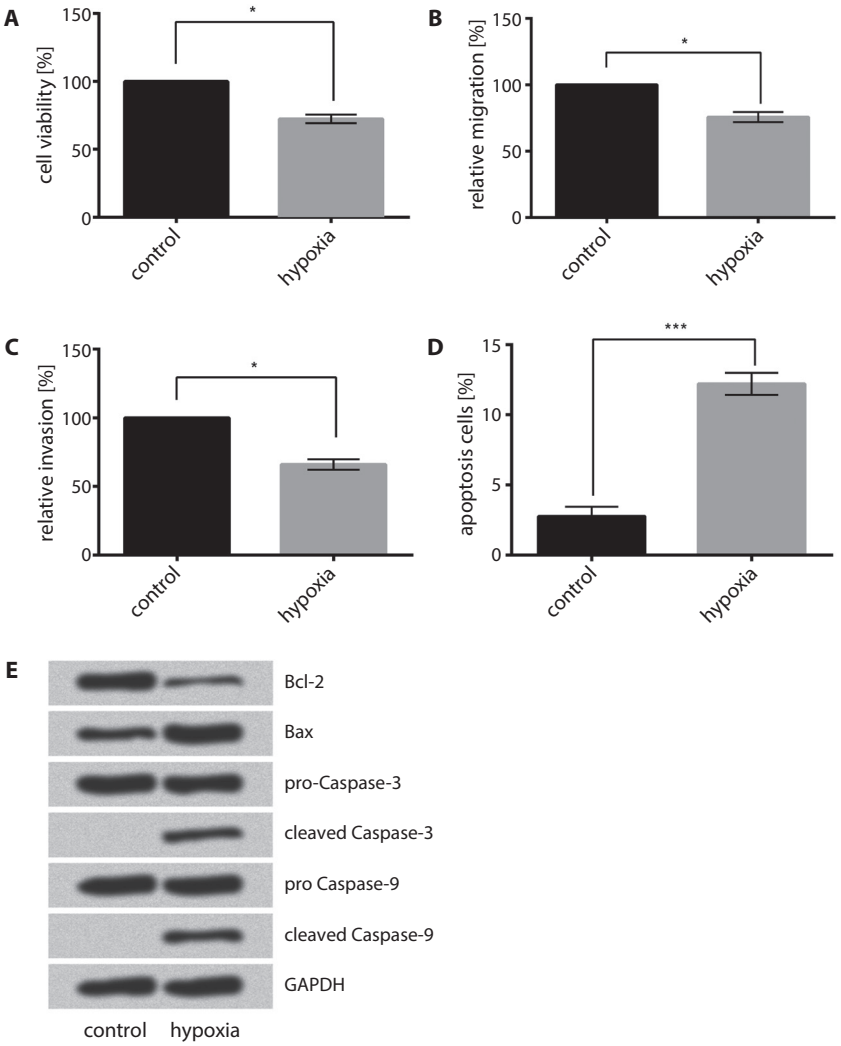

Fig. 1. Effects of hypoxia on H9c2 cell viability, migration, invasion, and apoptosis. Cell viability (A), migration (B), invasion (C), and apoptosis (D) after normoxia or hypoxia treatment was detected using trypan blue exclusion, migration and invasion, and annexin V-FITC/PI staining, respectively. (E) Western blotting was used to analyze the expression levels of Bcl-2, Bax, caspase 3, and caspase 9 in H9c2 cells after normoxia or hypoxia treatment. *p < 0.05; ***p < 0.005

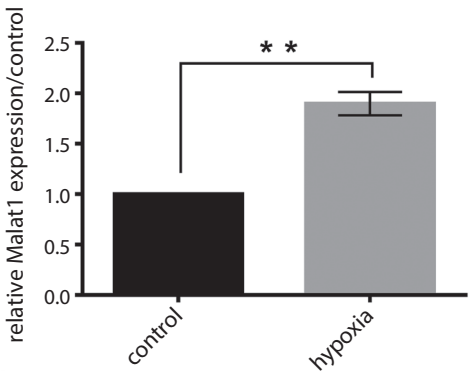

Fig. 2. Effect of hypoxia on expression of Malat1 in H9c2 cells. Quantitative real-time polymerase chain reaction (qRT-PCR) was performed to measure the expression level of Malat1 in H9c2 cells after hypoxia treatment. **p < 0.01

miR-217 negatively regulates the expression of Sirt1 in H9c2 cells

Sirt1 was hypothesized to be a potential target of miR-217. As shown in Fig. 6A, the expression level of Sirt1 was remarkably upregulated after hypoxia treatment (p < 0.01). Moreover, the expression of Sirt1 was obviously downregulated after miR-217 mimic transfection (p < 0.005) and noticeably upregulated after si-miR-217 transfection (p < 0.01), which suggests that miR-217 negatively regulated the expression of Sirt1 in H9c2 cells. To verify whether miR-217 was able to directly bind to the 3' untranslated region (3'UTR) of Sirt1, Sirt1-wt and Sirt1-mt containing the wild-type and mutant binding sequences of miR-217 were generated, respectively (Fig. 6B). A luciferase reporter assay revealed that the relative luciferase activity was significantly reduced when co-transfected with Sirt1-wt and miR-217 mimics (p < 0.05). However, the luciferase activity revealed no significant difference when co-transfected with Sirt1-mt and miR-217 mimics. These results indicate that Sirt1 was a direct target gene of miR-217 in H9c2 cells.

Overexpression of Sirt1 alleviates the hypoxia-induced H9c2 cell injury

To analyze the functions of Sirt1, the full-length Sirt1 sequences and short-hairpin RNA directed against Sirt1 were constructed in pEX-2 and U6/GFP/Neo plasmids, respectively. They were referred to as pEX-Sirt1 and sh-Sirt1.

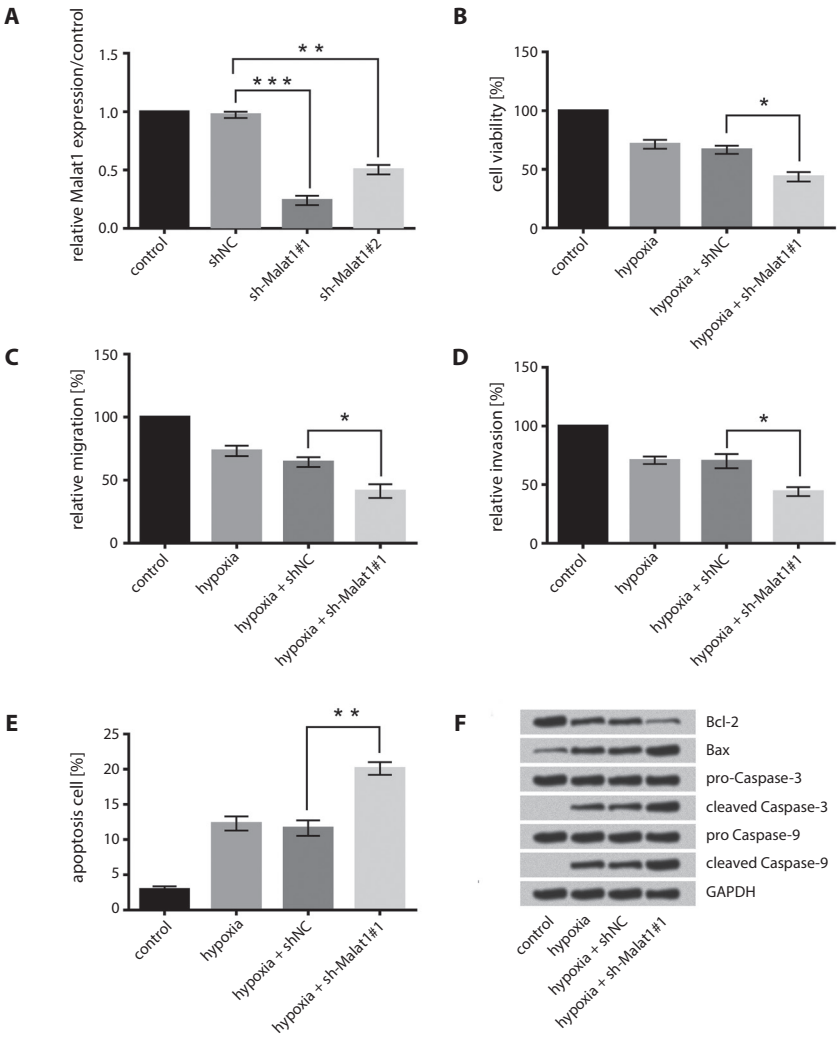

Fig. 3. Effects of suppression of Malat1 on hypoxia-induced H9c2 cell injury. (A) quantitative real-time polymerase chain reaction (qRT-PCR) was used to detect the expression level of Malat1 after sh-Malat1#1 or sh-Malat1#2 transfection. Cell viability (B), migration (C), invasion (D), and apoptosis (E) after hypoxia treatment and/or sh-Malat1 transfection were measured using trypan blue exclusion, migration and invasion, and annexin V-FITC/PI staining, respectively. (F) Western blotting was performed to analyze the expression levels of Bcl-2, Bax, caspase 3, and caspase 9 in H9c2 cells after hypoxia treatment and/or sh-Malat1 transfection. *p < 0.05; **p < 0.01; ***p < 0.005

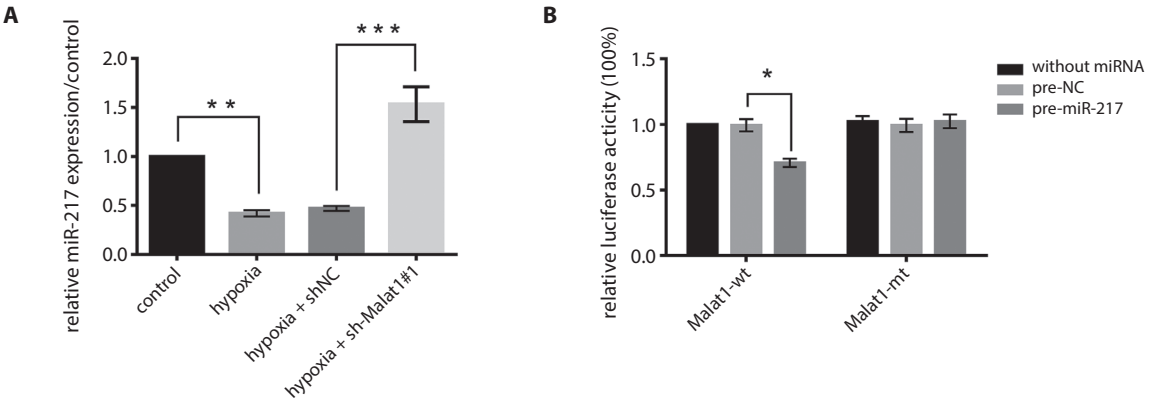

Fig. 4. The relationship between Malat1 and miR-217. (A) The expressions of miR-217 in H9c2 cells after hypoxia treatment and/or sh-Malat1 transfection were determined using quantitative real-time polymerase chain reaction (qRT-PCR). (B) The relative luciferase activity was detected after co-transfected miR-217 with Malat1-wt or Malati-mt. **p < 0.01; ***p < 0.005

As presented in Fig. 7A, the relative Sirt1 expression was obviously increased after pEX-Sirt1 transfection ($p < 0.05$) and significantly decreased after sh-Sirt1 transfection ($p < 0.01$). Overexpression of Sirt1 significantly reversed the hypoxia-induced cell viability, migration and invasion inhibition (Fig. 7B–D, $p < 0.05$) as well as cell apoptosis enhancement (Fig. 7E, $p < 0.05$). As expected, suppression of Sirt1 showed opposite results (Fig. 7B–E). These results suggest that overexpression of Sirt1 protects H9c2 cells from hypoxia-induced injury.

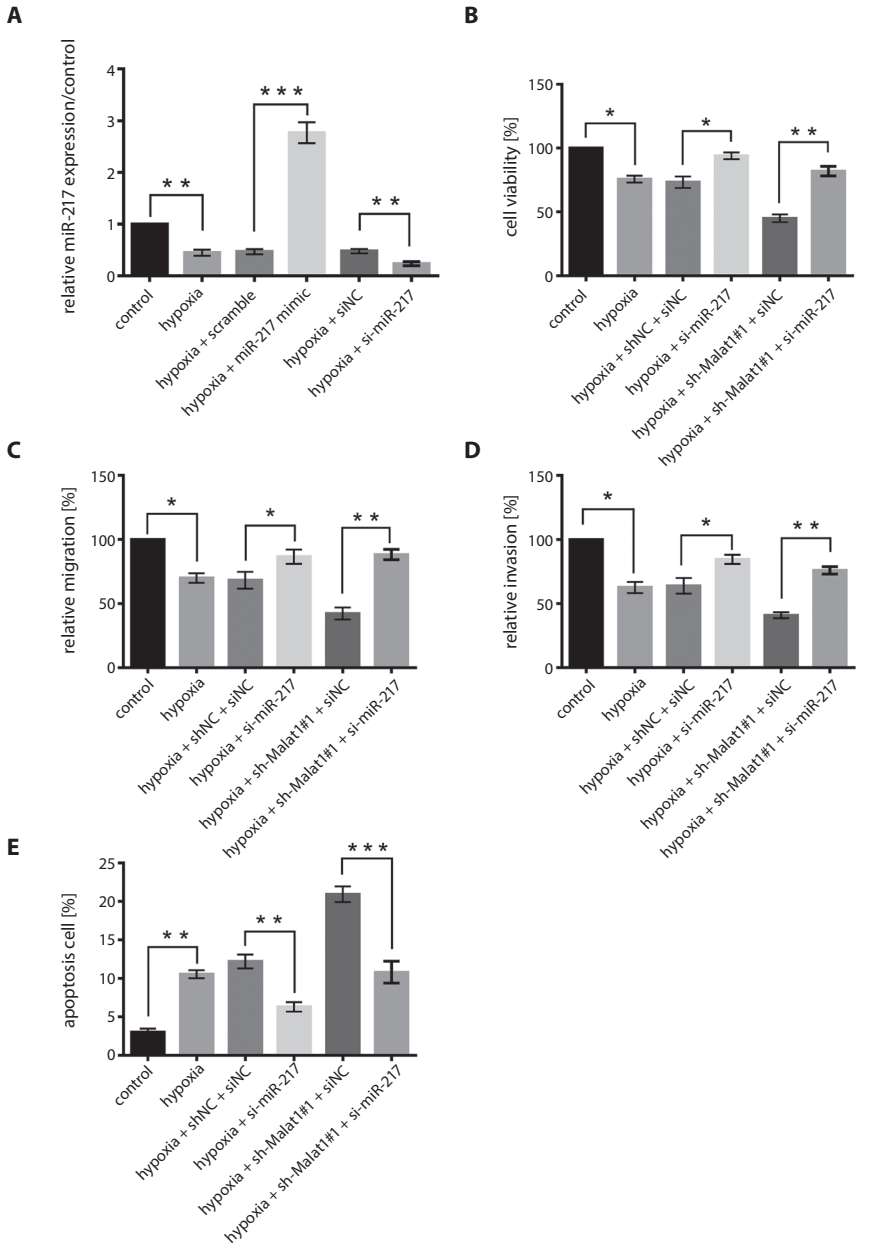

Fig. 5. Roles of miR-217 in hypoxia and sh-Malat1-induced H9c2 cell injury. (A) The expressions of miR-217 were measured after hypoxia treatment and miR-217 mimic or si-miR-217 transfection. Cell viability (A), migration (B), invasion (C), and apoptosis (E) after hypoxia treatment and/or Malat1#1 as well as si-miR-217 transfection were detected using trypan blue exclusion, migration and invasion, and annexin V-FITC/PI staining, respectively. *p < 0.05; **p < 0.01; ***p < 0.005

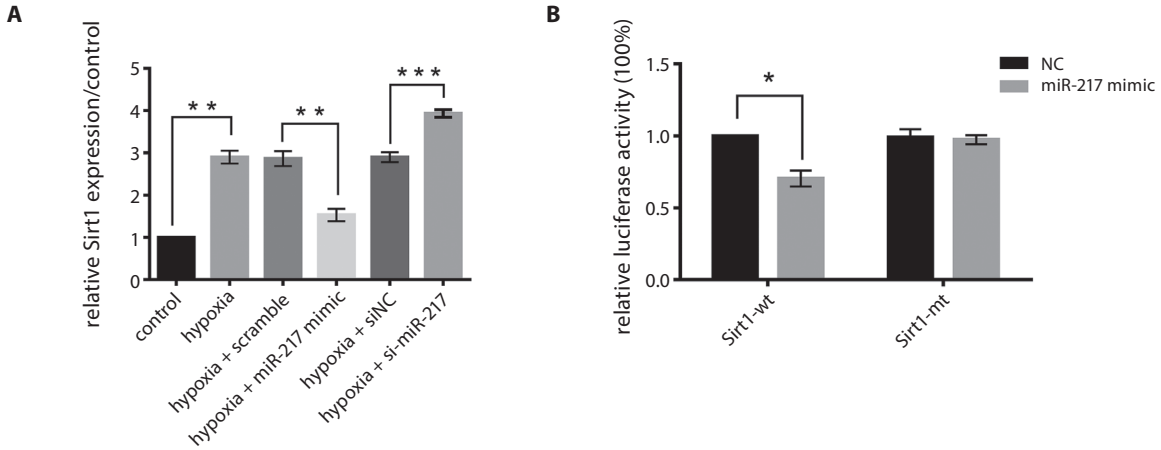

Fig. 6. The relationship between miR-217 and Sirt1. (A) Quantitative real-time polymerase chain reaction (qRT-PCR) was performed to detect the expressions of Sirt1 in H9c2 cells after hypoxia treatment and/or miR-217 mimic/si-miR-217 transfection. (B) The relative luciferase activity was measured after co-transfection with miR-217 mimic and Sirt1-wt or Sirt1-mt. **p < 0.01; ***p < 0.005

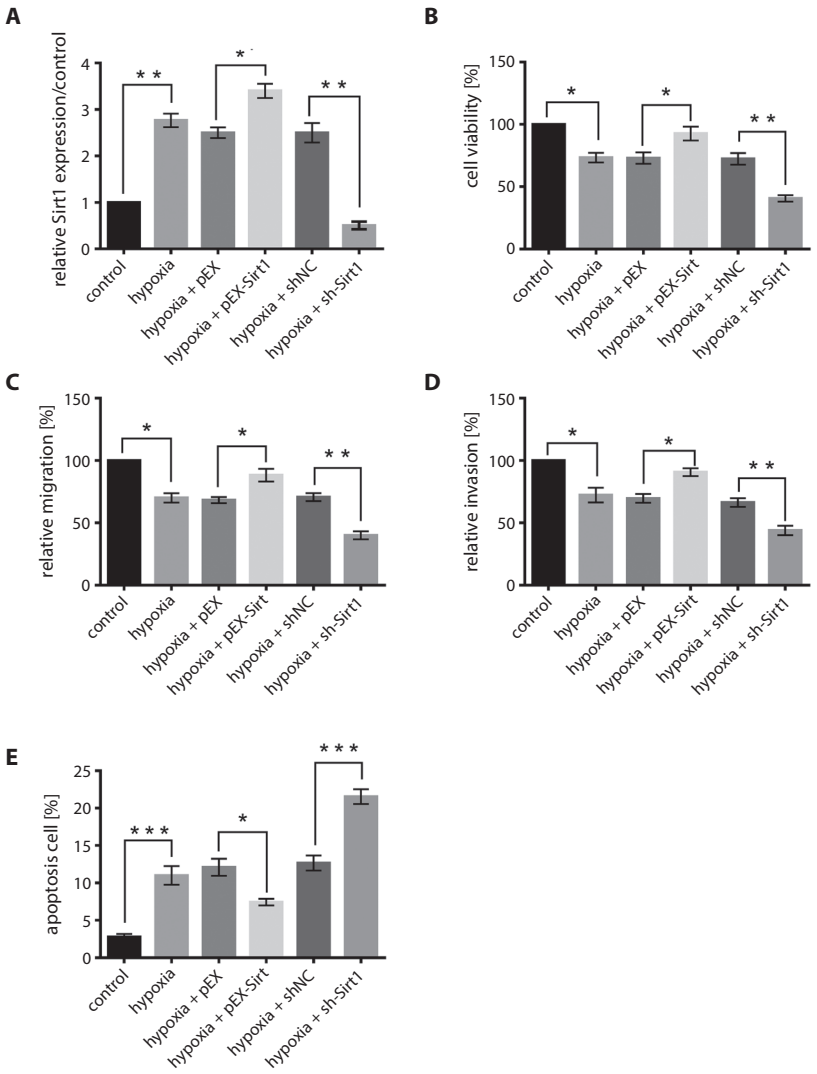

Fig. 7. Effects of Sirt1 on hypoxia-induced H9c2 cell injury. (A) The expressions of Sirt1 in H9c2 cells were detected after hypoxia treatment and/or pEX-Sirt1/sh-Sirt1 transfection. Cell viability (B), migration (C), invasion (D), and apoptosis (E) after hypoxia treatment and/or pEX-Sirt1/sh-Sirt1 transfection were measured using trypan blue exclusion, migration and invasion, and annexin V-FITC/PI staining, respectively. *p < 0.05; **p < 0.01; ***p < 0.005

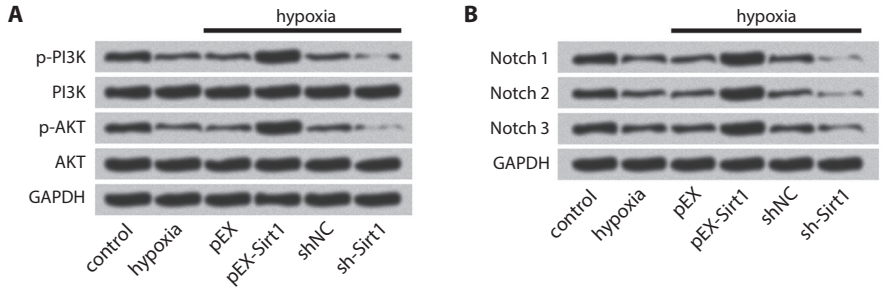

Fig. 8. PI3K/AKT and Notch signaling pathways. (A) Western blotting was used to analyze the expressions of p-PI3K, PI3K, p-AKT, and AKT in H9c2 cells after hypoxia treatment and/or pEX-Sirt1/sh-Sirt1 transfection. (B) The expressions of Notch 1, Notch 2 and Notch 3 in H9c2 cells were detected after hypoxia treatment and/or pEX-Sirt1/sh-Sirt1 transfection

PI3K/AKT and Notch signaling pathways

Western blot analysis was performed to analyze the roles of PI3K/AKT and Notch signaling pathways in hypoxia-induced H9c2 cell injury. The results displayed that the expression levels of p-PI3K and p-AKT were decreased after hypoxia treatment (Fig. 8A). Overexpression of Sirt1 reversed the hypoxia-induced decreases of p-PI3K and p-AKT but suppression of Sirt1 further aggravated the hypoxia-induced decreases of p-PI3K and p-AKT. Similar results were found in Notch signaling pathway, which showed that the expressions of Notch 1, Notch 2 and Notch 3 were decreased after hypoxia treatment and further downregulated after sh-Sirt1 transfection (Fig. 8B). These results indicate that overexpression of Sirt1 alleviates hypoxia-induced H9c2 cell injury by activating PI3K/AKT and Notch pathways.

Discussion

We studied the effects and mechanisms of Malat1 on the hypoxia-induced injury in H9C2 cells. We showed that hypoxia induced H9c2 cell injury by inhibiting cell

viability, migration and invasion, and promoting cell apoptosis. Suppression of Malat1 aggravates the hypoxia-induced H9c2 cell injury (Fig. 3). Malat1 negatively regulates the expression of miR-217 in H9c2 cells (Fig. 4). Knockdown of Malat1 aggravates hypoxia-induced H9c2 cell injury by overexpression of miR-217 (Fig. 5). Moreover, miR-217 negatively regulates Sirt1 expression and Sirt1 was a target of miR-217 (Fig. 6 and 7). Overexpression of Sirt1 activates PI3K/AKT and Notch signaling pathways, which might be involved in H9c2 cell survival (Fig. 8).

Hypoxia-induced cell death is a major concern and plays a critical role in various pathophysiological processes, such as hypoxic/ischemic disease, organ transplantation, angiogenesis, or tumor invasion.[29–31] Cardiomyocyte injury comprises a series of events that may occur together or separately, such as: reperfusion, arrhythmias, myocardial stunning in "reversible mechanical dysfunction", microvascular damage, and cell death.[32,33]

Malat1 was initially discovered as a tumor-associated lncRNA, which is mainly involved in the splicing and epigenetic regulation of gene expression.[34] A recent study reports that Malat1 also acts as a regulator of cardiovascular disease.[35] Zhao et al. reported that Malat1 plays a key regulatory role in mediating the cardioprotective effects of fentanyl against ischemic/reperfusion injury.[17] In our research, we found that the expression of Malat1 in H9c2 cells was significantly increased after hypoxia treatment. Knockdown of Malat1 aggravates hypoxia-induced H9c2 cell injury by enhancing cell viability, migration and invasion inhibition, and promoting cell apoptosis. However, Zhang et al. indicated that downregulation of Malat1 reduced cardiomyocyte apoptosis and improved left ventricular function in diabetic rats.[36] The regulation of intracellular signaling pathways is very complex. The same molecules may have different regulatory effects in different cell types and in different conditions. The disparity effect of Malat1 on cardiomyocyte cell proliferation and apoptosis might be associated with different cell types and different treatment processes.

Our study indicates that Malat1 negatively regulates the expression of miR-217, which is consistent with another study on human cancers.[37] Our study is the first to demonstrate that miR-217 binds to Malat1 in cardiomyocytes and the role of miR-217 in cardiomyocyte injury induced by hypoxia. Luciferase activity reveals that miR-217 was able to directly bind to the 3'UTR of Sirt1 and, therefore, Sirt1 was identified as a direct target of miR-217 in H9c2 cells. Several other studies have also confirmed that Sirt1 was a target of miR-217,[38] which is consistent with our findings.

Sirt1 is a member of a protein family known as sirtuins, which belongs to the Sirt2 family and has been identified as nicotinamide-adenine dinucleotide $(NAD)^+$ dependent deacetylases.[39,40] Sirt1 has been demonstrated to participate in cancer, aging, metabolic diseases, and cardiovascular dysfunctions.[41,42] Sirt1 can protect endothelial cells from oxidative stress and oxidative low-density lipoprotein-induced apoptosis.[43–45] In our study, we found that overexpression of Sirt1 alleviates the hypoxia-induced H9c2 cell injury by promoting cell viability, migration and invasion but inhibiting cell apoptosis.

The PI3K/Akt and Notch signaling pathways are essential for cell survival and proliferation.[39,46] It has been reported that the activation of PI3K/Akt pathway is closely associated with vascular remodeling and angiogenesis. Li et al. demonstrated that Sirt1 promoted the migration and proliferation of endothelial progenitor cells through PI3K/AKT pathway.[46] Our study results similarly proved that Sirt1 activates PI3K/AKT and Notch signaling pathways, which were involved in the promotion of cell survival in H9c2 cells.

In conclusion, these findings suggest that knockdown of Malat1 aggravates hypoxia-induced cardiomyocyte injury by upregulating miR-217 expression. The aforementioned results demonstrated negative regulation of Sirt1 expression by miR-217 and Sirt1 as a target of miR-217. Also, Sirt1 activated PI3K/AKT and Notch signaling pathways, which in turn promoted H9c2 cell survival.

References

1. Thygesen K, Alpert JS, White HD. Joint ESC/ACCF/AHA/WHF Task Force for the Redefinition of Myocardial Infarction. Universal definition of myocardial infarction. *Eur Heart J*. 2007;28(20):2525–2538.
2. Zhu HM, Deng L. Evaluation of cardiomyocyte hypoxia injury models for the pharmacological study in vitro. *Pharm Biol*. 2012;50(2):167–174.
3. Gui L, Liu B, Lv G. Hypoxia induces autophagy in cardiomyocytes via a hypoxia-inducible factor 1-dependent mechanism. *Exp Ther Med*. 2016;11(6):2233–2239.
4. Coventry LL, Bremner AP, Williams TA, Jacobs IG, Finn J. Symptoms of myocardial infarction: Concordance between paramedic and hospital records. *Prehosp Emerg Care*. 2014;18(3):393–401.
5. Lippi G, Sanchis-Gomar F, Cervellin G. Chest pain, dyspnea and other symptoms in patients with type 1 and 2 myocardial infarction: A literature review. *Int J Cardiol*. 2016;215:20–22.
6. Tong W, Xiong F, Li Y, Zhang L. Hypoxia inhibits cardiomyocyte proliferation in fetal rat hearts via upregulating TIMP-4. *Am J Physiol Regul Integr Comp Physiol*. 2013;304(8):R613–R620.
7. Botting KJ, McMillen IC, Forbes H, Nyengaard JR, Morrison JL. Chronic hypoxemia in late gestation decreases cardiomyocyte number but does not change expression of hypoxia-responsive genes. *J Am Heart Assoc*. 2014;3(4). doi:10.1161/JAHA.113.000531
8. Ramjiawan A, Bagchi RA, Blant A, et al. Roles of histone deacetylation and AMP kinase in regulation of cardiomyocyte PGC-1α gene expression in hypoxia. *Am J Physiol Cell Physiol*. 2013;304(11):C1064–1072.
9. Wang W, Peng Y, Wang Y, Zhao X, Yuan Z. The anti-apoptotic effect of heat shock protein 90 on hypoxia-mediated cardiomyocyte damage through the PI3K/Akt pathway. *Clin Exp Pharmacol Physiol*. 2009;36(9):899–903.
10. Wang K, Liu CY, Zhou LY, et al. APF lncRNA regulates autophagy and myocardial infarction by targeting miR-188-3p. *Nat Commun*. 2015;6:6779.
11. Wang JX, Zhang XJ, Li Q, et al. MicroRNA-103/107 regulate programmed necrosis and myocardial ischemia/reperfusion injury through targeting FADD. *Circ Res*. 2015;117(4):352–363.
12. Reik W. Evolution and functions of long noncoding RNAs. *Cell*. 2009;136(4):629–641.
13. Zhang X, Tang X, Liu K, Hamblin MH, Yin KJ. Long non-coding RNA Malat1 regulates cerebrovascular pathologies in ischemic stroke. *J Neurosci*. 2017;37(7):1797–1806.
14. Lin R, Maeda S, Liu C, Karin M, Edgington TS. A large noncoding RNA is a marker for murine hepatocellular carcinomas and a spectrum of human carcinomas. *Oncogene*. 2007;26(6):851–858.

15. Wei Y, Niu B. Role of MALAT1 as a Prognostic factor for survival in various cancers: A systematic review of the literature with meta-analysis. *Dis Markers*. 2015;2015:164635.
16. Gutschner T, Hammerle M, Eissmann M, et al. The noncoding RNA MALAT1 is a critical regulator of the metastasis phenotype of lung cancer cells. *Cancer Res*. 2013;73(3):1180–1189.
17. Zhao ZH, Hao W, Meng QT, Du XB, Lei SQ, Xia ZY. Long non-coding RNA MALAT1 functions as a mediator in cardioprotective effects of fentanyl in myocardial ischemia-reperfusion injury. *Cell Biol Int*. 2016;41(1):62–70.
18. Vausort M, Wagner DR, Devaux Y. Long noncoding RNAs in patients with acute myocardial infarction. *Circ Res*. 2014;115(7):668–677.
19. Janssen R, Zuidwijk MJ, Muller A, et al. MicroRNA 214 is a potential regulator of thyroid hormone levels in the mouse heart following myocardial infarction, by targeting the thyroid-hormone-inactivating enzyme deiodinase type III. *Front Endocrinol (Lausanne)*. 2016;7:22.
20. Xin Y, Yang C, Han Z. Circulating miR-499 as a potential biomarker for acute myocardial infarction. *Ann Transl Med*. 2016;4(7):135.
21. Li R, Yan G, Li Q, et al. MicroRNA-145 protects cardiomyocytes against hydrogen peroxide (H_2O_2)-induced apoptosis through targeting the mitochondria apoptotic pathway. *PLoS One*. 2012;7(9):e44907.
22. Wang K, Liu F, Zhou LY, et al. The long noncoding RNA CHRF regulates cardiac hypertrophy by targeting miR-489. *Circ Res*. 2014;114(9):1377–1388.
23. Wang K, Long B, Zhou LY, et al. CARL lncRNA inhibits anoxia-induced mitochondrial fission and apoptosis in cardiomyocytes by impairing miR-539-dependent PHB2 downregulation. *Nat Commun*. 2014;5:3596.
24. Yang J, Chen L, Ding J, et al. Cardioprotective effect of miRNA-22 on hypoxia/reoxygenation induced cardiomyocyte injury in neonatal rats. *Gene*. 2015;579(1):17–22.
25. Liu Y, Li G, Lu H, et al. Expression profiling and ontology analysis of long noncoding RNAs in post-ischemic heart and their implied roles in ischemia/reperfusion injury. *Gene*. 2014;543(1):15–21.
26. Liu Y, Zhou D, Li G, et al. Long non coding RNA-UCA1 contributes to cardiomyocyte apoptosis by suppression of p27 expression. *Cell Physiol Biochem*. 2015;35(5):1986–1998.
27. Michalik KM, You X, Manavski Y, et al. Long noncoding RNA MALAT1 regulates endothelial cell function and vessel growth. *Circ Res*. 2014;114(9):1389–1397.
28. Doulamis IP, Tzani AI, Konstantopoulos PS, et al. A sirtuin 1/MMP2 prognostic index for myocardial infarction in patients with advanced coronary artery disease. *Int J Cardiol*. 2017;230:447–453.
29. Rayner BS, Duong TTH, Myers SJ, Witting PK. Protective effect of a synthetic anti-oxidant on neuronal cell apoptosis resulting from experimental hypoxia re-oxygenation injury. *J Neurochem*. 2006;97(1):211–221.
30. Hartel FV, Holl MM, Aslam M, et al. Transient hypoxia induces ERK-dependent anti-apoptotic cell survival in endothelial cells. *Am J Physiol Cell Physiol*. 2010;298(6):1501–1509.
31. Bhogal RH, Weston CJ, Curbishley SM, Bhatt AN, Adams DH, Afford SC. Variable responses of small and large human hepatocytes to hypoxia and hypoxia/reoxygenation (H–R). *FEBS Letters*. 2011;585(6):935–941.
32. Hess ML, Barnhart GR, Crute S, Komwatana P, Krause S, Greenfield LJ. Mechanical and biochemical effects of transient myocardial ischemia. *J Surg Res*. 1979;26(2):175–184.
33. Bolli R, Marbán E. Molecular and cellular mechanisms of myocardial stunning. *Physiol Rev*. 1999;79(2):609–634.
34. Qiu MT, Hu JW, Yin R, Xu L. Long noncoding RNA: An emerging paradigm of cancer research. *Tumour Biol*. 2013;34(2):613–620.
35. Lorenzen JM, Thum T. Long noncoding RNAs in kidney and cardiovascular diseases. *Nat Rev Nephrol*. 2016;12(6):360–373.
36. Zhang M, Gu H, Xu W, Zhou X. Down-regulation of lncRNA MALAT1 reduces cardiomyocyte apoptosis and improves left ventricular function in diabetic rats. *Int J Cardiol*. 2016;203:214–216.
37. Wang X, Li M, Wang Z, et al. Silencing of long noncoding RNA MALAT1 by miR-101 and miR-217 inhibits proliferation, migration, and invasion of esophageal squamous cell carcinoma cells. *J Biol Chem*. 2015;290(7):3925.
38. Menghini R, Casagrande V, Cardellini M, et al. MicroRNA 217 modulates endothelial cell senescence via silent information regulator 1. *Circulation*. 2009;120(15):1524–1532.
39. Guarani V, Deflorian G, Franco CA, et al. Acetylation-dependent regulation of endothelial Notch signalling by the SIRT1 deacetylase. *Nature*. 2011;473(7346):234–238.
40. Nakahata Y, Sahar S, Astarita G, Kaluzova M, Sassone-Corsi P. Circadian control of the NAD+ salvage pathway by CLOCK-SIRT1. *Science*. 2009;324(5927):654–657.
41. Picard F, Kurtev M, Chung N, et al. Sirt1 promotes fat mobilization in white adipocytes by repressing PPAR-gamma. *Nature*. 2004;429(6993):771–776.
42. Cho SH, Chen JA. SIRT1 deficiency in microglia contributes to cognitive decline in aging and neurodegeneration via epigenetic regulation of IL-1beta. *J Neurosci*. 2015;35(2):807–818.
43. Nadtochiy SM, Yao H, McBurney MW, et al. SIRT1-mediated acute cardioprotection. *Am J Physiol Heart Circ Physiol*. 2011;301(4):H1506–1512.
44. Hsieh-Cheng Chen MS, Yung-Ming Jeng MD, PhD. SIRT1 promotes tumorigenesis and resistance to chemotherapy in hepatocellular carcinoma and its expression predicts poor prognosis. *Ann Surg Oncol*. 2012;19(6):2011–2019.
45. Yang J, Wang N, Zhu Y, Feng P. Roles of SIRT1 in high glucose-induced endothelial impairment: Association with diabetic atherosclerosis. *Arch Med Res*. 2011;42(5):354–360.
46. Li W, Du D, Wang H, et al. Silent information regulator 1 (SIRT1) promotes the migration and proliferation of endothelial progenitor cells through the PI3K/Akt/eNOS signaling pathway. *Int J Clin Exp Pathol*. 2015;8(3):2274–2287.

The importance of hypoalbuminemia in peritoneal dialysis patients: Impact of gender

Dorota Sikorska[1,A–F], Anna Olewicz-Gawlik[2,A–F], Ewa Baum[3,A–F], Krzysztof Pawlaczyk[4,A–F], Andrzej Oko[4,A–F]

[1] Department of Rheumatology and Rehabilitation, Poznan University of Medical Sciences, Poland
[2] Department of Infectious Diseases, Hepatology and Acquired Immune Deficiencies, Poznan University of Medical Sciences, Poland
[3] Department of Philosophy and Bioethics, Poznan University of Medical Sciences, Poland
[4] Department of Nephrology, Transplantology and Internal Diseases, Poznan University of Medical Sciences, Poland

A – research concept and design; B – collection and/or assembly of data; C – data analysis and interpretation;
D – writing the article; E – critical revision of the article; F – final approval of the article

Advances in Clinical and Experimental Medicine, ISSN 1899–5276 (print), ISSN 2451–2680 (online) *Adv Clin Exp Med*. 2019;28(6):729–735

Address for correspondence
Dorota Sikorska
E-mail: dorotasikorska@ump.edu.pl

Funding sources
None declared

Conflict of interest
None declared

Acknowledgements
We would like to thank Janusz Witowski for his comments, which greatly improved the manuscript.

Received on May 31, 2017
Reviewed on October 12, 2017
Accepted on November 2, 2017

Published online on August 14, 2018

Abstract

Background. High mortality in peritoneal dialysis (PD) patients is associated with the presence of non-traditional cardiovascular risk factors, such as malnutrition. However, hypoalbuminemia in patients undergoing PD may have gender-dependent consequences.

Objectives. The aim of the study was to evaluate the relationship between hypoalbuminemia, overhydration (OH), inflammation, and cardiovascular risk, depending on gender.

Material and methods. The group studied consisted of 54 PD patients: 26 male (mean age: 59 ±19 years) and 28 female (mean age: 52 ±15 years). Serum albumin levels were measured routinely by the hospital central laboratory. The degree of OH was assessed by bioelectrical impedance analysis (BIA). Serum concentrations of C-reactive protein (CRP) and interleukin (IL)-6 were measured as inflammatory markers. Levels of N-terminal prohormone of brain natriuretic peptide (NT-proBNP) and troponin T (TnT) were used to assess cardiovascular risk.

Results. Median serum albumin concentration was 3.9 g/dL (3.6–4.2 g/dL). Both genders were comparable regarding most parameters except body weight (79 ±16 kg vs 67 ±16 kg; $p = 0.009$), but no differences were observed in body mass index (BMI) (26.3 ±5.0 kg/m^2 vs 26.2 ±5.9 kg/m^2; non significant (NS)). There was also no difference in the prevalence of hypoalbuminemia between female and male PD patients (23% vs 21%; NS). In females, low serum albumin concentrations were associated with OH, inflammation and cardiovascular risk, while in males serum albumin levels correlated with the parameters of dialysis and cardiovascular risk.

Conclusions. The impact of hypoalbuminemia may be gender-dependent. It seems that hypoalbuminemia is more important for female patients. It is also possible that different mechanisms regulate serum albumin concentration in female and male PD patients.

Key words: inflammation, cardiovascular risk, peritoneal dialysis, overhydration, hypoalbuminemia

Cite as
Sikorska D, Olewicz-Gawlik A, Baum E, Pawlaczyk K, Oko A. The importance of hypoalbuminemia in peritoneal dialysis patients: Impact of gender. *Adv Clin Exp Med*. 2019;28(6):729–735. doi:10.17219/acem/79653

DOI
10.17219/acem/79653

Introduction

High mortality in peritoneal dialysis (PD) patients is associated with the presence of non-traditional cardiovascular risk factors, such as malnutrition, chronic inflammation and fluid overload.[1,2] It appears that malnutrition plays a key role in the development of complications in PD patients.[3] Hypoalbuminemia in PD patients may result from the combined effects of high protein loss, malnutrition, inflammation, overhydration (OH), and comorbidity.[2]

It appears that hypoalbuminemia is an important determinant of the hydration status in PD patients.[4] Large cross-sectional studies have revealed that malnutrition is common in PD patients and is associated with OH.[5] Protein-energy wasting associated with OH predicts both all-cause and cardiovascular mortality in PD patients.[6]

Many authors suggest an association between the nutritional status and inflammation, which may have an impact on the development of many complications. The coexistence of protein-calorie malnutrition, chronic non-specific inflammation and accelerated development of atherosclerosis is known as the malnutrition-inflammation-atherosclerosis (MIA) syndrome.[7]

Moreover, it seems that in PD patients malnutrition occurs even more often, because body mass index (BMI) is not a reliable indicator of malnutrition in that group of patients.[8] In PD patients, muscle may account for a smaller percentage of body weight because of wasting or edema. Peritoneal dialysis patients often have normal (or even elevated) BMI and, at the same time, hypoalbuminemia, with all its complications.[6] The poor diagnostic performance of BMI may potentially explain the paradoxical association between higher BMI and lower mortality in that group of patients.[6]

There are apparent anthropometric and physiological differences between male and female patients. On the other hand, there is not a lot of data regarding the effect of gender on nutritional parameters in PD patients.[9]

The main aim of the study was to evaluate the relationship between hypoalbuminemia, OH, inflammation, and cardiovascular risk, depending on gender. This study also investigated the frequency of malnutrition in PD patients.

Material and methods

Patients

In this cross-sectional study, patients were recruited consecutively from 3 regional dialysis centers between 2011 and 2014. The studied group consisted of 54 patients undergoing PD. Inclusion criteria for the study were: 1. age >18 years; 2. time on PD ≥3 months; and 3. informed consent for participation in the study. Exclusion criteria were: 1. the presence of acute inflammatory disease within 3 months prior to enrolment; 2. after amputation; or 3. the presence of a cardioverter-defibrillator or pacemaker. Only 1 patient was excluded from the study because of amputation. No patients were excluded from the analysis. The patients were fully informed and each of them provided a written consent for participation in the study. The study was approved by the Poznan University of Medical Sciences Bioethics Committee (decisions No. 85/09 and 424/13) and was conducted in accordance with the Declaration of Helsinki.

Nutritional status

Serum albumin levels were measured routinely by the hospital central laboratory, with the reference value >3.5 g/dL. To assess the nutritional status in more detail, the following parameters and techniques were also used: weight and BMI, subjective global assessment (SGA) questionnaire, and fat and lean tissue mass (LTM) in bioelectric impedance analysis (BIA), using Body Composition Monitor (BCM) (Fresenius Medical Care, Bad Homburg vor der Höhe, Germany).[10,11]

Inflammatory markers

Serum C-reactive protein (CRP) was measured routinely by the hospital central laboratory. Serum concentrations of interleukin (IL)-6 were measured using the Quantikine High-Sensitivity IL-6 Immunoassay (R&D Systems, Minneapolis, USA). The immunoassays were performed according to the manufacturer's instructions. The sensitivity of the assays were 0.1 pg/mL and 33 pg/mL, respectively.

Hydration status

The hydration status was assessed by clinical symptoms and BIA, using BCM. The study used whole-body BIA. The measurements were performed under the standardized conditions recommended by the manufacturer, in the supine position after 2 min of rest. Reference values for the bioelectrical impedance measurements considered the hydration status to be from –1.1 L to 1.1 L.[12] Clinical assessment of OH was based on the presence of peripheral edema, dyspnea, jugular vein distension, and blood pressure measurements.

Cardiovascular risk

The N-terminal prohormone of brain natriuretic peptide (NT-proBNP) and troponin T (TnT) were used as biomarkers for cardiovascular diseases.

Assessment of peritoneal membrane function and laboratory measurements

Peritoneal membrane function was measured with the peritoneal equilibration test (PET) during a 4-hour dwell,

using 2.27% glucose dialysate.[13] All laboratory tests were made by standard methods, using automated biochemical analyzers in the hospital central laboratory.

Statistical analysis

The analyzed data is presented as medians and interquartile ranges (IQRs) or percentage, as appropriate. Comparisons between the groups were tested for significance using the Mann-Whitney U test. Categorical data was analyzed with the χ^2 test or the Fisher-Freeman-Halton test. The relationship between variables was analyzed with Spearman's rank correlation coefficient. All results were considered significant at $p < 0.05$. Statistical analyses were performed with STATISTICA v. 10.0 PL (StatSoft Polska, Kraków, Poland).

Results

Patient characteristics according to serum albumin levels

Serum albumin concentration in the group of 54 patients ranged from 2.6 g/dL to 4.9 g/dL. Median serum albumin concentration was 3.9 g/dL (3.6–4.2 g/dL). Patients were divided into 2 subgroups, depending on median serum albumin levels:

Table 1. Patients' characteristics according to serum albumin

Parameters	Albumin <3.9 g/dL (n = 29)	Albumin ≥3.9 g/dL (n = 25)	Mann-Whitney or χ^2 p-value
Demographic and PD-related parameters			
Men, n [%]	14 (48)	12 (48)	NS
Age [years]	60 (51–70)	51 (34–66)	NS
Diabetic nephropathy, n [%]	12 (41)	2 (8)	0.005
DM, n [%]	14 (48)	5 (20)	0.030
Time on PD [months]	28 (17–56)	28 (17–38)	NS
APD mode, n [%]	7 (24)	8 (32)	NS
Ultrafiltration [mL/day]	1,400 (600–2,000)	1,000 (900–1,200)	NS
Residual diuresis [mL/day]	1,500 (500–2,200)	1,600 (1,300–2,400)	NS
4-hour D/P creatinine in PET	0.68 (0.59–0.77)	0.61 (0.54–0.67)	0.034
Parameters of nutritional status			
Weight [kg]	71 (63–81)	71 (63–82)	NS
BMI [kg/m^2]	25.2 (22.3–30.3)	25.9 (21.1–28.6)	NS
Lean tissue [%] in BIA	45 (36–60)	49 (44–56)	NS
Fat tissue [%] in BIA	36 (27–45)	36 (30–40)	NS
Lean tissue [kg] in BIA	31 (27–42)	34 (28–41)	NS
Fat tissue [kg] in BIA	27 (18–34)	25 (19–34)	NS
SGA	9.0 (8.0–9.0)	8.0 (7.0–9.0)	0.026
Inflammatory markers			
CRP [mg/L]	5.9 (2.6–9.7)	2.1 (1.1–5.7)	0.038
hs IL-6 [pg/mL]	1.2 (0.8–1.8)	1.0 (0.5–1.3)	0.046
Hydration status in BIA and clinical examination			
Hydration status [L]	2.0 (0.7–2.7)	0.6 (0.2–1.0)	0.003
Hydration status/weight [%]	2.6 (1.1–3.9)	0.9 (0.2–1.3)	0.002
Patients with edema, n [%]	9 (31)	1 (4)	0.011
Cardiovascular parameters			
SBP [mm Hg]	140 (130–150)	130 (120–130)	0.001
DBP [mm Hg]	80 (70–94)	80 (70–80)	NS
TnT [pg/mL]	54 (26–109)	28 (16–37)	0.005
NT-proBNP [pg/mL]	3,024 (1,172–9,404)	1,240 (619–3,201)	0.020

Data presented as median (interquartile range (IQR)) or as n [%]. NS – non significant; PD – peritoneal dialysis; DM – diabetes mellitus; APD – automated peritoneal dialysis; D/P – dialysate and plasma ratio; PET – peritoneal equilibration test; BMI – body mass index; BIA – bioimpedance analysis; SGA – subjective global assessment; CRP – C-reactive protein; hs IL-6 – high-sensitivity interleukin-6; SBP – systolic blood pressure; DBP – diastolic blood pressure; TnT- troponin T; NT-proBNP – N-terminal prohormone of brain natriuretic peptide.

– group A: albumin <3.9 g/dL (n = 29);
– group B: albumin ≥3.9 g/dL (n = 25).

Patient characteristics according to serum albumin are shown in Table 1. There were no differences in body weight, BMI or body composition in BIA between the subgroups. In contrast, there were significant differences in the SGA.

The data showed significantly higher levels of serum IL-6 and a tendency for higher levels of CRP in patients with lower serum albumin. As expected, serum albumin correlated negatively with IL-6 levels (r = –0.35; p = 0.009).

Clinical signs of OH were found in 18% (10/54) of all patients, and OH as measured by BIA was found in 41% (22/54) of patients. There was a significant difference in the distribution of those patients (Table 1). In the group with higher albumin level, only 20% (5/25) of patients were overhydrated (as measured by BIA), while OH occurred in 62% (18/29) of patients in the group with lower albumin level. Indeed, there was an inverse correlation between the hydration status and serum albumin (r = –0.55; p < 0.001).

There was also a tendency to higher blood pressure and increased serum concentrations of TnT and NT-proBNP in patients with hypoalbuminemia.

Patient characteristics according to gender

The study group consisted of 26 (48%) male and 28 (52%) female patients. Both gender subgroups were comparable regarding most of the investigated parameters. Differences between genders occurred only in body weight in kg, but there was no differences in BMI and LTM in BIA.

Albumin in male patients

Serum albumin concentration ranged from 2.6 g/dL to 4.9 g/dL. Median serum albumin concentration was 3.9 (3.6–4.1). Six out of 26 (23%) investigated males had hypoalbuminemia. In male patients, serum albumin levels correlated with PD parameters: diuresis (r = 0.59; p = 0.001), ultrafiltration (r = –0.33; p = 0.098), peritoneal

Table 2. Male (n = 26) patients' characteristics according to serum albumin

Parameters	Albumin <3.9 g/dL (n = 14)	Albumin ≥3.9 g/dL (n = 12)	Mann-Whitney or χ^2 p-value
Demographic and PD-related parameters			
Age [years]	64 (52–70)	63 (51–70)	NS
Diabetic nephropathy, n [%]	6 (43)	1 (8)	0.048
DM, n [%]	7 (50)	3 (25)	NS
Time on PD [months]	48 (19–66)	26 (14–35)	NS
Ultrafiltration [mL/day]	1,450 (900–1,800)	950 (550–1,200)	0.047
Residual diuresis [mL/day]	1,400 (200–2,000)	2,350 (1,600–2,800)	0.022
4-hour D/P creatinine in PET	0.69 (0.61–0.75)	0.61 (0.53–0.65)	NS
Parameters of nutritional status			
Weight [kg]	72.8 (65.0–85.0)	78.4 (65.0–85.0)	NS
BMI [kg/m^2]	24.7 (21.4–29.1)	26.6 (22.3–28.7)	NS
Lean tissue [%] in BIA	48.7 (36.1–64.5)	51.5 (44.4–62.6)	NS
Fat tissue [%] in BIA	33.8 (25.7–44.0)	33.6 (26.9–38.9)	NS
Lean tissue [kg] in BIA	41.4 (28.2–44.5)	39.8 (34.8–46.4)	NS
Fat tissue [kg] in BIA	24.4 (17.2–33.0)	26.2 (18.9–34.4)	NS
SGA	9.0 (8.0–9.0)	8.5 (7.5–9.0)	NS
Inflammatory markers			
CRP [mg/L]	2.7 (2.1–8.4)	3.4 (1.0–6.7)	NS
hs IL-6 [pg/mL]	1.10 (0.80–1.70)	0.91 (0.70–1.41)	NS
Hydration status in BIA			
Hydration status [%]	1.2 (0.3–4.4)	0.8 (0.6–1.8)	NS
Hydration status/weight [%]	1.6 (0.5–5.9)	1.2 (0.8–2.3)	NS
Cardiovascular parameters			
TnT [pg/mL]	80 (33–127)	31 (22–40)	0.020
NT-proBNP [pg/mL]	2,498 (1,159–6,714)	868 (689–4,637)	NS

Data presented as median (interquartile range (IQR)) or as n [%]. NS – non significant; PD – peritoneal dialysis; DM – diabetes mellitus; D/P – dialysate and plasma ratio; PET – peritoneal equilibration test; BMI – body mass index; BIA – bioimpedance analysis; SGA – subjective global assessment; CRP – C-reactive protein; hs IL-6 – high-sensitivity interleukin-6; TnT- troponin T; NT-proBNP – N-terminal prohormone of brain natriuretic peptide.

equilibration test (PET) dialysate and plasma ratio (D/P) creatinine (r = –0.59; p = 0.002) and PD vintage (r = –0.43; p = 0.028). The study also showed a relationship between albumin levels and biomarkers for cardiovascular diseases: TnT (r = –0.60; p = 0.001) and NT-proBNP (r = –0.43; p = 0.028). The differences after the division into 2 subgroups according to the median serum level of albumin (A <3.9 g/dL; B ≥3.9 g/dL) are shown in Table 2.

Albumin in female patients

Median serum albumin concentration in female patients was 3.9 (3.6–4.2) and ranged from 2.7 g/dL to 4.6 g/dL. Six out of 28 (21%) female patients presented hypoalbuminemia. In female patients, the study showed statistically significant correlations of albumin levels with OH (r = –0.74, p < 0.001) and hs IL-6 (r = –0.45; p = 0.015). There was also a clear tendency to a significant correlation regarding albumin concentration and CRP (r = –0.45; p = 0.052). Serum albumin levels also correlated with TnT (r = –0.44; p = 0.026) and NT-proBNP (r = –0.46; p = 0.014). The differences after the division into 2 subgroups according to the median albumin level (A <3.9 g/dL; B ≥3.9 g/dL) are shown in Table 3.

Discussion

Hypoalbuminemia in patients undergoing PD is known to be an important prognostic factor of their clinical outcome.[14] In this study we investigated hypoalbuminemia and its gender differences in a group of PD patients in relation to OH, inflammation, nutritional status, and cardiovascular risk.

First, we found that the prevalence of fluid overload by BIA in PD patients was 41%. The prevalence of hypoalbuminemia was 21% in females and 23% in males. Fluid overload in PD patients was associated with low albumin levels. The finding was not a surprise, as fluid overload has been associated with hypoalbuminemia.[15] Despite the fact

Table 3. Female (n = 28) patients' characteristics according to serum albumin

Parameters	Albumin <3.9 g/dL (n = 14)	Albumin ≥3.9 g/dL (n = 14)	Mann-Whitney or χ^2 p-value
Demographic and PD-related parameters			
Age [years]	58 (34–66)	46 (33–64)	NS
Diabetic nephropathy, n [%]	6 (43)	1 (7)	NS
DM, n [%]	7 (50)	2 (14)	NS
Time on PD [months]	26 (15–46)	32 (14–43)	NS
Ultrafiltration [mL/day]	1,200 (500–2,000)	1,000 (900–1,400)	NS
Residual diuresis [mL/day]	1,300 (500–2,200)	1,450 (1,000–2,100)	NS
4-hour D/P creatinine in PET	0.68 (0.58–0.80)	0.61 (0.55–0.69)	NS
Parameters of nutritional status			
Weight [kg]	69.5 (59.7–81.5)	62.8 (54.2–72.0)	NS
BMI [kg/m^2]	28.9 (22.3–31.0)	24.7 (20.4–27.2)	NS
Lean tissue [%] in BIA	42.5 (32.5–60.4)	47.9 (39.8–50.7)	NS
Fat tissue [%] in BIA	41.0 (27.7–48.5)	38.6 (35.2–43.2)	NS
Lean tissue [kg] in BIA	28.2 (24.0–33.5)	28.0 (26.8–32.1)	NS
Fat tissue [kg] in BIA	27.7 (18.2–36.0)	24.4 (19.4–31.4)	NS
SGA	9.0 (8.0–9.0)	8.0 (7.0–8.0)	0.028
Inflammatory markers			
CRP (mg/L)	6.5 (4.0–18.1)	2.6 (1.5–4.0)	0.049
hs IL-6 [pg/mL]	1.27 (0.82–2.08)	0.67 (0.51–1.04)	0.012
Hydration status in BIA			
Hydration status [L]	1.7 (0.8–2.6)	0.4 (–0.7–0.8)	0.003
Hydration status/weight [%]	2.4 (1.4–4.0)	0.6 (0.0–1.2)	0.003
Cardiovascular parameters			
TnT [pg/mL]	34 (23–90)	26 (13–33)	0.044
NT-proBNP [pg/mL]	5,592 (1,402–21,553)	1,421 (609–3,201)	0.011

Data presented as median (interquartile range (IQR)) or as n [%]. NS – non significant; PD – peritoneal dialysis; DM – diabetes mellitus; D/P – dialysate and plasma ratio; PET – peritoneal equilibration test; BMI – body mass index; BIA – bioimpedance analysis; SGA – subjective global assessment; CRP – C-reactive protein; hs IL-6 – high-sensitivity interleukin-6; TnT- troponin T; NT-proBNP – N-terminal prohormone of brain natriuretic peptide.

that patients on PD lose about 5 g of albumin per day, many of them can compensate for this loss by increased liver albumin synthesis.[16] However, Yeun and Kaysen showed that low-grade chronic inflammation reduces this compensative ability.[17] This is in agreement with our results, which showed a significant inverse correlation between albumin levels and IL-6 concentration, which typically reflects ongoing chronic inflammation. Unexpectedly, further analysis in regard to gender of the investigated patients showed that inflammatory parameters (IL-6 and CRP) were associated with hypoalbuminemia only in females. This finding is difficult to interpret, as there is a lack of literature investigating gender differences in PD patients. One possible reason for the observed gender differences is that females have stronger behavioral and somatic responses to stress and more potent immune and inflammatory reactions than males.[18] Further, in patients with acute or chronic respiratory diseases, the the inflammatory response was reported to be higher in females than in males.[19] Moreover, in children with chronic inflammatory diseases, i.e., asthma, cystic fibrosis and sickle cell anemia, symptoms and the inflammatory status were more prominent in females.[20] The fact that hypoalbuminemia in PD patients is usually a consequence of low-grade chronic inflammation being a part of the MIA syndrome, and that the gender differences seem to be evident in chronic inflammatory diseases, may explain the association between the inflammation and hypoalbuminemia observed only in females in the presented study.[21]

All the above could also elucidate the association between OH and hypoalbuminemia observed in this study only in the female subgroup. In more detail, the results of large cross-sectional studies have revealed that BIA-determined OH is associated with loss of residual renal function, malnutrition and inflammation.[5,22] The close association between inflammation, hypoalbuminemia and OH was also confirmed by other studies, which found inflammation and hypoalbuminemia being the strongest determinants of OH.[23,24] On one hand, malnutrition and low albumin level contribute to systemic inflammation through tissue OH, while on the other hand, as a result of a kind of vicious circle, chronic inflammation leads to hypoalbuminemia, and ultimately to OH.[4,25]

Furthermore, diabetes and diabetic nephropathy may be an additional risk factor for malnutrition in PD patients. It is possible that diabetes mellitus (DM) is consistently linked with chronic low-grade inflammation driven by oxidative stress and changed protein glycation.[26]

Surprisingly, only in male patients was hypoalbuminemia positively associated with diuresis and negatively with PD parameters. It is well-known that patients with preserved residual renal function have better nutritional status, with all its beneficial consequences.[27] As mentioned above, women present more potent immune and inflammatory reactions than males, which could diminish the positive influence of residual diuresis in the presented study.[18] The negative correlation between low albumin levels and PD parameters can result from a changed rate of transperitoneal transport in favor of a faster rate, with subsequent decreased ultrafiltration, increased protein loss and malnutrition.[28] In what way gender affects this mechanism, remains to be explored. Of note, the results of Tang et al. showed that gender was an independent determinant of the edema status in PD patients.[29]

In both gender groups, patients with hypoalbuminemia had significantly elevated levels of NT-proBNP and TnT. This finding points to albumin level as a useful additional marker in the assessment of cardiovascular risk in PD patients and is concordant with the results of a previous study, which showed a connection between hypoalbuminemia and poor cardiovascular outcome.[30] Moreover, Yamamoto et al. noted an inverse correlation between brain natriuretic peptide (BNP) change and albumin, and confirmed by multivariate analysis that both factors are independent predictors of major adverse cardiac events.[31]

Conclusions

There was no difference in malnutrition prevalence between female and male PD patients. However, hypoalbuminemia in patients undergoing PD may have gender-dependent consequences. It is also possible that different factors are responsible for hypoalbuminemia in female and male PD patients. It seems that hypoalbuminemia is more important for female patients (at comparable concentrations of serum albumin). In female patients, lower values of serum albumin were associated with OH, inflammation and cardiovascular risk, while in male patients the only relationship observed was between albumin levels and the parameters of dialysis and cardiovascular risk. Probably, malnutrition and low albumin contribute to systemic inflammation through tissue OH and it is known that all these factors have an impact on cardiovascular risk.

Limitations

Our study has some limitations, including a regional center design, a small sample size and lack of stepwise multivariate analysis. Additionally, some patients had comorbid medical illnesses.

References

1. Markaki A, Gkouskou K, Ganotakis E, Margioris A, Daphnis E. A longitudinal study of nutritional and inflammatory status in patients on dialysis. *J Ren Care*. 2014;40(1):14–22. doi:10.1111/jorc.12048
2. Davies SJ, Phillips L, Griffiths AM, Russell LH, Naish PF, Russell GI. Impact of peritoneal membrane function on long-term clinical outcome in peritoneal dialysis patients. *Perit Dial Int.* 1999;19(Suppl 2): S91–94.
3. Huang R, Liu Y, Wu H, et al. Lower plasma visceral protein concentrations are independently associated with higher mortality in patients on peritoneal dialysis. *Br J Nutr.* 2015;113(4):627–633. doi:10.1017/S0007114514004061

4. John B, Tan BK, Dainty S, Spanel P, Smith D, Davies SJ. Plasma volume, albumin, and fluid status in peritoneal dialysis patients. *Clin J Am Soc Nephrol.* 2010;5(8):1463–1470. doi:10.2215/cjn.09411209
5. Van Biesen W, Williams JD, Covic AC, et al. Fluid status in peritoneal dialysis patients: The European Body Composition Monitoring (EuroBCM) study cohort. *PLoS ONE.* 2011;6(2):e17148. doi:10.1371/journal.pone.0017148
6. Agarwal R, Bills JE, Light RP. Diagnosing obesity by body mass index in chronic kidney disease: An explanation for the "obesity paradox?" *Hypertension.* 2010;56(5):893–900. doi:10.1161/HYPERTENSIONAHA.110.160747
7. Stenvinkel P, Heimburger O, Lindholm B, Kaysen GA, Bergstrom J. Are there two types of malnutrition in chronic renal failure? Evidence for relationships between malnutrition, inflammation and atherosclerosis (MIA syndrome). *Nephrol Dial Transplant.* 2000;15(7):953–960.
8. Salamon K, Woods J, Paul E, Huggins C. Peritoneal dialysis patients have higher prevalence of gastrointestinal symptoms than hemodialysis patients. *J Ren Nutr.* 2013;23(2):114–118. doi:10.1053/j.jrn.2012.02.007
9. Kaya T, Sipahi S, Karacaer C, et al. Evaluation of nutritional status with different methods in geriatric hemodialysis patients: Impact of gender. *Int Urol Nephrol.* 2014;46(12):2385–2391. doi:10.1007/s11255-014-0776-0
10. Kalantar-Zadeh K, Kleiner M, Dunne E, Lee GH, Luft FC. A modified quantitative subjective global assessment of nutrition for dialysis patients. *Nephrol Dial Transplant.* 1999;14(7):1732–1738.
11. Konings CJ, Kooman JP, Schonck M, et al. Influence of fluid status on techniques used to assess body composition in peritoneal dialysis patients. *Perit Dial Int.* 2003;23(2):184–190.
12. Wabel P, Chamney P, Moissl U, Jirka T. Importance of whole-body bioimpedance spectroscopy for the management of fluid balance. *Blood Purif.* 2009;27(1):75–80. doi:10.1159/000167013.
13. Twardowski ZJ, Nolph KD, Khanna R, Prowant BF, Ryan LP, Moore HL. Peritoneal equilibration test. *Perit Dial Bull.* 1987;7:138–147.
14. Kaysen GA. Biological basis of hypoalbuminemia in ESRD. *J Am Soc Nephrol.* 1998;9(12):2368–2376.
15. Guo Q, Yi C, Li J, Wu X, Yang X, Yu X. Prevalence and risk factors of fluid overload in Southern Chinese continuous ambulatory peritoneal dialysis patients. *PLoS ONE.* 2013;8(1):e53294. doi:10.1371/journal.pone.0053294
16. Kaysen GA, Schoenfeld PY. Albumin homeostasis in patients undergoing continuous ambulatory peritoneal dialysis. *Kidney Int.* 1984;25(1):107–114.
17. Yeun JY, Kaysen GA. Acute phase proteins and peritoneal dialysate albumin loss are the main determinants of serum albumin in peritoneal dialysis patients. *Am J Kidney Dis.* 1997;30(6):923–927.
18. Chrousos GP. Stress and sex versus immunity and inflammation. *Sci Signal.* 2010;3(143):pe36. doi:10.1126/scisignal.3143pe36
19. Gan WQ, Man SF, Postma DS, Camp P, Sin DD. Female smokers beyond the perimenopausal period are at increased risk of chronic obstructive pulmonary disease: A systematic review and meta-analysis. *Respir Res.* 2006;7:52. doi:10.1186/1465-9921-7-52
20. Casimir GJ, Mulier S, Hanssens L, et al. Chronic inflammatory diseases in children are more severe in girls. *Shock.* 2010;34(1):23–26. doi:10.1097/SHK.0b013e3181ce2c3d
21. Stenvinkel P, Heimburger O, Paultre F, et al. Strong association between malnutrition, inflammation, and atherosclerosis in chronic renal failure. *Kidney Int.* 1999;55(5):1899–1911. doi:10.1046/j.1523-1755.1999.00422.x
22. Fan S, Sayed RH, Davenport A. Extracellular volume expansion in peritoneal dialysis patients. *Int J Artif Organs.* 2012;35(5):338–345.
23. Mostovaya IM, Bots ML, van den Dorpel MA, et al. Left ventricular mass in dialysis patients, determinants and relation with outcome. Results from the COnvective TRansport STudy (CONTRAST). *PloS ONE.* 2014;9(2):e84587. doi:10.1371/journal.pone.0084587
24. Barberato SH, Bucharles SG, de Souza AM, Costantini CO, Costantini CR, Pecoits-Filho R. Association between inflammatory markers and left atrial enlargement in patients on hemodialysis. *Arq Bras Cardiol.* 2013;100(2):141–146.
25. Davies SJ. What are the consequences of volume expansion in chronic dialysis patients?: Volume expansion in peritoneal dialysis patients. *Semin Dial.* 2015;28(3):239–242. doi:10.1111/sdi.12350
26. Shelbaya S, Amer H, Seddik S, et al. Study of the role of interleukin-6 and highly sensitive C-reactive protein in diabetic nephropathy in type 1 diabetic patients. *Eur Rev Med Pharmacol Sci.* 2012;16(2):176–182.
27. Aguilera A, Codoceo R, Selgas R, et al. Anorexigen (TNF-alpha, cholecystokinin) and orexigen (neuropeptide Y) plasma levels in peritoneal dialysis (PD) patients: Their relationship with nutritional parameters. *Nephrol Dial Transplant.* 1998;13(6):1476–1483.
28. Kim YL. Update on mechanisms of ultrafiltration failure. *Perit Dial Int.* 2009;29(Suppl 2):S123–127.
29. Tang W, Xue T, Lu XH, Luo YJ, Wang T. Factors contributing to formation of edema in volume overloaded continuous ambulatory peritoneal dialysis patients. *Perit Dial Int.* 2011;31(2):160–167. doi:10.3747/pdi.2010.00055
30. Furth SL, Cole SR, Fadrowski JJ, et al. The association of anemia and hypoalbuminemia with accelerated decline in GFR among adolescents with chronic kidney disease. *Pediatr Nephrol.* 2007;22(2):265–271. doi:10.1007/s00467-006-0313-1
31. Yamamoto E, Sato Y, Sawa T, Fujiwara T, Fujiwara H, Takatsu Y. Correlation between serum concentrations of B-type natriuretic peptide and albumin in patients with chronic congestive heart failure. *Int Heart J.* 2012;53(4):234–237.

Expression profile of Galp, alarin and their receptors in rat adrenal gland

Marianna Tyczewska[1,A–F], Paulina Milecka[2,B,C,F], Marta Szyszka[1,B,C,F], Piotr Celichowski[1,B,C,F], Karol Jopek[1,B,C,F], Hanna Komarowska[3,B,C,F], Ludwik Kazimierz Malendowicz[1,E,F], Marcin Ruciński[1,A,F]

[1] Department of Histology and Embryology, Poznan University of Medical Sciences, Poland
[2] Central Laboratory of Microbiology, H. Swiecicki Clinical Hospital at the Poznan University of Medical Sciences, Poland
[3] Department of Endocrinology, Metabolism and Internal Medicine, Poznan University of Medical Sciences, Poland

A – research concept and design; B – collection and/or assembly of data; C – data analysis and interpretation; D – writing the article; E – critical revision of the article; F – final approval of the article

Advances in Clinical and Experimental Medicine, ISSN 1899–5276 (print), ISSN 2451–2680 (online) *Adv Clin Exp Med*. 2019;28(6):737–746

Address for correspondence
Marianna Tyczewska
E-mail: maritycz@ump.edu.pl

Funding sources
Grant No. 2015/17/D/NZ4/02294, National Science Centre, Poland.

Conflict of interest
None declared

Received on June 26, 2018
Reviewed on July 9, 2018
Accepted on September 10, 2018

Published online on March 6, 2019

Abstract

Background. Galanin-like peptide (Galp) and alarin (Ala) are 2 new members of the galanin peptide family. Galanin (Gal), the "parental" peptide of the entire family, is known to regulate numerous physiological processes, including energy and osmotic homeostasis, reproduction, food intake, and secretion of adrenocortical hormones. Galp and Ala are known to regulate food intake. In the rat, Galp mRNA has been found in the brain, exclusively in the hypothalamic arcuate nucleus (ARC) and median eminence, which are involved in the regulation of energy homeostasis. Alarin-like immunoreactivity is present in the locus coeruleus (LC) and the ARC of rats and mice.

Objectives. The aim of the study was to investigate the expression of *Ala*, *Galp* and their receptors in the organs of the hypothalamo–pituitary–adrenal (HPA) axis of the rat.

Material and methods. The expression of the examined genes was measured in different models of adrenal growth of the rat in vivo (postnatal ontogenesis, compensatory adrenal growth, adrenocortical regeneration, adrenocorticotropic hormone (ACTH) administration). The expression was evaluated using the Affymetrix® microarray system or quantitative polymerase chain reaction (qPCR).

Results. The expression of *Ala* gene was observed in each organ of the HPA axis (the hypothalamus, hypophysis and adrenal gland). The elevated level of expression of this gene was observed in the pituitary of 2-day rats, while very low levels of *Ala* mRNA were observed in the adrenals. *Galp* mRNA expression was observed only in the hypothalamus and the hypophysis during postnatal ontogenesis. The expression of Gal receptors was demonstrated in the hypothalamus, the hypophysis and the adrenal gland. In different compartments of the adrenal glands of adult, intact male and female rats, the expression of *Ala*, *Galp* and galanin receptor 1 (*Galr1*) genes was negligible, but the expression of galanin receptor 2 (*Galr2*), galanin receptor 3 (*Galr3*) and neurotrophic receptor tyrosine kinase 2 (*Ntrk2*) genes was noticeable.

Conclusions. The examined genes showed different expression levels within the studied HPA axis; some of them were neither expressed in the hypothalamus or the pituitary gland, nor in the adrenal gland.

Key words: galanin-like peptide, alarin, adrenal gland

Cite as
Tyczewska M, Milecka P, Szyszka M, et al. Expression profile of Galp, alarin and their receptors in rat adrenal gland. *Adv Clin Exp Med*. 2019;28(6):737–746. doi:10.17219/acem/95039

DOI
10.17219/acem/95039

Introduction

Galanin (Gal), a biologically active peptide composed of 29 amino acid residues, was discovered in 1983.[1] This peptide is widely distributed in the nervous system and gut, and acts through 3 subtypes of G protein-coupled receptors, named galanin receptor 1 (Galr1), galanin receptor 2 (Galr2) and galanin receptor 3 (Galr3).[2]

Further research allowed the identification of other proteins that make up the common 'galanin peptide family'. In 1999, Ohtaki et al. identified a new peptide – galanin-like peptide (Galp).[3] A few years later, a splice variant of *Galp* gene was isolated and named alarin (*Ala*). Galanin-like peptide, a 60-amino acid-long peptide, was first isolated and cloned from porcine hypothalamus as an endogenous ligand of the galanin type 2 receptor (Galr2).[3,4] Alarin is a 25-amino acid peptide, formed in the process of modification of GALP mRNA as a result of exclusion of exon 3, was first identified in the gangliocytes of human neuroblastic tumors.[5] Over the last 20 years, the expression of Galp and Ala mRNAs and their function have been analyzed. Both peptides are known to regulate food intake, for example centrally administered Galp inhibited feeding in mice, while intraparaventricular (ipv.) Galp injection stimulated food intake in rats.[6,7] A high expression of Galp was observed in porcine gastrointestinal tract. In rat brain, Galp mRNA has been found in cell bodies residing exclusively in the hypothalamic arcuate nucleus (ARC) and median eminence.[8–10] In this context, it should be noted that both Gal and Galp regulate a number of physiological processes, including arousal/sleep regulation, energy and osmotic homeostasis, reproduction, and food intake.[11–13]

Taking into account the role of Gal and Galp in the regulation of energy homeostasis, it should be stressed that some experimental data indicates a correlation between such peptides and the adrenal cortex function. It is known that numerous neuropeptides affect, directly or indirectly, the secretion of corticosteroids. On the other hand, steroid hormones of the adrenal gland regulate the synthesis and secretion of various orexigenic and anorexigenic peptides. For example, both corticosteroid and dexamethasone increase the expression in the hypothalamus and the secretion of orexigenic neuropeptide Y (NPY).[14] Furthermore, orexins exert a potent stimulating effect on corticosteroid secretion.[15]

Numerous studies indicate that peptides involved in the regulation of energy homeostasis also regulate the growth, differentiation and secretory function of the adrenal cortex. Regarding this, the role of Gal in the regulation of the hypothalamo–pituitary–adrenal (HPA) axis is relatively well known.[16] Gal and its receptors are expressed in the hypothalamus, the anterior pituitary and the adrenal medulla. Experimental data indicates that Gal stimulates the HPA axis acting on the secretion of corticotropin-releasing hormone (CRH) and adrenocorticotropic hormone (ACTH), and exerts a direct stimulating effect on the secretion of corticosterone by isolated adrenocortical cells. Unlike Gal, the expression of genes of other galanin peptide family members within the HPA axis and the role of the proteins encoded by them in the regulation of the secretory function of the HPA axis are not known well.

Objectives

The aim of the study was to investigate the expression of Ala, Galp and their receptors Galr1, Galr2, Galr3, and neurotrophic receptor tyrosine kinase 2 (Ntrk) in the organs of the HPA axis. The studies were performed on intact rats of both sexes, during ontogenesis and in altered adrenal cortex function caused by ACTH administration, unilateral adrenalectomy and enucleation of the gland.

Material and methods

Animals and reagents

Male and female Wistar rats from the Laboratory Animal Breeding Center, Department of Toxicology, Poznan University of Medical Sciences, Poland, were used. The number of rats, their sex, age and body mass are given in the descriptions of the individual experiments or the descriptions of relevant figures. The study protocol was approved by the Local Ethics Committee for Animal Studies (No. LKE-11/2015 and LKE-24/2015). Animals were maintained under standardized conditions of light (12:12 h light-dark cycle, illumination onset at 6.00 a.m.), with the airflow exchange 8–10 times/h, at 55–60% air humidity and the temperature of 22 ±1°C, with free access to standard pellets and tap water.[17] Unless otherwise stated, all reagents were obtained from Sigma-Aldrich (St. Louis, USA) or from Avantor Performance Materials Poland S.A. (Gliwice, Poland). Animals were decapitated between 9.00 a.m. and 10.00 a.m.

Experiments

Expression analysis of Ala, Galp and their receptors in the hypothalamo–pituitary–adrenal axis during postnatal ontogenesis

Organs were harvested from intact male rats 2, 21, 60, 120, and 360 days after birth (postnatal ontogenesis). The animals were decapitated and the tissues quickly removed. Fragments of the hypothalamus were collected as described by Rucinski et al.[18] The neural lobe was removed from the pituitary gland using a stereoscopic microscope (ZEISS, Oberkochen, Germany), while the adrenals were cleaned of adherent fat and samples were taken from the entire gland. All samples were immersed in RNAlater® (Thermo Fisher Scientific, Inc., Waltham, USA) and

frozen at –80°C for quantitative polymerase chain reaction (qPCR) analysis. Each age group consisted of 5 animals.

Expression analysis of Ala, Galp and their receptors in different compartments of the adrenal glands of adult, intact male and female rats

The study was performed on tissues used in previous research.[19] Intact adult female and male Wistar rats (12 weeks old; body weight: 120–150 g) were used. The females were used in the estrus cycle phase, which was determined on the basis of the cell types observed in the vaginal smear. The animals (females: n = 6, males: n = 6) were decapitated, and the adrenals were removed, freed of adherent fat and divided into 3 zones: zona glomerulosa (ZG), zona fasciculata/reticularis (ZF/R) and medulla (M). After that, the samples were sunk in RNAlater and frozen at –80°C for microarray and qPCR analysis. Identification of adrenal compartments was anatomy-based and conducted under a stereomicroscope.

Expression analysis of Ala, Galp and their receptors in the hypothalamo–pituitary–adrenal axis of rats administered adrenocorticotropic hormone

The experiment was performed on 10 adult (3–4 months old; body weight: 250–300 g) male rats. Adrenocorticotropic hormone (Cortrosyn®; Organon Pharmaceuticals, West Orange, USA) was administered by intraperitoneal (ip.) injection at a dose of 2.5 μg/100 g. Control rats were administered 0.2 mL of physiological saline (0.9% NaCl). Each group consisted of 5 animals. The rats were decapitated 1 h after injection. The hypothalami, as well as the pituitary and adrenal glands were collected as described above, preserved in RNAlater and stored at –80°C for qPCR analysis. The dose of ACTH was selected according to previous studies.[20]

Enucleation-induced adrenocortical regeneration

Female Wistar rats (18 animals; final body weight: 100–150 g) were used.[21] In the rats, under standard ketamine (100 mg/kg, ip.) and xylazine (10 mg/kg, ip.) anesthesia, via the dorsal approach, both adrenal glands were enucleated according to the classic method.[21] The operated rats were given 0.9% NaCl to drink for 3 days. One, 2, 3, 5, 8, or 15 days after the surgery, the rats were sacrificed (3 per group), and their regenerating adrenals were immediately removed, freed of adherent fat, sunk in RNAlater, and stored at –80°C for microarray and qPCR analysis. The adrenals from sham-operated rats (removed on day 1 after the surgery) were used as control glands.[21]

Compensatory adrenal growth

The experiment was described earlier.[17] In brief, under standard ketamine (100 mg/kg, ip.) and xylazine (10 mg/kg, ip.) anesthesia, left adrenal glands were removed from the dorsal incision at the last rib height of the rat (left hemiadrenalectomy). The decapitation of the animals was performed 24 and 72 h after the procedure (experimental group). The animals from the sham-operated group were decapitated 24 h after the sham surgery. The adrenals were removed, the samples were sunk in RNAlater and frozen at –80°C for microarray and qPCR analysis. In each group there were 10 rats. The surgical procedures as well as the completion of the experiment were carried out between 10 a.m. and 11 a.m.

Microarray analysis

The entire analysis procedure was described in previous publications.[19,21] Microarray analysis was used in the experiments regarding the compartments of the adrenal glands of adult, intact male and female rats, the enucleation-induced adrenocortical regeneration and the compensatory growth of the adrenal gland. From the adrenal glands, total RNA was isolated using the Tri-Reagent method and purified on columns (RNeasy® Mini Kit; Qiagen, Hilden, Germany). The RNA quantity and quality were analyzed with gel electrophoresis and spectrophotometry (NanoDrop® ND-1000; Thermo Fisher Scientific, Inc.). Microarray analyses were performed using Affymetrix® Rat Gene 1.1 ST Array Strip (Thermo Fisher Scientific, Inc.).[21] The obtained CEL files were imported into downstream data analysis software (Bioconductor package of R language (https://www.bioconductor.org/). Every CEL file was merged with a description file. To correct for background, to normalize and summarize the results, the authors used the Robust Multi-array Averaging (RMA) method. Statistical significance of the expression levels of the analyzed genes was examined using moderated t-statistics from the empirical Bayes method. The obtained p-values were corrected for multiple comparisons using the Benjamini and Hochberg's false discovery rate (FDR) (a statistical method incorporated into Bioconductor calculations).[22]

Ribonucleic acid isolation

From the obtained tissues (hypothalami, pituitary glands, adrenals) total RNA was extracted using NucleoSpin® RNA mini spin columns (MACHEREY-NAGEL GmbH & Co. KG, Düren, Germany). The RNA isolation procedure was performed as previously described.[19] To each sample 150 μL of chloroform was added and the samples were centrifuged for 10 min at 12,000 × g at 4°C. The supernatant was collected and 350 μL of 70% ethanol was added to each sample. The mixture was transferred to pure mini-columns and centrifuged for 1 min at 11,000 × g. The next 3 steps included the addition of a rinsing buffer at appropriate concentrations. After each addition, the samples were centrifuged again under the abovementioned conditions (30 s – the first 2 steps or 2 min – the 3rd step). At the final stage of the procedure, the mini-columns

were placed in clean tubes and to each tube 30 µL of water was added. The amount of total RNA was determined by optical density at 260 nm and its purity was estimated by 260/280 nm absorption ratio (>1.8) (NanoDrop spectrophotometer). The samples were stored at –80°C for further qPCR analysis.

Reverse transcription polymerase chain reaction

Reverse transcription was performed using Transcriptor High Fidelity cDNA Synthesis Kit (Roche, Basel, Switzerland) at the temperature of 42°C for 60 min (Thermocycler UNO II; Biometra (Göttingen, Germany). The primers were designed by Primer 3 software (Whitehead Institute for Biomedical Research, Cambridge, USA) and purchased from the Laboratory of DNA Sequencing and Oligonucleotide Synthesis, Institute of Biochemistry and Biophysics, Polish Academy of Sciences, Warszawa, Poland (Table 1). Only Ala primer sequences were taken from the publication of Santic et al.[23]

Quantitative polymerase chain reaction

The expression levels of the studied genes (Table 1) were measured by means of real-time qPCR using the LightCycler® 2.0 instrument with 4.05 software version (Roche). Using the primers presented in Table 1, the SYBR® Green detection system was applied according to the specific protocol, except for Ala. Each 20 µL of the reaction mixture contained 4 µL template cDNA (standard or control), 0.5 µM of each gene-specific primer and a previously determined optimum $MgCl_2$ concentration (3.5 µM for 1 reaction). The LightCycler® FastStart DNA Master SYBR Green I mix (Roche) was used. The real-time qPCR program included a 10-minute initial denaturation step to activate Taq DNA Polymerase (95°C), followed by a 3-step amplification program – denaturation at 95°C for 10 s, annealing at 58°C or 60°C for 5 s, and extension at 72°C for 10 s. Only the qPCR analyses to detect Ala mRNA expression levels were performed using the data from Santic et al.[23] The alarin real-time qPCR program was as follows: A 10-minute initial denaturation step to activate Taq DNA Polymerase (95°C), followed by a 2-step amplification program – denaturation at 95°C for 5 s and annealing at 60°C for 20 s. The specificity of the reaction products was checked by the determination of melting points (transition rate: 0.1°C/s).

Statistics

Microarray data was statistically evaluated with a moderated t-statistics test with Benjamini and Hochberg's FDR correction.[24] The qPCR results were presented as means ± standard error of the mean (SEM). For multiple comparisons, statistical analysis of the data was performed using one-way analysis of variance (ANOVA) followed by Tukey's post-hoc test. The calculations were performed using R × 64 software v. 3.4.1 with the multicomp library. Following one-way ANOVA, if $p < 0.05$ was obtained, Tukey's post-hoc test was performed and differences were considered to be statistically significant at $p < 0.05$. The results of Tukey's post-hoc test are marked by letters (a, b, c). Groups sharing the same letter are not significantly different from each other according to Tukey's post-hoc test.

Table 1. Conventional reverse transcription polymerase chain reaction (RT-PCR) and quantitative polymerase chain reaction (qPCR) analyses of galanin-like peptide (Galp), alarin (Ala), galanin receptor 1 (Galr1), galanin receptor 2 (Galr2), galanin receptor 3 (Galr3), and neurotrophic receptor tyrosine kinase 2 (Ntrk2; also known as TrkB). Oligonucleotide sequences for sense (S) and antisense (A) primers are shown. Hypoxanthine phosphoribosyltransferase (Hprt) was the reference gene

cDNA	Genbank accession number	Primer	Primer sequence (5'-3')	Position	PCR product size [bp]
Galp	NM_022633.1	S A	TGCTCACAGGGGACGAGGA CCGGAACATTCTTGTCCAC	200–218 429–447	248
Ala	NM_022633.1	S A	ACAGGTCCTCCACCTTTCC CATTGACCTTTTGGTCATCCTTGG	205–233 314–337	133
Galr1	NM_012958.3	S A	TTCATCGGGACAGCAACCA GCCAAATACCACAACGACCA	755–774 974–994	239
Galr2	NM_019172.5	S A	CATCCTGTGCTGCGTGCC CTAGCCCCCAGATGAGCCC	251–269 468–487	236
Galr3	NM_019173.1	S A	AGGACTGAGGAAGATGGCTGA ATTGCCCACCATGCCCAAC	13–34 112–131	118
Ntrk2	NM_012731.2	S A	TCGGATGACAGTGGGAAACAA TGAAGTGCTGGCTTGGGGT	1430–1451 1592–1608	179
Hprt	NM_012583	S A	CAGTCAACGGGGGACATAAAAG ATTTTGGGGCTGTACTGCTTGA	391–412 515–536	146

Results

Expression analysis of Ala, Galp and their receptors in the hypothalamo–pituitary–adrenal axis during postnatal ontogenesis

The studies were carried out on male rats at the age of 2–360 days. The expression of *Ala* gene was observed in the hypothalamus, the hypophysis and the adrenal glands (Fig. 1). The level of expression of this gene increased in rats on the 120th and 360th day of life. An elevated level of expression of this gene was observed in the pituitary of 2-day rats, while very low levels of Ala mRNA were observed in the adrenals; however, they did not change during ontogenesis. On the other hand, in the course of postnatal ontogenesis, *Galp* gene expression was observed in the hypothalamus and the hypophysis, while in the adrenal glands it was negligible throughout the period under study (Fig. 1). In the hypothalamus, this expression increased temporarily in rats on the 120th day of life, and in the pituitary – on the 2nd day after birth.

The expression of *Galr1* gene was observed in the hypothalamus and the adrenal glands of a growing rat, but it was negligible in the hypophysis (Fig. 2). In the course of ontogenesis, the level of expression of this gene did not change in the hypothalamus, but increased in the adrenals of the oldest rats studied. The presence of Galr2 mRNA was noted in the hypothalamus, the hypophysis and the adrenal glands of a growing rat (Fig. 2). During ontogenesis, the level of expression of the gene did not change in the hypothalamus and the pituitary, but increased temporarily in the adrenals of 60-day rats. The presence of Galr3 mRNA was also found in all examined organs of a growing rat (Fig. 2). During ontogenesis, the level of expression of the gene increased only at individual observation points: the hypothalamus – day 120, the hypophysis – day 360, and the adrenals – day 120. The expression of *Ntrk2* gene was demonstrated in all studied organs. In the course of postnatal ontogenesis, it did not change in the hypothalamus, but increased in the pituitary and the adrenal glands of the rat on the 21st day of life.

Expression analysis of Ala, Galp and their receptors in different compartments of the adrenal glands of adult, intact male and female rats

In these studies, the levels of expression of the studied genes were determined using the qPCR method in individual compartments (ZG, ZF/R, M) of the adrenal glands of male and female rats. In all these cases, the expression of *Ala*, *Galp* and *Galr1* genes was negligible (data not shown). The expression of *Galr2*, *Galr3* and *Ntrk2* genes was demonstrated in all adrenal compartments of rats of both sexes (Fig. 3). Their expression was similar in all adrenal zones in males. In females, *Galr2* expression was higher in ZF/R than in other compartments. The expression of *Ntrk2* gene, on the other hand, was the highest in ZG.

Expression analysis of Ala, Galp and their receptors in the hypothalamo–pituitary–adrenal axis of rats administered adrenocorticotropic hormone

Within 60 min after ACTH administration, the level of expression of the studied neuropeptide genes in the pituitary and the adrenal glands of male rats did not change (data not shown). Similarly, in the hypothalamus, the expression of *Ala* and *Galp* genes did not change, but the level of expression of *Galr1* gene decreased (Fig. 4).

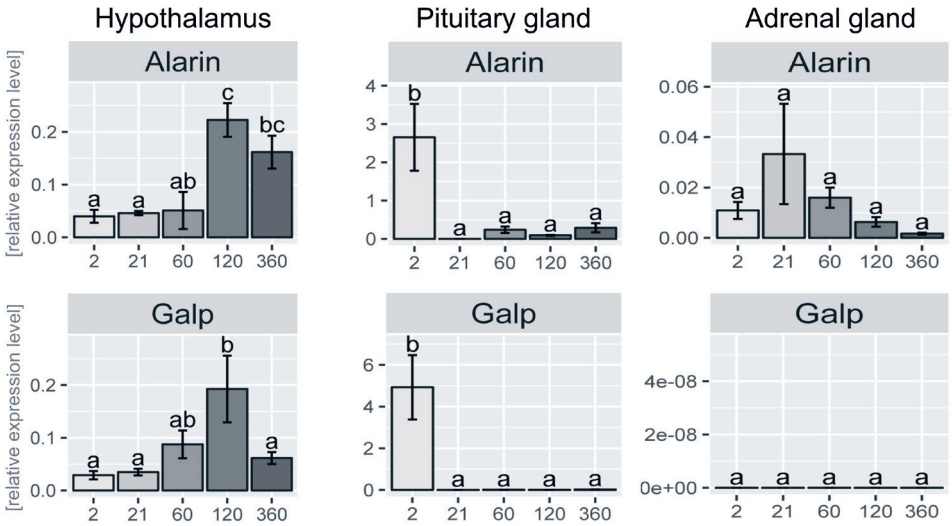

Fig. 1. Relative expression of Ala and Galp mRNAs in the hypothalamus, the pituitary and the adrenal glands of male rats during postnatal ontogenesis (days 2–360). Reverse transcription-quantitative polymerase chain reaction (RT-qPCR) was performed to determine the mRNA expression levels

Data is presented as the mean ± standard error of the mean (SEM); n = 5 per group. Statistical analysis of the data was performed using one-way analysis of variance (ANOVA) followed by Tukey's post-hoc test. Groups sharing the same letter are not significantly different, while different letters indicate groups that are significantly different from each other, with $p < 0.05$.

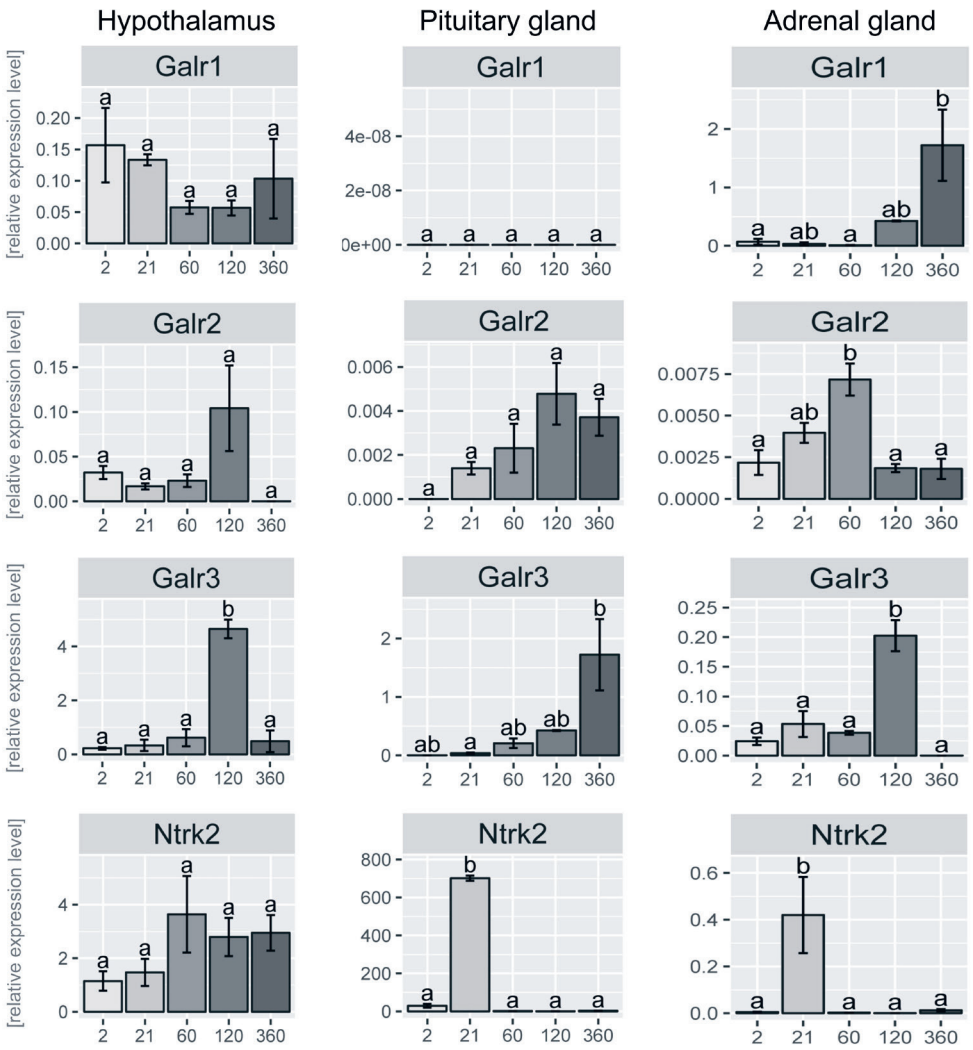

Fig. 2. Relative mRNA expression of *Galr1–3* and *Ntrk2* genes in the hypothalamus, the pituitary and the adrenal glands of male rats during postnatal ontogenesis (days 2–360). Reverse transcription-quantitative polymerase chain reaction was performed to determine the mRNA expression levels

Data and statistical analysis as in Fig. 1; n = 5 per group.

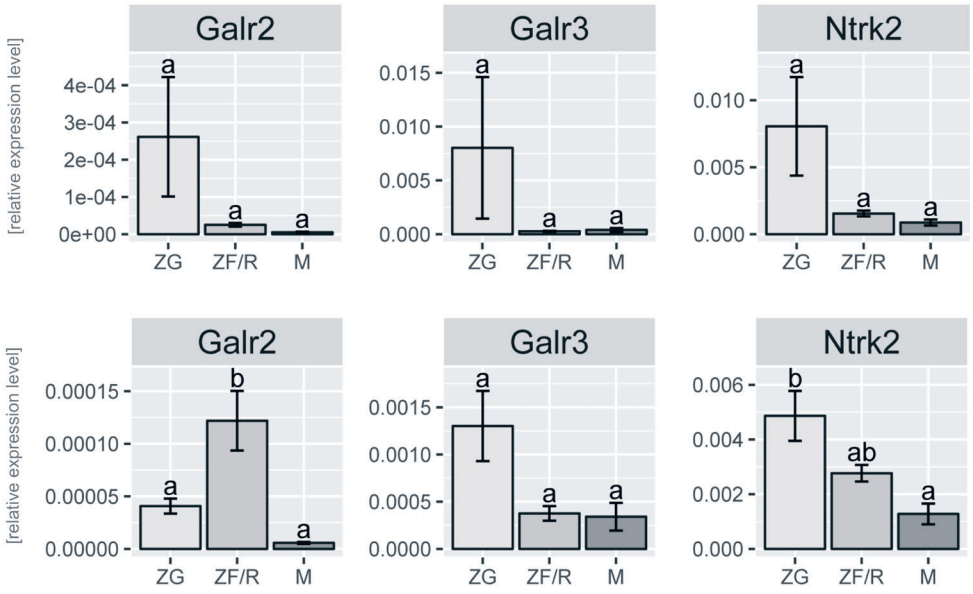

Fig. 3. Relative mRNA expression of *Galr2–3* and *Ntrk2* genes in different compartments of the adrenal glands of adult, intact male (upper row) and female rats. Reverse transcription-quantitative polymerase chain reaction was performed to determine the mRNA expression levels

Data and statistical analysis as in Fig. 1; n = 6 per group; ZG – zona glomerulosa; ZF/R – zona fasciculata/reticularis; M – medulla.

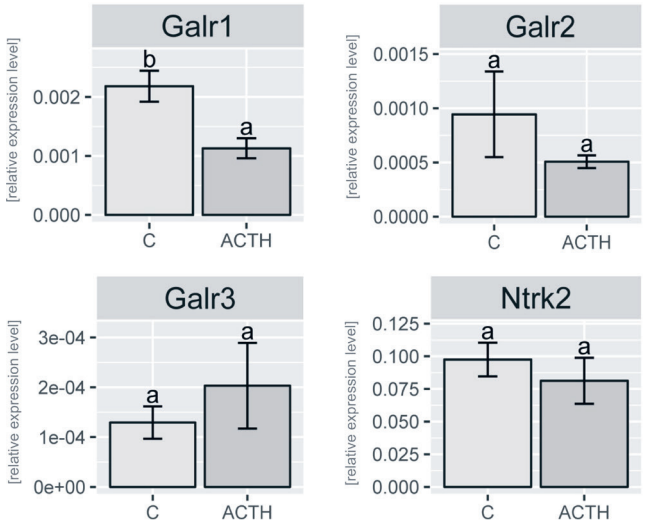

Fig. 4. Relative mRNA expression of *Galr1–3* and *Ntrk2* genes in the hypothalamus adult male rats administered adrenocorticotropic hormone (ACTH). Adrenocorticotropic hormone (Cortrosyn®) was administered by intraperitoneal (ip.) injection at a dose of 2.5 µg/100 g. Control rats were administered 0.2 mL physiological saline (0.9% NaCl). Rats were decapitated 1 h after injection. Reverse transcription-quantitative polymerase chain reaction was performed to determine the mRNA expression levels

Data and statistical analysis as in Fig. 1; n = 5 per group.

Enucleation-induced adrenocortical regeneration

Enucleation-induced adrenal regeneration is one of the types of in vivo gland growth. The data obtained from the microarray analysis suggested the expression of Galp, Galr1–3 receptors and Ntrk2 receptor genes in the regenerating adrenals of the rat. This data was validated using the qPCR method and showed only a minimal expression of *Galp*, *Ala*, *Galr1*, and *Galr3* genes. In the regenerating adrenal glands, the expression of *Galr2* gene, which even at the last point of the study (15 days) was much lower than in the control (Fig. 5), decreased significantly. The levels of *Ntrk2* mRNA did not change throughout the observed regeneration period of the adrenals.

Compensatory adrenal growth

Unilateral adrenalectomy-induced compensatory adrenal growth is another type of growth of the gland. As in the case of enucleation-induced adrenal regeneration, the data from the microarray analysis suggested the expression of both neuropeptides (Galp and Ala) and their receptors in the growing adrenals. However, the validation of the data by means of qPCR in the studied adrenals did not reveal the expression of *Ala*, *Galp* and *Galr1* genes (data not shown). Compared to the control, the expression of *Galr2*, *Galr3* and *Ntrk2* genes in the adrenal gland after hemiadrenalectomy did not change within 72 h after surgery (Fig. 6).

Discussion

Body weight regulation and energy homeostasis is controlled by a myriad of metabolic pathway intermediates and endocrine control systems. There are 2 principal mechanisms of energy homeostasis regulation, central and peripheral. Peptides involved in food intake – orexigenic, such as NPY, agouti-related peptide (AgRP), orexins (Ox), apelin (Apln), Gal, and anorexigenic, such as cocaine- and amphetamine-regulated transcript (CART), proopiomelanocortin (Pomc) and Crh, play a significant role in these regulatory processes. It is well known that glucocorticoids stimulate/inhibit the secretion of numerous orexigenic and anorexigenic peptides, which in turn control the growth, structure and function of the adrenal gland.[25,26] Today, the group of neuropeptides involved in the regulation

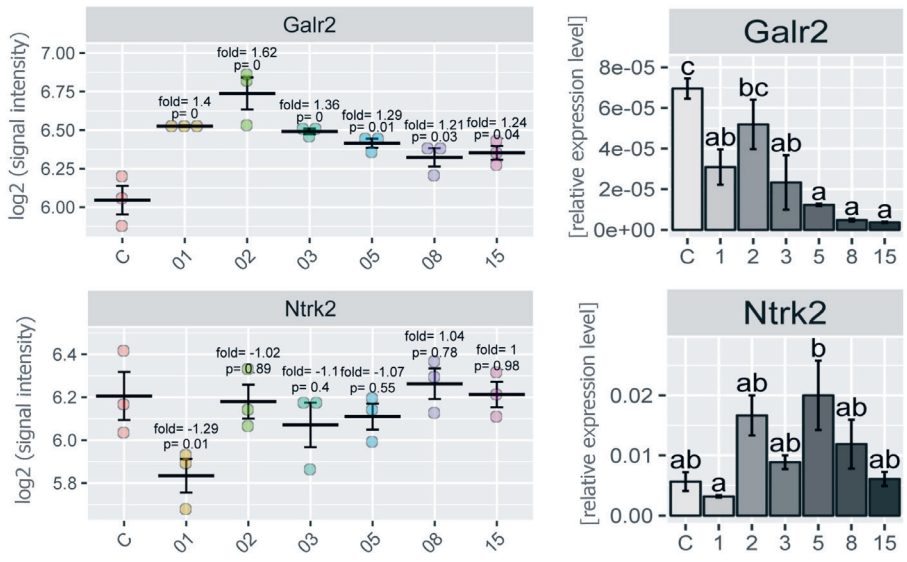

Fig. 5. Relative expression levels of adrenal *Galr2* and *Ntrk2* genes in the course of enucleation-induced adrenal regeneration. Adult female rats were sacrificed 1, 2, 3, 5, 8, and 15 days after surgery. The adrenals from sham-operated rats (day 1 after surgery) were used as control glands

Reanalyzed microarray data (graphs on the left) was obtained from an earlier study.[21] Graphs on the right (bars) present data obtained in qPCR. Each circle represents a single rat. Data and statistical analysis as in Fig. 1.

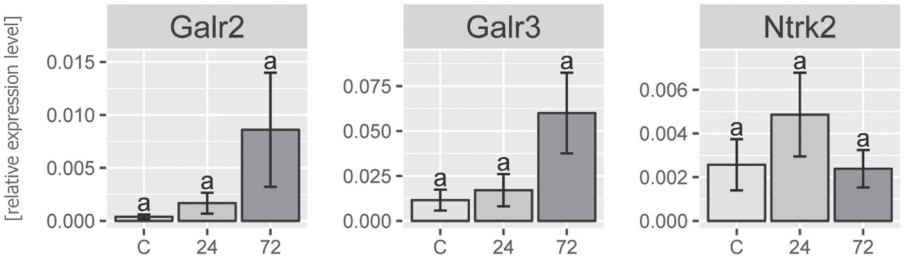

Fig. 6. Relative expression levels of adrenal *Galr2–3* and *Ntrk2* genes in the course of the compensatory adrenal growth. Adult male rats were hemiadrenalectomized and their adrenals studied after 24 and 72 h. Animals from the sham-operated group (control) were decapitated 24 h after the sham surgery. Reverse transcription-quantitative polymerase chain reaction was performed to determine the mRNA expression levels

Data and statistical analysis as in Fig. 1; n = 10 per group.

of energy homeostasis includes 2 subsequent peptides of galanin peptide family – Galp and Ala.

Galp was isolated and cloned as an endogenous ligand of Galr2, but a later study provided evidence that Galp interacted also with other Gal receptor isoforms, such as Galr1 and Galr3.[3,4] This is most probably due to the fact that the amino acids 9–21 of Galp peptide are identical to the first 13 amino acids of Gal peptide. This sequence of amino acids is able to activate Gal receptors.[3] Furthermore, studies on genetic knockouts of Galr1, Galr2 and Galr3 suggested that the effect of Galp might not be dependent on Gal receptors in the regulation of feeding.[27–29] However, no other receptors through which Galp could regulate food intake have yet been identified.

Previously, it has also been suggested that Ala exerts a biological effect through known Gal receptors. The exclusion (deletion) of exon 3 in Galp mRNA in post-translational processes, however, led to a loss of the Gal receptor binding domain of Ala, which is a key site for the binding of Galp to Gal receptors. And in fact, Ala is unable to bind to membranes expressing Gal receptors, and therefore it has been suggested that Ala acts through an unidentified receptor(s).[23,30] Regarding this, only recently, in 2017, Zhuang et al. demonstrated that Ala might act through TrkB receptor (receptor for brain-derived neurotrophic factor; known also as Ntrk2) in its antidepressant activity and cause changes in ERK and AKT signaling pathways.[31]

Galp is known to be involved in the neuroendocrine regulation of feeding, body weight and temperature. It was demonstrated earlier that intracerebroventricular (icv.) infusion of Galp stimulated food intake in rats in the first 2 h.[6,32–34] This acute effect of Galp was at first identical to the feeding response observed after icv. injection of Gal; however, 24 h after Galp administration, both food intake and body weight decreased.[6,33] These observations pointed to the possibility that Galp could have dual and opposing effects on energy homeostasis. On the other hand, the other peptide (Ala) was demonstrated to be involved in the regulation of feeding behavior in male rats. Regarding this, Boughton et al. found that acute icv. Ala administration stimulated food intake and increased circulating luteinizing hormone (LH) levels in male rats.[30]

All the above information suggests that both Galp and Ala may be involved in the regulation of energy homeostasis. In this context, immunohistochemical studies demonstrated that ca. 85% of ARC-Galp-positive neurons also expressed leptin receptors.[10] Other Galp neurons express orexin-1 receptors and melanocyte-stimulating hormone (MSH). Some Galp-positive cells are innervated by NPY- and Ox-terminals, while Ox- and MCH-neurons of the lateral hypothalamus and gonadotropin-releasing hormone (GnRH)-neurons are innervated by Galp.[35] Moreover, Ala-like immunoreactivity is present in the locus coeruleus (LC) and the ARC of rats and mice. Both regions are known to be involved in feeding behavior.

Taking into account the interrelationships between corticosteroids, orexigenic and anorexigenic neuropeptides, we analyzed the expression patterns of Galp and Ala mRNAs and their receptors in individual components of the rat's HPA axis. In further experiments, we investigated the expression patterns of these neuropeptides and their receptors during ontogenesis, after adrenal stimulation with corticotropin, in compensatory adrenal growth, and in the course of enucleation-induced adrenal regeneration.

Considering the presence and role of the galaninergic system in the HPA axis, the role of Gal itself and its receptors is relatively well known.[16] Data for Galp and Ala in this system is limited.

Immunohistochemical studies and in situ hybridization show that cells expressing Galp peptide are located almost exclusively in the hypothalamic ARC and median eminence as well as in the posterior pituitary of both rats and mice.[8–10,36] The analysis of the expression of both peptides at the RNA level, based on the qPCR method, presented by us confirms previous reports – Galp and Ala peptide mRNA is expressed both in the hypothalamus and in the pituitary glands, but not in the adrenals. It is interesting to note that in the hypothalamus, the expression of both Galp and Ala mRNA was low in the first days of postnatal ontogenesis, and then it increased statistically significantly, especially on the 120th day of the development, while the expression of both genes in the pituitary was high on the 2nd day of ontogenesis, and then it decreased significantly.

In the available literature, there are many reports concerning the expression of Gal receptors. There is a consensus that the expression of Galr1 and Galr3 mRNA occurs mainly in the central nervous system, while the expression of Galr2 is widespread throughout the body.[37] Previous data indicates that in rats, within the HPA axis,

Galr1–3 receptors are expressed in the hypothalamus and Galr1 receptors are not expressed in the pituitary gland. The expression of Galr2 and Galr3 was also described in the adrenal gland, both in the cortex and in the medulla of the gland. The expression of various isoforms of Ntrk2 was also described in the hypothalamus and in the pituitary gland, while in the adrenal glands of rats it was negligible.[38,39]

Only a few publications on the expression of Galp, Ala and their receptors during ontogenesis are available. The results of our studies indicate a very variable and diversified expression of the studied genes in the HPA system in the course of ontogenesis. Ala and Galp mRNAs were found to be present in the hypothalamus and in the hypophysis; however, in the adrenal gland only Galp mRNA was identified. Our research indicates that the level of expression of *Galp* and *Ala* genes in the hypothalamus of the rat is low in the initial periods of postnatal development and it increases on the 120th day of life. In the pituitary gland, in turn, the level of expression of both genes was high on the 2nd day of ontogenesis, after which it decreased significantly. In general, the expression of the studied receptors (Galr1–3 and Ntrk2) in the HPA axis during the rat ontogenesis is consistent with the above data. The levels of Galr1 mRNA did not change in the hypothalamus, but increased in the adrenals of the oldest animals. The expression of other receptors of the studied system did not show any significant changes in the hypothalamus, in the pituitary gland or the adrenal glands, either. In an earlier publication, Faure-Virelizier et al. observed a higher expression of *Galr1* gene in the hypothalamus of adult female rats compared to male rats.[40] We have not shown such a difference in our research.

In this study, we also analyzed the expression of the studied genes in various adrenal compartments of adult male and female rats. It is well known that adult adrenal glands of female rats differ from male adrenal glands of the same age. This difference appears after puberty and is dependent on sex hormones since testosterone exerts an inhibitory effect on the HPA axis.[17,19] The expression of *Ala*, *Galp* and *Galr1* genes was negligible in all adrenal glands of males and females. The expression of *Galr2*, *Galr3* and *Ntrk2* genes was observed in all samples studied, with the level of this expression being similar in ZG, ZF/R and M. The only exception is the expression of *Galr2* gene in adult females, which in ZF/R was higher than in ZG and M. The obtained results suggest that the expression of the studied genes of the galaninergic system in the adrenal glands of adult rats does not show any differences depending on sex.

The results obtained by us in the adrenals of the rat confirm the data obtained by Yu et al.[39] Using the RNA-seq method, the authors studied gene expression, among others, in the adrenals of the Fischer strain of rats, males and females, in 4 developmental periods: juvenile (2 weeks), adolescence (6 weeks), adult (21 weeks) and aged (104 weeks). In the adrenals of these rats, the authors did not show the expression of *Galp* gene. A very low expression of *Galr1* gene was observed only in adolescent rats. The expression of *Galr2*, *Galr3* and *Ntrk2* genes took place at all stages of ontogenetic development, with the level of this expression not changing during ontogenesis. In addition, Yu et al. did not observed any sex differences in the expression of these genes in the adrenals.[39]

The next step of the study was to investigate the effect of acute administration of ACTH on the expression of the studied genes in the HPA axis of the rat. Within 60 min after a single administration of ACTH, no statistically significant changes in the level of expression of the examined genes were observed in the analyzed system (the HPA axis). The only exception was the expression of *Galr1* gene in the hypothalamus, which decreased significantly. This may suggest that the galaninergic system of the HPA axis in the rat can be regulated by ACTH via Galr1.

In the present research we also examined the expression of *Galp* and *Ala* genes and their receptors in the enucleation-induced regeneration of the adrenal gland of the rat and in the compensatory adrenal growth induced by hemiadrenalectomy. These tests were based on microarrays, the results of which were validated by means of qPCR. It is well known that data obtained from microarray analyses usually indicates a larger number of differentially expressed genes; therefore, the data from qPCR seems to be more reliable. With qPCR we showed only an insignificant expression of *Galp*, *Galr1–3* receptors and *Ntrk2* receptor genes in the regenerating adrenal glands of the rat. During gland regeneration, however, the expression of *Galr2* gene decreased significantly, while the expression of *Ntrk2* did not change. The expression of the studied genes did not change also in the case of the compensatory adrenal growth. The obtained results suggest that Galp, Ala and their receptors do not play a significant role in the adrenal growth caused by ACTH elevation (i.e., in enucleation-induced regeneration) or hemiadrenalectomy (neurally depending growth).

To summarize, we conducted systematic studies on the expression of *Galp*, *Ala*, *Galr1–3,* and *Ntrk2* genes in the HPA axis of rats, with particular emphasis on the adrenal glands. These genes show different expression within the studied axis, some of them are not expressed, whether in the hypothalamus, the pituitary gland or the adrenal glands. In the course of adrenal ontogenesis, no significant changes in the level of expression of the studied genes were observed. Apart from *Galr2*, the expression of the studied genes did not change in the enucleation-induced adrenal gland regeneration. These observations suggest that neither Galp nor Ala plays a significant role in the growth of the rat adrenal glands. After acute administration of ACTH, the expression of Galr1 in the hypothalamus significantly decreased in the studied axis. Our observations suggest that corticotropin may regulate the expression of genes of the galaninergic system of the hypothalamus.

References

1. Hökfelt T, Tatemoto K. Galanin – 25 years with a multitalented neuropeptide. *Cell Mol Life Sci*. 2008;65(12):1793–1795.
2. Lang R, Gundlach AL, Kofler B. The galanin peptide family: Receptor pharmacology, pleiotropic biological actions, and implications in health and disease. *Pharmacol Ther*. 2007;115(2):177–207.
3. Ohtaki T, Kumano S, Ishibashi Y, et al. Isolation and cDNA cloning of a novel galanin-like peptide (GALP) from porcine hypothalamus. *J Biol Chem*. 1999;274(52):37041–37045.
4. Lang R, Berger A, Santic R, et al. Pharmacological and functional characterization of galanin-like peptide fragments as potent galanin receptor agonists. *Neuropept*. 2005;39:(3)179–184.
5. Santic R, Fenninger K, Graf K, et al. Gangliocytes in neuroblastic tumors express alarin, a novel peptide derived by differential splicing of the galanin-like peptide gene. *J Mol Neurosci*. 2006;29(2):145–152.
6. Krasnow SM, Fraley GS, Schuh SM, Baumgartner JW, Clifton DK, Steiner RA. A role for galanin-like peptide in the integration of feeding, body weight regulation, and reproduction in the mouse. *Endocrinol*. 2003;144(3):813–822.
7. Patterson M, Murphy KG, Thompson EL, et al. Microinjection of galanin-like peptide into the medial preoptic area stimulates food intake in adult male rats. *J Neuroendocrinol*. 2006;18(10):742–747.
8. Juréus A, Cunningham MJ, McClain ME, Clifton DK, Steiner RA. Galanin-like peptide (GALP) is a target for regulation by leptin in the hypothalamus of the rat. *Endocrinol*. 2000;141(7):2703–2706.
9. Larm JA, Gundlach AL. Galanin-like peptide (GALP) mRNA expression is restricted to arcuate nucleus of hypothalamus in adult male rat brain. *Neuroendocrinol*. 2000;72(2):67–71.
10. Takatsu Y, Matsumoto H, Ohtaki T, et al. Distribution of galanin-like peptide in the rat brain. *Endocrinol*. 2001;142(4):1626–1634.
11. Gundlach AL. Galanin/GALP and galanin receptors: Role in central control of feeding, body weight/obesity and reproduction? *Eur J Pharmacol*. 2002;440(2–3):255–268.
12. Crawley JN, Austin MC, Fiske SM, et al. Activity of centrally administered galanin fragments on stimulation of feeding behavior and on galanin receptor binding in the rat hypothalamus. *J Neurosci*. 1990;10(11):3695–3700.
13. Shiba K, Kageyama H, Takenoya F, Shioda S. Galanin-like peptide and the regulation of feeding behavior and energy metabolism. *FEBS J*. 2010;277(24):5006–5013.
14. Corder R, Pralong F, Turnill D, Saudan P, Muller AF, Gaillard RC. Dexamethasone treatment increases neuropeptide Y levels in rat hypothalamic neurones. *Life Sci*. 1988;43(23):1879–1886.
15. Malendowicz LK, Tortorella C, Nussdorfer GG. Orexins stimulate corticosterone secretion of rat adrenocortical cells, through the activation of the adenylate cyclase-dependent signaling cascade. *J Steroid Biochem Mol Biol*. 1999;70(4–6):185–188.
16. Tortorella C, Neri G, Nussdorfer GG. Galanin in the regulation of the hypothalamic-pituitary-adrenal axis (Review). *Int J Mol Med*. 2007;19(4):639–647.
17. Jopek K, Tyczewska M, Celichowski P, Malendowicz LK, Rucinski M. Transcriptome profile in unilateral adrenalectomy-induced compensatory adrenal growth in the rat. *Int J Mol Sci*. 2018;19(4):1111.
18. Rucinski M, Ziolkowska A, Szyszka M, Hochol A, Malendowicz LK. Evidence suggesting that ghrelin O-acyl transferase inhibitor acts at the hypothalamus to inhibit hypothalamo–pituitary–adrenocortical axis function in the rat. *Peptides*. 2012;35(2):149–159.
19. Trejter M, Jopek K, Celichowski P, Tyczewska M, Malendowicz LK, Rucinski M. Expression of estrogen, estrogen related and androgen receptors in adrenal cortex of intact adult male and female rats. *Folia Histochem Cytobiol*. 2015;53(2):133–144.
20. Paschke L, Zemleduch T, Rucinski M, Ziolkowska A, Szyszka M, Malendowicz LK. Adiponectin and adiponectin receptor system in the rat adrenal gland: Ontogenetic and physiologic regulation, and its involvement in regulating adrenocortical growth and steroidogenesis. *Peptides*. 2010;31(9):1715–1724.
21. Tyczewska M, Rucinski M, Trejter M, Ziolkowska A, Szyszka M, Malendowicz LK. Angiogenesis in the course of enucleation-induced adrenal regeneration – expression of selected genes and proteins involved in development of capillaries. *Peptides*. 2012;38(2):404–413.
22. Gentleman RC, Carey VJ, Bates DM, et al. Bioconductor: Open software development for computational biology and bioinformatics. *Genome Biol*. 2004;5(10):80.
23. Santic R, Schmidhuber SM, Lang R, et al. Alarin is a vasoactive peptide. *Proc Natl Acad Sci U S A*. 2007;104(24):10217–10222.
24. Benjamini Y, Hochberg Y. Controlling the false discovery rate: A practical and powerful approach to multiple testing. *J R Stat Soc Ser B*. 1995;57:289–300.
25. Hochol A, Tortorella C, Rucinski M, Ziolkowska A, Nussdorfer GG, Malendowicz LK. Effects of neuropeptides B and W on the rat pituitary-adrenocortical axis: In vivo and in vitro studies. *Int J Mol Med*. 2007;19(2):207–211.
26. Rucinski M, Ziolkowska A, Szyszka M, Malendowicz LK. Cerebellin and des-cerebellin exert ACTH-like effects on corticosterone secretion and the intracellular signaling pathway gene expression in cultured rat adrenocortical cells – DNA microarray and QPCR studies. *Int J Mol Med*. 2009;23(4):539–546.
27. Fraley GS, Shimada I, Baumgartner JW, Clifton DK, Steiner RA. Differential patterns of Fos induction in the hypothalamus of the rat following central injections of galanin-like peptide and galanin. *Endocrinol*. 2003;144(4):1143–1146.
28. Krasnow SM, Hohmann JG, Gragerov A, Clifton DK, Steiner RA. Analysis of the contribution of galanin receptors 1 and 2 to the central actions of galanin-like peptide. *Neuroendocrinol*. 2004;79(5):268–277.
29. Man PS, Lawrence CB. The effects of galanin-like peptide on energy balance, body temperature and brain activity in the mouse and rat are independent of the GALR2/3 receptor. *J Neuroendocrinol*. 2008;20(1):128–137.
30. Boughton CK, Patterson M, Bewick GA, et al. Alarin stimulates food intake and gonadotrophin release in male rats. *Br J Pharmacol*. 2010;161(3):601–613.
31. Zhuang F, Li M, Gao X, et al. The antidepressant-like effect of alarin is related to TrkB-mTOR signaling and synaptic plasticity. *Behav Brain Res*. 2016;313:158–171.
32. Lawrence CB, Baudoin FM, Luckman SM. Centrally administered galanin-like peptide modifies food intake in the rat: A comparison with galanin. *J Neuroendocrinol*. 2002;14(11):853–860.
33. Lawrence CB, Williams T, Luckman SM. Intracerebroventricular galanin-like peptide induces different brain activation compared with galanin. *Endocrinol*. 2003;144(9):3977–3984.
34. Seth A, Stanley S, Dhillo W, Murphy K, Ghatei M, Bloom S. Effects of galanin-like peptide on food intake and the hypothalamo-pituitary-thyroid axis. *Neuroendocrinol*. 2003;77(2):125–131.
35. Takenoya F, Hirayama M, Kageyama H, et al. Neuronal interactions between galanin-like-peptide- and orexin- or melanin-concentrating hormone-containing neurons. *Regul Pept*. 2005;126(1–2):79–83.
36. Eberhard N, Mayer C, Santic R, et al. Distribution of alarin immunoreactivity in the mouse brain. *J Mol Neurosci*. 2012;46(1):18–32.
37. Lang R, Gundlach AL, Kofler B. The galanin peptide family: Receptor pharmacology, pleiotropic biological actions, and implications in health and disease. *Pharmacol Ther*. 2007;115(2):177–207.
38. Otani K, Okada M, Yamawaki H. Diverse distribution of tyrosine receptor kinase B isoforms in rat multiple tissues. *J Vet Med Sci*. 2017;79(9):1516–1523.
39. Yu Y, Fuscoe JC, Zhao C, et al. A rat RNA-Seq transcriptomic BodyMap across 11 organs and 4 developmental stages. *Nat Commun*. 2014;5:3230.
40. Faure-Virelizier C, Croix D, Bouret S, et al. Effects of estrous cyclicity on the expression of the galanin receptor Gal-R1 in the rat preoptic area: A comparison with the male. *Endocrinol*. 1998;139(10):4127–4139.

Audiologic prognostic factors for hearing preservation following vestibular schwannoma surgery

Aleksandra Ochal-Choińska[1,A–F], Magdalena Lachowska[1,A,C–F], Katarzyna Kurczak[2,D–F], Kazimierz Niemczyk[1,E,F]

[1] Department of Otolaryngology, Medical University of Warsaw, Poland
[2] Center for Foreign Languages, Medical University of Warsaw, Poland

A – research concept and design; B – collection and/or assembly of data; C – data analysis and interpretation;
D – writing the article; E – critical revision of the article; F – final approval of the article

Advances in Clinical and Experimental Medicine, ISSN 1899–5276 (print), ISSN 2451–2680 (online) *Adv Clin Exp Med*. 2019;28(6):747–757

Address for correspondence
Magdalena Lachowska
E-mail: mlachowska@wum.edu.pl

Funding sources
None declared

Conflict of interest
None declared

Received on July 26, 2017
Reviewed on November 19, 2017
Accepted on May 5, 2018

Published online on February 19, 2019

Abstract

Background. Postoperative hearing loss after vestibular schwannoma (VS) removal still remains a lifelong problem for the patients. The present study analyzes the problem of hearing preservation after VS removal from a different angle than available professional literature on this topic.

Objectives. To identify audiologic factors which determine the extent of hearing loss in patients operated on for VS.

Material and methods. The study group included 86 patients operated on due to VS accessed via the middle cranial fossa. The analyses involved the effect on absolute hearing loss, which was calculated on the basis of the results of pure-tone audiometry performed pre- and postoperatively, and factors included in the preoperative audiologic tests, such as pure-tone audiometry, speech audiometry, auditory brainstem response (ABR), and impedance audiometry.

Results. The following parameters were demonstrated to have a prognostic value: 1. hearing thresholds at 125 Hz, 500 Hz and 1,000 Hz for the operated ear, Pure Tone Average (PTA) – calculated specifically at 500 Hz, 1,000 Hz and 2,000 Hz and at 500 Hz, 1,000 Hz, 2,000 Hz, and 4,000 Hz for the operated ear, and normal audiometric curve; 2. speech discrimination ranging from 55 dB to 75 dB for the operated ear, speech detection threshold (SDT) in the operated ear and interaural difference at 25–35 dB (non-operated vs operated ear); 3. presence of wave V, the values of I–V and III–V intervals for the operated ear, the amplitude of wave V, and the interaural ratio of wave V amplitudes; 4. intensity level for obtaining stapedial reflex or an abnormal reflex at Ipsi 500 Hz, 1,000 Hz and 2,000 Hz, and Contra 500 Hz, 1,000 Hz, 2,000 Hz, and 4,000 Hz.

Conclusions. The better the preoperative hearing status, the more substantial surgery-related hearing loss was observed. A number of preoperative parameters of the basic diagnostic set of audiologic tests present a prognostic value for the degree of surgery-related hearing loss in VS patients.

Key words: hearing loss, neuroma, middle cranial fossa, audiometry, auditory evoked potentials

Cite as
Ochal-Choińska A, Lachowska M, Kurczak K, Niemczyk K. Audiologic prognostic factors for hearing preservation following vestibular schwannoma surgery. *Adv Clin Exp Med*. 2019;28(6):747–757. doi:10.17219/acem/90768

DOI
10.17219/acem/90768

Background

The development in the field of medicine has facilitated the shift of the primary aim of vestibular schwannoma (VS) removal surgery from tumor removal to the smallest possible impairment of neurological functions. The impairment of facial nerve function is mostly transient. However, postoperative hearing impairment still remains a lifelong problem for the patients.

It is therefore necessary to determine the factors responsible for the extent of hearing loss resultant from the surgery and to employ them in the optimization of the therapeutic process. A review of the professional literature revealed a paucity of detailed and multidimensional analyses of possible prognostic factors included in the basic panel of audiologic diagnostic tests for VS patients which would determine the extent of surgery-related hearing loss.

Objectives

The main aim of the study was to identify audiologic factors which determine the extent of hearing loss in patients operated on for VS. The analysis included the following audiologic tests: pure-tone audiometry, speech audiometry, auditory brainstem response (ABR), and impedance audiometry with particular attention paid to stapedial reflex.

Some authors have attempted to investigate the role of pure-tone audiometry or speech audiometry outcomes as prognostic factors. However, studies describing the predictive value of ABR are scarce. The available analyses have concentrated on few parameters of response recording, neglecting such data as the values of amplitudes of individual waves.

Material and methods

This retrospective analysis covered data obtained from audiologic tests and case histories of patients operated on for VS via middle cranial fossa approach which is a technique facilitating hearing preservation. The study involved 86 patients with a postoperative histopathological confirmation of VS.

All the surgical procedures were performed by the same experienced otosurgeon with substantial expertise in skull base surgery. The surgeries of the patients analyzed were carried out within 6 years, however, the potential influence of his gradually growing experience and on surgery-related hearing loss was ruled out ($p > 0.05$).

Each study group patient underwent diagnostic and medical procedures according to a standard protocol implemented by Department of Otolaryngology, Medical University of Warsaw (Poland) concerning patients with a suspected tumor of the cerebellopontine angle. According to the protocol, each patient underwent audiologic tests, including pure-tone audiometry, speech audiometry, impedance audiometry with stapedial reflex testing, and ABR no later than a month prior to the procedure. Magnetic resonance imaging (MRI) was used to confirm the presence of a tumor in the cerebellopontine angle region in each patient.

The follow-up tests included pure-tone audiometry alone or pure-tone audiometry and speech audiometry performed 3 months after the surgery.

This study presents the analysis of a number of factors (157 individual parameters) included in the parameters of the audiologic tests, imaging test data and case histories in terms of their possible influence on surgery-related hearing loss.

The following parameters were assessed with pure-tone audiometry: the values of hearing thresholds at individual frequencies, air- and bone-conduction, Pure Tone Average (PTA) calculated on the side affected with VS based on hearing thresholds at 500 Hz, 1,000 Hz, 2,000 Hz, and 3,000 Hz (this parameter is more commonly used in North America and recommended by the American Academy of Otolaryngology-Head and Neck Surgery (AAO-HNS)),[1] interaural differences in the values of hearing thresholds for each of the test frequencies from 125 Hz to 8,000 Hz, for air-conduction (the value of hearing threshold in the operated ear minus the value of hearing threshold in the non-operated ear), and interaural differences between PTA (the value of PTA in the operated ear minus the value of PTA in the non-operated ear). Moreover, the preoperative shape of the air-conduction audiometric curve was assessed, with the curve classified as normal, sharply falling, rising, flat, U-shaped, inverted U-shaped, and complete deafness.

The following parameters were assessed with speech audiometry in terms of being potentially prognostic factors: 1. speech discrimination for individual sound intensities with particular attention paid to the value of 55–65 dB of sound pressure level (dB SPL) as it corresponds with typical speech intensity; 2. interaural differences in speech discrimination for individual values of sound intensity (speech discrimination for the non-operated minus speech discrimination for the operated ear at a specific intensity); 3. speech detection threshold (SDT) expressed in dB SPL; 4. speech reception threshold (SRT) – expressed in dB SPL; 5. speech discrimination score (SDS) – expressed as percentages; 6. interaural difference between SDS (value for the non-operated ear minus value for the operated ear); 7. achieving 100% of speech discrimination by the patient – with the zero-one method.

Impedance audiometry was used to assess the presence or absence of stapedial reflex and the value of sound intensity at which stapedial reflex was obtained. However, if the reflex was absent, its value was recorded as 130 dB in order to facilitate the analyses. Moreover, the patients were grouped based on normal or pathological stapedial reflex (with the pathological reflex described as: test intensity

exceeding reference values – 100 dB SPL, positive Metz symptom and a complete lack of stapedial response).

Type A tympanograms were obtained in each patient. Therefore, tympanogram curve shape was disregarded as a prognostic factor.

Auditory brainstem response tests were conducted with the Smart Box platform integrated with Smart-EP software (Intelligent Hearing Systems, Corp., Miami, USA). A 90 dB nHL (decibels above normal adult hearing level) broadband click was used as an acoustic stimulus. The rate of stimulus delivery was 31/s.

The following ABR testing parameters were assessed as possible prognostic factors: 1. waveform morphology – the presence of waves I, III and V; 2. the value of wave I, III and V latency; 3. the values of I–III, I–V and III–V intervals; 4. interaural latency differences (ILD) for waves I, III and V; 5. ILD for I–III, I–V and III–V; 6. wave I, III and V amplitudes measured as the average of 3 records for each wave; 7. interaural amplitude differences for waves I, III and V; 8. interaural amplitude ratios of waves I, III and V – the value of amplitudes recorded on the side of the tumor and the value of contralateral amplitudes of individual waves; 9. amplitude ratios of waves V and I (ARI_V); 10. interaural ARI_V ratio – ipsilateral to the tumor vs contralateral side, compliance with referenced values according to Hall et al.[2]

Apart from the individual parameters for selected audiologic tests (pure-tone, speech, impedance audiometry, and ABR) as possible prognostic factors of hearing preservation, we also assessed the preoperative hearing capacity calculated according to the AAO-HNS classification[1] and the Classification of Hearing Impairments by the International Bureau for Audiophonology (BIAP).[3]

Assessment of surgery-related hearing loss

The abovementioned parameters of the assessment of pre- and postoperative hearing status, calculated on the basis of data obtained from pure-tone audiometry, were used to evaluate surgery-related hearing loss by determining absolute hearing loss. The majority of analyses in the present study refer to this parameter.

Absolute hearing loss was defined as a difference between PTA before and after the surgery for the operated ear.

Statistical analysis

All statistical calculations were performed with IBM SPSS statistical software (IBM Corp., Armonk, USA). Qualitative data was described with the use of the number and percentage of occurrence of a category, while quantitative variables were characterized with the following descriptive statistics: median (M), mean, standard deviation (SD), minimum (Min), and maximum (Max). Prior to analyses, all the quantitative variables had been examined in terms of data distribution with 2 measures of distribution: skewness and kurtosis. A result was considered statistically significant with a p-value below 0.05 ($p < 0.05$). The following analyses were conducted in this study: 1. χ^2 test in cross tabulations (combined with comparison of column proportions with Bonferroni correction); 2. correlation analysis (Pearson's r/Spearman's rho); 3. polynomial logistic regression analysis; 4. k-means cluster analysis; 5. one-way analysis of variance (ANOVA; intra-group and inter-group design).

Ethical considerations

The study was approved by the local Institutional Ethics Committee Review Board. The project conforms to the Code of Ethics of the World Medical Association (Declaration of Helsinki).

Results

Study group division into 4 groups based on absolute hearing loss

Based on absolute hearing loss (difference between PTA pre- and postoperatively for the operated ear), the patients were divided into 4 categories of differences: ≤10.00; 10.01–20.00; 20.01–40.00; and ≥40.01 (Table 1). The division aimed at distinguishing groups with low and high grades of hearing loss. This division into 4 groups became the basis for further analyses concerning possible factors influencing surgery-related hearing loss. The table presents the number and percentage of patients along with the average tumor size in each group.

Table 1. The division into groups based on surgery-related hearing loss, comprising the difference in Pure Tone Average (PTA; according to AAO-HNS classification) before and after the surgery. The table presents number and percentage of patients along with average tumor size in each group

Patient group depending on surgery-related hearing loss [dB HL]	Number of patients	Percentage of patients [%]	Average tumor size [mm]
≤10.00	27	31.40	10.14
10.01–20.00	21	24.42	11.77
20.01–40.00	16	18.60	13.42
≥40.01	22	25.58	10.75

Pure-tone audiometry

One-way ANOVA revealed a correlation between hearing thresholds for individual frequencies before the operation and preoperative PTA and the degree of surgery-related hearing loss. A thorough post hoc analysis with an S-N-K test showed that patients with hearing loss below 10 dB HL (decibels hearing level) preserved considerably higher values of hearing threshold for the 1,000 Hz frequency than the remaining groups (a result at the level of statistical tendency

Table 2. Pure Tone Averages (PTA) at individual frequencies and preoperative PTA [dB HL] depending on the extent of surgery-related hearing loss – statistically significant parameters

The parameter of pure-tone audiometry	Hearing loss in individual groups [dB HL]				F-test	p-value
	≤10.00	10.01–20.00	20.01–40.00	≥40.01		
Hearing threshold at 125 Hz	24.07 ±15.81	17.73 ±8.13	14.67 ±6.67	16.82 ±10.53	2.817	0.044
Hearing threshold at 250 Hz	25.56 ±16.49	15.46 ±11.12	15.33 ±9.90	15.46 ±9.12	4.067	0.010
Hearing threshold at 500 Hz	28.33 ±20.33	19.09 ±15.17	17.67 ±15.34	17.05 ±10.43	2.634	0.055
Hearing threshold at 1,000 Hz	38.33 ±24.22	27.73 ±19.19	25.33 ±21.25	18.41 ±13.49	4.133	0.009

Table 3. Correlations between surgery-related hearing loss (the difference in pre- and postoperative Pure Tone Averages (PTA)) and the preoperative degree of hearing impairment (according to BIAP classification)

Surgery-related hearing loss	Preoperative degree of hearing impairment				Total [%]
	normal [%]	slight [%]	moderate [%]	severe [%]	
≤10.00 dB HL	22.6[a]	24.0[a]	42.9[a,b]	100.0[b]	31.40
10.01–20.00 dB HL	25.8[a]	20.0[a]	32.1[a]	–	25.60
20.01–40.00 dB HL	16.1[a]	20.0[a]	17.9[a]	–	17.40
≥40.01 dB HL	35.5[a]	36.0[a]	7.1[b]	–	25.60
Total	100.00	100.00	100.00	100.00	100.00

Each superscript letter ([a,b]) means a subset of "hearing impairment" category whose column proportions do not differ significantly at the level of 0.05.

was obtained only for 500 Hz frequency). The remaining differences revealed no statistical significance (Table 2).

The χ^2 analysis in cross tabulations did not confirm any correlation between the type of audiogram and surgery-related hearing loss ($\chi^2 = 21.81$; $p > 0.05$). It showed no correlation between surgery-related hearing loss (the difference between pre- and postoperative PTA) and the degree of BIAP hearing impairment ($\chi^2 = 13.62$; $p > 0.05$). It is worth mentioning that the column proportions test with Bonferroni correction showed that the lowest degree of surgery-related hearing loss was obtained considerably more frequently in patients who had been preoperatively diagnosed with moderate or severe hearing impairment according to BIAP.[3] Detailed results are presented in Table 3.

The χ^2 analysis in cross tabulations showed no correlation between surgery-related hearing loss (the difference between pre- and postoperative PTA) and the preoperative hearing status described with the AAO-HNS classification ($\chi^2 = 4.62$; $p > 0.05$).

Speech audiometry

Pearson's r correlation analysis was used to determine whether there was a correlation between the parameters of speech audiometry and the surgery-related hearing loss. The pre- and postoperative differences between PTA were compared in the analysis.

A correlation between the results of both tests was confirmed. It was demonstrated that the more marked the surgery-related hearing loss, the lower the preoperative SDT and SRT indexes found in the patients and the more patients achieved 100% of speech discrimination in the operated ear preoperatively.

The SDS parameter was found to have the weakest correlation with postoperative hearing loss. However, a trend was visible which showed that hearing loss experienced by patients as a result of surgery was more marked in the case of better preoperative speech discrimination. Detailed results are presented in Table 4.

Pearson's r calculated for the correlation between the percentage of speech discrimination at individual intensities and the surgery-related hearing loss showed a significant correlation for the intensities of 45 dB and higher, the surgery-related hearing loss increased with the increase of the percentage of speech discrimination for the intensities of 45 dB SPL and higher.

The results of Pearson's r correlation between preoperative interaural differences in speech discrimination during speech audiometry for individual intensities and surgery-related hearing loss showed a significant correlation for intensities above 50 dB SPL. Surgery-related hearing loss

Table 4. Correlations between the indexes of speech audiometry (speech reception threshold – SRT, speech detection threshold – SDT, peak percentage of speech discrimination in the operated ear – SDS, and whether the patient achieved 100% of speech discrimination – SDS100) and surgery-related hearing loss (the difference between pre- and postoperative Pure Tone Averages (PTA)) – the values of Pearson's r correlation coefficient

Index	Surgery-related hearing loss
SDT	–0.324**
SRT	–0.341**
SDS	0.220
SDS100	0.325**

* $p < 0.05$; ** $p < 0.01$; ** statistically significant parameters.

Table 5. Correlations between statistically significant preoperative indexes of speech audiometry for the operated ear and surgery-related hearing loss (the difference between pre- and postoperative Pure Tone Averages – PTA) – descriptive statistics (±SD) and F statistics

Speech audiometry parameters	≤10.00 dB HL	10.01–20.00 dB HL	20.01–40.00 dB HL	≥40.01 dB HL	F-test	p-value
SDT	45.42 ±18.29	40.00 ±17.24	38.33 ±18.48	30.26 ±10.07	3.047	0.034
55 dB SPL	38.96 ±38.95	47.00 ±40.80	55.33 ±36.03	70.00 ±25.66	2.785	0.047
60 dB SPL	47.08 ±39.48	54.75 ±39.69	65.00 ±32.13	78.68 ±22.48	3.193	0.028
65 dB SPL	55.63 ±38.46	61.25 ±36.41	71.33 ±28.69	83.95 ±19.19	3.031	0.035
70 dB SPL	64.17 ±37.20	68.25 ±33.57	77.67 ±27.70	89.21 ±18.20	2.672	0.054
75 dB SPL	69.17 ±36.32	73.50 ±26.81	79.67 ±28.19	91.32 ±15.97	2.347	0.080
Interaural difference 25 dB SPL	7.04 ±10.63	−0.23 ±5.17	1.67 ±9.94	7.96 ±10.20	4.056	0.010
Interaural difference 30 dB SPL	12.69 ±22.11	−0.68 ±10.27	2.67 ±20.34	13.41 ±17.42	3.344	0.023
Interaural difference 35 dB SPL	22.22 ±28.31	4.43 ±20.40	19.33 ±30.79	20.34 ±19.08	2.453	0.069

Table 6. The distribution of mean values and standard deviation (SD) of statistically significant parameters in 4 individual groups of surgery-related hearing loss

Parameter	≤10.00 dB HL	10.01–20.00 dB HL	20.01–40.00 dB HL	≥40.01 dB HL	F-test	p-value
Pure-tone audiometry						
Hearing threshold at 125 Hz	24.07 ±15.81	17.73 ±8.13	14.67 ±6.67	16.82 ±10.53	2.817	0.044
Hearing threshold at 250 Hz	25.56 ±16.49	15.46 ±11.12	15.33 ±9.90	15.46 ±9.12	4.067	0.010
Hearing threshold at 500 Hz	28.33 ±20.33	19.09 ±15.17	17.67 ±15.34	17.05 ±10.43	2.634	0.055
Hearing threshold at 1,000 Hz	38.33 ±24.22	27.73 ±19.19	25.33 ±21.25	18.41 ±13.49	4.133	0.009
Speech audiometry						
SDT	45.42 ±18.29	40.00 ±17.24	38.33 ±18.48	30.26 ±10.07	3.047	0.034
65 dB SPL	55.63 ±38.46	61.25 ±36.41	71.33 ±28.69	83.95 ±19.19	3.031	0.035
70 dB SPL	64.17 ±37.20	68.25 ±33.57	77.67 ±27.7	89.21 ±18.20	2.672	0.054
75 dB SPL	69.17 ±36.32	73.50 ±26.81	79.67 ±28.19	91.32 ±15.97	2.347	0.080
Interaural difference 25 dB SPL	7.04 ±10.63	−0.23 ±5.17	1.67 ±9.94	7.96 ±10.20	4.056	0.010
Interaural difference 30 dB SPL	12.69 ±22.11	−0.68 ±10.27	2.67 ±20.34	13.41 ±17.42	3.344	0.023
Interaural difference 35 dB SPL	22.22 ±28.31	4.43 ±20.40	19.33 ±30.79	20.34 ±19.08	2.453	0.069
ABR						
III–V interval	2.09 ±0.44	1.88 ±0.15	1.74 ±0.24	2.22 ±0.49	4.701	0.005
Wave V amplitude	0.23 ±0.09	0.30 ±0.10	0.23 ±0.10	0.22 ±0.10	3.129	0.030
Interaural difference of III–V intervals	0.34 ±0.41	0.12 ±0.08	0.33 ±0.30	0.41 ±0.37	2.618	0.059
Impedance audiometry						
Reflex normality for 500 Hz in the operated ear	0.30 ±0.47	0.71 ±0.46	0.67 ±0.49	0.76 ±0.44	4.313	0.008
Reflex normality for 1,000 Hz in the operated ear	0.22 ±0.42	0.52 ±0.51	0.5 ±0.52	0.71 ±0.47	3.643	0.017
Reflex normality for 2,000 Hz in the operated ear	0.09 ±0.29	0.33 ±0.48	0.33 ±0.49	0.53 ±0.51	3.392	0.023

increased with a more marked interaural diversity for intensities above 50 dB SPL. The same tendency occurred for the interaural difference of SDS parameters. Therefore, patients who had better preoperative speech discrimination in the operated ear compared to the non-operated ear experienced more marked surgery-related hearing loss.

One-way ANOVA was used to determine if there was a correlation between the indexes of the speech audiometry test and surgery-related hearing loss with the division into 4 groups (Table 5). Significant differences were only obtained for the SDT ($p < 0.05$) in the operated ear. A detailed SDT analysis showed that the only diversity was observed between groups of patients with the lowest and the most marked surgery-related hearing loss. The highest results were obtained in the group with the lowest hearing loss and the mean SDT value in this group was 45 dB SPL. Patients who lost over 40 dB HL of PTA had had the mean preoperative SDT value of 30 dB SPL. We also observed a trend showing that SDT values decreased with increased surgery-related hearing loss (Table 6).

The analysis of speech discrimination percentage for individual speech intensities showed significant differences

in regard to surgery-related hearing loss observed for the 55 dB to 75 dB SPL band, which includes the key intensity for interpersonal communication and 60 dB SPL band, which is typical for conversation (depending on the source: 55–65 dB SPL).

The analysis of interaural difference of speech discrimination for individual intensities confirmed the presence of differences in interaural difference of speech discrimination only for the intensities from 25 dB to 35 dB SPL. A thorough post hoc analysis with S-N-K test showed that patients with surgery-related hearing loss from 10.01 dB to 40.00 dB HL achieved considerably lower results of the analyzed indexes than the remaining groups (Table 6). The only exception in the case of interaural difference in speech discrimination for 35 dB SPL was noted in patients with the difference in pure-tone audiometry of 10.01–20.00 dB HL. The remaining differences revealed no statistical significance. The analysis proved that the patients more commonly experienced moderate surgery-related hearing loss (10–40 dB HL of PTA) if their speech discrimination on the side of the tumor was better and similar to speech discrimination on the non-operated side for the intensities of 25–35 dB SPL.

No intergroup differences were observed in case of the remaining parameters.

Auditory brainstem response testing

Pearson's r correlation analysis demonstrated an increasing surgery-related hearing loss in the operated ear along with the growing deviation of I–V and III–V intervals from the norm, regardless of the PTA index investigated. It was also demonstrated that the presence of wave V in the operated ear in ABR waveform morphology correlated with lower surgery-related hearing loss. Moreover, the analyses revealed that the hearing loss resulting from the surgery was more marked if the I–V interval presented higher values in the operated ear. Additionally, a negative correlation was observed between surgery-related hearing loss and the presence of wave V. Therefore, patients whose waveform morphology lacked wave V experienced a more marked surgery-related hearing loss. The remaining correlations revealed no statistical significance.

One-way ANOVA between ABR parameters and surgery-related hearing loss in the 4 groups demonstrated significant differences for the value of III–V interval ($p < 0.01$). A detailed post hoc analysis with S-N-K test showed that patients with the most abundant hearing loss (≥40.01 dB HL) achieved considerably higher values of III–V interval before the surgery than patients with a surgery-related PTA reduction ranging from 10.01 dB to 40.00 dB HL. The lowest values of III–V interval were achieved if PTA reduction ranged from 20.01 dB to 40.00 dB HL. No difference was observed between patients with the lowest and the most abundant surgery-related hearing loss. The resultant relationship is presented in Table 6. A significant difference was also found as regards the value of wave V amplitude ($p < 0.05$). S-N-K test analysis revealed that the subjects with a pre- vs postoperative difference between PTA ranging from 10.01 dB to 20.00 dB HL had markedly higher values of preoperative wave V amplitude compared to the remaining groups ($p = 0.050$). The remaining differences revealed no statistical significance. Differences at the level of statistical tendency ($p = 0.059$) were obtained for the interaural difference of III–V intervals. A detailed post hoc analysis with S-N-K test revealed that the patients with a pre- vs postoperative difference between PTA ranging from 10.01 dB to 20.00 dB HL had markedly lower values of interaural difference of III–V intervals compared to the remaining subjects.

The χ^2 test in cross tabulations also indicated a significant relationship in the assessment of normal values of III–V interval in the operated ear ($\chi^2 = 9.06$; $p < 0.05$). A thorough analysis of column comparisons with Bonferroni correction showed that III–V interval was more commonly normal in the group with surgery-related hearing loss ranging from 10.01 dB to 40.00 dB HL compared to the subjects with surgery-related hearing loss below 10 dB HL or over 40 dB HL. The remaining ABR parameters revealed no statistical significance.

Impedance audiometry

One-way ANOVA demonstrated significant differences for a parameter predefined as normal stapedial reflex at 500 Hz on the operated side ($p < 0.01$). A detailed S-N-K analysis showed that the subjects with surgery-related hearing loss lower than 10 dB HL significantly more often had an abnormal ipsilateral stapedial reflex at the frequency of 500 Hz in the operated ear compared to the remaining groups of patients (Table 6).

Moreover, significant differences were observed for the normality of ipsilateral stapedial reflex at 1,000 Hz and 2,000 Hz on the operated side ($p < 0.05$). S-N-K test analysis revealed significant differences between groups with the lowest and the most severe surgery-related hearing loss. Normal stapedial reflexes were observed in the group with surgery-related hearing loss of over 40 dB HL. The differences between the remaining groups revealed no statistical significance.

Significant differences at the statistical trend level were obtained for the index of stapedial reflex at the frequency of 4,000 Hz for the contralateral non-operated ear ($p = 0.085$). The obtained results indicate the presence of a negative correlation – the value of the parameter decreased with the increased surgery-related hearing loss.

The χ^2 analysis in cross tabulations was used to determine if there was any correlation between the normality of stapedial reflex (at the frequencies of 500 Hz, 1,000 Hz, 2,000 Hz, and 4,000 Hz) in the operated ear (ipsi) and surgery-related hearing loss. A correlation was confirmed for reflex normality at 500 Hz ($\chi^2 = 11.53$; $p < 0.01$). A thorough analysis of column comparisons with Bonferroni

correction showed a significantly lower percentage of reflex normality at 500 Hz in the operated ear in the group with the lowest surgery-related hearing loss in comparison to the remaining groups. The analysis also confirmed a correlation for reflex normality at the frequency of 1,000 Hz (χ^2 = 9.98; p < 0.05) and 2,000 Hz (χ^2 = 9.38; p < 0.05). A thorough analysis of column comparisons with Bonferroni correction showed a significantly lower percentage of reflex normality at 1,000 Hz in the group with the lowest surgery-related hearing loss in comparison with the remaining groups (except the group in which pure-tone audiometry revealed differences between 20.01 dB and 40.00 dB). However, no correlation was found for reflex normality at 4,000 Hz (χ^2 = 3.11; p < 0.05). It is worth emphasizing that the results obtained match the trend observed for reflex normality at 500 Hz, 1,000 Hz and 2,000 Hz. Pearson's r correlation analysis confirmed a correlation between the indexes of impedance audiometry and surgery-related hearing loss (pre- and postoperative differences between PTA). The analysis revealed an increase in absolute surgery-related hearing loss with the increasing reflex normality at 500 Hz, 1,000 Hz and 2,000 Hz. Moreover, surgery-related hearing loss became more marked with the reduction in the values of preoperative parameters of impedance audiometry, such as ipsilateral sound intensity for the stapedial reflex in the operated ear at the frequency of 2,000 Hz, and contralateral sound intensity for stapedial reflex in the non-operated ear at the frequencies of 500 Hz, 1,000 Hz, 2,000 Hz, and 4,000 Hz. The remaining correlations revealed no statistical significance.

Discussion

The present study analyzes the problem of hearing preservation after VS removal at a slightly different angle than available professional literature concerning this topic. In principle, previous studies classified patients according to various scales to assess the initial hearing status on a 3- to 5-grade scale according to which it was stated whether the hearing status improved, deteriorated or remained at the same level.[1,4–14]

The present study concentrates on the assessment of absolute hearing loss in order to identify the factors which influence the absolute value of "lost decibels" in pure-tone audiometry, and, what follows, the factors which determine the preservation or loss of initial hearing status irrespective of the preoperative status. The problem of "hearing preservation" was specifically approached in this study – to preserve hearing as similar as possible to the preoperative status. The study did not exclusively concern the issue of serviceable hearing criteria which may differ to a large extent depending on an implemented scale. Dugar et al. and Lassaletta et al. observed that the preservation of serviceable hearing may range from 0% to 56% depending on the selected scale.[15,16]

It is worth emphasizing that no scales were used to calculate the results in this study. Surgery-related hearing loss was reviewed objectively, exclusively on the basis of study group analysis. At the same time, our intention was not to use the described techniques of determining serviceable hearing and not to use scales (largely based on speech audiometry) for the main calculations. Nonetheless, a certain amount of data concerning not only hearing sounds but also sound perception as speech are not available. However, the aim of this study was not to repeat available studies, but to focus on a new approach to the topic.

To the best of our knowledge, detailed analyses concerning the possible prognostic audiologic factors of hearing preservation in patients with VS have not been published so far.

Pure-tone audiometry

The present study demonstrated that surgery-related hearing loss is influenced by BIAP hearing impairment degree determined before the surgery.[3] The lowest degree of surgery-related hearing loss, below 10 dB HL of PTA, was obtained considerably more frequently in patients who had been preoperatively diagnosed with moderate or severe hearing impairment. Additionally, it was demonstrated that the most marked surgery-related hearing loss was observed in patients with previously normal hearing status.

Ferber-Viart et al. assessed the prognostic value of selected parameters of pure-tone audiometry for hearing preservation in patients operated on due to VS.[17] Hearing preservation was defined by the maintenance of AAO-HNS hearing status grade A, B or C. The assessment covered the hearing thresholds for individual frequencies: 250 Hz, 500 Hz, 1,000 Hz, 2,000 Hz, 4,000 Hz, and 8,000 Hz, and PTA for the following frequencies: 500 Hz, 1,000 Hz, 2,000 Hz, and 4,000 Hz. Statistical significance was confirmed for hearing threshold values at 250 Hz, 4,000 Hz and 8,000 Hz, and PTA. The authors stated that the possibility of hearing preservation significantly decreased above the value of 50 dB HL PTA. According to Rohit et al., preoperative PTA markedly contributes to surgery-related hearing loss.[18] However, the value of postoperative PTA negatively correlated with the size of the tumor. Similar correlations were not confirmed by a study by Slattery et al.[19] and Brackmann et al.,[20] as well as the results of the present analyses. Rastogi et al. analyzed the influence of preoperative hearing thresholds at 4,000 Hz and 8,000 Hz on surgery-related hearing status in patients operated on due to VS.[21] However, no statistically significant correlations were demonstrated.

Speech audiometry

The present study revealed a trend showing that preoperative SDT values decreased with increased surgery-related hearing loss. Based on statistical analyses, patients with SDT ≥45 dB SPL are expected to lose ≤10 dB HL of PTA as a result of the surgery, while patients with SDT ≤30 dB

SPL are at risk of the most marked surgery-related hearing loss (loss of >40 dB HL of PTA). The analysis of the influence of speech discrimination for individual intensities on surgery-related hearing loss, both with and without the division into 4 groups, showed that surgery-related hearing loss increased with the percentage of speech discrimination for individual intensities. Moreover, correlation analysis demonstrated that surgery-related hearing loss significantly increased with the growing percentage of speech discrimination for the intensities of 45 dB SPL and above. Significant differences concerning surgery-related hearing loss in the specified 4 groups were observed for speech discrimination for the 55 dB to 75 dB SPL band, which includes the key intensity band for interpersonal communication typical for conversation (55–65 dB SPL). The present study results may indicate that the surgery affects those parameters of hearing which appear to be critical for interpersonal communication and a similar physical nerve fiber destruction is responsible for a disproportionately large reduction in perception. The issue requires confirmation in further research because of the lack of other publications in this field.

The analysis of interaural differences in speech discrimination for individual intensities and surgery-related hearing loss without the division into 4 groups showed that surgery-related hearing loss became more marked with increasing interaural diversity for intensities above 50 dB SPL. The division into 4 groups additionally showed that the better the speech audiometry result in the operated ear for the intensities of 25–35 dB SPL, the more frequently the patients experienced moderate surgery-related hearing loss (10–40 dB HL PTA).

Therefore, the analyses of speech audiometry results showed that patients who had had better preoperative speech discrimination in the operated ear vs non-operated ear experienced more marked surgery-related hearing loss. The review of the professional literature revealed that speech audiometry parameters including speech detection threshold (SDT), speech reception threshold (SRT) and speech discrimination score (SDS) were most commonly assessed in terms of their influence on hearing loss. According to some previous research, mean preoperative SDS was estimated at 66–96%.[8,9,18,22,23]

Shelton et al.[8] stated that SDT and SDS did not affect hearing status postoperatively, while 10 years later a similar study conducted by Ferber-Viart et al.[17] revealed a significant influence of SDT on hearing preservation postoperatively. Moreover, it was stated that 45 dB SPL was the SDT level above which patients experienced a marked surgery-related deterioration of hearing. The present study also indicated no influence of SDS on postoperative hearing status. Rohit et al. also found no correlation between SDS and surgery-related hearing loss.[18] Rastogi et al. conducted a study including 44 VS patients which demonstrated no influence of SRT or SDS on postoperative hearing status[21].

Auditory brainstem response testing

The present analyses which did not comprise the division into groups demonstrated increasing surgery-related hearing loss in the operated ear along with a growing deviation of I–V and III–V intervals from the reference values, regardless of the PTA parameter investigated. Moreover, the analyses revealed that the hearing loss resulting from the surgery was more marked if the I–V interval presented higher values in the operated ear (according to BIAP[3]).

Additionally, a negative correlation was observed between surgery-related hearing loss and the presence of wave V. Therefore, patients whose waveform morphology lacked wave V experienced a more marked surgery-related hearing loss. Additionally, the analysis of surgery-related hearing loss including the division into 4 groups showed that patients in whom hearing loss was the most marked (≥40.01 dB HL) achieved considerably higher values of III–V interval before the surgery. It was also demonstrated that the subjects with a pre- vs postoperative difference between PTA ranging from 10.01 dB to 20.00 dB HL achieved markedly higher values of preoperative wave V amplitude compared to the remaining groups.

The analysis of the normality of selected ABR parameters in terms of reference values according to Hall et al. in 4 selected groups demonstrated that III–V interval was more commonly normal compared to subjects whose surgery-related hearing loss was below 10 dB HL or above 40 dB HL.[2] This may indicate that patients with the abnormal value of III–V interval had poorer conduction of bioelectric arousal, and what follows, poorer hearing. Therefore, surgery-related hearing loss was not as marked. However, this requires further study due to the fact that hearing loss is the most marked in such patients. It was demonstrated that surgery-related hearing loss was not affected by the normality of parameters like I and V latency for the operated and non-operated ear, I–III intervals for the operated and non-operated ear, I–V intervals for the operated and non-operated ear, interaural latency difference for wave V, and the amplitude ratio of waves I and V for the operated and non-operated ear.

Additionally, cluster analysis demonstrated that surgery-related hearing loss most commonly ranged between 10.01 dB and 40.00 dB HL in patients with normal ABR parameters according to Hall's reference values,[2] while patients whose ABR parameters were abnormal most commonly lost over 40 dB HL. This was consistent with the tendency identified in the present study which was observed in all audiologic tests and indicated that the absolute surgery-related hearing loss was more marked if the preoperative hearing status was better.

Ferber-Viart et al. analyzed ABR recordings in terms of their prognostic value for the postoperative hearing status in order to assess the presence of waves I, III and V, their latency and the duration of I–V interval.[17] The study demonstrated that wave III was present in waveform morphology

and wave V latency was over 6.5 ms in a group with preserved postoperative hearing, which was defined by the authors as the preservation of hearing at the level of AAO-HNS class A, B or C.[1] Matthies and Samii analyzed 420 preoperative ABRs and proved that the presence of waves I, III and V in waveform morphology correlated with a higher SDS in postoperative speech audiometry.[24] Shelton et al. confirmed a negative correlation of postoperative SDS with abnormal interaural latency difference for wave V.[8] Patients with a value of interaural latency difference for wave V not exceeding 0.4 ms preserved hearing at a rate of 78% (according to the authors' own classification). In the case of values ranging from 0.5 ms to 2 ms, the percentage of patients with preserved hearing decreased to 58%.

Browning et al. conducted a study on a group of 36 patients operated on with a hearing preservation technique.[25] They demonstrated a correlation between preserved intraoperative ABR waveform morphology and a slight loss in postoperative PTA. However, the correlation revealed no statistical significance. Auditory brainstem response waveform morphology as a factor contributing to hearing loss was undermined by a study conducted by Kanzaki et al., who analyzed the recordings of 27 patients who had undergone hearing preservation surgery.[26] They demonstrated a correlation between the presence of wave V and the interaural latency difference for wave V vs postoperative hearing preservation, but the factors were not statistically significant.

A study including 71 patients was conducted by Dornhoffer et al., who demonstrated a statistically significant correlation between wave V latency and low surgery-related hearing loss.[23] The patients with results not exceeding 6.8 ms had significantly better hearing after the surgery. However, interaural latency difference for wave V appeared to have no influence on postoperative hearing status.

A study including 104 patients conducted by Rohit et al. showed no statistically significant difference in regard to ABR waveform morphology, I–V interval and interaural latency difference for wave V between a group with preserved hearing and a group with surgery-related hearing loss.[18] Vincent et al. conducted a study in which they assessed hearing after VS removal in 77 patients.[27] They demonstrated that prolonged wave V latency in preoperative ABR recording is linked to a poorer prognosis regarding hearing status. Gardener et al. emphasized that even the preoperative lack of ABR data was not a factor which negatively correlated with postoperative hearing preservation.[10] However, the study was conducted on a small sample size (9 subjects). Therefore, it requires a confirmation by research covering a larger population.

Impedance audiometry

The analysis of the normality of the stapedial reflex conducted in the present study, with the study group divided into patients with a normal and pathological reflex, demonstrated a trend which indicates that normal stapedial reflex was correlated with more marked hearing loss and a pathological reflex – with a less marked hearing loss. This was probably due to the initial hearing status on the side of the tumor and remained consistent with a tendency demonstrated in the present paper indicating that more marked absolute surgery-related hearing loss was observed in patients with better preoperative hearing status.

Berrettini et al. analyzed a pathological reflex as abnormal reflex, the lack of stapedial reflex and a positive Metz test result in patients with VS only at 1 frequency of 1,000 Hz.[28] Abnormal reflex was found in 59.5% of patients, which is consistent with the present study group (53%) and confirms a proper selection of patients for further analyses.

This study shows that the subjects with surgery-related hearing loss lower than 10 dB HL significantly more often had an abnormal ipsilateral stapedial reflex at the frequency of 500 Hz in the operated ear compared to the remaining groups of patients. Regarding the frequency of 1,000 Hz, it was demonstrated that the patients with a normal stapedial reflex significantly more commonly experienced major hearing loss (over 40 dB HL of PTA). Analogous results were also obtained for the frequency of 2,000 Hz.

A significant correlation was observed between surgery-related hearing loss and intensity value for the contralateral stapedial reflex at the frequency of 2,000 Hz for the non-operated ear. Considerably lower intensities were obtained in the group where the absolute hearing loss was the most marked (PTA over 40 dB HL), and the highest intensities were obtained in the group where surgery-related hearing loss was the least marked (PTA below 10 dB HL).

Moreover, surgery-related hearing loss increased with a reduction in the values of some preoperative parameters of impedance audiometry. This also indicates that a higher risk of marked absolute hearing loss did not only correlate with better hearing status.

To the best of our knowledge, no professional literature is available which would cover the topic of possible prognostic factors of hearing preservation regarding impedance audiometry.

Conclusions

Univariate analyses of audiologic results, such as pure-tone audiometry, speech audiometry, ABR test, and impedance audiometry coherently demonstrated that the better the preoperative hearing, the more substantial surgery-related hearing loss was observed.

The following preoperative audiologic parameters were demonstrated to have a prognostic value for the extent of surgery-related hearing loss in patients with vestibular schwannoma (Table 7): 1. pure-tone audiometry parameters such as: hearing threshold at 125 Hz, 500 Hz, 1,000 Hz,

Table 7. Statistically significant ($p < 0.5$) parameters influencing the extent of hearing loss following VS removal

Parameter
Pure-tone audiometry
hearing threshold at 125 Hz
hearing threshold at 250 Hz
hearing threshold at 500 Hz
hearing threshold at 1,000 Hz
Pure Tone Average – PTA
Hearing capacity
Hearing impairment according to BIAP
Speech audiometry
SDT
SRT
Did the patient achieve 100% of speech discrimination?
55 dB SPL
60 dB SPL
65 dB SPL
70 dB SPL
75 dB SPL
interaural difference 25 dB SPL
interaural difference 30 dB SPL
interaural difference 35 dB SPL
Auditory brainstem response testing
the presence of wave V
the value of I–V interval
deviation from the reference values of I–V interval
deviation from the reference values of III–V interval
normality of the amplitude ratio of waves V and I against reference values
Impedance audiometry
Ipsi 2,000 Hz for the operated ear
Contra 500 Hz for the non-operated ear
Contra 1,000 Hz for the non-operated ear
Contra 2,000 Hz for the non-operated ear
Contra 4,000 Hz for the non-operated ear
reflex normality for 500 Hz in the operated ear
reflex normality for 1,000 Hz in the operated ear
reflex normality for 2,000 Hz in the operated ear

and PTA for the affected ear; 2. speech audiometry parameters such as: speech discrimination between 55 Hz and 75 dB SPL, SDT for the affected ear, interaural difference in speech discrimination between 25 dB and 35 dB SPL; 3. speech audiometry showed that the surgery mostly affects those parameters of hearing which appear to be critical for interpersonal communication (speech intensity of 60 dB SPL) and a similar physical nerve fiber destruction is responsible for a disproportionately large reduction in perception compared to the perception of a different range of speech intensity; 4. auditory brainstem response test parameters such as: the presence of V wave, the values of I–V and III–V intervals and the amplitude of wave V; 5. impedance audiometry with parameters such as intensity level for obtaining stapedial reflex or an abnormal reflex at Ipsi 500 Hz, 1,000 Hz and 2,000 Hz, and Contra 500 Hz, 1,000 Hz, 2,000 Hz, and 4,000 Hz.

References

1. AAO-HNS. Committee on Hearing and Equilibrium guidelines for the evaluation of hearing preservation in acoustic neuroma (vestibular schwannoma). American Academy of Otolaryngology-Head and Neck Surgery Foundation, INC. *Otolaryngol Head Neck Surg.* 1995; 113(3):179–180. doi:10.1016/S0194-5998(95)70101-X
2. Hall JW III, Mueller HG III, eds. *Audiologists' Desk Reference: Volume I. Diagnostic Audiology Procedures and Practices.* San Diego, CA: Singular Publishing Group; 1997.
3. International Bureau for Audiophonology BIAP. Recommendation 02/1 bis – Audiometric classification of hearing impairments. www.biap.org. https://www.biap.org/en/recommandations/recommendations/tc-02-classification. Published October 26, 1996. Updated July 10, 2017. Accessed July 21, 2017.
4. Sanna M, Khrais T, Piccirillo E, Russo A, Augurio A. Hearing preservation surgery in vestibular schwannoma: The hidden truth. *Ann Otol Rhinol Laryngol.* 2004;113(2):156–163.
5. Samii M, Matthies C. Management of 1000 vestibular schwannomas (acoustic neuromas). The facial nerve: Preservation and restitution of function. *Neurosurgery.* 1997;40(4):684–695.
6. Kanzaki J, Tos M, Sanna M, Moffat DA. New and modified reporting systems from the consensus meeting on systems for reporting results in vestibular schwannoma. *Otol Neurotol.* 2003;24(4):642–649.
7. Kanzaki J, Kunihiro T, Inoue Y. Some proposals on reporting systems in acoustic neuroma. In: Kanzaki J, ed. *Acoustic Neuroma: Consensus on Systems for Reporting Results*. Keio University International Symposia for Life Sciences and Medicine. Vol 10. Tokyo–New York: Springer; 2003:107–112.
8. Shelton C, Brackmann DE, House WF, Hitselberger WE. Acoustic tumor surgery: Prognostic factors in hearing conservation. *Arch Otol Head Neck Surg.* 1989;115(10):1213–1216.
9. Hecht CS, Honrubia VF, Wiet RJ, Sims HS. Hearing preservation after acoustic neuroma resection with tumor size used as a clinical prognosticator. *Laryngoscope.* 1997;107(8):1122–1126.
10. Gardner G, Robertson JH. Hearing preservation in unilateral acoustic neuroma surgery. *Ann Otol Rhinol Laryngol.* 1988;97(1):55–66.
11. Koos WT, Day JD, Matula C, Levy DI. Neurotopographic considerations in the microsurgical treatment of small acoustic neurinomas. *J Neurosurg.* 1998;88(3):506–512.
12. Caye-Thomasen P, Dethloff T, Hansen S, Stangerup S-E, Thomsen J. Hearing in patients with intracanalicular vestibular schwannomas. *Audiol Neurotol.* 2007;12(1):1–12.
13. Kanzaki J, ed. Acoustic Neuroma: *Consensus on Systems for Reporting Results*. Keio University International Symposia for Life Sciences and Medicine. Springer. 2003;10:183–192.
14. Fukushima T. Patient selection and method of evaluation for hearing preservation in acoustic neuroma surgery. In: Kanzaki J, ed. *Acoustic Neuroma: Consensus on Systems for Reporting Results*. Keio University International Symposia for Life Sciences and Medicine. Vol 10. Tokyo–New York: Springer; 2003:101–105.
15. Dugar J, Nikolopoulos TP, O'Donoghue GM. Hearing preservation in acoustic neuroma surgery: The impact of different patient selection criteria. *Laryngoscope.* 2002;112(11):2051–2053.
16. Lassaletta L, Fontes L, Melcon E, Sarria MJ, Gavilan J. Hearing preservation with the retrosigmoid approach for vestibular schwannoma: Myth or reality? *Otolaryngol Head Neck Surg.* 2003;129(4):397–401.
17. Ferber-Viart C, Laoust L, Boulud B, Duclaux R, Dubreuil C. Acuteness of preoperative factors to predict hearing preservation in acoustic neuroma surgery. *Laryngoscope.* 2000;110(1):145–150.
18. Rohit, Piccirillo E, Jain Y, Augurio A, Sanna M. Preoperative predictive factors for hearing preservation in vestibular schwannoma surgery. *Ann Otol Rhinol Laryngol.* 2006;115(1):41–46.
19. Slattery WH III, Brackmann DE, Hitselberger W. Middle fossa approach for hearing preservation with acoustic neuromas. *Otol Neurotol.* 1997; 18(5):596–601.
20. Brackmann DE, Owens RM, Friedman RA, et al. Prognostic factors for hearing preservation in vestibular schwannoma surgery. *Otol Neurotol.* 2000;21(3):417–424.
21. Rastogi P, Cacace AT, Lovely TJ. Factors influencing hearing preservation in acoustic tumor surgery. *Skull Base Surg.* 1995;5(3):137–142.

22. Glasscock ME III, Hays JW, Minor LB, Haynes DS, Carrasco VN. Preservation of hearing in surgery for acoustic neuromas. *J Neurosurg*. 1993;78(6):864–870.
23. Dornhoffer JL, Helms J, Hoehmann DH. Hearing preservation in acoustic tumor surgery: Results and prognostic factors. *Laryngoscope*. 1995;105(2):184–187.
24. Matthies C, Samii M. Management of vestibular schwannomas (acoustic neuromas): The value of neurophysiology for evaluation and prediction of auditory function in 420 cases. *Neurosurgery*. 1997; 40(5):919–930.
25. Browning S, Mohr G, Dufour JJ, et al. Hearing preservation in acoustic neuroma surgery. *J Otolaryngol*. 2001;30(5):307–315.
26. Kanzaki J, Ogawa K, Inoue Y, Shiobara R. Hearing preservation surgery in acoustic neuroma patients with normal hearing. *Skull Base Surg*. 1997;7(3):109–113.
27. Vincent C, Bonne N-X, Guérin C, et al. Middle fossa approach for resection of vestibular schwannoma: Impact of cochlear fossa extension and auditory monitoring on hearing preservation. *Otol Neurotol*. 2012;33(5):849–852.
28. Berrettini S, Ravecca F, Sellari-Franceschini S, Bruschini P, Casani A, Padolecchia R. Acoustic neuroma: Correlations between morphology and otoneurological manifestations. *J Neurol Sci*. 1996;144(1):24–33.

VEGF serum concentration and irreversible bronchoconstriction in adult asthmatics

Krzysztof Gomułka[1,A,B,D], Jerzy Liebhart[1,F], Urszula Gładysz[2,C], Wojciech Mędrala[1,E]

[1] Department of Internal Medicine and Allergology, Wroclaw Medical University, Poland
[2] Institute of Informatics, University of Wrocław, Poland

A – research concept and design; B – collection and/or assembly of data; C – data analysis and interpretation;
D – writing the article; E – critical revision of the article; F – final approval of the article

Advances in Clinical and Experimental Medicine, ISSN 1899–5276 (print), ISSN 2451–2680 (online) *Adv Clin Exp Med*. 2019;28(6):759–763

Address for correspondence
Krzysztof Gomułka
E-mail: krzysztof.gomulka@umed.wroc.pl

Funding sources
This study was supported by the grant for young scientists No. Pbmn 150 from Wroclaw Medical University in Poland (granted to Krzysztof Gomułka).

Conflict of interest
None declared

Acknowledgements
The authors thank Barbara Majewska for performing spirometry tests and Emilia Królewicz for laboratory analyses.

Received on October 22, 2017
Reviewed on February 1, 2018
Accepted on June 6, 2018

Published online on February 8, 2019

Abstract

Background. Vascular endothelial growth factor (VEGF) is an angiogenic, heparin-binding glycoprotein playing an important role in the pathogenesis of many diseases and disorders, including asthma. It has been reported that increased VEGF serum concentration is a biomarker of neovascularization, which could suggest that higher VEGF expression may be relevant to asthmatics with airway remodeling and irreversible bronchoconstriction.

Objectives. The aim of this study was to assess the possible association between VEGF serum concentration and irreversible bronchoconstriction in adult patients with a diagnosis of asthma.

Material and methods. This study involved 82 adult patients with asthma (42 persons with and 40 persons without irreversible bronchoconstriction) and 40 healthy adult controls. Vascular endothelial growth factor serum concentration was analyzed using enzyme-linked immunosorbent assay (ELISA).

Results. Vascular endothelial growth factor serum concentration in patients with asthma was higher than in healthy controls ($p = 0.0131$), particularly in those from the subgroup of irreversible bronchoconstriction ($p = 0.0133$). The rising tendency was confirmed using the Kruskal–Wallis rank sum test that showed a significant difference ($p = 0.0374$) in VEGF values among the 3 groups examined: healthy controls (Me = 246.6 pg/mL), asthmatics with reversible bronchoconstriction (Me = 288.6 pg/mL) and asthmatics with irreversible bronchoconstriction (Me = 340.6 pg/mL). However, the direct comparison between the 2 asthmatics groups (reversible vs irreversible bronchoconstriction) did not show a statistically significant difference ($p = 0.5521$).

Conclusions. Increased VEGF serum concentration is characteristic of patients with asthma, especially those with irreversible bronchoconstriction.

Key words: asthma, vascular endothelial growth factor, remodeling, bronchoconstriction

Cite as
Gomułka K, Liebhart J, Gładysz U, Mędrala W. VEGF serum concentration and irreversible bronchoconstriction in adult asthmatics. *Adv Clin Exp Med*. 2019;28(6):759–763. doi:10.17219/acem/92012

DOI
10.17219/acem/92012

Introduction

Vascular endothelial growth factor (VEGF) is a dimeric, heparin-binding glycoprotein with a molecular weight of 46 kDa. The VEGF family consists of several members, e.g.: VEGF-A (discovered first and called just VEGF), VEGF-B, VEGF-C, VEGF-D, and placenta growth factor (PGF). The *VEGF* gene has the chromosomal locus on 6p21.3 and contains a 14-kb coding region with 8 exons and 7 introns. Splicing of a single gene results in transcription of VEGF variants with different numbers of amino acids identified in human cells. Among them, $VEGF_{121}$ and $VEGF_{165}$ are secreted as soluble forms, whereas $VEGF_{189}$ and $VEGF_{206}$ are associated with the cells' surface.[1,2] Primarily, VEGF is expressed in epithelial cells, platelets, neutrophils, and macrophages. The biological activity of VEGF is dependent on interaction between soluble forms of this glycoprotein and one of the receptors (VEGF-R1, VEGF-R2 or VEGF-R3) that are mainly expressed in endothelial cells, activated macrophages and epithelial cells. Receptors for VEGF belong to the tyrosine kinase receptors which, after VEGF-stimulation, dimerize and become activated through transphosphorylation.[3] Vascular endothelial growth factor seems to specifically affect endothelial cells' growth, survival and permeability, and moreover, it enhances vascular permeability, modulates thrombogenicity, protects endothelial cells against apoptosis and delays endothelial cell senescence.[4,5]

Previous studies have reported that increased mean VEGF serum concentration may be related to tissue hypoxia and inflammation during age-related macular degeneration,[6] rheumatoid diseases,[7] sepsis,[8] coronary heart disease,[9] chronic obstructive pulmonary disease (COPD),[10] and cancers.[11,12] For this reason, the peripheral VEGF levels have been considered as a biomarker of neovascularization and vascular remodeling. Hypoxia as well as inflammation are also relevant to asthma – therefore the biological properties of VEGF have led to interest of this molecule within the lung, suggesting that the higher expression of VEGF may play a potential role in the pathogenesis of asthma and lung remodeling.[13–15] Vascular endothelial growth factor can promote proliferation of airway smooth muscle (ASM) cells. It upregulates disintegrin and metalloproteinase (ADAM-33) mRNA and protein levels in a dose- and time-dependent manner as well as phosphorylation of phospho-extracellular signal-regulated kinase 1/2 (ERK1/2) and phospho-Akt (Akt).[16] In addition, longitudinal analysis performed in a study by the Childhood Asthma Management Program (CAMP) showed an association of the rs4711750 VEGF genotype with FEV_1/FVC decline over 4.5 years of observation.[17]

Despite the existence of such strong indications that VEGF may play an important role in the asthma pathomechanism and the development of airway remodeling, we have not found in the available literature any report on the possible connection of VEGF serum concentration with irreversible bronchoconstriction in adult asthmatics. Therefore, the aim of the present study was to compare VEGF serum concentrations in asthmatics and healthy individuals and to assess whether they were associated with irreversible bronchoconstriction.

Material and methods

The study sample consisted of 122 participants (42 male) aged 20–70 years, of whom 40 subjects (14 male) did not manifest any allergies and had normal pulmonary function. Among this control group, 11 participants had a positive history toward smoking. In a group of 82 patients (28 male) aged 23–69 years, the diagnosis of asthma was established according to the Global Initiative for Asthma (GINA) recommendations. Patients diagnosed with ACO (asthma-COPD overlap) were excluded from our study. The degree of severity of asthma ranged from sporadic to severe and persistent. On the basis of the bronchodilation test, asthmatics were divided into 2 subgroups: patients with irreversible bronchoconstriction (42 patients, 17 male, aged 24–69 years) and patients without irreversible bronchoconstriction (40 patients, 11 male, aged 23–69 years). In the asthmatics with reversible bronchoconstriction, 6 patients had positive smoking history, 27 participants used inhaled corticosteroids (budesonide or fluticasone propionate), 28 patients were treated with long-acting β2 agonists (salmeterol or formoterol fumarate), and 38 patients declared using short-acting β2 agonists "on demand" (salbutamol or fenoterol hydrobromide + ipratropium bromide). Among the asthmatics with irreversible bronchoconstriction, 15 patients had positive smoking history, 37 participants used inhaled corticosteroids (budesonide or fluticasone propionate), 38 patients were treated with long-acting β2 agonists (salmeterol or formoterol fumarate), and 42 patients declared using short-acting β2 agonists "on demand" (salbutamol or fenoterol hydrobromide + ipratropium bromide). The population data is shown in Table 1.

The study protocol was approved by the Ethics Committee of Wroclaw Medical University, Poland.

Bronchodilation test

The pulmonary function test and bronchodilation test, specifying forced vital capacity (FVC) and forced expiratory volume in 1 s (FEV1) values, were performed using a MasterScope CT Spirometer (Erich Jaeger GmbH, Würzburg, Germany). The bronchodilation test was performed after inhalation with 5 mg of salbutamol (SteriNeb Salamol; Teva Pharmaceuticals, Warszawa, Poland) administered with a jet nebulizer (Model 4650-U; Devilbiss, Heston, UK). The postbronchodilator values of FEV1/FVC <0.7 and FEV1 <80% predicted were taken as a criterion of irreversible bronchoconstriction.

Table 1. Characteristics of study population

Parameter	Asthmatics – irreversible bronchoconstriction	Asthmatics – reversible bronchoconstriction	Controls
n	42	40	40
Male gender	17 (40.48%)	11 (27.5%)	14 (35%)
Age [years], $\bar{x}$ ±SD	53.71 ±10.40	50.03 ±13.65	47.95 ±13.66
Age [years], Me (min–max)	55 (24–69)	52 (23–69)	52.5 (20–70)
Disease duration [mean years]	21.94	10.04	–
FVC%, $\bar{x}$ ±SD	72.21 ±19.31	98.49 ±13.89	101.36 ±13.26
FEV1%, $\bar{x}$ ±SD	56.05 ±18.62	90.12 ±17.25	104.81 ±15.37
FEV1/FVC, $\bar{x}$ ±SD	0.61 ±0.11	0.73 ±0.10	0.82 ±0.06
Smoking (answer "yes")	15 (35.71%)	6 (15%)	11 (27.5%)
inhGKS	37 (88.1%)	27 (67.5%)	–
LABA	38 (90.48%)	28 (70%)	–
SABA "on demand"	42 (100%)	38 (95%)	–

$\bar{x}$ – mean; SD – standard deviation; Me – median; min–max – minimum–maximum; FVC% – forced vital capacity, % of predicted; FEV1% – forced expiratory volume in 1 s, % of predicted; inhGKS – inhaled corticosteroids; LABA – long-acting beta-2 agonists; SABA – short-acting beta-2 agonists.

VEGF serum concentration

To estimate the mean VEGF serum concentration, the "sandwich" enzyme-linked immunosorbent assay (ELISA) was used. The VEGF concentration was measured in pg/mL and the Quantikine Human VEGF Immunoassay Kit was used according to the recommendation of the manufacturer. The minimum detectable VEGF concentration was no less than 5.0 pg/mL. Individual blood samples were assayed twice and the average value was taken for further analysis. The normal values of VEGF serum concentration extend from 62.0 pg/mL to 707.0 pg/mL.

Statistical analysis

Statistical analysis was performed using the STATISTICA v. 10 for Windows statistical program (StatSoft Inc., Tulsa, USA). Data distribution was evaluated using the Shapiro-Wilk W test. Nonparametric statistics were used for variables without normal distribution. The data was analyzed using descriptive statistics methods and Kruskal-Wallis and Mann-Whitney U tests. A p-value <0.05 was considered statistically significant.

Results

Statistical analyses (Tables 2, 3) showed that VEGF serum concentration in all patients with asthma was higher than in healthy controls (p = 0.0131; odds ratio (OR) = 2.38; 95% confidence interval (95% CI) = 1.00–5.69), particularly in those from the subgroup of irreversible bronchoconstriction (p = 0.0133; OR = 3.48; 95% CI = 0.62–4.67). The increasing tendency was confirmed with the Kruskal-Wallis rank sum test that showed a significant difference (p = 0.0374) in VEGF values among the 3 groups examined:

Table 2. VEGF serum concentrations [pg/mL] in the study sample

Examined groups	Me (min–max)
Asthmatics – irreversible bronchoconstriction	340.65 (85.9–1,470.0)
Asthmatics – reversible bronchoconstriction	288.6 (71.7–1,134.0)
Asthmatics – whole examined group	314.35 (71.7–1,470.0)
Controls	246.6 (57.3–714.7)

Me – median; min–max – minimum–maximum.

Table 3. Comparisons of VEGF serum concentration [pg/mL] between groups examined

Compared groups	p-value
Asthmatics with irreversible bronchoconstriction vs asthmatics with reversible bronchoconstriction vs controls	0.0374#
Asthmatics with reversible bronchoconstriction vs controls	0.0705*
Asthmatics with irreversible bronchoconstriction vs controls	0.0133*
Asthmatics with irreversible bronchoconstriction vs asthmatics with reversible bronchoconstriction	0.5221*
Asthmatics/whole examined group/vs controls	0.0131*

* – Mann-Whitney U test; # – Kruskal-Wallis ANOVA test.

healthy controls (median (Me) = 246.6 pg/mL), asthmatics with reversible bronchoconstriction (Me = 288.6 pg/mL) and asthmatics with irreversible bronchoconstriction (Me = 340.6 pg/mL). However, the direct comparison between the 2 latter groups (asthmatics with reversible vs irreversible bronchoconstriction) did not show a statistically significant difference (p = 0.5521; OR = 2.05; 95% CI = 0.67–6.39). Spearman's rank correlation coefficient did

not show any significant difference in asthmatics between VEGF serum concentration and spirometric values (FVC%, FEV1% and FEV1/FVC) and between the age of patients and FEV1% value. The comparison between asthmatics with and without irreversible bronchoconstriction and with positive smoking history showed a statistically significant difference (p = 0.0317; OR = 3.15; 95% CI = 0.97–10.62).

Discussion

Vascular endothelial growth factor was first described in 1983 by Senger et al. as the vascular permeability factor (VPF) secreted by tumor cells.[18] Its protein structure and significance were later identified by Ferrara and Henzel.[19] Since then, several studies have also investigated circulating VEGF levels in patients with asthma, indicating its role in inflammation and neovascularization.[20–22] The clinical picture of asthma depends on a variety of factors, probably including (among other things) the *VEGF* gene polymorphism.[15] Significant differences in VEGF concentration between patients with asthma and controls have been shown not only in induced sputum, but also in bronchoalveolar lavage or bronchial biopsies.[23,24] The authors observed higher overall levels of VEGF in samples taken from patients with asthma. The findings also suggest the influence of VEGF on the hyperactivity of airways and reduction of bronchial diameter by thickening the bronchial wall during the remodeling process. In a previous study, Barbato et al.[25] observed an inverse correlation between FEV1 values and the number of vessels in the lamina propria of airways in patients with asthma and atopy. Results obtained by Abdel-Rahman et al.[26] showed that VEGF concentration is increased and proportional to the severity of asthma in children during exacerbations of asthma associated with respiratory tract infection. The results of the current study have shown that VEGF serum concentrations are elevated in patients with asthma, especially in those with irreversible bronchoconstriction. However, the difference between the groups with reversible and non-reversible bronchoconstriction was not statistically significant, which could be partly attributed to the relatively small sample size.

It has been known that VEGF levels may depend on, among others, status of smoking, the effect of inhaled corticosteroids, duration of asthma, or eosinophilic inflammatory profiles.[27] According to the Global Initiative for Asthma (GINA) report,[28] cigarette smoking is a modifiable risk factor connected with asthma exacerbation and persistence of airway obstruction. The results obtained confirm that a positive history toward smoking promotes the development of irreversible bronchoconstriction in asthmatics. However, smoking cannot be regarded as a single and dominant factor for remodeling because the majority of asthmatics with irreversible bronchoconstriction have never smoked. In the groups examined, a relationship between therapy with inhaled corticosteroids and degree of bronchoconstriction was not revealed. In asthmatics, treatment with inhaled corticosteroids was declared mostly in the group with irreversible bronchoconstriction, which suggests that inhaled corticosteroids may delay the progression of airway remodeling but is unable to effectively prevent bronchoconstriction. Another factor that may correlate with the VEGF level and severity of remodeling in the airways is the asthma duration. In our study, longer duration of asthma was demonstrated in patients with irreversible bronchoconstriction, which seems to confirm that for remodeling connected with irreversible airway narrowing, the duration of the disease also should be taken into account. On the other hand, it is difficult to determine the influence of the sex and age of the patients examined on the severity of the remodeling and bronchoconstriction, as the percentage of women and men was similar and the median age and age range of patients in the examined groups were similar. A limitation in our study was not taking into account the atopic status of patients, family history toward allergy, place of living (city or village), additional diseases (e.g., pulmonary and cardiac failure), or the number of eosinophils. Also, the measurements of bronchial wall thickness using computed tomography (CT) were not performed. This issue is undoubtedly worth conducting further extensive studies because VEGF seems to be an emerging target for novel asthma therapies. It should be noted that several anti-VEGF drugs are already available (e.g., ranibizumab or bevacizumab), licensed for use in various diseases (mainly in oncological disorders and eye diseases).[29,30]

References

1. Ferrara N, Gerber HP, LeCouter J. The biology of VEGF and its receptors. *Nat Med*. 2003;9(6):669–676.
2. Gomułka K, Liebhart J. Vascular endothelial growth factor: Structure, function and role in airways inflammation and the clinical course of asthma [in Polish]. *Pneumonol Alergol Pol*. 2009;77(6):549–553.
3. Gover-Proaktor A, Granot G, Shapira S, et al. Ponatinib reduces viability, migration, and functionality of human endothelial cells. *Leuk Lymphoma*. 2017;58(6):1455–1467.
4. Yamamoto H, Rundqvist H, Branco C, Johnson RS. Autocrine VEGF isoforms differentially regulate endothelial cell behavior. *Front Cell Dev Biol*. 2016;4:99.
5. Xin H, Zhong C, Nudleman E, Ferrara N. Evidence for pro-angiogenic functions of VEGF-Ax. *Cell*. 2016;167(1):275–284.
6. Campochiaro PA, Aiello LP, Rosenfeld PJ. Anti-vascular endothelial growth factor agents in the treatment of retinal disease: From bench to bedside. *Ophthalmology*. 2016;123(10S):78–88.
7. Paradowska-Gorycka A, Pawlik A, Romanowska-Prochnicka K, et al. Relationship between VEGF gene polymorphisms and serum VEGF protein levels in patients with rheumatoid arthritis. *PLoS One*. 2016; 11(8):e0160769.
8. Heitrich M, García DM, Stoyanoff TR, Rodríguez JP, Todaro JS, Aguirre MV. Erythropoietin attenuates renal and pulmonary injury in polymicrobial induced-sepsis through EPO-R, VEGF and VEGF-R2 modulation. *Biomed Pharmacother*. 2016;82:606–613.
9. Bulysheva AA, Hargrave B, Burcus N, Lundberg CL, Murray L, Heller RR. Vascular endothelial growth factor-A gene electrotransfer promotes angiogenesis in a porcine model of cardiac ischemia. *Gene Ther*. 2016;23(8–9):649–656.
10. García-Lucio J, Argemi G, Tura-Ceide O, et al. Gene expression profile of angiogenic factors in pulmonary arteries in COPD: Relationship with vascular remodeling. *Am J Physiol Lung Cell Mol Physiol*. 2016; 310(7):583–592.

11. Wheler JJ, Janku F, Naing A, et al. TP53 alterations correlate with response to VEGF/VEGFR inhibitors: Implications for targeted therapeutics. *Mol Cancer Ther*. 2016;15(10):2475–2485.
12. Wojtukiewicz MZ, Sierko E, Skalij P, et al. Granulocyte-colony stimulating factor receptor, tissue factor, and VEGF-R bound VEGF in human breast cancer in loco. *Adv Clin Exp Med*. 2016;25(3):505–511.
13. Grzela K, Litwiniuk M, Krejner A, Zagorska W, Grzela T. Increased angiogenic factors in exhaled breath condensate of children with severe asthma: New markers of disease progression? *Respir Med*. 2016;118:119–121.
14. Lee KY, Lee KS, Park SJ, et al. Clinical significance of plasma and serum vascular endothelial growth factor in asthma. *J Asthma*. 2008;45(9): 735–739.
15. Lachheb J, Chelbi H, Dhifallah IB, et al. Association of vascular endothelial growth factor polymorphisms with asthma in Tunisian children. *Gene Regul Syst Bio*. 2008;2:89–96.
16. Pei QM, Jiang P, Yang M, et al. Upregulation of a disintegrin and metalloproteinase-33 by VEGF in human airway smooth muscle cells: Implications for asthma. *Cell Cycle*. 2016;15(20):2819–2826.
17. Sharma S, Murphy AJ, Soto-Quiros ME, et al. Association of VEGF polymorphisms with childhood asthma, lung function and airway responsiveness. *Eur Respir J*. 2009;33(6):1287–1294.
18. Senger DR, Galli SJ, Dvorak AM, Perruzzi CA, Harvey VS, Dvorak HF. Tumor cells secrete a vascular permeability factor that promotes accumulation of ascites fluid. *Science*. 1983;219(4587):983–985.
19. Ferrara N, Henzel WJ. Pituitary follicular cells secrete a novel heparin-binding growth factor specific for vascular endothelial cells. *Biochem Biophys Res Commun*. 1989;161(2):851–858.
20. Czarniakowska-Bołtuć M, Ziętkowski Z, Bodzenta-Łukaszyk A. Rola wybranych czynników wzrostowych w astmie. *Alergia Astma Immunol*. 2012;17:172–179.
21. Meyer N, Akdis CA. Vascular endothelial growth factor as a key inducer of angiogenesis in the asthmatic airways. *Curr Allergy Asthma Rep*. 2013;13(1):1–9.
22. Li X, Wilson JW. Increased vascularity in the bronchial mucosa in mild asthma. *Am J Respir Crit Care Med*. 1997;156(1):229–233.
23. Lee C, Ma B, Takyar S, et al. Studies of vascular endothelial growth factor in asthma and chronic obstructive pulmonary disease. *Proc Am Thorac Soc*. 2011;8(6):512–515.
24. Koczy-Baron E, Kasperska-Zając A. Rola naczyniowo-śródbłonkowego czynnika wzrostu w procesach zapalnych. *Postepy Hig Med Dosw (Online)*. 2014;68:57–65.
25. Barbato A, Turato G, Baraldo S, et al. Airway inflammation in childhood asthma. *Am J Respir Crit Care Med*. 2003;168(7):798–803.
26. Abdel-Rahman AM, el-Sahrigy SA, Bakr SI. A comparative study of two angiogenic factors: Vascular endothelial growth factor and angiogenin in induced sputum from asthmatic children in acute attack. *Chest*. 2006;129(2):266–271.
27. Asai K, Kanazawa H, Kamoi H, Shiraishi S, Hirata K, Yoshikawa J. Increased levels of vascular endothelial growth factor in induced sputum in asthmatic patients. *Clin Exp Allergy*. 2003;33(5):595–599.
28. Global Initiative for Asthma. Global Strategy for Asthma Management and Prevention 2017 (revision). https://ginasthma.org/wms-GINA-2017-main-report-tracked-changes-for-archive.pdf
29. Chebib R, Verlingue L, Cozic N, et al. Angiogenesis inhibition in the second-line treatment of metastatic colorectal cancer: A systematic review and pooled analysis. *Semin Oncol*. 2017;44(2):114–128.
30. Evans J, Virgili G. Anti-VEGF drugs: Evidence for effectiveness. *Community Eye Health*. 2014;27(87):48.

The clinical significance of intrahepatic Th22 cells in liver cirrhosis

Shanyu Qin[A,D,F], Mei Chen[B,C], Xiaoyun Guo[B,F], Wei Luo[C,D,F], Jiaxu Wang[B,C,F], Haixing Jiang[A,E,F]

Department of Gastroenterology, First Affiliated Hospital of Guangxi Medical University, Nanning, China

A – research concept and design; B – collection and/or assembly of data; C – data analysis and interpretation;
D – writing the article; E – critical revision of the article; F – final approval of the article

Advances in Clinical and Experimental Medicine, ISSN 1899–5276 (print), ISSN 2451–2680 (online) *Adv Clin Exp Med*. 2019;28(6):765–770

Address for correspondence
Haixing Jiang
E-mail: gxjianghx@163.com

Funding sources
None declared

Conflict of interest
None declared

Received on November 23, 2015
Reviewed on December 30, 2015
Accepted on August 8, 2018

Published online on February 8, 2019

Abstract

Background. Th22 cells are a recently identified $CD4^+$ T helper subset and have been implicated in the pathogenesis of certain diseases in humans, but the role of Th22 cells in liver cirrhosis (LC) remains unclear.

Objectives. The aim of the study was to investigate the expression and clinical significance of intrahepatic Th22 cells in LC tissues.

Material and methods. Samples of liver tissue of 20 LC patients and 12 normal controls (NC) were collected. Interleukin 22 (IL-22), IL-22R1 mRNA and aryl hydrocarbon receptor (AHR) expression were examined using quantitative reverse transcription polymerase chain reaction (RT-PCR). The protein expression of Th22 and $CD4^+$ cells in liver tissue was measured with immunohistochemistry.

Results. The number of intrahepatic Th22 and $CD4^+$ cells increased markedly in LC patients and the number of Th22 cells positively correlated with the number of $CD4^+$ cells ($p < 0.05$). Moreover, the number of Th22 cells positively correlated with the serum levels of alanine aminotransferase (ALT) and aspartate aminotransferase (AST), as well as the Child-Pugh score in LC patients ($p < 0.05$). The expression of IL-22, IL-22R1 and AHR in LC patients was significantly increased compared with the NC group ($p < 0.05$).

Conclusions. Our findings suggest that the expression of intrahepatic Th22 cells increased in LC patients and was associated with the progression of LC.

Key words: Th22 cells, liver cirrhosis, clinical significance

Cite as
Qin S, Chen M, Guo X, Luo W, Wang J, Jiang H. The clinical significance of intrahepatic Th22 cells in liver cirrhosis. *Adv Clin Exp Med*. 2019;28(6):765–770. doi:10.17219/acem/94062

DOI
10.17219/acem/94062

Introduction

Chronic hepatitis B (CHB) infection affects approx. 350 million individuals worldwide. It has become a major public health threat, especially in China, where 0.5–1.0 million individuals die due to HBV-associated liver diseases each year.[1] Liver cirrhosis (LC) is defined as the accumulation of extracellular matrix (ECM) forming fibrous scars that distort the hepatic architecture, and the subsequent development of nodules of regenerating hepatocytes.

It has been demonstrated that $CD4^+$ cells are essential to controlling HBV infection.[2] Th22 cells are a recently identified $CD4^+$ T helper subset distinct from Th17 and Th1 cells. They are characterized by particularly high interleukin 22 (IL-22) production, but not IL-17 or interferon gamma (IFN-γ), and they express the chemokine receptors CCR4, CCR6 and CCR10.[3,4] Th22 cells have been implicated in the pathogenesis of certain diseases in humans, such as psoriasis,[5] Crohn's disease[6] and gastric cancer.[7] However, the nature of Th22 cells in HBV-associated LC remains poorly understood.

In the present study, we investigated the number of Th22 and $CD4^+$ cells in the liver tissue of patients with HBV-associated LC and analyzed possible associations between Th22 and $CD4^+$ cells and various clinical parameters, as well as the expression of transcription factor aryl hydrocarbon receptor (AHR), IL-22 and IL-22R1, aiming to reveal the possible mechanism of Th22 cell involvement in HBV-associated liver cirrhosis.

Material and methods

Patient selection

Between October 2012 and May 2014, liver biopsies or surgically removed specimens were collected from 20 HBV-LC patients; samples from 12 patients who had undergone hepatic hemangiomas or cysts and had normal liver tissues were used as normal controls (NC). The diagnoses of LC were made according to previously described criteria.[8,9] Patients who were co-infected with human immunodeficiency virus (HIV) or other hepatitis viruses or autoimmune diseases were excluded from the study group. None of the participants received anti-HBV agents or steroids within 6 months prior to the sampling. Patients with viral hepatitis, autoimmune hepatitis and alcoholic liver diseases were excluded from the NC group. Written informed consent was obtained from each participant and the study protocol was approved by the Ethics Committee of the First Affiliated Hospital of Guangxi Medical University, Nanning, China.

Real-time polymerase chain reaction analysis

The total RNA of the liver samples was isolated from the liver tissues using Invitrogen TRIzol Reagent (Thermo Fisher Scientific Inc., Waltham, USA). cDNA synthesis was performed using PrimeScript RT Reagent Kits (Roche Diagnostics Corp., Indianapolis, USA). Real-time polymerase chain reaction (RT-PCR) was performed using Real-Time PCR Master Mix (Roche Diagnostics) according to the manufacturer's protocol. The primers are described as follows: IL-22 forward: ACT GGA TTT GCT GTT TAT GTC TCT G; IL-22 reverse: GGC TTC CCA TCT TCC TTT TG; IL-22R1 forward: TGG CAA AGA AGG GCT GTC AG; IL-22R1 reverse: GCG GTG ACC CTG GCA TAG T; AHR forward: TGT CGT CTA AGG TGT CTG CTG GA; AHR reverse: ACA AAG CCA ACT GAG GTG GAA GTA; *GAPDH* forward: GCA CCG TCA AGG CTG AGA AC; *GAPDH* reverse: TGG TGA AGA CGC CAG TGG A. *GAPDH* was measured as a housekeeping gene. Real-time PCR was performed using SYBR Green PCR Master Mix (Roche Diagnostics) on an ABI 7500 Real-Time PCR System (Applied Biosystems, Thermo Fisher Scientific). After an initial denaturation step for 3 min at 94°C, a 3-step cycling procedure (denaturation at 94°C for 30 s, annealing at 60°C for 30 s and extension at 72°C for 60 s) was used for 35 cycles. Samples were assayed in triplicate. The expression ratio of each gene of interest (GOI) between different groups was analyzed using the ΔΔCT method.

Immunohistochemistry

Immunohistochemical staining was performed with the streptavidin-biotin complex method, using streptavidin and biotin (Thermo Fisher Scientific), according to the manufacturer's instructions. Paraffin-embedded, formalin-fixed liver tissues were cut into 3-μm sections and placed on polylysine-coated slides. Each paraffin section was deparaffinized and rehydrated through a graded series of ethanol. Endogenous peroxidase was blocked using a 3% H_2O_2 methanol solution, and 5% goat serum albumin (Zhongshan Golden Bridge Biotech, Beijing, China) was applied to block non-specific staining. A 1:500 dilution of rabbit anti-human IL-22 (Thermo Fisher Scientific) and ready-to-use rabbit anti-human CD4 antibody (Zhongshan Golden Bridge Biotech) were used for the immunohistochemistry staining of IL-22 and CD4. Incubation of a biotin-free secondary antibody and horseradish peroxidase (Zhongshan Golden Bridge Biotech) was subsequently performed, followed by development with diaminobenzidine (Zhongshan Golden Bridge Biotech) and counterstaining with hematoxylin. Instead of a primary antibody, non-immune goat serum was taken as a control. The rates of positive staining in 5 randomly chosen high-power (×400) fields of view were counted separately by 2 experienced pathologists. The numbers of positive cells in the same 5 high-power fields of view were also counted. The mean frequency of positive staining in each slide was then obtained. None of the pathologists were aware of the clinical diagnosis of the patient associated with any tissue section at the time of analysis.

Statistical analysis

All the data was analyzed using SPSS software v. 16.0 for Windows (SPSS Inc., Chicago, USA). The results are presented as means with standard deviation (SD) using GraphPad Prism 5 software (GraphPad Software Inc., La Jolla, USA). Demographic and clinical data between groups was compared using the χ^2 test or Student's t-test, as appropriate. Pearson's correlation coefficient or Spearman's rank correlation coefficient were used for correlation analysis depending on the data distribution. A value of $p < 0.05$ was considered significant.

Results

Clinical data of the subjects

Table 1 shows the clinical data of the LC and NC groups. There were statistically significant differences in the serum concentrations of alanine aminotransferase (ALT0), aspartate aminotransferase (AST), total bilirubin (TBIL), the hepatitis Be antigen (HBeAg) positive rates, and Child-Pugh scores between the LC and NC patients ($p < 0.05$). No significant differences were found between the LC and NC patients in terms of gender or age ($p > 0.05$).

Table 1. Clinical characteristics of the study participants

Parameters	LC group	NC group	p-value
Cases, n	20	12	–
Gender, n (male/female)	16/4	7/5	0.240
Age [years]	42 (13.75)	44.5 (12.5)	0.421
ALT serum level [U/L]	32 (21.75)	22.5 (16.25)	0.025
AST serum level [U/L]	26 (15.75)	20.5 (10.75)	0.015
TBIL serum level [μmol/L]	20.45 (13.83)	10.55 (6.93)	0.000
HBeAg (+/–)	7/13	0/12	0.029
HBV DNA (+/–)	11/9	ND	–
Child-Pugh score (A/B/C)	12/8/0	12/0/0	0.014

LC group – HBV-associated liver cirrhosis patients; NC group – normal controls; ALT – alanine aminotransferase; AST – aspartate aminotransferase; TBIL – total bilirubin; HBeAg – hepatitis Be antigen; ND – not determined; The data for age group, ALT, AST, and TBIL are shown as medians (interquartile range).

Distribution of Th22 and CD4$^+$ cells in liver tissues

Immunohistochemistry showed that IL-22 had a cytoplasmic staining pattern, and a large number of lymphocytes had infiltrated the livers of patients with HBV-associated LC (Fig. 1A,B). Th22 cells were mainly located in the portal area of the liver and could also be found in the lobes, especially in the inflammatory regions (Fig. 1B). In contrast, few or no Th22 cells were observed in the NC group (Fig. 1C). The CD4$^+$T cells had mainly infiltrated the portal areas of the liver in the LC group, and were distinctly expressed in the membranes of the cells (Fig. 1D,E), but were rarely found in the NC group (Fig. 1F).

A significantly stronger expression of Th22 cells was detected in the LC patients (65.06 ±35.01) than in the NC group (4.17 ±2.79, $p < 0.001$, Fig. 2A). The frequencies of CD4$^+$T cells were significantly increased in the LC group (70.94 ±25.13) compared with the NC group (4.5 ±1.76, $p < 0.001$, Fig. 2B). According to the immunohistochemistry results, the number of Th22 cells in the liver was positively correlated with the number of CD4$^+$T cells in both the NC group ($r = 0.944$, $p = 0.005$; Fig. 2C) and the LC group ($r = 0.966$, $p < 0.01$; Fig. 2D).

Correlation between the number of Th22 cells and clinical parameters

In the LC patients, the number of Th22 cells was positively correlated with the serum levels of ALT ($r = 0.642$,

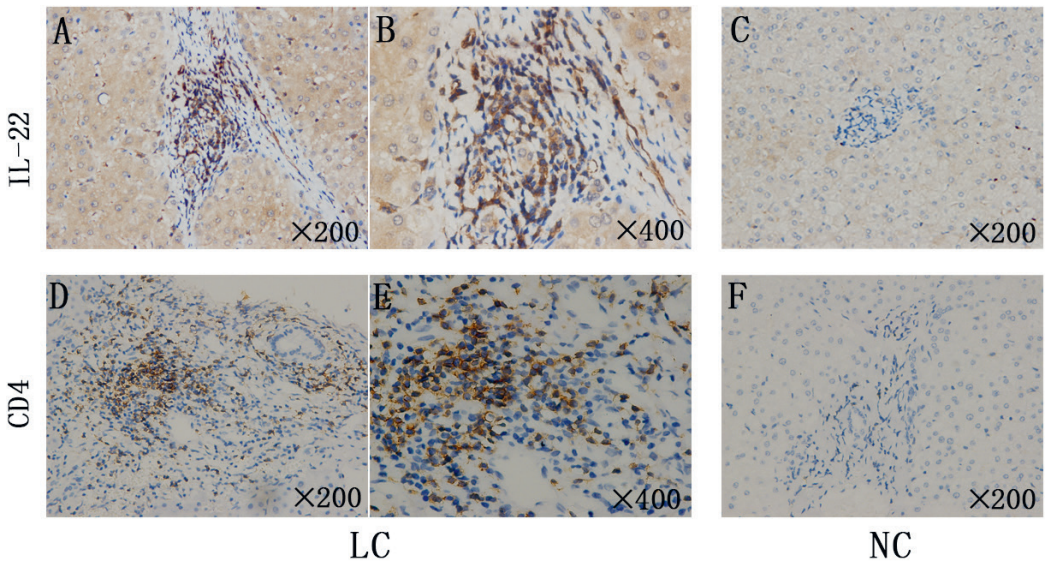

Fig. 1. Liver infiltration of Th22 and CD4$^+$ T cells

Representative distribution of IL-22 and CD4 positive cells in liver samples of liver cirrhosis (LC) patients (A, B, D, E) and normal controls (NC) (C, F). Positive staining is shown as a claybank color (×200). The micrographs at higher magnification (×400) show IL-22 distinctly expressed in the cytoplasm of the lymphocytes (B) while CD4 show membrane staining (E).

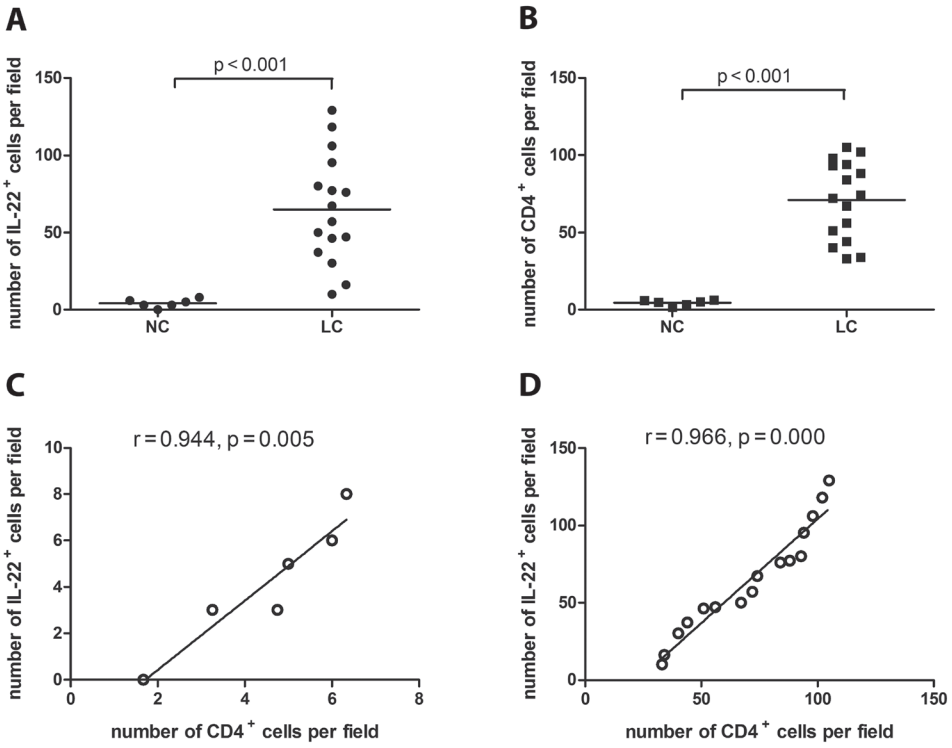

Fig. 2. Th22 cells and CD4+ cells accumulate in the livers of liver cirrhosis (LC) patients

(A, B) The number of Th22 and CD4+ lymphocytes per field (×400) in the liver of LC compared with normal controls (NC). The number of Th22 lymphocytes per field (×400) in the liver is positively correlated with the number of CD4+ lymphocytes in NC (C) and LC groups (D).

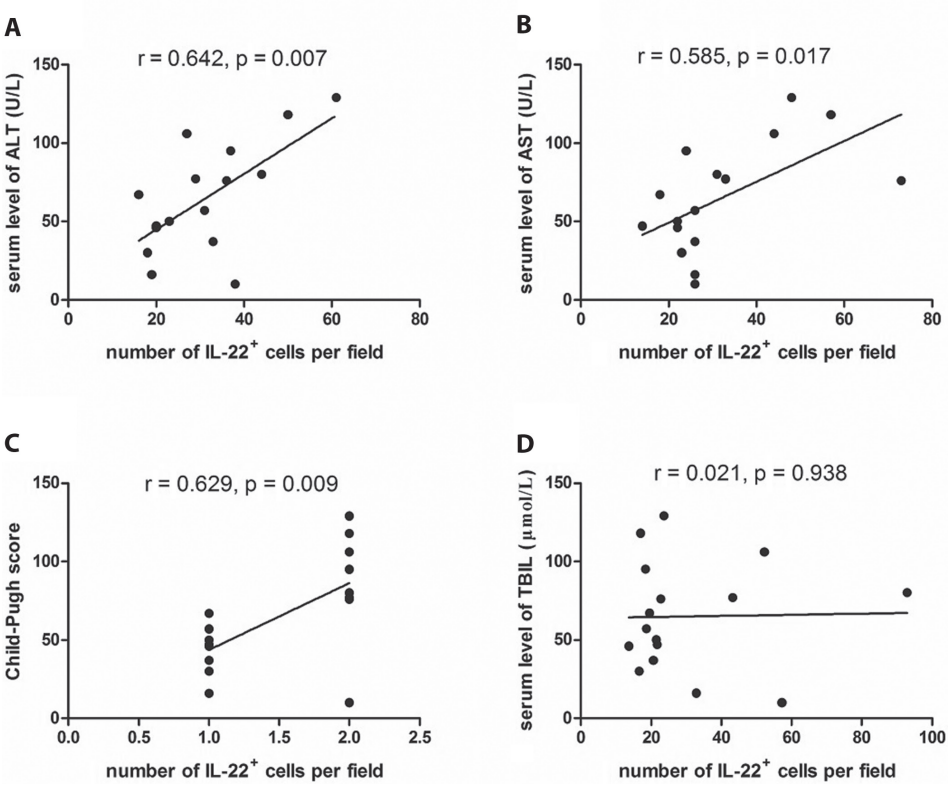

Fig. 3. Correlation between the number of Th22 cells and the clinical parameters in the liver cirrhosis (LC) group.

The number of Th22 cells was positively correlated with serum level of alanine aminotransferase (ALT) (A) and aspartate aminotransferase (AST) (B) and the Child-Pugh score (C). There was no correlation between the number of Th22 cells and serum level of total bilirubin (TBIL) (D).

p = 0.007, Fig. 3A), AST (r = 0.585, p = 0.017, Fig. 3B) and the Child-Pugh score (r = 0.629, p = 0.009, Fig. 3C). There was no correlation between the number of Th22 cells and the serum level of TBIL (r = 0.021, p = 0.938, Fig. 3D).

Increased Th22 cell-related cytokines in the LC patients' livers

Interleukin 22 is the effector cytokine of Th22 cells, and plays its role through a heterodimeric transmembrane receptor complex consisting of IL-10R2 and IL-22R1.

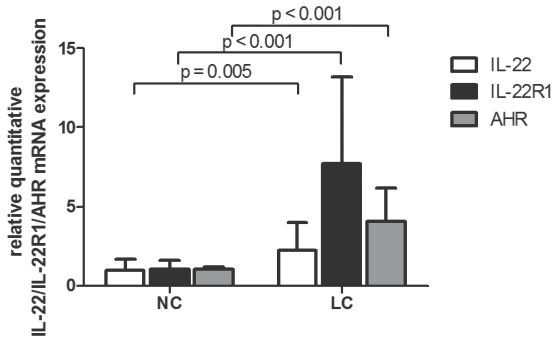

Fig. 4. Relative liver gene expressions of interleukin 22 (IL-22), IL-22R1 and aryl hydrocarbon receptor (AHR) were detected using real-time polymerase chain reaction (RT-PCR)

Because signaling through IL-22R1 is restricted to IL-22, we focused on IL-22 and IL-22R1. Aryl hydrocarbon receptor is the key transcription factor of Th22 cells, which control the production of IL-22. In the present study, we found that the amounts of IL-22, IL-22R1 and AHR mRNA were significantly increased in the LC patients as compared with the NC group ($p < 0.05$, Fig. 4).

Discussion

Liver cirrhosis is a chronic progressive disease characterized by the formation and accumulation of ECM and the activation of hepatic stellate cells (HSCs).[10] Liver injury caused by HBV is strongly linked with cellular immunity and the immune tolerance of the organism.[11] $CD4^+$T cells participate in the immune response of the body and play a key role in the process of liver inflammation and fibrosis.[12] Although previous studies have found that Th22 cells play an important role in certain autoimmune diseases, such as gastric cancer,[7] the mechanism of Th22 cells in HBV-associated LC has not been fully elucidated. In the present study, we confirmed that, like Th17 cells and Th1 cells, Th22 cells were present in liver injury,[13] and that the number of Th22 cells and $CD4^+$T cells in LC was much higher than in the NC group. Moreover, we found that Th22 cells were correlated with $CD4^+$T cells in LC, suggesting that Th22 cells may be involved in the pathogenesis of HBV-associated LC.

As Th22 cells are abundantly expressed in cirrhotic liver tissues, to further understand their relationship with liver inflammation and fibrosis indices, we conducted a correlation analysis between the number of Th22 cells and the serum parameters of ALT, AST and TBIL, and the Child-Pugh score. Our data showed that the number of Th22 cells was positively correlated with serum levels of ALT and AST and the Child-Pugh score, but the correlation with serum levels of TBIL did not reach statistical significance. These results were in line with findings of Park et al., who reported that the number of Th22 cells correlated positively with the serum levels of AST and ALT in patients with viral hepatitis.[14] Taken together, these results indicate that Th22 cells are associated with the severity of the disease and contribute to the prognosis.

The effector cytokine of Th22 cells is IL-22, which mediates its effects through IL-22R1 and IL-10R2.[15,16] The former is mainly expressed at the highest levels in the pancreas, followed by the small intestine, colon, kidney, and liver.[16] Kong et al. demonstrated that HSCs express high levels of IL-10R2 and IL-22R1.[17] In the current study, we also found that the amount of IL-22 and IL-22R1 mRNA were significantly elevated in LC patients compared with the NC group. A high expression of IL-22 and IL-22R1 mRNA in liver tissue may effectively support signaling directionality from the immune system to the liver, and thus participate in the pathological process of LC.

Aryl hydrocarbon receptor is the major transcriptional factor of Th22 cells.[4] $CD4^+$T cells from AHR-deficient mice fail to produce IL-22 when exposed to AHR ligands, while they still develop normal Th17 cell responses.[18] Trifari et al. also reported that transfection of AHR-specific siRNA into $CD4^+$ memory T cells resulted in significantly lesser IL-22 production, but had no effect on IL-17; AHR agonists promote IL-22 production in humans.[4] In accordance with previous studies, we observed that the expression of AHR in the LC patients was significantly increased in comparison with the control participants. We therefore deduced that overexpression of AHR induces Th22 cells to secrete more IL-22, which is closely related to Th22 cell function activities.

Conclusions

Our data showed that intrahepatic Th22 cells were significantly increased in LC patients and had a positive correlation with $CD4^+$T cells. Additionally, overexpression of IL-22, IL-22R1 and AHR confirmed that Th22 cells may participate in the immunopathogenesis of HBV-associated LC. Th22 cells also contribute to the progression of liver fibrosis and can be used as a marker for the severity of LC.

References

1. Harrington LE, Hatton RD, Mangan PR, et al. Interleukin 17–producing $CD4^+$ effector T cells develop via a lineage distinct from the T helper type 1 and 2 lineages. *Nat Immunol*. 2005;6(11):1123–1132.
2. Vierling JM. The immunology of hepatitis B. *Clin Liver Dis*. 2007;11(4):727–759.
3. Duhen T, Geiger R, Jarrossay D, Lanzavecchia A, Sallusto F. Production of interleukin 22 but not interleukin 17 by a subset of human skin-homing memory T cells. *Nat Immunol*. 2009;10(8):857–863.
4. Trifari S, Kaplan CD, Tran EH, Crellin NK, Spits H. Identification of a human helper T cell population that has abundant production of interleukin 22 and is distinct from T(H)-17, T(H)1 and T(H)2 cells. *Nat Immunol*. 2009;10(8):864–871.
5. Kagami S, Rizzo HL, Lee JJ, Koguchi Y, Blauvelt A. Circulating Th17, Th22, and Th1 cells are increased in psoriasis. *J Invest Dermatol*. 2010;130(5):1373–1383.
6. Brand S, Beigel F, Olszak T, et al. IL-22 is increased in active Crohn's disease and promotes pro-inflammatory gene expression and intestinal epithelial cell migration. *Am J Physiol Gastrointest Liver Physiol*. 2006;290(4):G827–838.

7. Liu T, Peng L, Yu P, et al. Increased circulating Th22 and Th17 cells are associated with tumor progression and patient survival in human gastric cancer. *J Clin Immunol*. 2012;32(6):1332–1339.
8. Mookerjee RP, Stadlbauer V, Lidder S, et al. Neutrophil dysfunction in alcoholic hepatitis superimposed on cirrhosis is reversible and predicts the outcome. *Hepatology*. 2007;46(3):831–840.
9. Tritto G, Bechlis Z, Stadlbauer V, et al. Evidence of neutrophil functional defect despite inflammation in stable cirrhosis. *J Hepatol*. 2011; 55(3):574–581.
10. Friedman SL. Mechanisms of hepatic fibrogenesis. *Gastroenterology*. 2008;134(6):1655–1669.
11. Liaw Y-F, Chu C-M. Hepatitis B virus infection. *Lancet*. 2009;373(9663): 582–592.
12. Karlmark KR, Wasmuth HE, Trautwein C, Tacke F. Chemokine-directed immune cell infiltration in acute and chronic liver disease. *Expert Rev Gastroenterol Hepatol*. 2008;2(2):233–242.
13. Lai R, Xiang X, Mo R, et al. Protective effect of Th22 cells and intrahepatic IL-22 in drug induced hepatocellular injury. *J Hepatol*. 2015;63(1): 148–155.
14. Park O, Wang H, Weng H, et al. In vivo consequences of liver-specific interleukin-22 expression in mice: Implications for human liver disease progression. *Hepatology*. 2011;54(1):252–261.
15. Dumoutier L, Louahed J, Renauld JC. Cloning and characterization of IL-10-related T cell-derived inducible factor (IL-TIF), a novel cytokine structurally related to IL-10 and inducible by IL-9. *J Immunol*. 2000;164(44):1814–1819.
16. Kotenko SV, Izotova LS, Mirochnitchenko OV, et al. Identification of the functional interleukin-22 (IL-22) receptor complex: The IL-10R2 chain (IL-10Rbeta) is a common chain of both the IL-10 and IL-22 (IL-10-related T cell-derived inducible factor, IL-TIF) receptor complexes. *J Biol Chem*. 2001;276(4):2725–2732.
17. Kong X, Feng D, Wang H, et al. Interleukin-22 induces hepatic stellate cell senescence and restricts liver fibrosis in mice. *Hepatology*. 2012;56(3):1150–1159.
18. Veldhoen M, Hirota K, Westendorf AM, et al. The aryl hydrocarbon receptor links TH17-cell-mediated autoimmunity to environmental toxins. *Nature*. 2008;453(7191):106–109.

Long-term administration of fenspiride has no negative impact on bone mineral density and bone turnover in young growing rats

Agnieszka Matuszewska[1,A–F], Beata Nowak[1,A–F], Diana Jędrzejuk[2,B,C], Marcin Landwójtowicz[2,B,C], Marek Bolanowski[2,C,E], Wojciech Dziewiszek[1,B], Anna Merwid-Ląd[1,D,E], Ewa Szeląg[3,B,C], Krzysztof Zduniak[4,B,C], Joanna Kwiatkowska[1,B,C], Adam Szeląg[1,A,E,F]

[1] Department of Pharmacology, Wroclaw Medical University, Poland
[2] Department of Endocrinology, Diabetology and Isotope Therapy, Wroclaw Medical University, Poland
[3] Department of Maxillofacial Orthopedics and Orthodontics, Wroclaw Medical University, Poland
[4] Department of Pathomorphology, Wroclaw Medical University, Poland

A – research concept and design; B – collection and/or assembly of data; C – data analysis and interpretation; D – writing the article; E – critical revision of the article; F – final approval of the article

Advances in Clinical and Experimental Medicine, ISSN 1899–5276 (print), ISSN 2451–2680 (online) *Adv Clin Exp Med*. 2019;28(6):771–776

Address for correspondence
Beata Nowak
E-mail: beata.nowak@umed.wroc.pl

Funding sources
The research was supported with a Wroclaw Medical University Grant for Young Researchers (Pbmn 138).

Conflict of interest
None declared

Received on March 1, 2018
Reviewed on June 5, 2018
Accepted on July 24, 2018

Published online on March 6, 2019

Abstract

Background. Fenspiride is an antagonist of H1-histamine receptors that is used to treat acute and chronic respiratory tract infections and otitis media in children and adolescents.

Objectives. The aim of the study was to assess the influence of long-term administration of fenspiride on bone mineral density (BMD) and bone turnover in young growing rats.

Material and methods. The experiment was carried out on 18 young (8-week-old) male Wistar rats receiving either fenspiride 15 mg/kg intragastrically (ig) (group F) or saline solution 4 mL/kg ig (group C) for 3 months. On days 1 and 93, blood samples were collected and serum levels of calcium, phosphorus and markers of bone turnover were measured. On days 2 and 92, BMD was measured with dual-energy X-ray absorptiometry (DXA) using small animal software.

Results. We detected no influence of fenspiride on weight gain, total body BMD (0.212 ±0.010 g/cm^2 vs 0.204 ±0.024 g/cm^2), hind limb BMD (0.264 ±0.016 g/cm^2 vs 0.252 ±0.027 g/cm^2), or bone macroscopic parameters. There were no significant differences between group F and group C in serum levels of osteocalcin (group F: 0.42 ±0.09 ng/mL vs group C: 0.43 ±0.08 ng/mL), C-terminal telopeptide of type I collagen (F: 0.31 ±0.08 ng/mL vs C: 0.29 ±0.08 ng/mL), osteoprotegerin (F: 5.47 ±0.78 pg/mL vs C: 5.35 ±1.65 pg/mL), receptor activator of nuclear factor kappa B ligand (F: 0.65 ±0.85 pg/mL vs C: 0.56 ±0.86 pg/mL), parathormone (F: 237 ±182 pg/mL vs C: 289 ±200 pg/mL), total calcium (F: 6.38 ±1.50 mg/dL vs C: 6.83 ±1.71 mg/dL), or inorganic phosphorus (F: 5.19 ±1.76 mg/dL vs C: 5.50 ±1.32 mg/dL).

Conclusions. Long-term administration of fenspiride has no negative impact on BMD and bone metabolism in young growing rats.

Key words: rats, histamine, bone mineral density, bone, fenspiride

Cite as
Matuszewska A, Nowak B, Jędrzejuk D, et al. Long-term administration of fenspiride has no negative impact on bone mineral density and bone turnover in young growing rats. *Adv Clin Exp Med*. 2019;28(6):771–776. doi:10.17219/acem/93729

DOI
10.17219/acem/93729

Osteoporosis is a generalized bone disease characterized by low bone mass and disorders of bone architecture leading to increased susceptibility and, in consequence, to fractures.[1] Osteoporosis and osteoporotic fractures generate high costs of medical care, physical disability and increased mortality. In 2010, it was estimated that in Europe osteoporosis affects 22 million women and 5.5 million men, with 3.5 million new bone fractures per year, including 610,000 hip fractures, 520,000 vertebral fractures, 560,000 forearm fractures, and 1.8 million fractures in other localizations.[2]

Achieving the proper peak bone mass (PBM) in young people (25–30 years) is extremely important for decreasing the risk of osteoporosis and fractures in adulthood[3] and possibly in the elderly.[4] In young organisms, intensive bone turnover is observed, with bone formation predominant over bone resorption. As a result, the skeleton achieves the appropriate size, shape, and weight of bones.[5] The maximum PBM value depends on many different variables, such as genetic, hormonal and environmental factors.[4] Many drugs may have significant impact on bone mineral density (BMD) and bone metabolism in children (glucocorticoids, methotrexate, antiepileptic drugs).[6,7] Therefore, it is important to assess the influence of various drugs on growing bones.

Fenspiride is used to treat acute and chronic respiratory tract infections and otitis media in children and adolescents. It is an H1-antihistamine agent that decreases the synthesis of pro-inflammatory mediators (cytokines, tumor necrosis factor α (TNF-α), prostaglandins, leukotrienes, and free radicals) and relaxes the smooth muscles, similarly to papaverine.[8–10] The presence of H1-histamine receptors on both osteoblasts and osteoclasts has been confirmed.[11] Pro-inflammatory cytokines, e.g., interleukin-1, interleukin-6 and TNF-α, increase osteoclast activity through the RANK/RANKL/OPG pathway and inhibit osteoblast activity. Prostaglandins may stimulate both bone formation and bone resorption.[12] Leukotrienes inhibit osteoblast proliferation, decrease the number of foci of bone tissue mineralization and stimulate the formation of bone cavities by osteoclasts.[13] These findings suggest that fenspiride may influence bone metabolism and BMD. The impact of different antagonists of H1-receptors (e.g., loratadine, cetirizine, pheniramine maleate) on bone metabolism has been studied,[11,14,15] but to the best of our knowledge, the action of fenspiride on bone metabolism has not been investigated.

The aim of the study was to assess the influence of long-term administration of fenspiride on BMD and selected markers of bone turnover in young growing rats.

Material and methods

Drugs and chemicals

The drugs used in the study included Pulneo (fenspiride hydrochloricum) 25 mg/1 mL oral drops solution (Aflofarm Farmacja Polska Sp. z o.o., Pabianice, Poland); normal saline solution (B. Braun Melsungen AG, Melsungen, Germany); ketamine 10% solution for injection for veterinary use, 100 mg/mL (Biowet Puławy Sp. z o.o., Puławy, Poland); and Relanium (diazepam) ampules, 5 mg/mL (Polfa S.A., Warszawa, Poland).

The animals and the experiment

The experiment was carried out on 18 8-week-old male Wistar rats with body weight of 190–270 g (mean weight 227.8 ±22.6 g). The animals were housed at room temperature (21–23°C) with 12:12-hour light–dark cycles. They were fed with a standard diet (LSM, Agropol sp. j., Motycz, Poland) that contained 1.2% calcium and 0.7% phosphates. Food and water were provided ad libitum.

Once acclimated, the rats were randomly assigned to 1 of 2 groups (9 animals in each group): group F received fenspiride at a dose of 15 mg/kg (dosing based on a publication by Kuzubova et al.[16]), or group C (the control group) which received saline solution. The fenspiride and saline solution were given intragastrically (ig) once daily for 90 days (the time needed to cause significant changes in BMD).

Body weights were checked once daily throughout the experimental period. On day 1 and day 93, blood samples were collected from the tail vein for serum isolation. The serum was separated by centrifugation (at 1500 × g) and then stored at –70°C until required for bone metabolic marker assays. On days 2 and 92, dual-energy X-ray absorptiometry (DXA) was performed under general anesthesia with ketamine (50 mg/kg intraperitoneally (ip)) and diazepam (3 mg/kg ip).

The animals were sacrificed in deep narcosis with ketamine (50 mg/kg ip) and diazepam (3 mg/kg ip) on day 93. Femurs and tibias were collected from each animal for further examination.

Ethical approval

All applicable international, national and/or institutional guidelines for the care and use of animals were followed. The experiment was performed with the approval of the Local Ethics Committee for Experiments on Animals at the Wroclaw Medical University, Poland (approval No. 25/2016). All the procedures involving animals performed during the study were in accordance with the ethical standards and practices of the institution where the study was conducted.

Parameters of bone turnover

Total calcium concentration and inorganic phosphorus measurements were performed by a certified laboratory with an Architect Plus ci4100 chemistry analyzer (Abbott Laboratories, Lake Bluff, USA) using commercial tests (Architect/Aeroset Calcium Assay and Architect

Phosphorus Assay, both from Abbott Laboratories) according to the manufacturer's instructions. Levels of parathormone (PTH), osteocalcin, C-terminal telopeptide of type I collagen (bCTX), osteoprotegerin (OPG), and receptor activator of nuclear factor kappa B ligand (RANKL) were measured with the following commercial enzyme-linked immunosorbent assay (ELISA) kits: Rat Intact PTH ELISA Kit (Immutopics Inc., San Clemente, USA); Rat Osteocalcin ELISA Kit (SEA471Ra, USCN Life Science Inc., Houston, USA); Rat Beta-Crosslaps ELISA Kit (USCN Life Science Inc.); Rat Osteoprotegerin ELISA Kit (USCN Life Science Inc.); and Rat Receptor Activator of Nuclear Factor Kappa B Ligand ELISA Kit (USCN Life Science Inc.), respectively, according to manufacturers' instructions.

Dual-energy X-ray absorptiometry

Dual-energy X-ray absorptiometry (DXA) was performed on a high-resolution Discovery W (S/N) 81507 device (Hologic Inc., Marlborough, USA). Bone mineral density and fat content were measured.

Macrometric measurements

After sacrificing the animals, the right tibia and right femur were collected from each rat. The bones were weighed using electronic scales (Radwag, Radom, Poland). The bone lengths and mid-length diameter of the diaphysis were measured using digital calipers with a resolution of 0.01 mm (Pro sp.z o.o., Bielsko-Biała, Poland). For each bone, the femur index, defined as the ratio of femur weight and body weight ((femur mass [g]) / (body mass [g]) × 100), or tibial index ((tibia mass [g]) / (body mass [g]) × 100) were calculated.

Statistical analysis

The significance of differences between values was assessed using Student's t-test. P-values of less than 0.05 were considered statistically significant. The results were presented as means ± standard deviation (SD).

The statistical analysis was performed using STATISTICA v. 10 software (StatSoft, Inc., Tulsa, USA).

Results

Age and body weight

On day 1, groups F and C were homogenous in terms of age (59.11 ±1.05 days vs 60 ±3.87 days, $p > 0.05$), body weight (274.4 ±26.4 g vs 272.2 ±23.9 g, $p > 0.05$) and fat content (15.0 ±2.0% of body weight vs 14.2 ±3.1% of body weight, $p > 0.05$). No significant difference between the groups in the dynamic of body weight gain was observed throughout the experimental period, and therefore on day 93 body weight (413.3 ±41.2 g in group F vs 424.4 ±35.0 g in group C, $p > 0.05$) and fat content were comparable in the 2 groups (20.5 ±4.2% of body weight in group F vs 19.7 ±4.4% of body weight in the controls, $p > 0.05$).

Parameters of bone turnover

The results are presented in Table 1. On days 1 and 93, no significant differences between groups F and C were found in any of the analyzed serum bone turnover markers (osteocalcin, bCTX), regulatory proteins (RANKL, OPG) or total calcium and inorganic phosphorus concentrations.

Table 1. The effect of fenspiride treatment on the serum concentration of selected markers of bone turnover

Parameter		Fenspiride group (n = 9)	Control group (n = 9)	p-value
Day 1	osteocalcin [ng/mL]	1.00 ±0.11	0.95 ±0.18	NS
	bCTX [ng/mL]	0.28 ±0.05	0.29 ±0.12	NS
	RANKL [pg/mL]	0.17 ±0.41	1.02 ±1.27	NS
	OPG [pg/mL]	3.50 ±0.63	3.80 ±0.69	NS
	total calcium [mg/dL]	9.14 ±0.76	8.60 ±1.02	NS
	inorganic phosphorus [mg/dL]	6.63 ±0.42	6.26 ±0.87	NS
Day 93	osteocalcin [ng/mL]	0.42 ±0.09	0.43 ±0.08	NS
	bCTX [ng/mL]	0.31 ±0.08	0.29 ±0.08	NS
	RANKL [pg/mL]	0.65 ±0.85	0.56 ±0.86	NS
	OPG [pg/mL]	5.47 ±0.78	5.35 ±1.65	NS
	total calcium [mg/dL]	6.38 ±1.50	6.83 ±1.71	NS
	inorganic phosphorus [mg/dL]	5.19 ±1.76	5.50 ±1.32	NS
	PTH [pg/mL]	237 ±182	289 ±200	NS

bCTX – C-terminated telopeptide of type I collagen; RANKL – receptor activator of nuclear factor kappa B ligand; OPG – osteoprotegerin; PTH – parathormone; NS – not significant; SD – standard deviation. Values are presented as means ±SD.

Table 2. The effect of fenspiride treatment on BMD and bone macrometric parameters

Parameter		Fenspiride group (n = 9)	Control group (n = 9)	p-value
Day 2	total body BMD [g/cm^2]	0.160 ±0.007	0.161 ±0.006	NS
	lower limbs BMD [g/cm^2]	0.188 ±0.028	0.1788 ±0.034	NS
	femur BMD [g/cm^2]	0.232 ±0.006	0.226 ±0.008	NS
	tibia BMD [g/cm^2]	0.181 ±0.018	0.175 ±0.016	NS
Day 93	total body BMD [g/cm^2]	0.212 ±0.010	0.204 ±0.024	NS
	lower limbs global BMD [g/cm^2]	0.264 ±0.016	0.252 ±0.027	NS
	femur BMD [g/cm^2]	0.292 ±0.016	0.276 ±0.033	NS
	tibia BMD [g/cm^2]	0.236 ±0.017	0.228 ±0.024	NS
	tibia mass [g]	1.12 ±0.12	1.04 ±0.10	NS
	tibia index [%]	0.27 ±0.04	0.25 ±0.02	NS
	tibia length [mm]	42.43 ±0.79	42.27 ±1.05	NS
	mid-length diameter of tibia [mm]	3.77 ±0.16	3.67 ±0.29	NS
	femur mass [g]	1.44 ±0.11	1.38 ±0.12	NS
	femur index [%]	0.35 ±0.04	0.32 ±0.01	NS
	femur length [mm]	37.74 ±0.69	38.01 ±0.62	NS
	mid-length diameter of femur [mm]	4.88 ±0.25	4.76 ±0.28	NS
	neck diameter of femur [mm]	6.08 ±0.42	6.12 ±0.25	NS

BMD – bone mineral density; NS – not significant; SD – standard deviation. Values are presented as means ± SD.

Parathyroid hormone levels were measured only on day 93, and no significant difference between the 2 groups was detected.

Bone mineral density and macrometric bone parameters

Bone mineral density and macrometric bone parameters are presented in Table 2. No significant influence of fenspiride was detected on the parameters analyzed.

Discussion

Histamine exerts its action through membrane receptors (H1, H2, H3, and H4) localized in most of the tissues and cells in the organism.[17] H1-antihistamines are widely used in the treatment of allergic disorders and acute or chronic urticarial.[18] However, little is known about the action of H1-antihistamines on bones during the developmental phase in immature organisms.[19]

Histamine is a biogenic amine widely distributed throughout the peripheral tissues of the body, and is found in neurons in the central nervous system.[17] The influence of histamine on bone metabolism and the development of osteoporosis was suggested after some observational studies indicating that in patients with systemic mastocytosis, osteoporosis is relatively frequent.[20] It is now well known that histamine is involved in the regulation of osteoclast differentiation through autocrine and paracrine signaling. Histamine increases the number of both osteoclasts and precursors of osteoclasts. What is more, preosteoclasts are also able to synthetize and release histamine. In primary osteoclasts, histamine increases the ratio of RANKL to osteoprotegerin (OPG).[21] It has been documented that histamine increases the synthesis of osteoclast differentiation factor/RANKL in osteoblasts.[22] The RANK/RANKL/OPG system plays an important and crucial role in bone metabolism regulation.[23]

Due to the common use of fenspiride in clinical practice, especially in pediatrics, and very often in long-term therapy, the aim of our study was to assess the impact of fenspiride on bone metabolism during intensive bone growth to answer the question of whether the use of the drug negatively influences bone growth and metabolism. We chose a well-established experimental model on young growing rats, often used in this type of experiments.[24–26] We checked selected markers of bone metabolism, such as serum concentrations of osteocalcin, C-terminal telopeptide of type I collagen, RANKL, osteoprotegerin, serum total calcium, inorganic phosphorus, and PTH. Bone mineral density was assessed with densitometric measurements. Additionally, macrometric bone parameters of each animal's right tibia and right femur were measured, tibia and femur indices were calculated (expressed per body mass), and the diameters of the tibias and femurs were measured in typical localizations. All the results demonstrated that the 3-month-long administration of fenspiride to young male rats did not exert any negative impact on bone metabolism parameters.

Observational studies in humans indicate that patients with allergic disorders (e.g., allergies to pollens) who are

not treated with any H1-antihistamine drugs suffer almost 3 times more frequently from low-energy bone fractures when compared to patients treated with such agents. Some authors have suggested that this might be due to higher histamine levels in untreated patients.[27] It has been shown in experimental studies that H1-histamine receptor antagonists can inhibit histamine-induced osteoclastogenesis[28] as well as age-related bone loss.[29] The results of some experimental studies suggest that H1-antihistamine agents have no negative impact on bone metabolism and may even have a beneficial influence.[30]

In relatively early experimental research, the administration of promethazine (an H1-antihistamine agent) to female ovariectomized rats decreased bone resorption and increased BMD.[29] Treatment with cetirizine (a 2nd generation H1-antihistamine) did not have any impact on BMD values or bone tissue properties in H(+)/K(+) ATPase β subunit knockout (KO) mice, which are genetically modified to have high histamine levels leading to secondary decreases in BMD.[11,31] Recently, Folwarczna et al.[14] administered loratadine (a 2nd generation H1-antihistamine) to ovariectomized and non-ovariectomized rats with bone metabolism disorders. Short-term loratadine administration significantly improved bone metabolism and biomechanical bone properties in the non-ovariectomized rats.

The function of osteoclasts and osteoblasts may be influenced not only by histamine alone, but also by chronic inflammatory processes, directly and indirectly. Bone metabolism strongly depends on the interaction of a variety of substances (growth factors, cytokines, hormones) with bone cells. The final effect of these interactions in cases of chronic inflammation leads to bone loss rather than bone formation.[23] There is data suggesting close relationships between prostaglandins, leukotrienes and pro-inflammatory cytokines, and bone turnover.[32] In vitro studies have shown increased differentiation of mesenchymal stem cells in the presence of pranlukast (a CysLT1 receptor antagonist).[33] In experimental animal models of bone fractures, both zileuton (a 5-lipooxygenase inhibitor) and montelukast (a CysLT1 receptor antagonist) increased chondrocyte proliferation and led to quicker bone formation.[34]

Our results demonstrate that long-term therapy with fenspiride does not have a negative impact on the growing skeleton. Taking into account the negative impact on bone metabolism of increased histamine levels connected with chronic allergic reactions, it may be assumed that in children with allergic disorders, fenspiride may even have a protective effect.

References

1. Kanis JA. Osteoporosis III: Diagnosis of osteoporosis and assessment of fracture risk. *Lancet*. 2002;359(9321):1929–1936. doi:10.1016/S0140-6736(02)08761-5
2. Hernlund E, Svedbom A, Ivergård M, et al. Osteoporosis in the European Union: Medical management, epidemiology and economic burden. *Arch Osteoporos*. 2013;8(1–2):136. doi:10.1007/s11657-013-0136-1
3. Ferrari S, Bianchi ML, Eisman JA, et al. Osteoporosis in young adults: Pathophysiology, diagnosis, and management. *Osteoporos Int*. 2012; 23(12):2735–2748. doi:10.1007/s00198-012-2030-x
4. Rizzoli R, Bianchi ML, Garabédian M, McKay HA, Moreno LA. Maximizing bone mineral mass gain during growth for the prevention of fractures in the adolescents and the elderly. *Bone*. 2010;46(2):294–305. doi:10.1016/j.bone.2009.10.005
5. Heaney RP, Abrams S, Dawson-Hughes B, et al. Peak bone mass. *Osteoporos Int*. 2000;11(11):985–1009. doi:10.1007/s001980070020
6. Viswanathan A, Sylvester FA. Chronic pediatric inflammatory diseases: Effects on bone. *Rev Endocr Metab Disord*. 2008;9(2):107–122. doi:10.1007/s11154-007-9070-0
7. Zhang Y, Zheng YX, Zhu JM, Zhang JM, Zheng Z. Effects of antiepileptic drugs on bone mineral density and bone metabolism in children: A meta-analysis. *J Zhejiang Univ Sci B*. 2015;16(7):611–621. doi:10.1631/jzus.B1500021
8. Shmelev EI, Kunicina YL. Comparison of fenspiride with beclomethasone as adjunctive anti-inflammatory treatment in patients with chronic obstructive pulmonary disease. *Clin Drug Investig*. 2006;26(3): 151–159.
9. Volkova LI, Budkova AA, Filonova NN, et al. Efficacy of a complementary anti-inflammatory treatment with erespal in chronic obstructive and nonobstructive bronchitis. *Ter Arkh*. 2004.
10. Khawaja AM, Liu YC, Rogers DF. Effect of fenspiride, a non-steroidal anti-inflammatory agent, on neurogenic mucus secretion in ferret trachea in vitro. *Pulm Pharmacol Ther*. 1999;12(6):363–368. doi:10.1006/pupt.1999.0221
11. Aasarod KM, Stunes AK, Mosti MP, et al. Effects of the histamine 1 receptor antagonist cetirizine on the osteoporotic phenotype in H+/K+ ATPase beta subunit KO mice. *J Cell Biochem*. 2016;117(9):2089–2096. doi:10.1002/jcb.25514
12. Blackwell KA, Raisz LG, Pilbeam CC. Prostaglandins in bone: Bad cop, good cop? *Trends Endocrinol Metab*. 2010;21(5):294–301. doi:10.1016/j.tem.2009.12.004
13. Hikiji H, Takato T, Shimizu T, Ishii S. The roles of prostanoids, leukotrienes, and platelet-activating factor in bone metabolism and disease. *Prog Lipid Res*. 2008;47(2):107–126. doi:10.1016/j.plipres.2007.12.003
14. Folwarczna J, Janas A, Pytlik M, Śliwiński L, Wiercigroch M, Brzęczek A. Modifications of histamine receptor signaling affect bone mechanical properties in rats. *Pharmacol Reports*. 2014;66(1):93–99. doi:10.1016/j.pharep.2013.08.010
15. Ezzat BA, Abbass MMS. The ability of H1 or H2 receptor antagonists or their combination in counteracting the glucocorticoid-induced alveolar bone loss in rats. *J Oral Pathol Med*. 2014;43(2):148–156. doi:10.1111/jop.12104
16. Kuzubova NA, Lebedeva ES, Fedin AN, Dvorakovskaya IV, Preobrazhenskaya TN, Titova ON. Effect of fenspiride on bronchial smooth muscle of rats with chronic obstructive pulmonary disease. *J Smooth Muscle Res*. 2013;49:46–54. doi:10.1540/jsmr.49.46
17. Cataldi M, Borriello F, Granata F, Annunziato L, Marone G. Histamine receptors and antihistamines: From discovery to clinical applications. *Chem Immunol Allergy*. 2014;100:214–226. doi:10.1159/000358740
18. Fitzsimons R, van der Poel L-A, Thornhill W, du Toit G, Shah N, Brough HA. Antihistamine use in children. *Arch Dis Child Educ Pract Ed*. 2015; 100(3):122–131. doi:10.1136/archdischild-2013-304446
19. De Benedictis FM, De Benedictis D, Canonica GW. New oral H1 antihistamines in children: Facts and unmet needs. *Allergy Eur J Allergy Clin Immunol*. 2008;63(10):1395–1404. doi:10.1111/j.1398-9995.2008.01771.x
20. Barete S, Assous N, de Gennes C, et al. Systemic mastocytosis and bone involvement in a cohort of 75 patients. *Ann Rheum Dis*. 2010; 69(10):1838–1841. doi:10.1136/ard.2009.124511
21. Biosse-Duplan M, Baroukh B, Dy M, de Vernejoul M-C, Saffar J-L. Histamine promotes osteoclastogenesis through the differential expression of histamine receptors on osteoclasts and osteoblasts. *Am J Pathol*. 2009;174(4):1426–1434. doi:10.2353/ajpath.2009.080871
22. Deyama Y, Kikuiri T, Ohnishi GI, et al. Histamine stimulates production of osteoclast differentiation factor/receptor activator of nuclear factor-kappaB ligand by osteoblasts. *Biochem Biophys Res Commun*. 2002;298(2):240–246. doi:10.1016/S0006-291X(02)02440-3

23. Neumann E, Müller-Ladner U, Frommer KW. Entzündung und Knochenmetabolismus. *Z Rheumatol*. 2014;73(4):342–348. doi:10.1007/s00393-013-1288-5
24. Lelovas PP, Xanthos TT, Thorma SE, Lyritis GP, Dontas IA. The laboratory rat as an animal model for osteoporosis research. *Comp Med*. 2008;58(5):424–430.
25. Tauer JT, Hofbauer LC, Jung R, et al. Impact of long-term exposure to the tyrosine kinase inhibitor imatinib on the skeleton of growing rats. *PLoS One*. 2015;10(6):e0131192. doi:10.1371/journal.pone.0131192
26. Lin S, Huang J, Zheng L, et al. Glucocorticoid-induced osteoporosis in growing rats. *Calcif Tissue Int*. 2014;95(4):362–373. doi:10.1007/s00223-014-9899-7
27. Ferencz V, Meszaros S, Csupor E, et al. Increased bone fracture prevalence in postmenopausal women suffering from pollen-allergy. *Osteoporos Int*. 2006;17(3):484–491. doi:10.1007/s00198-005-0011-z
28. Ikawa Y, Yonekawa T, Ohkuni Y, Kuribayashi M, Fukino K, Ueno K. A comparative study of histamine activities on differentiation of osteoblasts and osteoclasts. *J Toxicol Sci*. 2007;32(5):555–564. doi:10.2131/jts.32.555
29. Rico H, Gómez M, Revilla M, et al. Effects of promethazine on bone mass and on bone remodeling in ovariectomized rats: A morphometric, densitometric, and histomorphometric experimental study. *Calcif Tissue Int*. 1999;65(4):272–275. doi:10.1007/s002239900697
30. Kinjo M, Setoguchi S, Solomon DH. Antihistamine therapy and bone mineral density: Analysis in a population-based US sample. *Am J Med*. 2008;121(12):1085–1091. doi:10.1016/j.amjmed.2008.06.036
31. Meh A, Sprogar Š, Vaupotic T, et al. Effect of cetirizine, a histamine (H1) receptor antagonist, on bone modeling during orthodontic tooth movement in rats. *Am J Orthod Dentofac Orthop*. 2011;139(4):e323–329. doi:10.1016/j.ajodo.2009.11.013
32. Gatti D, Senna G, Viapiana O, Rossini M, Passalacqua G, Adami S. Allergy and the bone: Unexpected relationships. *Ann Allergy Asthma Immunol*. 2011;107(3):202–206. doi:10.1016/j.anai.2011.03.018
33. Akino K, Mineda T, Mori N, Hirano A, Imaizumi T, Akita S. Attenuation of cysteinyl leukotrienes induces human mesenchymal stem cell differentiation. *Wound Repair Regen*. 2006;14(3):343–349. doi:10.1111/j.1743-6109.2006.00130.x
34. Wixted JJ, Fanning PJ, Gaur T, et al. Enhanced fracture repair by leukotriene antagonism is characterized by increased chondrocyte proliferation and early bone formation: A novel role of the cysteinyl IL-1 receptor. *J Cell Physiol*. 2009;221(1):31–39. doi:10.1002/jcp.21809

Management of crossing vessels in children and adults: A multi-center experience with the transperitoneal laparoscopic approach

Wojciech Panek[1,A–D], T.P.V.M de Jong[2,E], Tomasz Szydełko[1,E], Rafał Chrzan[3,C–F]

[1] Division of Oncology and Palliative Care, Faculty of Health Sciences, Wroclaw Medical University, Poland
[2] Department of Pediatric Urology, UMC-WKZ Utrecht, the Netherlands
[3] Department of Pediatric Urology, Jagiellonian University Medical College, Kraków, Poland

A – research concept and design; B – collection and/or assembly of data; C – data analysis and interpretation; D – writing the article; E – critical revision of the article; F – final approval of the article

Advances in Clinical and Experimental Medicine, ISSN 1899–5276 (print), ISSN 2451–2680 (online) *Adv Clin Exp Med*. 2019;28(6):777–782

Address for correspondence
Wojciech Panek
E-mail: wojtpan84@gmail.com

Funding sources
None declared

Conflict of interest
None declared

Acknowledgements
The data collection of the pediatric population for this study was conducted during a scholarship program provided by the European Society for Pediatric Urology to Dr. Wojciech Panek, who visited the Departments of Pediatric Urology in UMC Utrecht and AMC Amsterdam, the Netherlands.

Received on September 30, 2017
Reviewed on April 10, 2018
Accepted on August 9, 2018

Published online on April 5, 2019

Cite as
Panek W, de Jong TPVM, Szydełko T, Chrzan R. Management of crossing vessels in children and adults: A multi-center experience with the transperitoneal laparoscopic approach. *Adv Clin Exp Med*. 2019;28(6):777–782. doi:10.17219/acem/94142

DOI
10.17219/acem/94142

Abstract

Background. Crossing vessels (CVs) are common in older children and adults with hydronephrosis but no gold standard exists on how to treat this condition. The final decision is made intraoperatively by the surgeon.

Objectives. To assess the outcome of the laparoscopic dismembered pyeloplasty with translocation of the CVs in children and adults.

Material and methods. Prospectively collected data from 3 departments was reviewed. Inclusion criteria were: 1) a transperitoneal laparoscopic approach; 2) dismembered pyeloplasty; and 3) the same operating pediatric urologist (RC) or urologist (TS). In the case of CVs, pyeloplasty with vessel transposition (children) or with cephalad translocation (adults) was performed. Forty-eight children and 41 adults met these criteria. Patients were divided into 4 groups: children with (group 1A) and without (group 1B) CVs, and adults with (group 2A) and without (group 2B) CVs. Any surgical reintervention at the uretero–pelvic junction (UPJ) was deemed a failure.

Results. The overall reintervention rate was 3/48 (6.25%) in children and 2/41 (4.9%) in adults ($p > 0.05$), and involved the following: 4 endopyelotomies and 1 redo pyeloplasty. Crossing vessels were identified in 28/48 (58%) children and 12/41 (29%) adults. The mean operation time was 152 min in group 1A and 161 min in group 2A ($p > 0.5$). Reintervention was needed in 2/28 patients in group 1A and in 1/12 patients in group 2A ($p > 0.05$). There was no difference in the failure rate between group 1A and group 1B, nor between group 2A and group 2B ($p > 0.05$).

Conclusions. Crossing vessels should be meticulously looked for during pyeloplasty in older children and adults. Dismembered laparoscopic pyeloplasty (LP) with dorsal transposition or cephalad translocation are comparable methods in terms of success rate for the treatment of UPJ obstruction in these patients.

Key words: laparoscopic, hydronephrosis, pyeloplasty, UPJO

Introduction

A wide range of acquired and congenital conditions can lead to dilation of the renal collecting system. Uretero–pelvic junction (UPJ) stenosis is the most common cause of hydronephrosis in the pediatric population, with a prevalence between 1:750 and 1:1,500, and a male to female ratio of 2:1.[1,2] Impaired transmission of the peristaltic waves due to abnormal development of the smooth muscles and connective tissue, intraureteral valves and polyps are intrinsic reasons for obstruction.[3,4] Crossing vessels (CVs), adhesions around the UPJ and kinking of the proximal ureter are among the extrinsic factors.[2] Furthermore, infections, stones and iatrogenic trauma can also deteriorate the urinary outflow from the renal pelvis.

Lower pole CVs are reported in 11–15% of young and up to 58% of older symptomatic children with hydronephrosis.[5,6] In adults, CVs are present intraoperatively in 39–71% of all patients operated on due to UPJ obstruction.[2] It is still unclear whether these vessels can be the sole reason for obstruction or if this entity coexists with the intrinsic pathology.

Dismembered pyeloplasty, described by Kuster and popularized by Anderson and Hynes, is the gold standard surgical treatment for UPJ stenosis.[7] Laparoscopic pyeloplasty (LP) was first performed in 1993 in adults and in 1995 in children, and over the years, it has almost replaced the open technique in both groups.[8–10] Nowadays, LP can also be safely done in very young children.[3,11] When CVs are found during surgery, additional maneuvers are performed to keep the vessels away from the UPJ. However, there is no consensus on how to deal with this finding and the operating surgeon usually makes the final decision intraoperatively.

The goal of the study it to assess the outcome of laparoscopic dismembered pyeloplasty with translocation of the CVs in children and adults.

Material and methods

Patients

A retrospective analysis of the prospectively collected data from 3 departments – 2 pediatric urology centers and 1 department of urology – was conducted. Inclusion criteria were as follows: 1) a transperitoneal laparoscopic approach without conversion in all patients; 2) dismembered Anderson–Hynes pyeloplasty in all patients; and 3) the same operating pediatric urologist (RC) for children or urologist (TS) for adults, each using one method for CVs management. Children with CVs (group 1A) and adults with CVs (group 2A) were selected. The control groups consisted of the remaining patients without CVs: group 1B – children and group 2B – adults.

Clinical symptoms of obstruction (pain, hypertension), worsening of hydronephrosis on repeated ultrasounds, and renal function impairment revealed on the diuretic renography (DR) are the indications for surgical treatment according to the existing recommendations.[12] In some centers, a cumulative curve with a prolonged half-time to tracer clearance (T1/2 > 20 min) and an excretory urography (IVP) are also used to confirm the diagnosis.[2,13]

In this study, the follow-up was longer than 12 months for all patients (range: 1–9 years). In children, the first ultrasound after pyeloplasty was done 4–6 weeks after removal of the double J catheter (JJC) and then at 3–6-month intervals. A DR was done only in selected cases: symptomatic patients and/or increased dilation on ultrasound. In adults, the first ultrasound and DR are performed 6 weeks after removal of the JJC and then 1 year later.

Complications were classified according to Clavien–Dindo criteria.[14] A short-term complication is defined as any unsolicited event before the JJC removal. Special attention was paid to any temporary diversion or secondary procedure due to persistent UPJ obstruction after JJC removal, which was classified as a late-term complication. Fisher's exact test was used for the statistical analysis.

Surgical technique

Children

Diagnostic cystoscopy and antegrade pyelography are done first and a Foley catheter is left in the bladder. Antegrade pyelography was performed for 2 reasons: to assess the distal part of the ipsilateral ureter and to measure the length of the ureter from the orifice to the UPJ. As the JJC is introduced in the antegrade manner and the length of the ureter in children varies from 12 to 26 cm, it is important to estimate the proper length of the stent beforehand. The patient is turned in the supine position with a 30° elevation of the affected site. The first trocar is put in the umbilicus in the open manner. A pneumoperitoneum is created and then 2 working trocars are introduced under direct visual control. The pressure is between 8 mm Hg and 12 mm Hg, depending on the age. For the right-sided pyeloplasty, the colon is mobilized and for the left-sided one, a transmesocolic approach is preferred. The renal pelvis and the proximal ureter are exposed and isolated. Crossing vessels are looked for. After transection of the renal pelvis 1 cm above the UPJ, the narrow part of the ureter is excised and the proximal ureter is spatulated. The posterior wall of the anastomosis is done with interrupted 5–0 sutures (polyglactin). Then, a JJC catheter (4.0 of 4.7 Fr) is placed percutaneously and finally the anastomosis is completed. The Foley catheter is removed on the 1st day and the JJC 3 weeks later.

Adults

The main steps of the procedure are similar in adults, although a 5 or 7 Fr JJC are put in a retrograde manner during cystoscopy if technically possible. In a 45% supine

position, the first 10 mm trocar for the camera is put just below the umbilicus. Then, a pneumoperitoneum to 12 mm Hg is created and the other working 5 mm working trocars are inserted. A transmesocolic approach on the left side is used in non-obese patients. During mobilization of the renal pelvis and the proximal ureter, the CVs are looked for. Then, the pelvis wall is transected diagonally from the medial to the lateral edge. Next, the UPJ and the upper part of the ureter are incised downward laterally over the length of 1.5 cm and the stenotic part is resected. The anastomosis between the pelvis and the spatulated ureter is performed with 4–0 sutures. A wound drain is left next to the anastomosis and removed 3 days after the procedure. The Foley catheter is retrieved after 2 days and the JJC 4–6 weeks postoperatively.

Crossing vessels management

Dorsal transposition of the CVs is performed in children (Fig. 1,2). In adults, cephalad translocation is done. For this maneuver, the crossing vein is ligated and transected, and the crossing artery is fixed using 2 or 3–0 absorbable sutures to the Gerota fascia. The sutures with perivascular tissue are applied to preserve the arcuate run of the artery and to avoid postoperative arterial hypertension (Fig. 3,4).

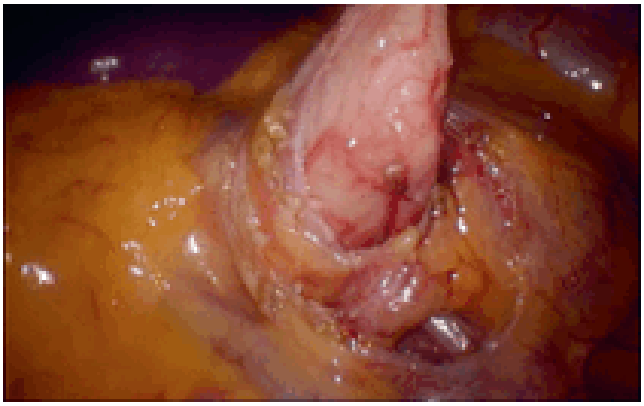

Fig. 1. Dorsal transposition of crossing vessels (CVs): intraoperative view before transection of the ureter. Crossing vessel in front of the ureter

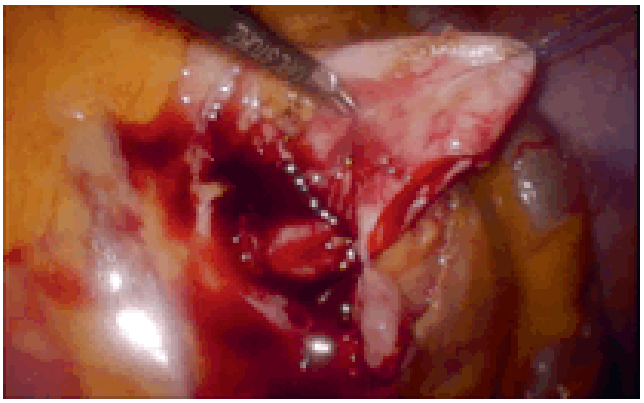

Fig. 2. Dorsal transposition of crossing vessels (CVs): intraoperative view after transection of the ureter and placing of the first stitch

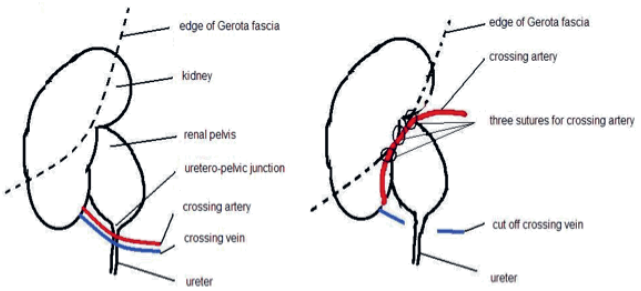

Fig. 3. Sequential steps of cephalad translocation maneuver

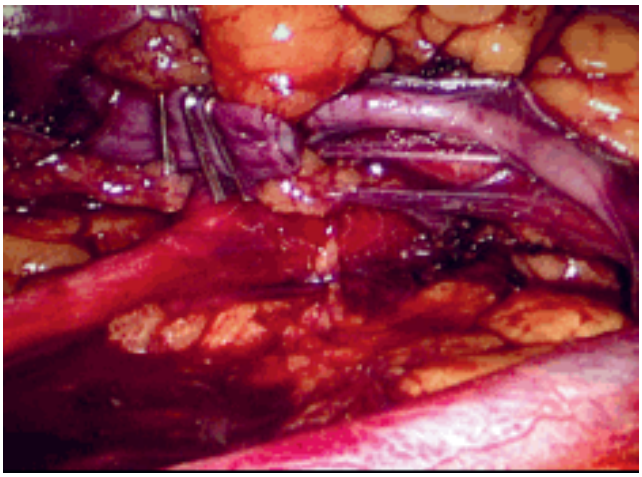

Fig. 4. Translocated crossing artery and cut off crossing vein (adult)

Results

In all, 76 consecutive LPs in children and 71 LPs in adults were analyzed. Forty-eight children and 41 adults met the inclusion criteria. The mean age was 9.9 years (mode – 5.1 years, range: 3.0–17.7 years) and 35.5 years (mode – 30.5 years, range: 18–72 years), respectively. The mean follow-up was 4.2 years (range: 1–9 years) for children and 2.6 years (range: 1–4 years) for adults. Twenty-eight children and 12 adults had CVs. The patients' characteristics are presented in Table 1. The mean operative time was 150 min in children and 161 min in adults (Table 2).

Table 1. Patients' data

Variables		Children (n = 48)	Adults (n = 41)
Gender	female	17 (35.4%)	28 (68.3%)
	male	31 (64.6%)	13 (31.7%)
Side	left	28 (58.3%)	17 (41.5%)
	right	20 (41.7%)	24 (58.5%)
CVs	yes	28 (58.3%)	12 (29.3%)
	left side	17	3
	right side	11	9
	no	20 (41.7%)	29 (70.7%)

CVs – crossing vessels.

Table 2. Mean operative time

Variables	Children	Mean operative time [min]	Adults	Mean operative time [min]
CVs	IA (dorsal transposition)	152	IIA (cephalad translocation)	160.80
No CVs	IB	149	IIB	161.03

CVs – crossing vessels.

Table 3. Characteristic of short- and long-term complications in both groups

Complication	C–D	Number of cases	Solution
Children			
Short-term			
Prolonged postoperative pain	I	2 (4.2%)	painkillers
Leakage of urine and peritonitis	IIIb	1 (2.0%)	percutaneous peritoneal drainage and change of the JJC; no UPJ intervention
Pelvic dilation and pain	IIIb	1 (2.0%)	nephrostomy tube placement, no UPJ intervention
Long-term			
Chronic abdominal pain	IIIb	1 (2.0%)	JJC placement; no UPJ intervention
Pain and dilation	IIIb	3 (6.2%)	endopyelotomy (1 patient had pyeloplasty redone afterwards)
Adults			
Short-term			
Pain/pyelonephritis	IIIa	4 (9.7%)	JJC replacement
Bleeding from the skin wound	IIIa	1 (2.4%)	wound inspection and hemostasis
Long-term			
Pain and dilation	IIIb	2 (4.9%)	undopyelotomy

C–D – Clavien–Dindo classification; JJC – double J catheter; UPJ – uretero–pelvic junction.

Complications occurred in 8 (16.6%) pediatric patients. Three patients needed reinterventions due to persistent UPJ obstruction over the long-term. Endopyelotomy was performed in all of these patients and 1 of them required a redo pyeloplasty due to failure of the endoscopic procedure. Two of those 3 patients had CVs. One patient, with chronic abdominal pain and moderate dilation, temporarily received a JJC 5 years after pyeloplasty to exclude UPJ obstruction (Table 3).

There were 7 (17%) complications in the adult group. Four patients needed the JJC changed under local anesthesia over the short-term. In 1 patient, prolonged bleeding from the wound required surgical exploration. None of those patients needed a secondary procedure on the UPJ. Two patients needed surgical reintervention due to persistent UPJ obstruction over the long-term (endopyelotomy). One of them had CVs. The mean time to the second surgical treatment was 5.33 months in children and 34.5 months in adults (p = 0.29). In patients with CVs, it was 3 months vs 25 months, respectively. The overall success rate over the long-term was 92.9% in patients after LP with dorsal transposition of the CVs (group 1A) vs 91.7% in patients after LP with cephalad translocation (group 2A) (Table 4).

Table 4. Reinterventions in relation to crossing vessels (CVs) management

CVs	Children (n = 48)	Adults (n = 41)
Yes	dorsal transposition 1A – 2/28 (7.1%)	cephalad translocation 2A – 1/12 (8.3%)
No	1B – 1/20 (5.0%)	2B – 1/29 (3.4%)

Discussion

Ureteropelvic junction obstruction is the most common congenital abnormality of the ureter that leads to hydronephrosis, which has a wide spectrum of signs and symptoms. Nowadays, hydronephrosis is usually diagnosed during antenatal screening, but only 10–25% of these patients need surgical treatment – referred to as a pyeloplasty.[1] The main goal of the treatment is to relieve the symptoms and to protect the affected kidney from damage and loss of function.

A few epidemiological discrepancies between our cohort and the data from the literature were found. The CVs were identified only in 29% of adult patients, which is a rather low prevalence, compared to 39–71%, as published by Leavitt et al.[15] Furthermore, the CVs were more common in adult female patients (68.3%) and on the right side, while other authors claim the CVs present more often in men and on the left side.[1,15] The characteristics of our pediatric population have comparable distribution to the other series.[16–18] We analyzed the consecutive procedures performed by 2 experienced laparoscopic surgeons employing

the transperitoneal approach, which theoretically should minimize the risk that the CVs were overlooked.

Dismembered pyeloplasty with excision of the UPJ region, as proposed by Kusters and modified by Anderson and Hynes, has become the gold standard procedure for treating UPJ stenosis. Non-dismembered methods (Fenger, Foley, Y-V, Culp and DeWeerd's, Scardino and Prince), as well as endoscopic endopyelotomy, have also been developed, but they were found to be less effective.[19] The laparoscopic technique was introduced in adults in 1993 and 2 years afterwards in children. Over time, it has been proven to be at least as effective as the open technique, providing less morbidity, shorter postoperative hospital stays and better cosmetic outcomes.[20,21] Transperitoneal and retroperitoneal approaches have similar outcomes and are used depending on the urologist's preferences.[17] In our cohort, 5% of adult patients and 6% of children needed secondary intervention on the UPJ after transperitoneal dismembered LP, which is comparable with the other series, as published by Seixas–Mikelus et al.[18]

Intrinsic stenosis is the most common underlying pathology leading to obstruction. Extrinsic factors (e.g., CVs) can also play a role, but to this day, it is not clear if the CVs are the sole factor causing obstruction. This implies that there is no consensus on how to deal with this intraoperative finding. Dismembered pyeloplasty with dorsal transposition of the CVs is one of the options.[22,23] However, since Hellström first described the "vascular hitch" in 1949, many surgeons prefer this method in adults and children.[24–28] Simforoosh et al. published his experience with cephalad translocation of the CVs in children and adults with good outcomes in more than 90% of cases.[16,29] Blanc et al. showed a 95% success rate for retroperitoneal LP with posterior transposition in pediatric patients.[30] We had a similar success rate of posterior transposition in children and cephalad translocation in adults using the transperitoneal approach.

In our cohort, all patients had an Anderson–Hynes type dismembered pyeloplasty using the same approach and we believe that it is the strongest point of our research. An additional maneuver was used to fix the CVs. The CVs were translocated in different ways but in the same manner in each age group by the same surgeon. No statistically significant differences were found between groups with and without CVs in children and adults. We observed a similarly low number of secondary interventions due to persistent UPJ obstruction after LP with dorsal transposition in children and cephalad translocation in adults. Our analysis revealed shorter time to reintervention after failed LP in children. We cannot explain this phenomenon but it could be related, on the one hand, to more reliable follow-up in children, and, on the other hand, a tendency to postpone the reintervention with an attempt to solve a problem with an internal diversion using a JJC in adults.

The mean operative time was similar in all groups – 150 min in children and 160 min in adults – indicating that in experienced hands, the additional maneuvers to handle the CVs do not hinder the procedure. The operative time of LP in pediatric patients varies depending on the series. Blanc et al. published his experience with retroperitoneal LP and the mean duration was 185 min (range: 160–235 min).[30] The operative time using the transperitoneal approach presented by van der Toorn et al. was 177 min (range: 115–324 min).[31] Transposition of the CVs was done for adults, but the authors did not differentiate between patients with and without CVs. In our series, the mean operation time is comparable to this data. Furthermore, the additional maneuver to fix the crossing vessels does not significantly prolong the surgery.

The obvious limitation of our paper is the low number of patients. We are also aware that there are many factors that can influence the final outcome of a pyeloplasty: the method, the approach and the technique, as well as the manner of suturing and stenting. Furthermore, comparison of a different surgical technique in the different age groups could be confusing and is statistically not justified. To minimize the bias in both groups, only patients who had the Anderson–Hynes procedure done by the same surgeon and using the transperitoneal approach were selected. In case of CVs, an additional maneuver was used to fix the problem. The results have been assessed in relation to the those who had no CVs – in the pediatric or the adult population, respectively. Hence, we compare the outcome of the dismembered pyeloplasty with transposition of the CV done in a slightly different manner.

We can conclude that LP combined with cephalad translocation, as compared to with dorsal transposition, provide the same results as LP alone when no CVs are present. Another limitation of our study involves the diagnostic and follow-up protocols, which are not the same in children and adults. However, only 1 protocol was consistently used in each group. Finally, the Clavien–Dindo classification may be misleading when used for the pediatric and adult populations. Similar complications that are solved in a comparable manner have a different grade of severity because of the need for general anesthesia (e.g., to insert/change a JJC) in children.

Conclusions

Crossing vessels should be meticulously looked for during pyeloplasty in older children and adults. Dismembered LP with dorsal transposition or cephalad translocation are comparable methods in terms of success rate for treatment of UPJ obstruction in those patients.

References

1. Fefer S, Ellsworth P. Prenatal hydronephrosis. *Pediatr Clin North Am*. 2006;53(3):429–447.
2. Hashim H, Woodhouse CRJ. Ureteropelvic junction obstruction. *European Urology Supplements: Official Journal of the European Association of Urology*. 2012;11(2):25–32.

3. Menon P, Rao KLN, Sodhi KS, Bhattacharya A, Saxena AK, Mittal BR. Hydronephrosis: Comparison of extrinsic vessel versus intrinsic ureteropelvic junction obstruction groups and a plea against the vascular hitch procedure. *J Pediatr Urol*. 2015;11(2):80.e1–6.
4. Szydelko T, Apoznanski W, Koleda P, Rusiecki L, Janczak D. Laparoscopic pyeloplasty with cephalad translocation of the crossing vessel – a new approach to the Hellström technique. *Wideochir Inne Tech Maloinwazyjne*. 2015;10(1):25–29.
5. Singh RR, Govindarajan KK, Chandran H. Laparoscopic vascular relocation: Alternative treatment for renovascular hydronephrosis in children. *Pediatr Surg Int.* 2010;26(7):717–720.
6. Cain MP, Rink RC, Thomas AC, Austin PF, Kaefer M, Casale AJ. Symptomatic ureteropelvic junction obstruction in children in the era of prenatal sonography: Is there a higher incidence of crossing vessels? *Urology*. 2001;57(2):338–341.
7. Anderson JC, Hynes W: Retrocaval ureter: A case diagnosed preoperatively and treated successfully by a plastic operation. *Br J Urol*. 1949;21(3):209.
8. Schuessler WW, Grune MT, Tecuanhuey LV, Preminger GM. Laparoscopic dismembered pyeloplasty. *J Urol.* 1993;150(6):1795–1799.
9. Peters CA, Schlussel RN, Retic AB. Pediatric laparoscopic dismembered pyeloplasty. *J Urol.* 1995;153(6):1962–1965.
10. Knoedler J, Han L, Granberg C, et al. Population-based comparison of laparoscopic and open pyeloplasty in pediatric pelvi-ureretic junction obstruction. *BJU Int.* 2013;111(7):1141–1147.
11. García-Aparicio L, Blazquez-Gomez E, Martin O, et al. Pyeloplasty in patients less than 12 months old. Is the laparoscopic approach safe and feasible? *J Endourol*. 2014;28(8):906–908.
12. Tekgül S, Dogan HS, Erdem E, et al. *Guidelines on Paediatric Urology*. European Association of Urology Guidelines; 2015:43. https://uroweb.org/wp-content/uploads/EAU-Guidelines-Paediatric-Urology-2015.pdf.
13. Szydełko T, Kasprzak J, Lewandowski J, Apoznański W, Dembowski J. Dismembered laparoscopic Anderson–Hynes pyeloplasty versus non-dismembered laparoscopic Y-V pyeloplasty in the treatment of patients with primary ureteropelvic junction obstruction: A prospective study. *J Endourol.* 2012;26(9):1165–1170.
14. Dindo D, Demartines N, Clavien PA. Classification of surgical complications: A new proposal with evaluation in a cohort of 6336 patients and results of a survey. *Ann Surg*. 2004;240(2):205–213.
15. Leavitt DA, Nicholson AF, Ortiz-Alvarado O, et al. Nature of crossing vessels in patients with radiographically normal ureteropelvic junctions: Prevalence and anatomic characteristics. *Urology*. 2013;81(6):1168–1172.
16. Simforoosh N, Tabibi A, Nouralizadeh A, Nouri-Mahdavi K, Shayaninasab H. Laparoscopic management of ureteropelvic junction obstruction by division of anterior crossing vein and cephalad relocation of anterior crossing artery. *J Endourol.* 2005;19(7):827–830.
17. Badawy H, Zoair A, Ghoneim T, Hanno A. Transperitoneal versus retroperitoneal laparoscopic pyeloplasty in children: Randomized clinical trial. *J Pediatr Urol*. 2015;11(3):122.e1–6.
18. Seixas-Mikelus SA, Jenkins LC, Williot P, Greenfield SP. Pediatric pyeloplasty: Comparison of literature meta-analysis of laparoscopic and open techniques with open surgery at a single institution. *J Urol*. 2009;182(5):2428–2432.
19. Carr MC, El-Ghoneimi A. Anomalies and surgery of the ureteropelvic junction in children. In: Wein AJ, Novick AC, Partin A, Peters CA, eds. *Campbell-Walsh Urology, Vol. 4*. 9th ed. Philadelphia, PA: Elsevier Saunders; 2007:3370.
20. Autorino R, Eden C, El-Ghoneimi A, et al. Robot-assisted and laparoscopic repair of ureteropelvic junction obstruction: A systematic review and meta-analysis. *Eur Urol.* 2014;65(2):430–452.
21. Moon DA, El-Shazly MA, Chang CM, Gianduzzo TR, Eden CG. Laparoscopic pyeloplasty: Evolution of a new gold standard. *Urology*. 2006;67(5):932–936.
22. Türk IA, Davis JW, Winkelmann B, et al. Laparoscopic dismembered pyeloplasty: The method of choice in the presence of an enlarged renal pelvis and crossing vessels. *Eur Urol*. 2002;42(3):268–275.
23. Inagaki T, Rha KH, Ong AM, et al. Laparoscopic pyeloplasty: Current status. *BJU Int.* 2005;95(Suppl 2):102–105.
24. Meng MV, Stoller ML. Hellström technique revisited: Laparoscopic management of ureteropelvic junction obstruction. *Urology*. 2003;62(3):404–408.
25. Zhang X, Xu K, Fu B, et al. The retroperitoneal laparoscopic Hellström technique for pelvi-ureteric junction obstruction from a crossing vessel. *BJU Int.* 2007;100(6):1335–1338.
26. Gundeti MS, Reynolds WS, Duffy PG, Mushtaq I. Further experience with the vascular hitch (laparoscopic transposition of lower pole crossing vessels): An alternate treatment for pediatric ureterovascular ureteropelvic junction obstruction. *J Urol.* 2008;180(4 Suppl):1832–1836.
27. Schneider A, Ferreira CG, Delay C, Lacreuse I, Moog R, Becmeur F. Lower pole vessels in children with pelviureteric junction obstruction: Laparoscopic vascular hitch or dismembered pyeloplasty? *J Pediatr Urol.* 2013;9(4):419–423.
28. Singh RR, Govindarajan KK, Chandran H. Laparoscopic vascular relocation: Alternative treatment for renovascular hydronephrosis in children. *Pediatr Surg Int.* 2010;26(7):717–720.
29. Simforoosh N, Javaherforooshzadeh A, Aminsharifi A, Soltani MH, Radfar MH, Kilani H. Laparoscopic management of ureteropelvic junction obstruction in pediatric patients: A new approach to crossing vessels, crossing vein division, and upward transposition of the crossing artery. *J Pediatr Urol.* 2010;6(2):161–165.
30. Blanc T, Muller C, Abdoul H, et al. Retroperitoneal laparoscopic pyeloplasty in children: Long-term outcome and critical analysis of 10-year experience in a teaching center. *Eur Urol*. 2013;63(3):565–572.
31. van der Toorn F, van den Hoek J, Wolffenbuttel KP, Scheepe JR. Laparoscopic transperitoneal pyeloplasty in children from age of 3 years: Our clinical outcomes compared with open surgery. *J Pediatr Urol*. 2013;9(2):161–168.

Serum testosterone depression as a factor influencing the general condition in chronic obstructive pulmonary disease patients

Renata Rubinsztajn[A–D,F], Tadeusz Przybyłowski[B,C,E,F], Marta Maskey-Warzęchowska[B,E,F], Krzysztof Karwat[B,F], Ryszarda Chazan[A,E,F]

Department of Internal Medicine, Pulmonary Diseases and Allergy, Medical University of Warsaw, Poland

A – research concept and design; B – collection and/or assembly of data; C – data analysis and interpretation;
D – writing the article; E – critical revision of the article; F – final approval of the article

Advances in Clinical and Experimental Medicine, ISSN 1899–5276 (print), ISSN 2451–2680 (online) *Adv Clin Exp Med*. 2019;28(6):783–788

Address for correspondence
Renata Rubinsztajn
E-mail: rrubinsztajn@wum.edu.pl

Funding sources
National Centre for Research and Development; project "Chronic obstructive pulmonary disease (COPD) – systemic disease, the biggest threat of the 21st century" (No. 13 0034 06/2009).

Conflict of interest
None declared

Acknowledgements
We would like to thank Barbara Mackiewicz MD, PhD for her help in data collection.

Received on July 27, 2017
Reviewed on January 24, 2018
Accepted on August 9, 2018

Published online on March 6, 2019

Abstract

Background. Testosterone has been recognized for its anabolic properties. It has been documented that in patients with chronic obstructive pulmonary disease (COPD), chronic hypoxia, disease severity, smoking, and corticosteroid treatment may contribute to low testosterone levels.

Objectives. The aim of the study was to evaluate the incidence of decreased serum testosterone concentration in male COPD patients and its influence on their condition.

Material and methods. The study group consisted of 90 male patients, aged 67.2 ±8.8 years in all stages of airflow limitation severity (mild n = 6, moderate n = 43, severe n = 28 and very severe n = 13) Serum testosterone concentration was evaluated using ELISA method (Testosterone ELISE LDN). Decreased serum testosterone level was defined as a value of less than 3 ng/mL. Testosterone levels were related clinical features of COPD.

Results. Serum testosterone concentration did not differ in patients with different stages of airflow limitation severity (3.8 ±0.7 ng/mL for mild: 3.6 ±2.1 ng/mL for moderate; 3.4 ±1.2 ng/mL for severe and 3.7 ±1.7 ng/mL for very severe, respectively). Decreased serum testosterone was found in 30 patients (group A). There were no differences in age, the number of exacerbations or CRP concentration between patients with decreased and the normal serum testosterone group (group B). Group A was characterized by a lower FEV1, shorter 6-minute walking distance, longer smoking history and higher BMI, but no differences in body composition and densitometry results were found.

Conclusions. Serum testosterone depression may occur in as much as 30% of male COPD patients in all COPD stages of severity. The relationship between serum testosterone and negative COPD prognostic factors indicates its influence on the natural history of the disease.

Key words: quality of life, body composition, COPD, testosterone

Cite as
Rubinsztajn R, Przybyłowski T, Maskey-Warzęchowska M, Karwat K, Chazan R. Serum testosterone depression as a factor influencing the general condition in chronic obstructive pulmonary disease patients. *Adv Clin Exp Med*. 2019;28(6):783–788. doi:10.17219/acem/94153

DOI
10.17219/acem/94153

Introduction

Male hypogonadism is a clinical syndrome caused by androgen deficiency which may adversely affect the function of multiple organs and the patient's quality of life. It is due to the disruption of 1 or several levels of the hypothalamic–pituitary–gonadal axis.[1] Male ageing is characterized by a progressive decline in circulating testosterone by approx. 1–2% per year.[2,3] In the European Male Ageing Study, testosterone concentration was lower than 8 nmol/L in 4.1% of patients and lower than 11 nmol/L in 17%.[4] The results show that the symptoms of poor morning erection, low sexual desire, erectile dysfunction, inability to perform vigorous activity, depression, and fatigue were significantly related to testosterone level.[4] According to the US Hypogonadism in Males Study, 38.7% of men aged 45 and above have testosterone deficiency (with the cut-off value set at 300 ng/dL).[5]According to the PolSenior study, 19.9% of male subjects over 65 years had testosterone concentrations below normal values, in 78.2% it was within the normal range and in 1.8% it was over the normal value.[6] Hypogonadism is associated with such symptoms as body composition changes, gynecomastia, muscular atrophy, osteoporotic fracture, loss of height, sleep disturbance, fatigue, decreased energy, muscle aches, and poor memory.[1] Some studies have shown that hypogonadism occurs more frequently in some medical conditions, including type 2 diabetes, obesity, dyslipidemia, obstructive sleep apnea, chronic obstructive pulmonary disease (COPD), rheumatoid arthritis, osteoporosis, chronic corticosteroid use, and others.[1] Important factors that predicted and correlated with hypogonadism were advanced age, obesity, a diagnosis of metabolic syndrome, and a poor general health status.[7] Decreased plasma testosterone may suggest the presence of cardiovascular risk factors and potentially increased risk for heart disease.[8] Low testosterone levels may be linked to increased all-cause mortality. The risk for all-cause mortality during an average of 4–16 years' follow-up period was 24–124% higher in men with low testosterone.[7] The prevalence of hypogonadism in male COPD patients ranges from 22 to 69%,[9] but some studies have shown an insignificant difference in testosterone concentration between COPD and healthy men.[2,10,11] The mechanism of hypogonadism in COPD patients is unclear. Age, chronic hypoxia and hypercapnia, smoking status, comorbidities and corticosteroid therapy are likely reasons for this condition.[9,12]

The aim of the study was to evaluate the incidence of decreased serum testosterone concentration in male COPD patients and its influence on the general condition.

Material and methods

The study group consisted of 90 male patients with COPD diagnosis, in all stages of airflow limitation. Chronic obstructive pulmonary disease was diagnosed according to the Global Initiative for Chronic Obstructive Lung Disease (GOLD) definition.[13] The patients were consecutively enrolled from patients treated on an out-patient basis at the Department of Internal Medicine, Pulmonary Diseases and Allergy at the Medical University of Warsaw. The inclusion criteria were: male sex, age over 50 years, COPD diagnosis, and signed informed consent. The exclusion criteria were: COPD exacerbation in the 4 weeks prior to the study, prostate cancer, treated with testosterone in the 4 weeks prior to the study. The characteristics of study group are presented in Table 1. Medical history and physical examination, including body weight and height, were conducted. The BMI (kg/m^2) was calculated. An analysis of body composition was performed using bioimpedance (Tanita T5896, TANITA Corporation of America, Inc., Arlington Heights, USA). Fat mass (FM), fat free mass (FFM), muscle mass (MM), and total body water (TBW) were expressed as indexes – kg/m^2 (FMI, FFMI, MMI, TBWI). Bone mineral density (BMD) within the postero-anterior lumbar spine (level L1–L4) and the femoral neck were assessed by dual-energy X-ray absorptiometry (DEXA) with the use of a Discovery Densitometer (Hologic, Waltham, USA) according to the manufacturer's recommended standard procedures. Spirometry with bronchial reversibility testing after the administration of salbutamol (400 µg) via a spacer was performed in accordance with the ATS/ERS recommendations (Lungtest 1000, MES, Skawina, Poland).[14] Six-minute walk test (6MWT) was performed in accordance with

Table 1. Characteristics of the study group (median and IQR)

Age	66.5 (60–75)
Pack-years	40.0 (26–50)
Ex-smokers, n [%] Active smokers Never smokers	63 (70.0) 23 (25.6) 4 (4.4)
BMI [kg/m^2]	28.3 (24.6–32.0)
Number of exacerbations/year	1.0 (0–2.0)
mMRC	2.0 (1.0–2.0)
BODE index	2.0 (0.0–3.0)
Post-bronchodilator FEV$_1$L/%predicted	1.53 (1.2–1.9) 53.2 (44.3–63.1)
Post-bronchodilator FVC L/%predicted	3.2 (2.7–3.8) 81.7 (67.4–94.5)
SpO$_2$ (%) at rest	95.0 (93.0–96.0)
6MWD [m]	445.0 (370.0–508.0)
Airflow limitation, n [%] mild moderate severe very severe	 6 (10) 43 (45.5) 28 (35.5) 13 (9)
Chronic inhaled corticosteroid treatment, n [%]	46 (51.1)

BMI – body mass index; BODE index – Body-mass index, airflow Obstruction, Dyspnea, and Exercise; FEV$_1$ – forced expiratory volume in the first second; FVC – forced vital capacity; 6MWD – 6-minute walking test distance.

ATS recommendations.[15] Dyspnea was assessed according to mMRC score.[16] BODE (Body-mass index, airflow Obstruction, Dyspnea, and Exercise) index was calculated for 53 patients.[17] Complete blood count and serum levels of C-reactive protein (CRP), lipid profile and testosterone concentration were evaluated. Serum testosterone concentration was measured with the enzyme-linked immunosorbent assay (ELISA) method, using Testosterone ELISA LDN (Labor Diagnostika Nord GmbH & Co.KG, Nordhorn, Germany). Decreased serum testosterone level for male adults was defined as a value lower than 3 ng/mL.[5] Quality of life was evaluated using the St. George's Respiratory Questionnaire (SGRQ).[18] The variables described above (anthropometric data, lung function, body composition, bone density, exercise performance, basic blood biochemical tests, and quality of life) defined the general condition of COPD patients in our study. The study was funded by the National Center for Research and Development; project "Chronic obstructive pulmonary disease (COPD) – systemic disease, the biggest threat of the 21st century" (13 0034 06/2009). The study received the permission of the Ethics Committee of the Medical University of Warsaw (No. KB/207/2008).

Statistical analysis

Statistical analysis was performed using STATISTICA for Windows software v. 10 (StatSoft, Inc., Tulsa, USA). The Shapiro–Wilk test was used to confirm normal distribution of the data. Normally distributed variables were represented as a mean ± standard deviation. Variables outside the normal distribution were represented as a median (interquartile range – IQR). Student's t-test or Mann–Whitney U tests were used depending on the distribution of the variables analyzed for intergroup comparisons. The significance of the correlation coefficient was assessed on the basis of the Spearman's rank correlation coefficient. Linear regression was used to analyze the differences in 6MWT distance (6MWTD) between groups with normal and decreased serum testosterone. Six-minute walking test distance was entered into the statistical model as a dependent variable, and BMI, FEV_1 and FVC were used as independent factors. Statistical significance was set to a value of $p < 0.05$ for all tests.

Results

The median testosterone concentration was 3.53 (2.7–4.3 ng/mL) in all patients. Serum testosterone concentration did not differ in patients at different stages of airflow limitation (4.1 (3.5–4.6 ng/mL) for mild, 3.4 (2.8–4.3 ng/mL) for moderate, 4.0 (2.6–4.2 ng/mL) for severe, and 2.8 (1.6–3.9 ng/mL) for very severe (Fig. 1). Decreased serum testosterone was found in 30 (33.3%) patients (hypogonadal, group A). There were no differences

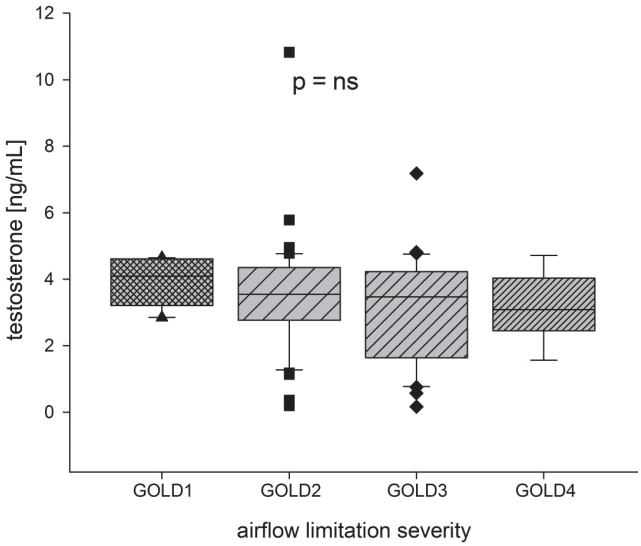

Fig. 1. Serum testosterone in patients at different stages of airflow limitation

The horizontal line within the box indicates the median. The boundaries of the box indicate the 25th and 75th percentiles. The error bars mark the 90th and 10th percentiles. Dotted points represent the outlying values. GOLD1 – FEV_1%FVC <0.7 and FEV_1 ≥80% of predicted; GOLD2 – FEV_1%FVC <0.7 and 50 ≤ FEV_1 <80% of predicted; GOLD3 – FEV_1%FVC <0.7 and 30 ≤ FEV_1 <50% of predicted; GOLD4 – FEV_1%FVC <0.7 and FEV_1 <30% of predicted.

in age, the number of exacerbations, CRP or lipid concentrations, or inhaled corticosteroid treatment between patients with decreased and normal serum testosterone. Group A had a higher BMI, a more relevant smoking history and a worse functional performance (Table 2). Sixteen patients (53.3%) in group A were treated with inhaled corticosteroids (p = ns) and 6 (20.0%) were active smokers (p = ns). Despite differences in BMI between the eugonadal and hypogonadal groups, we found no differences in body composition (FMI, FFMI, MMI, or TBWI). The results

Table 2. Differences in variables studied between hypogonadal (A) and eugonadal groups (B), presented as median and IQR

Variables	Group A	Group B	p-value
BMI [kg/m^2]	30.9 (24.6–34.3)	26.9 (24.0–31.0)	0.01
Pack-years	40.0 (35.0–67.0)	37.0 (20.0–50.0)	0.02
Post-bronchodilator FVC [L]	2.9 (2.4–3.5)	3.4 (2.8–4.1)	0.03
Post-bronchodilator FEV_1 [L]	1.3 (1.0–1.6)	1.6 (1.2–2.1)	0.005
Post-bronchodilator FEV_1 (%pred.)	47.5 (39.0–58.0)	57.5 (45.5–65.5)	0.03
SpO_2 (%) at rest	94.0 (89.0–95.0)	95.0 (93.0–96.0)	0.04
6MWD [m]	365.0 (341.0–455.0)	452.5 (395.0–560.0)	0.006
Hemoglobin [g/dL]	14.3 (12.6–14.9)	14.8 (14.0–15.7)	0.01

BMI – body mass index; FVC – forced vital capacity; FEV_1 – forced expiratory volume in the first second; SpO_2 (%) – arterial oxygen saturation; 6MWD – 6-minute walking test distance.

Table 3. Results of the St. George's Respiratory Questionnaire in the groups studied, presented as median and IQR

Domains of SGRQ	Group A	Group B	p-value
Symptoms	48.2 (26.9–60.6)	48.9 (35.0–62.7)	0.7
Activity	66.3 (57.2–85.8)	66.2 (47.7–75.0)	0.6
Impact	41.1 (24.8–58.1)	34.5 (26.2–46.1)	0.1
Total	51.8 (38.9–63.1)	46.5 (36.6–53.8)	0.8

Table 4. Correlations between testosterone concentration and studied variables

Variables		r	p-value
Serum testosterone concentration	SpO_2 at rest (%)	0.25	0.02
	6MWD	0.32	0.03
	post-bronchodilator FEV_1 (%pred)	0.23	0.02
	post-bronchodilator FEV_1 [L]	0.28	0.005
	post-bronchodilator FVC [L]	0.23	0.02
	BMI [kg/m^2]	–0.25	0.01
	hemoglobin [g/dL]	0.24	0.03
Lumbar vertebrae	L1–L4 BMD	–0.38	0.006
	L1–L4 T score	–0.38	0.006
	L1–L4 Z score	–0.33	0.01

BMD – bone mass density; FEV_1 – forced expiratory volume in the first second; FVC – forced vital capacity; SpO_2 (%) – oxygen saturation; 6MWD – 6-minute walking distance; L1–L4 – lumbar vertebrae; T-score – bone mineral density at the site when compared to the young normal reference mean; Z score – comparison to age-matched normal.

of densitometry were also comparable between groups, as were the mMRC score and BODE index. We did not observe any relationships between the quality of life assessed using the St. George's Respiratory Questionnaire and testosterone concentration, but the results show a tendency for a decreased quality of life (Table 3). There were 15 hypogonadal patients under 65 years of age. The median testosterone concentration in these patients was 3.38 ng/mL (IQR 4.0–0.8 ng/mL) vs 3.52 ng/mL (IQR 2.6–4.4) in patients above 65 years (p = ns). The following relationships between serum testosterone and the variables investigated were found (Table 4): multivariate analysis showed that inclusion into the analysis was based on independent variables: BMI, FEV_1 (% of predicted) and FVC (% of predicted) did not change the statistically significant relationship between 6MWT distance and the decreased or normal serum concentration of testosterone (linear regression, corrected R^2 of the model = 0.10; $p < 0.01$).

Discussion

Our study showed that 1/3 of the investigated cohort of patients with COPD had serum testosterone concentrations below the normal value and this was not dependent on age or inhaled corticosteroid treatment. Although we failed to show differences in serum testosterone concentrations in the 4 degrees of airway obstruction (GOLD1-4), low testosterone patients were characterized by lower FEV_1, FVC, SpO_2 at rest and a shorter 6-minute walking distance. Given the above, it seems that our results confirm the role of testosterone in the general impact of the disease in male patients with COPD.

Smoking is the main COPD risk factor. The influence of smoking on the total testosterone concentration has been the topic of previous studies. Halmenschlager et al. found no relation between smoking and testosterone level[19] but the results of a meta-analysis showed that in a group of healthy men aged 18–61 years, smokers had a higher mean testosterone than non-smokers.[20] Moreover, the Tromsø Study showed differences between testosterone concentration in current, ex- and never-smokers.[21] Our study did not confirm these results.

The next factor associated with COPD is hypoxia. Hypoxia suppresses gonadotropin and testosterone secretion in men with COPD.[9] A strong correlation between the degree of hypoxia and the degree of testosterone reduction was found by Sempleet al.[22] Gosney et al. found smaller testis volume and Leydig-cell atrophy in the necropsy of COPD patients.[23] In our group, oxygen saturation was lower in the hypogonadal group, which is in line with other results. Akbas et al. studied endocrine changes in COPD patients with acute respiratory failure admitted to the intensive care unit. Testosterone concentration tended to be lower in these male patients than in healthy subjects. In 5 (62.5%) COPD patients, testosterone concentration was below the lower limit. In this group, 3 patients had normal LH and FSH levels (hypogonadotropic hypogonadism) and in 2 patients LH and FSH levels were high (hypergonadotropic hypogonadism).[24] According to some authors, hypogonadism could be related to acute illnesses and inflammation.[24] However, other authors disagreed with this hypothesis.[11,25,26] We found no differences between studied groups with regards to CRP concentration or the number of exacerbations. Chronic obstructive pulmonary disease is characterized by persistent airflow limitation that is usually progressive.[13] In the Tromsø Study, the reduction in pulmonary function tests was associated with lower levels of free and total testosterone.[21] Hormones were independently associated with both FVC%pred. and FEV_1%pred., and their concentrations were significantly lower in patients with severe and very severe airflow limitation.[21] In our study, serum testosterone levels did not differ among patients with the 4 degrees of airway obstruction severity (GOLD 1–4), however, we found that patients with lower testosterone levels not only had lower FEV_1 and FVC, but were also characterized by lower SpO_2 at rest and shorter 6-minute walking distance. This seems to confirm the earlier findings that testosterone levels impact functional performance in male patients with COPD.

Low testosterone level as an anabolic hormone was associated with muscle wasting. Peripheral muscle wasting is associated with reduced exercise capacity.[21] Van Vliet et al. found a positive relationship between low androgen status and quadriceps muscle weakness in COPD male patients, but they found no correlations between circulating testosterone concentration and 6MWD.[25] Lagchi et al. found no differences in 6MWD between hypogonadal and eugonadal patients.[27] In our hypogonadal group, the 6MWD was shorter, along with resting oxygen saturation. Moreover, lower 6MWD may be related to lower hemoglobin concentration in the low testosterone group. Our results regarding higher BMI in hypogonadal men were the same as in the Laghi study.[27] Although hypogonadism is associated with the shift in body composition towards more adipose tissue,[28] we found no differences in FFMI, FMI, MMI, and TBWI.

Hypogonadism is one of the risk factors of osteoporosis.[9] No differences in bone mass density were found, but L1–L4 BMD, T-score and Z-score correlated with testosterone concentration. The influence of chronic diseases on the quality of life has been studied by different authors.[29,30] In our previous study, we reported differences in the individual components of the St George's Respiratory Questionnaire depending on the frequency of exacerbations.[31] In this study, we found no differences in the SGRQ score between patients with low and normal testosterone concentration. Our results are in line with the Laghi study.[27] On the other hand, sexual dysfunction is frequent in COPD patients.[32,33] and it has a negative impact on the quality of life.[33] According to Collins et al., the prevalence of low testosterone levels was equal in patients with and without sexual dysfunction.[33] In this study, we did not examine depression as one of the COPD comorbidities, and its correlation with hypogonadism. This was the question of Halabi et al., who found no association between testosterone deficiency and the prevalence of depression.[34] In medical practice, we should remember that critically ill patients develop significant changes in neuroendocrine axes, including changes in testosterone concentration.[35] The question is the impact of testosterone supplementation therapy on COPD patients. Atlantis et al. conducted a meta-analysis of 9 observational studies and concluded that testosterone therapy improves exercise capacity.[36]

Study limitations

This study is limited by the lack of a control group of age-matched healthy smokers. In our opinion, we can compare the COPD patients investigated to the subjects studied in the PolSenior Study. As mentioned in the introduction, in the PolSenior Study, 19.9% of male subjects over 65 years had testosterone concentrations below normal values.[6] Furthermore, we cannot exclude that the lack of some earlier, strongly-confirmed correlations, such as the correlation between testosterone level and FEV_1, may be attributed to the relatively small number of patients studied. However, we would like to emphasize that the earlier observed relationships between testosterone levels and FEV_1 have been indirectly confirmed by our findings of lower FEV_1 in patients with serum testosterone below the lower limit of normal.

Conclusions

Serum testosterone depression may occur in as many as 30% of male COPD patients in all COPD stages of severity. The correlation between serum testosterone and negative COPD prognostic factors may suggest its influence on the natural history of the disease. Larger, multicenter clinical trials are needed to confirm these conclusions and use it in clinical management.

References

1. Hassan J, Barkin J. Testosterone deficiency syndrome: Benefits, risks, and realities associated with testosterone replacement therapy. *Can J Urol*. 2016;23(Suppl 1):20–30.
2. Harman SM, Metter EJ, Tobin JD, Pearson J, Blackman MR; Baltimore Longitudinal Study of Aging. Longitudinal effects of aging on serum total and free testosterone levels in healthy men. Baltimore Longitudinal Study of Aging. *J Clin Endocrinol Metab*. 2001;86(2):724–731.
3. Huhtaniemi I. Late-onset hypogonadism: Current concepts and controversies of pathogenesis, diagnosis and treatment. *Asian J Androl*. 2014;16(2):192–202.
4. Wu FC, Tajar A, Beynon JM, et al; EMAS Group. Identification of late-onset hypogonadism in middle-aged and elderly men. *N Engl J Med*. 2010;363(2):123–135.
5. Mulligan T, Frick MF, Zuraw QC, Stemhagen A, McWhirter C. Prevalence of hypogonadism in males aged at least 45 years: The HIM study. *Int J Clin Pract*. 2006;60(7):762–769.
6. Milewicz A, Krzyżanowska-Świniarska B, Miazgowski T, et al. The reference values of sex hormones and SHBG serum levels in subjects over 65 years old – The PolSenior Study. *Endokrynol Pol*. 2013;64(2):82–93.
7. Zarotsky V, Huang MY, Carman W, et al. Systematic literature review of the risk factors, comorbidities, and consequences of hypogonadism in men. *Andrology*. 2014;2(6):819–834.
8. Chock B, Lin TC, Li CS, Swislocki A. Plasma testosterone is associated with Framingham risk score. *Aging Male*. 2012;15(3):134–139.
9. Balasubramanian V, Naing S. Hypogonadism in chronic obstructive pulmonary disease: Incidence and effects. *Curr Opin Pulm Med*. 2012;18(2):112–117.
10. Leifke E, Gorenoi V, Wichers C, Von Zur Mühlen A, Von Büren E, Brabant G. Age-related changes of serum sex hormones, insulin-like growth factor-1 and sex-hormone binding globulin levels in men: Cross-sectional data from a healthy male cohort. *Clin Endocrinol (Oxf)*. 2000;53(6):689–695.
11. Karadag F, Ozcan H, Karul AB, Yilmaz M, Cildag O. Sex hormone alterations and systemic inflammation in chronic obstructive pulmonary disease. *Int J Clin Pract*. 2009;63(2):275–281.
12. Creutzberg EC, Casaburi R. Endocrinological disturbances in chronic obstructive pulmonary disease. *Eur Respir J Suppl*. 2003;46:76–80.
13. Global Strategy for the Diagnosis, Management and Prevention of COPD, Global Initiative for Chronic Obstructive Lung Disease (GOLD) 2010. www.goldcopd.org. Accessed March 31, 2017.
14. Miller MR, Hankinson J, Brusasco V, et al; ATS/ERS Task Force. Standardisation of spirometry. *Eur Respir J*. 2005;26(2):319–338.
15. Brooks D, Solway S, Gibbons WJ. ATS statement on six-minute walk test. *Am J Respir Crit Care Med*. 2003;167(9):1287.
16. Mahler DA, Wells CK. Evaluation of clinical methods for rating dyspnea. *Chest*. 1988;93(3):580–586.

17. Celli BR Cote C, Marin JM, et al. The body-mass index, airflow obstruction, dyspnoea, and exercise capacity index in chronic obstructive pulmonary disease. *N Engl J Med*.2004;350(10):1005–1012.
18. Jones PW, Quirk FH, Baveystock CM. The St George's Respiratory Questionnaire. *Respir Med.* 1991;85(Suppl B):25–31.
19. Halmenschlager G, Rossetto S, Lara GM, Rhoden EL. Evaluation of the effects of cigarette smoking on testosterone levels in adult men. *J Sex Med.* 2009;6(6):1763–1772.
20. Zhao J, Leung JY, Lin SL, Schooling CM. Cigarette smoking and testosterone in men and women: A systematic review and meta-analysis of observational studies. *Prev Med.* 2016;85:1–10.
21. Svartberg J, Schirmer H, Medbø A, Melbye H, Aasebø U. Reduced pulmonary function is associated with lower levels of endogenous total and free testosterone. *Eur J Epidemiol.* 2007;22(2):107–112.
22. Semple PD, Beastall GH, Watson WS, Hume R. Serum testosterone depression associated with hypoxia in respiratory failure. *Clin Sci (Lond)*. 1980;58(1):105–106.
23. Gosney JR. Atrophy of Leydig cells in the testes of men with longstanding chronic bronchitis and emphysema. *Thorax.* 1987;42(8):615–619.
24. Akbaş T, Karakurt S, Unlügüzel G, Celikel T, Akalin S. The endocrinologic changes in critically ill chronic obstructive pulmonary disease patients. *COPD.* 2010;7(4):240–247.
25. Van Vliet M, Spruit MA, Verleden G, et al. Hypogonadism, quadriceps weakness, and exercise intolerance in chronic obstructive pulmonary disease. *Am J Respir Crit Care Med*. 2005;172(9):1105–1111.
26. Kaparianos A, Argyropoulou E, Efremidis G, Spiropoulos K. Sex hormone alterations and systemic inflammation in a group of male COPD smokers and their correlation with the +138 insA/delA endothelin-1 gene polymorphism. A case-control study. *Eur Rev Med Pharmacol Sci.* 2011;15(10):1149–1157.
27. Laghi F, Antonescu-Turcu A, Collins E, et al. Hypogonadism in men with chronic obstructive pulmonary disease: Prevalence and quality of life. *Am J Respir Crit Care Med.* 2005;171(7):728–733.
28. Arver S, Lehtihet M. Current guidelines for the diagnosis of testosterone deficiency. *Front Horm Res.* 2009;37:5–20.
29. Wacker ME, Jorres RA, Karch A, et al. Relative impact of COPD and comorbidities on generic health-related quality of life: A pooled analysis of the COSYCONET patient cohort and control subjects from the KORA and SHIP studies. *Respir Res.* 2016;17:81.
30. Alonso J, Ferrer M, Gandek B, et al; IQOLA Project Group. Health-related quality of life associated with chronic conditions in eight countries: Results from the International Quality of Life Assessment (IQOLA) Project. *Qual Life Res*. 2004;13(2):283–298.
31. Rubinsztajn R, Przybyłowski T, Maskey-Warzechowska, Karwat K, Chazan R. Exacerbations of chronic obstructive pulmonary disease and quality of life of patients. *Adv Exp Med Biol.* 2016;884:69–74.
32. Köseoğlu N, Köseoğlu H, Ceylan E, Cimrin HA, Ozalevli S, Esen A. Erectile dysfunction prevalence and sexual function status in patients with chronic obstructive pulmonary disease. *J Urol.* 2005;174(1):249–252.
33. Collins EG, Halabi S, Langston M, Schnell T, Tobin MJ, Laghi F. Sexual dysfunction in men with COPD: Impact on quality of life and survival. *Lung.* 2012;190(5):545–556.
34. Halabi S, Collins EG, Thorevska N, Tobin MJ, Laghi F. Relationship between depressive symptoms and hypogonadism in men with COPD. *COPD.* 2011;8(5):346–353.
35. Akbaş T, Deyneli O, Sönmez FT, Akalın S. The pituitary-gonadal-thyroid and lactotroph axes in critically ill patients. *Endokrynol Pol.* 2016; 67(3):305–312.
36. Atlantis E, Fahey P, Cochrane B, Wittert G, Smith S. Endogenous testosterone level and testosterone supplementation therapy in chronic obstructive pulmonary disease (COPD): A systematic review and meta-analysis. *BMJ Open.* 2013;3(8):e003127.

Association of total, acylated and unacylated ghrelin with apolipoprotein A1 and insulin concentrations in acromegalic patients

Hanna Komarowska[1,A–D,F], Barbara Bromińska[1,B,C,F], Nadia Sawicka-Gutaj[1,C,D,F], Magdalena Jaskula-Świtek[1,B,F], Ryszard Waśko[1,A], Marek Ruchała[1,E,F], Gabriel Bromiński[2,C,F], Małgorzata Kotwicka[3,A,E,F]

[1] Department of Endocrinology, Metabolism and Internal Medicine, Poznan University of Medical Sciences, Poland
[2] Department of Urology and Urologic Oncology, Poznan University of Medical Sciences, Poland
[3] Department of Cell Biology, Poznan University of Medical Sciences, Poland

A – research concept and design; B – collection and/or assembly of data; C – data analysis and interpretation; D – writing the article; E – critical revision of the article; F – final approval of the article

Advances in Clinical and Experimental Medicine, ISSN 1899–5276 (print), ISSN 2451–2680 (online) *Adv Clin Exp Med*. 2019;28(6):789–795

Address for correspondence
Hanna Komarowska
E-mail: hkomar@ump.edu.pl

Funding sources
This research was funded by the National Science Centre of Poland (grant No. NN 402 523 040).

Conflict of interest
None declared

Received on July 18, 2018
Reviewed on August 14, 2018
Accepted on October 9, 2018

Published online on March 19, 2019

Abstract

Background. Ghrelin is a hormone that occurs in acylated (AG) or unacylated (UG) form. Ghrelin strongly stimulates growth hormone (GH) secretion from anterior pituitary, as well as regulates the energy balance and various metabolic parameters. Increased consideration is given to UG, thought to be inactive.

Objectives. We aimed to evaluate the levels of total ghrelin, AG and UG in medically naive and treated patients with biochemically active acromegaly, with respect to variables of lipid and glucose metabolism.

Material and methods. We studied total ghrelin, AG and calculated UG levels in a group of 24 patients with active acromegaly and 15 healthy controls. Plasma levels of GH, insulin-like growth factor 1 (IGF-1), insulin, glucose, total cholesterol (TC), high-density lipoprotein (HDL) cholesterol and calculated low-density lipoprotein (LDL) cholesterol, triglycerides (TG), apolipoproteins A1 (APO A1), and B-100 (APO B-100) were measured.

Results. Patients with acromegaly revealed lower levels of total ghrelin than healthy controls. In pooled data of all subgroups, simple linear regression analysis revealed that total ghrelin concentration was significantly associated with APO A1 concentration ($\beta = 0.8087$; $p = 0.0315$) and AG concentration was significantly associated with fasting insulin concentration ($\beta = 15.5183$; $p = 0.011$). There was an inverse association between UG and the patients' age, and positive association between UG and APO A1.

Conclusions. Our results suggest that ghrelin may influence metabolic disturbances in acromegaly. It seems that the assessment of AG and UG is superior to total ghrelin measurement. Mechanisms regulating ghrelin acylation and function of each form need elucidation in order to improve diagnostics and treatment of metabolic disturbances, not only acromegaly.

Key words: ghrelin, acromegaly, apolipoprotein A-1, apolipoprotein B-100

Cite as
Komarowska H, Bromińska B, Sawicka-Gutaj N, et al. Association of total, acylated and unacylated ghrelin with apolipoprotein A1 and insulin concentrations in acromegalic patients. *Adv Clin Exp Med*. 2019;28(6):789–795. doi:10.17219/acem/97403

DOI
10.17219/acem/97403

Introduction

Ghrelin is an endogenous ligand for the growth hormone secretagogue receptor (GHS-R). Its first discovered function was the stimulation of growth hormone (GH) release from the anterior pituitary. This 28 aminoacid peptide was described and named by Kojima et al. in 1999.[1] Post-translational modification-o-n-octanoylation at serine 3 enables binding with GHS-R1a receptor. This is essential for main biological functions of ghrelin: GH release stimulation, regulation of glucose and energy homeostasis.[2] Ghrelin also controls lipid metabolism, both centrally and peripherally. It is the main modulator of hypothalamic lipid metabolism and stimulator of lipogenesis in white adipose tissue.[3]

Ghrelin occurs in acylated (AG) or unacylated (UG) form. Unacylated protein (80–90% of ghrelin in bloodstream) until recently has been considered to be inactive. However, recent research suggests that both forms may have biological functions. They influence the cardiovascular system, adipogenesis and cell proliferation. The unacylated form regulates transport and metabolism of lipids in the human body, presumably through a different kind of receptor.[4,5]

Lipoproteins are particles with a central hydrophobic core containing cholesterol esters and triglycerides surrounded by an outer layer made out of free cholesterol, phospholipids and proteins (apolipoproteins).[6] Among serum apolipoproteins, APO B100 and APO A1 are the most important. Increased concentrations of lipoproteins rich in APO B-100 (VLDL – very low density lipoprotein, VLDL remnants, IDL – intermediate density lipoprotein, LDL – low density lipoprotein, lipoprotein(a)) and decreased levels of those containing mostly APO A1 is pro-atherogenic and facilitates progression of atherosclerosis.[7]

Acromegaly is a rare, chronic illness characterized by increased secretion of GH, most commonly by autonomous adenoma of the anterior pituitary. Rare underlying causes are ectopic GH releasing hormone (GHRH) or GH production by neuroendocrine tumors. Men and women are affected with equal frequency. Typical symptoms are accompanied by systemic disturbances, mainly in the cardiovascular (cardiomyopathy, hypertension and premature atherosclerosis damaging brain and coronary arteries) and respiratory systems (obstructive sleep apnea).[8]

Growth hormone oversecretion is associated with metabolic consequences such as glucose intolerance, insulin resistance and dyslipidemia. Mortality in acromegaly is 2–3 times higher than in the general population, mainly due to cardiovascular and respiratory diseases.[9] First line treatment is transsphenoidal surgery, sometimes preceded by long-acting somatostatin analogs (SSAs) administration.[10]

While in 70% of cases acromegaly is associated with pituitary macroadenoma,[11] most patients require additional treatment. For those with persistent disease following surgery, pharmacological treatment or/and radiotherapy is recommended.[10]

Metabolic complications in acromegalic patients, e.g., lipid profile disturbances, occur due to GH insulin-antagonistic effect. One of the functions of ghrelin is the regulation of glucose turnover and adipose tissue metabolism.[12] Ghrelin might be involved in acromegaly pathogenesis. What is more, ghrelin may be associated with disturbances in lipid and glucose metabolism in acromegalic patients.[13] Research concerning ghrelin in acromegaly is scarce and offers conflicting results. This study assesses total ghrelin, AG and UG in acromegalic patients. To our knowledge, the association between serum apolipoproteins and ghrelin has not been investigated before.

In this study we aimed to evaluate the levels of total ghrelin, AG and UG in medically naive and treated patients with biochemically active acromegaly with respect to variables of lipid and glucose metabolism.

Material and methods

Study design and patients

This was a case-control study. The study group consisted of 24 patients diagnosed with active acromegaly. The diagnosis of acromegaly was based on the lack of serum GH suppression to <1 μg/L during a 75 g oral glucose tolerance test (OGTT), as well as the elevated serum insulin-like growth factor 1 (IGF-1) level. The criteria for disease control were GH suppression below 1 μg/L and normal IGF-1 level for age and sex, during long acting SSAs treatment. Exclusion criteria for the current study were remission of acromegaly, history or clinical or laboratory evidence of chronic disease including liver failure or renal failure, active cancer, and active infectious disease. Fifteen healthy volunteers served as controls. The physical examination of each subject was performed. Height, weight and systolic and diastolic blood pressure were measured in each patient. Blood samples were obtained after an overnight fasting.

All procedures performed in the study were in accordance with the ethical standards of the institutional research committee and with the 1964 Helsinki Declaration and its later amendments or comparable ethical standards. Informed consent was obtained from all individual participants included in the study.

Methods

Fasting serum levels of total ghrelin, AG, GH, IGF-1, total cholesterol, high-density lipoprotein (HDL), low-density lipoprotein (LDL), triglycerides (TG), apolipoprotein A-1 (APO A1), apolipoprotein B-100 (APO B-100), glucose, and insulin levels were evaluated. Hormonal and biochemical measurements were performed using the following methods: total ghrelin – RIA (Phoenix Pharmaceuticals, Burlingame, USA); AG – enzyme-linked immunosorbent assay (ELISA) assay kit (Sceti, Tokyo, Japan); UG was calculated

by subtracting AG from total ghrelin. Growth hormone and IGF-1 – IRMA and RIA (Biosource Europe, Nivelles, Belgium); insulin and glucose – electrochemiluminescence (ECL) (Roche Diagnostics, Risch-Rotkreuz, Switzerland); total cholesterol – enzymatic colorimetric method, HDL cholesterol – homogenic colorimetric enzymatic method, TG – enzymatic colorimetric method with glycerophosphate oxidase and 4-aminophenazon. The LDL cholesterol was calculated on the basis of the concentrations of total and HDL cholesterol. Apolipoproteins A1 and B-100 were assessed using ELISA assay kit (AssayPro, St. Charles, USA). Insulin sensitivity was estimated with homeostasis model assessment (HOMA) index. The following formula was used: HOMA = (FG * FI)/22.5.

Statistical analysis

Statistical analysis was performed with MedCalc Statistical Software v. 16.8.4 (MedCalc Software bvba, Ostend, Belgium; https://www.medcalc.org; 2016). Normality was analyzed with the D'Agostino–Pearson test. When the data did not follow normal distribution, comparisons between 3 groups were performed with the Kruskal–Wallis test. One-way analysis of variance (ANOVA) was used to compare normally distributed parameters between all groups. A χ^2 test was used to compare discrete variables. Simple regression analysis was used to test for the relationships between them. Before inclusion to this statistical analysis, non-normally distributed parameters were logarithmically transformed. P-value <0.05 was considered statistically significant.

Results

In the study group, 8 patients were newly diagnosed and 16 patients received SSAs (9 lanreotide, 7 octreotide). Fourteen patients underwent transsphenoidal resection of GH-secreting adenoma. The remaining 2 patients on SSAs had cardiological contraindication for surgical treatment. Twelve patients treated with long acting SSAs did not meet the criteria for acromegaly control and 4 patients had controlled disease. Patients in the study and the control group did not differ according to sex, age and concomitant diseases. Clinical characteristics of both groups are presented in Table 1. The comparison of laboratory parameters between the study and the control groups is shown in Table 2. Patients with acromegaly had lower levels of total ghrelin than healthy controls (Fig. 1). Other analyzed parameters did not differ between both groups (Table 2). In pooled data of all subgroups, simple linear regression analysis revealed that the total ghrelin concentration was significantly associated with APO A1 concentration (β = 0.8087; p = 0.0315) (Fig. 2), and AG concentration was significantly associated with fasting insulin concentration (β = 15.5183; p = 0.011). There was no association between total ghrelin or AG and age, BMI, fasting glucose, TC, HDL, LDL, TG, APO A1 nor APO B levels, IGF-1, and GH (Table 3). There was an inverse association between UG and patients' age, and positive association between UG and APO A1. When acromegalic patients were analyzed separately, total ghrelin and UG were positively associated with APO A1 (β = 1.2126; p = 0.0003 and β = 1.6533; p = 0.0074, respectively). There was also a positive relationship between AG and insulin concentrations (β = 14.59; p = 0.0377).

Discussion

Foregoing studies concerning the role of ghrelin in acromegaly gave conflicting results.[14–18] Usually, the discrepancies were explained by small, heterogeneous studied groups, differences in treatment regimens and difficulties in assessing AG levels.[19,20] Lack of correlation between ghrelin, GH, IGF-1, and BMI in our research might be explained identically. In the majority of published studies, only AG or/and total ghrelin was assessed. Recently,

Table 1. Clinical characteristics of the study and the control group

Variable	Newly diagnosed acromegalic patients (n = 8)	Acromegalic patients treated with SSAs (n = 16)	Controls (n = 15)	p-value
Age [years] Me (IQR)	55 (53–62)	52 (44.0–56.5)	52 (44–58)	0.48
Sex	F: 4 M: 4	F: 6 M: 10	F: 8 M: 7	0.67
Weight [kg] Me (IQR)	81.5 (64.5–105.0)	93.5 (79.5–103.1)	89 (79.0–102.7)	0.54
Height [m] Me (IQR)	1.66 (1.55–1.79)	1.74 (1.63–1.96)	1.78 (1.62–1.79)	0.29
BMI [kg/m^2] Me (IQR)	30.6 (25.6–31.6)	29.5 (26.0–31.2)	30.8 (27.2–32.6)	0.70
Controlled hypertension, n [%]	6 (75)	8 (50)	7 (46.7)	0.40
Diabetes mellitus, n [%]	2 (25)	1 (6.25)	4 (26.7)	0.25

Me – median; F – females; M – males; IQR – interquartile range; SD – standard deviation; SSAs – long acting somatostatin analogs.

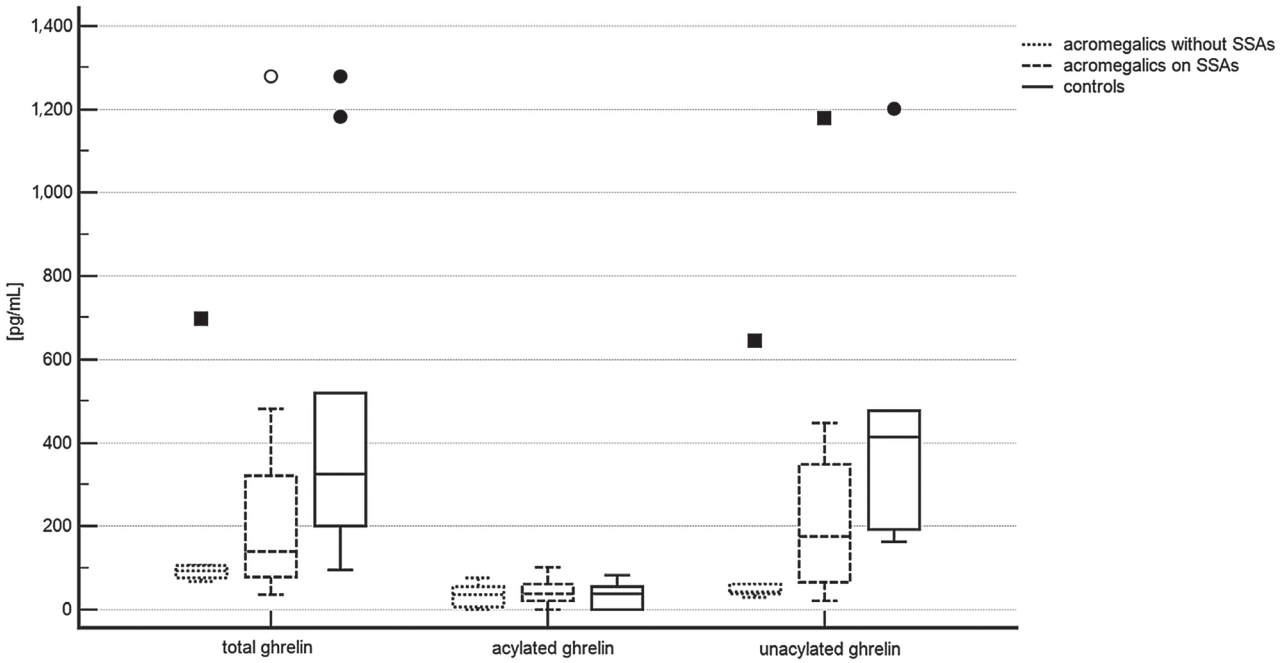

Fig. 1. Comparison of total ghrelin levels between the study and the control groups. The central box represents the values from the lower to upper quartile (25th to 75th percentile). The middle line represents the median. Whiskers extend to a multiple of ×1.5 the distance of the upper and lower quartile, respectively. Outliers are any values beyond the whiskers

Table 2. Laboratory parameters of the study and the control groups

Variable	Newly diagnosed acromegalic patients (n = 8)	Acromegalic patients treated with SSAs (n = 16)	Controls (n = 15)	p-value
Total ghrelin [pg/mL] Me (IQR)	91.94* (75.15–105.80)	140.27^ (79.05–320.14)	324.84*^ (201.06–519.58)	**0.0469**
AG [fmol/mL] Me (IQR)	15.65 (5.63–16.40)	12.5 (9.55–20.20)	15.58 (11.81–21.52)	0.6677
UG [pg/mL] Me (IQR)	42.7* (37.6–61.2)	174.8 (65.7–349.3)	414.8* (192.3–477.0)	**0.0365**
APO A1 [µg/mL] Me (IQR)	2032.5 (1189.5–4185.0)	2628 (1881.50–3729.75)	1470 (1292–2993)	0.2365
APO B [µg/mL] Me (IQR)	2208.5 (1909.5–2613.5)	2368 (2072.0–2528.5)	2207 (1722.5–2517.5)	0.9132
Fasting glucose [mg/dL] Me (IQR)	102 (97–119)	96 (102.5–120.0)	90 (89.0–98.7)	0.1492
Fasting insulin [µu/mL] Me (IQR)	8.68 (7.67–13.29)	7.81 (5.01–11.73)	9.62 (5.89–25.74)	0.7633
TC [mg/dL] Me (IQR)	198 (182.25–260.00)	198 (188–220)	216 (173.5–243.0)	0.9280
LDL [mg/dL] Me (IQR)	130 (111.85–173.05)	116 (97.60–140.85)	125.7 (88.0–171.2)	0.6679
HDL [mg/dL] Me (IQR)	48 (43.75–66.00)	56 (49–64)	42 (37.00–66.75)	0.3032
TG [mg/dL] Me (IQR)	121 (104.25–130.25)	122.5 (91–171)	163.5 (94–255)	0.3346
GH [ng/mL] Me (IQR)	5.455*^ (2.94–31.47)	2.02^ (1.26–4.68)	1.3* (0.77–1.83)	**0.0354**
IGF-1 [ng/mL] Me (IQR)	1081* (480–1297)	440 (328.0–927.5)	202* (125–279)	**0.0359**

Me – median; IQR – interquartile range; AG – acylated ghrelin; UG – unacylated ghrelin; APO A1 – apolipoprotein A1; APO B – apolipoprotein B; TC – total cholesterol; LDL – low-density lipoprotein; HDL – high-density lipoprotein; TG – triglycerides; GH – growth hormone; IGF-1 – insulin-like growth factor 1; SSAs – long acting somatostatin analogs; data followed with the same markers (* or ^) differed significantly; values in bold mean that the relationships were statistically significant.

Table 3. Simple linear regression analysis using total ghrelin and AG serum concentration as dependent variables in pooled data of study and control groups

Variable	Total ghrelin concentration (log)		AG concentration		UG concentration (log)	
	β	p-value	β	p-value	β	p-value
Age (log)	–0.9718	0.0744	1.5235	0.8764	**–1.4111**	**0.0498**
BMI	0.01939	0.3490	–0.4168	0.2795	0.0399	0.1756
APO A1 (log)	**0.8087**	**0.0315**	–9.4672	0.1356	**1.1473**	**0.0370**
APO B	0.0001	0.6141	0.0040	0.1503	0.0001	0.4524
Fasting glucose (log)	–0.0393	0.9575	–5.4848	0.6560	–0.0393	0.9579
Fasting insulin (log)	0.2505	0.5112	**15.5183**	**0.0110**	0.2597	0.6248
HOMA (log)	0.3271	0.4589	**20.9797**	0.0100	0.6632	0.3345
TC	0.0021	0.3207	–0.0390	0.3676	0.0036	0.2465
LDL	0.0018	0.4574	–0.0238	0.6140	0.0018	0.4574
HDL	–0.0015	0.7920	–0.1312	0.2014	–0.0057	0.4356
TG (log)	0.3342	0.4961	4.1919	0.6946	0.3342	0.4961
GH (log)	–0.1430	0.3425	0.2759	0.9149	–0.2851	0.1436
IGF-1	–0.0001	0.8076	0.0019	0.5536	–0.0002	0.3656

AG – acylated ghrelin; UG – unacylated ghrelin; BMI – body mass index; APO A1 – apolipoprotein A1; APO B – apolipoprotein B; HOMA – homeostatic model assessment; TC – total cholesterol; LDL – low-density lipoprotein; HDL – high-density lipoprotein; TG – triglycerides; GH – growth hormone; IGF-1 – insulin-like growth factor 1; values in bold mean that the relationships were statistically significant.

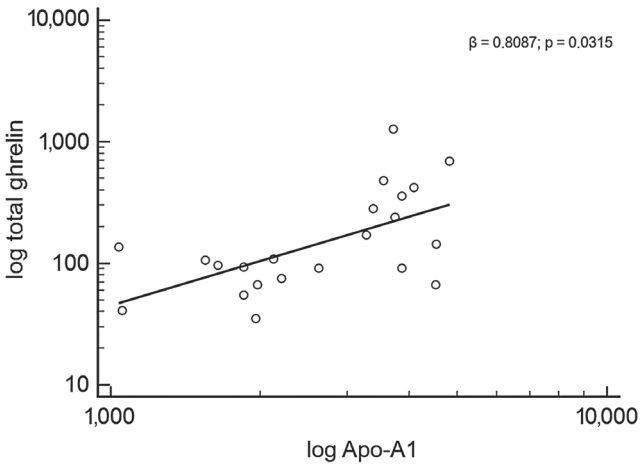

Fig. 2. Association between total ghrelin serum level and APO A1. Data was log-transformed to achieve normal distribution

attention has been focused on UG and AG. Only AG binds with GHR-R, which is why it is called "active". Thus, it was estimated that UG does not have any biological role. However, there is growing evidence against this thesis. The unacylated form, among other functions, positively influences glycemic control in diabetes and exerts regulatory effects on cardiovascular system.[21–24]

We assessed total ghrelin, AG and UG serum concentration, and found lowered total ghrelin levels in acromegalic patients when compared to healthy controls, which is in line with other studies[15–17] (Table 2). In contrast to other authors, the observed difference resulted from low UG concentration and it was not associated with a decrease in AG. A decrease in UG concentration was found in medically naive acromegalic patients, while the AG level was similar regardless of the activity of acromegaly. Cederberg et al. stressed the unfavorable effect of increased AG to the UG ratio leading to diabetes type 2, obesity and hyperphagia.[25] Muhammad et al. suggested the superiority of a ghrelin ratio assessment in comparison with a sole total ghrelin evaluation.[26] Previously, we have noticed that the mean concentrations of total ghrelin and AG were significantly higher in acromegalic patients presented with hypercholesterolemia compared with patients with normocholesterolemia.[13] The UG might inhibit the diabetogenic and atherogenic effects of AG. Thus, a decrease in UG might contribute to insulin resistance, diabetes and atherogenic lipid profile observed in acromegalic patients. Since SSA therapy improves glycemic control and lipid profile, it might explain the increase of serum UG concentration in treated acromegalic patients. Additionally, in our study UG correlated with the patient's age. Its concentration decreases in older people. We could speculate that insulin resistance and atherogenic lipid profile, very common in elderly patients, are associated with disturbances in ghrelin ratio.

Hyperinsulinemia is a very common metabolic disturbance in active acromegaly. Growth hormone normalization after transsphenoidal resection of somatotroph adenoma causes insulin sensitivity improvement.[15,27] Freda et al. suggested that it might be connected with an increase in ghrelin.[15] Additionally, Cappiello et al.[28] confirmed a negative correlation between insulin and ghrelin. In both studies, only total ghrelin was assessed. While most abundant ghrelin fraction in a bloodstream is UG (80–90%) this correlation probably refers to UG. Moreover, in research by Barazzoni et al., HOMA index correlated negatively with total ghrelin and UG.[29] Acylated form probably exerts contraindicatory effects, inducing insulin resistance. In our research, we concluded that AG is positively correlated with insulin. Moreover, when AG

levels rise, HOMA index values increase in both acromegalic patients and in the whole studied group. This might confirm the negative impact of AG on insulin metabolism.

There are ongoing studies on ghrelin-O-acyltransferase enzyme (GOAT), which acylates ghrelin. GOAT was identified in 2008 as a member of membrane bound O-acyl transferase (MBOAT) family, a group of integral membrane proteins involved in lipid-biosynthetic and lipid-signaling reactions.[30,31] The expression of GOAT is similar to that of ghrelin.[32] It is regulated by energy balance, metabolic status and hormones, such as leptin, somatostatin and ghrelin. Unacylated ghrelin does not seem to influence GOAT expression.[31] Most of the recently conducted studies have been performed on animal models.[33,34] Kouno et al. discovered that GOAT knockout mice consumed less amount of food, gained weight slower, and had better glucose metabolism and insulin sensitivity than wild-type littermates.[33] Moreover, GOAT inhibitors increase insulin secretion, enhance peripheral insulin sensitivity, and thereby prevent diabetes and diet-induced obesity.[35,36] Only a few studies concerning GOAT in human have been published.[36,37] Hopkins et al. showed that UG is activated by GOAT located in the target cell.[38] This suggests that UG is subjected to target cell-mediated activation, a novel mechanism for manipulating hormone activity. To our knowledge, there are no studies concerning GOAT expression in acromegaly. In the light of previous research and our results, the variation in ghrelin ratio may be one of the factors determining the development of metabolic disturbances in acromegaly. Therefore, further studies concerning GOAT and ghrelin acylation blockade in acromegaly would be of great value. In the future, drugs inhibiting GOAT could possibly be useful to prevent metabolic abnormalities in acromegalic patients.

Unacylated ghrelin may influence adipose tissue metabolism. Ghrelin inhibits lipolysis and stimulates adipogenesis by direct influence on adipocytes and preadipocytes through unknown receptor.[24] Ghrelin in serum interacts with lipoproteins.[39,40] Heksarelin after binding with CD26 receptor exerts anti-atherogenic effect. Low-density lipoprotein is a ligand for CD26 receptor.[40] It is possible that UG acts similarly to heksarelin. Outer layer of lipoproteins is made out of apolipoproteins, which function as a ligand for receptors. The receptor for UG is unknown. Perhaps UG is biologically active only after binding with lipoproteins and in this form is recognized by the receptor. In our study, we found a correlation between UG and APO A1. It might be suggested that ghrelin influences lipid metabolism through this mechanism.

To sum up, our results may suggest that ghrelin influences metabolic disturbances in acromegaly. It seems that the assessment of AG and UG is superior to total ghrelin measurement. However, the regulation of ghrelin secretion in acromegaly is complex, which might possibly explain the unequivocal results of studies on ghrelin in acromegaly. Even if there is a feedback loop between ghrelin, GH and/or IGF-1, the secretion of ghrelin has to be modulated by other factors. Mechanisms regulating ghrelin acylation and the function of each form are complex but need elucidation in order to improve diagnostics and the treatment of metabolic disturbances, not only in acromegaly. Further studies should answer if GOAT evaluation and its pharmacological blockade may be useful in the prevention of metabolic complications related to ghrelin disturbances.

The main limitation of the study is the small sample size, but it is one of the firsts papers assessing both total ghrelin, AG and UG in acromegalic patients and first paper about the association between serum apolipoproteins and ghrelin. Our results seem to be interesting and worth further analysis.

References

1. Kojima M, Hosoda H, Date Y, Nakazato M, Matsuo H, Kangawa K. Ghrelin is a growth-hormone-releasing acylated peptide from stomach. *Nature*. 1999;402(6762):656–660. doi:10.1038/45230
2. Kojima M, Kangawa K. Ghrelin: Structure and function. *Physiol Rev*. 2005;85(2):495–522. doi:10.1152/physrev.00012.2004
3. Varela L, Vázquez MJ, Cordido F, et al. Ghrelin and lipid metabolism: Key partners in energy balance. *J Mol Endocrinol*. 2011;46(2):R43–63. doi:10.1677/JME-10-0068
4. Harisseh R, Pillot B, Gharib A, et al. Unacylated ghrelin analog prevents myocardial reperfusion injury independently of permeability transition pore. *Basic Res Cardiol*. 2017;112(1):4. doi:10.1007/s00395-016-0595-9
5. Au CC, Furness JB, Brown KA. Ghrelin and breast cancer: Emerging roles in obesity, estrogen regulation, and cancer. *Front Oncol*. 2016; 6:265. doi:10.3389/fonc.2016.00265
6. Feingold KR, Grunfeld C. Introduction to lipids and lipoproteins. In: De Groot LJ, Chrousos G, Dungan K, et al., eds. *Endotext*. South Dartmouth, MA: MDText.com, Inc.; 2000. http://www.ncbi.nlm.nih.gov/books/NBK305896/. Accessed June 12, 2018.
7. Manjunath CN, Rawal JR, Irani PM, Madhu K. Atherogenic dyslipidemia. *Indian J Endocrinol Metab*. 2013;17(6):969–976. doi:10.4103/2230-8210.122600
8. Pivonello R, Auriemma RS, Grasso LFS, et al. Complications of acromegaly: Cardiovascular, respiratory and metabolic comorbidities. *Pituitary*. 2017;20(1):46–62. doi:10.1007/s11102-017-0797-7
9. Găloiu S, Poiană C. Current therapies and mortality in acromegaly. *J Med Life*. 2015;8(4):411–415.
10. Katznelson L, Laws ER, Melmed S, et al. Acromegaly: An endocrine society clinical practice guideline. *J Clin Endocrinol Metab*. 2014;99(11): 3933–3951. doi:10.1210/jc.2014-2700
11. Miranda-Rius J, Brunet-LLobet L, Lahor-Soler E, et al. GH-secreting pituitary macroadenoma (acromegaly) associated with progressive dental malocclusion and refractory CPAP treatment. *Head Face Med*. 2017;13(1):7. doi:10.1186/s13005-017-0140-6
12. Leite-Moreira AF, Soares J-B. Physiological, pathological and potential therapeutic roles of ghrelin. *Drug Discov Today*. 2007;12(7–8): 276–288. doi:10.1016/j.drudis.2007.02.009
13. Jaskula M, Wasko R, Komarowska H, Dziubandowska A, Sowinski J. Serum ghrelin levels and disturbances of the lipid profile in patients with acromegaly. *Neuro Endocrinol Lett*. 2009;30(2):245–255.
14. Jarkovská Z, Rosická M, Marek J, et al. Plasma levels of total and active ghrelin in acromegaly and growth hormone deficiency. *Physiol Res*. 2006;55(2):175–181.
15. Freda PU, Reyes CM, Conwell IM, Sundeen RE, Wardlaw SL. Serum ghrelin levels in acromegaly: Effects of surgical and long-acting octreotide therapy. *J Clin Endocrinol Metab*. 2003;88(5):2037–2044. doi:10.1210/jc.2002-021683
16. Kawamata T, Inui A, Hosoda H, Kangawa K, Hori T. Perioperative plasma active and total ghrelin levels are reduced in acromegaly when compared with in nonfunctioning pituitary tumors even after normalization of serum GH. *Clin Endocrinol (Oxf)*. 2007;67(1):140–144. doi:10.1111/j.1365-2265.2007.02851.x

17. Reyes-Vidal C, Fernandez JC, Bruce JN, et al. Prospective study of surgical treatment of acromegaly: Effects on ghrelin, weight, adiposity, and markers of CV risk. *J Clin Endocrinol Metab*. 2014;99(11): 4124–4132. doi:10.1210/jc.2014-2259
18. Wasko R, Jaskula M, Komarowska H, Zamyslowska H, Sowinski J, Waligorska-Stachura J. Ghrelin concentrations in acromegalic patients in relation to the administered therapy. *Neuro Endocrinol Lett*. 2006;27(1–2):162–168.
19. Delhanty PJD, Huisman M, Julien M, et al. The acylated (AG) to unacylated (UAG) ghrelin ratio in esterase inhibitor-treated blood is higher than previously described. *Clin Endocrinol (Oxf)*. 2015;82(1):142–146. doi:10.1111/cen.12489
20. Kosowicz J, Baumann-Antczak A, Ruchała M, Gryczyńska M, Gurgul E, Sowiński J. Thyroid hormones affect plasma ghrelin and obestatin levels. *Horm Metab Res*. 2011;43(2):121–125. doi:10.1055/s-0030-1269853
21. Özcan B, Neggers SJCMM, Miller AR, et al. Does des-acyl ghrelin improve glycemic control in obese diabetic subjects by decreasing acylated ghrelin levels? *Eur J Endocrinol*. 2014;170(6):799–807. doi:10.1530/EJE-13-0347
22. Delhanty PJ, Neggers SJ, van der Lely AJ. Des-acyl ghrelin: A metabolically active peptide. *Endocr Dev*. 2013;25:112–121. doi:10.1159/000346059
23. Kleinz MJ, Maguire JJ, Skepper JN, Davenport AP. Functional and immunocytochemical evidence for a role of ghrelin and des-octanoyl ghrelin in the regulation of vascular tone in man. *Cardiovasc Res*. 2006;69(1):227–235. doi:10.1016/j.cardiores.2005.09.001
24. Thompson NM, Gill DAS, Davies R, et al. Ghrelin and des-octanoyl ghrelin promote adipogenesis directly in vivo by a mechanism independent of the type 1a growth hormone secretagogue receptor. *Endocrinology*. 2004;145(1):234–242. doi:10.1210/en.2003-0899
25. Cederberg H, Rajala U, Koivisto V-M, et al. Unacylated ghrelin is associated with changes in body composition and body fat distribution during long-term exercise intervention. *Eur J Endocrinol*. 2011;165(2): 243–248. doi:10.1530/EJE-11-0334
26. Muhammad A, Delhanty PJD, Huisman M, Visser JA, Jan van der Lelij A, Neggers SJCMM. The acylated/unacylated ghrelin ratio is similar in patients with acromegaly during different treatment regimens. *J Clin Endocrinol Metab*. 2017;102(7):2425–2432. doi:10.1210/jc.2017-00147
27. Miya A, Nakamura A, Miyoshi H, et al. Glucose tolerance is improved following surgery for silent somatotroph adenoma. *International Journal of Diabetes and Clinical Research*. 2015;2:6–12.
28. Cappiello V, Ronchi C, Morpurgo PS, et al. Circulating ghrelin levels in basal conditions and during glucose tolerance test in acromegalic patients. *Eur J Endocrinol*. 2002;147(2):189–194.
29. Barazzoni R, Gortan Cappellari G, Semolic A, et al. Plasma total and unacylated ghrelin predict 5-year changes in insulin resistance. *Clin Nutr*. 2016;35(5):1168–1173. doi:10.1016/j.clnu.2015.10.002
30. González CR, Vázquez MJ, López M, Diéguez C. Influence of chronic undernutrition and leptin on GOAT mRNA levels in rat stomach mucosa. *J Mol Endocrinol*. 2008;41(6):415–421. doi:10.1677/JME-08-0102
31. Khatib MN, Gaidhane S, Gaidhane AM, Simkhada P, Zahiruddin QS. Ghrelin O acyl transferase (GOAT) as a novel metabolic regulatory enzyme. *J Clin Diagn Res*. 2015;9(2):LE01–05. doi:10.7860/JCDR/2015/9787.5514
32. Lim CT, Kola B, Grossman A, Korbonits M. The expression of ghrelin O-acyltransferase (GOAT) in human tissues. *Endocr J*. 2011;58(8): 707–710.
33. Kouno T, Akiyama N, Fujieda K, et al. Reduced intake of carbohydrate prevents the development of obesity and impaired glucose metabolism in ghrelin O-acyltransferase knockout mice. *Peptides*. 2016;86:145–152. doi:10.1016/j.peptides.2016.11.003
34. Barnett BP, Hwang Y, Taylor MS, et al. Glucose and weight control in mice with a designed ghrelin O-acyltransferase inhibitor. *Science*. 2010;330(6011):1689–1692. doi:10.1126/science.1196154
35. Teuffel P, Wang L, Prinz P, et al. Treatment with the ghrelin-O-acyltransferase (GOAT) inhibitor GO-CoA-Tat reduces food intake by reducing meal frequency in rats. *J Physiol Pharmacol*. 2015;66(4):493–503.
36. Ritze Y, Schollenberger A, Hamze Sinno M, et al. Gastric ghrelin, GOAT, leptin, and leptinR expression as well as peripheral serotonin are dysregulated in humans with obesity. *Neurogastroenterol Motil*. 2016;28(6):806–815. doi:10.1111/nmo.12773
37. Mihalache L, Gherasim A, Niță O, et al. Effects of ghrelin in energy balance and body weight homeostasis. *Hormones (Athens)*. 2016;15(2): 186–196. doi:10.14310/horm.2002.1672
38. Hopkins AL, Nelson TAS, Guschina IA, et al. Unacylated ghrelin promotes adipogenesis in rodent bone marrow via ghrelin O-acyl transferase and GHS-R1a activity: Evidence for target cell-induced acylation. *Sci Rep*. 2017;7:45541. doi:10.1038/srep45541
39. De Vriese C, Hacquebard M, Gregoire F, Carpentier Y, Delporte C. Ghrelin interacts with human plasma lipoproteins. *Endocrinology*. 2007;148(5):2355–2362. doi:10.1210/en.2006-1281
40. Purnell JQ, Weigle DS, Breen P, Cummings DE. Ghrelin levels correlate with insulin levels, insulin resistance, and high-density lipoprotein cholesterol, but not with gender, menopausal status, or cortisol levels in humans. *J Clin Endocrinol Metab*. 2003;88(12):5747–5752. doi:10.1210/jc.2003-030513

Polyphenols and dietary antioxidant potential, and their relationship with arterial hypertension: A cross-sectional study of the adult population in Poland (WOBASZ II)

Anna Waśkiewicz[1,A–F], Małgorzata Elżbieta Zujko[2,A,C,E,F], Danuta Szcześniewska[1,B,C,F], Andrzej Tykarski[3,B,E,F], Magdalena Kwaśniewska[4,B,E,F], Wojciech Drygas[4,1,B,E,F], Anna Maria Witkowska[2,A,C,E,F]

[1] Department of Epidemiology, Cardiovascular Disease Prevention and Health Promotion, National Institute of Cardiology, Warszawa, Poland
[2] Department of Food Biotechnology, Medical University of Bialystok, Poland
[3] Department of Hypertension, Angiology and Internal Medicine, Poznan University of Medical Sciences, Poland
[4] Department of Social and Preventive Medicine, Medical University of Lodz, Poland

A – research concept and design; B – collection and/or assembly of data; C – data analysis and interpretation; D – writing the article; E – critical revision of the article; F – final approval of the article

Advances in Clinical and Experimental Medicine, ISSN 1899–5276 (print), ISSN 2451–2680 (online) *Adv Clin Exp Med*. 2019;28(6):797–806

Address for correspondence
Anna Waśkiewicz
E-mail: awaskiewicz@ikard.pl

Funding sources
This study was supported by the National Institute of Cardiology (grant No. 2.17/I/16) and by the Medical University of Bialystok (grant No. N/ST/ZB/16/001/3317).

Conflict of interest
None declared

Acknowledgements
The authors express special thanks to the entire research team and collaborators from the field centers in the 16 voivodeships, and to all participants of the WOBASZ II study.

Received on November 23, 2017
Reviewed on January 30, 2018
Accepted on May 22, 2018

Published online on April 8, 2019

Abstract

Background. Oxidative stress plays a key role in the development of most non-communicable diseases, including arterial hypertension (AH). Diet is the major source of exogenous antioxidants, which support the body in the elimination of excessive free radicals.

Objectives. To assess dietary total antioxidant potential (DTAP) and dietary polyphenol intake (DPI), and to determine the relationship between DTAP, DPI and hypertension in the Polish adult population; to indicate dietary sources of DTAP and DPI in participants with and without AH.

Material and methods. Within the frame of the National Multicenter Health Survey (WOBASZ II), a random sample of the whole Polish population aged 20 years and above was screened during the years 2013–2014. Dietary habits and blood pressure were assessed in 2,554 men and 3,136 women. Dietary total antioxidant potential and DPI were calculated according to the amount of food consumed by the participants combined with the antioxidant potential and polyphenol contents in foods.

Results. The mean DTAP was 12.36 mmol/day in men and 12.27 mmol/day in women, and DPI was 2069 mg/day and 1989 mg/day, respectively. The DTAP and DPI were associated with reduced odds of AH in the Polish population. After adjusting for confounding variables, higher DTAP (by 1 mmol/day) had reduced odds of AH by 1.3% in men and by 1.8% in women and higher DPI (by 100 mg/day) by 1.1% and by 2.2%, respectively. Regardless of sex and AH, the main sources of DTAP and DPI were beverages, especially coffee and tea (over 50%), fruit (12–24%) and vegetables (12–18%).

Conclusions. The intake of food with high antioxidant potential and rich in polyphenols was associated, slightly but independently of other factors, with a lower chance of hypertension in the adult Polish population. Irrespective of sex and AH, coffee and tea were the basic dietary sources of the antioxidants.

Key words: arterial hypertension, polyphenols, Polish population, dietary antioxidant potential

DOI
10.17219/acem/91487

Cite as
Waśkiewicz A, Zujko ME, Szcześniewska D, et al. Polyphenols and dietary antioxidant potential, and their relationship with arterial hypertension: A cross-sectional study of the adult population in Poland (WOBASZ II). *Adv Clin Exp Med*. 2019;28(6):797–806. doi:10.17219/acem/91487

Oxidative stress plays a key role in the development of most non-communicable diseases, including circulatory disorders and arterial hypertension (AH). It results from an imbalance between the action of free radicals and the antioxidant potential of the body. Diet is the major source of exogenous antioxidants, such as polyphenols, certain vitamins (C, E, β-carotene) and mineral components (Se, Zn, Fe, Mn, Cu) which support the body in the elimination of excessive free radicals through suitable enzymatic proteins.[1,2]

A proper dietary supply of antioxidants exerts a beneficial effect on the lipid metabolism and endothelial function, reduces AH and decreases platelet aggregation, as well as seals and enhances vascular walls, leading to improvement in the peripheral circulation. However, the cardioprotective effect of polyphenols is based not only on the destruction of free radicals but also involves anti-aggregative properties and the ability to modulate numerous enzymatic pathways.[2–6]

Up to now, neither recommended dietary antioxidant potential nor the total content of polyphenols that would exert a beneficial effect on health have been established in a daily food ration. However, publications are available on antioxidant potential and polyphenol intake in the diets of people living in various countries as well as on the relationship between these parameters and cardiovascular disease (CVD), mainly in terms of mortality risk and rate.[7–15] At the same time, there are by far fewer reports concerning the relationship between antioxidant potential and polyphenol intake and AH.[16–19] In Poland, AH is diagnosed in approx. 42.7% of adult inhabitants, posing a substantial health hazard and generating social and economic costs.[20]

Taking into consideration the high prevalence of AH and the fact that oxidative stress is one of its promoting factors, it seems essential to investigate the consumption of bioactive substances that exhibit antioxidant properties in the Polish population.

The study objective was to:

– assess dietary total antioxidant potential (DTAP) and dietary polyphenol intake (DPI) in the Polish population in correlation with socioeconomic and health-related factors.
– evaluate the relationship between DTAP, DPI and AH;
– indicate and assess the differentiation of dietary sources of DTAP and DPI in participants with and without hypertension.

Material and methods

Study population

The study population involved a random sample of Polish residents aged 20 and older, examined in the years 2013–2014, as part of the Multicenter National Population Health Examination Survey (WOBASZ II). The project was conducted by the Institute of Cardiology in Warszawa, Poland, in cooperation with 5 medical universities in Poland. A total of 15,120 people of both sexes were drawn from the Department of State Registry database run by the Ministry of Internal Affairs (PESEL register). The selection was made as a 3-stage sampling, stratified according to administrative units (voivodeships), type of urbanization (community size) and sex. This type of random sampling, as well as the sample size, allowed reliable assessment of dietary habits in the Polish population. Altogether, 6,170 respondents were recruited to the study, whereas reliable dietary recalls were obtained from 5,689 people (2,554 men and 3,135 women). The aims of WOBASZ II, its organization scheme, methodological details, methods of information collection, and measurements were presented in an earlier paper.[21]

Arterial blood pressure

The level of arterial blood pressure was measured using automatic devices UA-631 (A&D Company Ltd, Japan), approved by the Association for the Advancement of Medical Instrumentation (Arlington, USA). Blood pressure was measured 3 times at the right shoulder, in a sitting position, at 1-minute intervals. The mean value of blood pressure obtained from the 2nd and 3rd measurements was taken for the assessment. Study participants were diagnosed with hypertension when their systolic blood pressure (SBP) was ≥140 mm Hg and/or diastolic blood pressure (DBP) was ≥90 mm Hg, and/or they took hypotensive drugs.[21]

Dietary assessment

Dietary habits were assessed by means of a 24-hour dietary recall. The consumption of products that are the source of the antioxidant potential and polyphenols was calculated on the basis of daily food intake and food formulation. Food products were combined into groups, taking into consideration their type, origin and production technology. A total of 367 products and dishes, i.e., various beverages, vegetables and their products, fruit and jams, nuts and seeds, cereals, bread, and chocolate were included in the study.

Determination of antioxidant potential and polyphenols in food

The antioxidant potential and the content of polyphenols in food products typical of the Polish market were determined in the Department of Food Biotechnology, Medical University of Bialystok, Poland. The analyses involved 3 independent samples of each product, purchased in retail, and in each case 2 versions were taken into consideration – the raw product and the product after culinary process. The distinction between raw and after culinary processes

is made due to the fact that culinary processes have an influence on investigated dietary antioxidants.[22] Solid food samples were dried and extracted using a methanol-acetate mixture, and the extracts were analyzed. Direct measurements were performed in fluid samples. The antioxidant potential was determined using the ferric-reducing antioxidant potential (FRAP) method, according to Benzie and Strain,[23] and the polyphenol content (expressed as aglycones) was measured using the method according to Singleton and Rossi.[24] For each of the products, an average of 3 measurements was assumed for further analysis. In the case of the very few products that were not subjected to laboratory analysis, the antioxidant potential and polyphenol content were obtained from the available database.[25,26] For each study participant, DTAP and DPI were determined taking into consideration the consumption of food products and the level of their antioxidant potential and polyphenol content.

Statistical methods

Methods of descriptive statistics were applied to describe continuous variables (mean, standard deviation (SD), quartiles) and the percentages of the respective values were used for categorized variables. Parametric tests (analysis of variance (ANOVA) and Student's t-test) and non-parametric tests (Mann–Whitney–Wilcoxon test and χ^2 test) were used to compare the groups, depending on whether they fulfil the assumption of normal distribution or not.

The analysis of covariance (generalized linear model (GLM) procedure) with age and season adjustment was applied to determine the mean DTAP and DPI in groups with different socioeconomic and health status. The association between DTAP, DPI and AH was assessed by logistic regression analyses (LOGISTIC procedure). Odds ratios (ORs) with the corresponding 95% confidence intervals (CIs) were calculated for unadjusted and adjusted models.

The level of significance for bilateral tests was considered to be at $p < 0.05$. The statistical analysis was performed with the statistical package SAS v. 9.2 (SAS Institute, Cary, USA).

Results

The mean total antioxidant potential of a daily food ration in the adult population of Poland (age- and season-adjusted) was 12.36 mmol/day in the group of men and 12.27 mmol/day in the group of women, whereas the total content of polyphenols was found to be 2,069 mg/day and 1,989 mg/day, respectively (Table 1, 2). The levels of the parameters studied depended on socioeconomic and health-related factors, such as age, marital status and paid employment in both sexes, and education only in women. Of the health-related factors, DTAP was determined by health self-assessment in both sexes, CVD in men and AH in women. In turn, DPI in men was influenced by CVD, and in women by AH, diabetes and health self-assessment (Table 1, 2).

The analysis of the relationship between DTAP, DPI and AH, having eliminated other factors, showed a significant decrease in the contribution of women with AH along with an increase in the quartile of the antioxidant potential (45% in 1st quartile vs 38% in 4th quartile) and polyphenols (45% vs 39%, respectively). In the group of men, the tendencies were similar, although statistically insignificant (Table 3).

The odds of AH with the antioxidant potential increased by 1 mmol/day was lower by 1.1% in the group of men and by 2.3% among women, and after adjustment for confounding variables (listed below Table 3), lower by 1.3% and 1.8%, respectively, in the sex groups. Similar results were obtained for polyphenols. The increase in the polyphenol supply by 100 mg/day, lowered the odds of AH by 0.8% in men and by 2.4% in women, and after adjustment for other AH-affecting factors, by 1.1% and 2.2%, respectively (Table 4).

Tables 5 and 6 present the contribution of food groups (beverages, vegetables, fruit, cereals, nuts and seeds, chocolate, and cacao) to DTAP and DPI intakes. Among adult residents of Poland, irrespective of sex and AH, beverages, especially tea and coffee, appeared to be the basic food sources of antioxidant potential and polyphenols. Over 50% of DTAP and more than 40% of DPI were obtained from beverages. Fruit provided approx. 12–18% of the antioxidant potential and 17–24% of polyphenols, and vegetables 14–18% and 12–14%, respectively, depending on sex and AH. Further places were occupied by cereal products, nuts and seeds, chocolate, and cacao. Of fruit, apples and strawberries, and of vegetables, potatoes and cabbage were a significant source of DTAP and DPI, and beetroots of DTAP only.

Some differences were found in dietary sources of DTAP and DPI between people with and without AH. Among men with AH, the contribution of DTAP and DPI from fruit was higher whereas from cereal products, nuts and seeds, chocolate and cacao, it was lower. The diet of women with AH was characterized by a lower contribution of DTAP and DPI obtained from beverages, cereal products, chocolate, and cacao. The quantities provided by vegetables and fruit were similar, irrespective of AH (Table 5, 6).

Discussion

The imbalance between pro- and antioxidant processes and the accumulation of reactive oxygen species (ROS) in the body which initiate cellular damage promote non-communicable diseases. A significant correlation was found between the dietary antioxidant potential and the antioxidant status of blood serum.[27] Thus, proper nutrition provided by dietary components which act as antioxidants can prevent the harmful effects of oxidative stress.

Table 1. Dietary total antioxidant potential (mmol/day) of Polish population according to socioeconomic and health-related factors (adjusted for age and season)

Variable	Men				Women			
	N[1]	mean	CI	p-value	N[1]	mean	CI	p-value
Total population	2,554	12.36	12.08–12.65		3,135	12.27	12.02–12.53	
Age group [years]								
20–35	574	11.69	11.08–12.30	<0.0001	635	11.77	11.21–12.33	<0.0001
36–50	706	13.43	12.88–13.98		832	13.16	12.67–13.65	
50–65	783	13.01	12.49–13.53		1,004	12.93	12.48–13.38	
≥65	491	10.64	9.98–11.30		664	10.60	10.05–11.15	
Educational level								
low	1,135	12.15	11.69–12.60	0.2898	1,136	11.54	11.09–12.00	0.0005
medium	938	12.68	12.20–13.17		1,200	12.49	12.08–12.90	
high	478	12.30	11.61–13.00		796	12.96	12.42–13.50	
Marital status								
married	1,792	12.78	12.43–13.13	<0.0001	2,003	12.54	12.22–12.86	0.0049
single	761	11.42	10.87–11.98		1,133	11.78	11.35–12.20	
Occupational activity								
yes	1,525	12.84	12.44–13.25	0.0011	1,453	12.64	12.24–13.03	0.0178
no	1,028	11.68	11.18–12.19		1,681	11.94	11.58–12.31	
CVD								
diagnosed with CVD	494	11.06	10.35–11.77	<0.0001	664	12.15	11.56–12.75	0.689
without history of CVD	2,060	12.69	12.36–13.02		2,492	12.29	12.00–12.58	
Diabetes								
diagnosed/glucose ≥7 mmol/L	290	11.80	10.89–12.71	0.1463	297	11.50	10.64–12.35	0.0625
fasting glucose <7 mmol/IL	2,155	12.52	12.20–12.85		2,685	12.36	12.08–12.64	
Blood pressure								
≥140/90 mm Hg/medication	1,249	12.13	11.70–12.57	0.1465	1,292	11.79	11.35–12.23	0.0118
<140/90 mm Hg	1,271	12.61	12.18–13.05		1,807	12.59	12.23–12.95	
Self-assessment of health status								
very good, good	1,733	12.67	12.30–13.03	0.0237	2,019	12.66	12.33–12.99	<0.0001
average	662	11.64	11.03–12.25		916	11.79	11.29–12.28	
bad, very bad	101	12.12	10.63–13.61		148	9.83	8.63–11.03	

[1] Differences in the size of groups derive from the lack of data for some people; CVD – cardiovascular disease; CI – confidence interval.

Table 2. Dietary polyphenol intake (mg/day) of Polish population according to socioeconomic and health-related factors (adjusted for age and season)

Variable	Men				Women			
	N[1]	mean	CI	p-value	N[1]	mean	CI	p-value
Total population	2,554	2,069	2,035–2,104		3,135	1,989	1,958–2,020	
Age group [years]								
20–35	574	2,007	1,930–2,083	<0.0001	635	1,930	1,865–1,996	<0.0001
36–50	706	2,189	2,120–2,258		832	2,098	2,041–2,155	
50–65	783	2,161	2,095–2,226		1,004	2,074	2,022–2,126	
≥65	491	1,837	1,754–1,920		664	1,771	1,708–1,835	
Educational level								
low	1,135	2,064	2,007–2,121	0.8672	1,136	1,921	1,868–1,974	0.0108
medium	938	2,085	2,024–2,146		1,200	2,013	1,965–2,061	
high	478	2,062	1,976–2,149		796	2,043	1,980–2,106	
Marital status								
married	1,792	2,114	2,070–2,159	0.0008	2,003	2,027	1,990–2,065	0.0004
single	761	1,971	1,901–2,040		1,133	1,915	1,866–1,965	
Occupational activity								
yes	1,525	2,133	2,082–2,183	0.0007	1,453	2,032	1,986–2,079	0.0129
no	1,028	1,982	1,919–2,046		1,681	1,948	1,905–1,991	
CVD								
diagnosed with CVD	494	1,948	1,859–2,037	0.003	664	1,935	1,865–2,004	0.1008
without history of CVD	2,060	2,101	2,060–2,143		2,492	2,001	1,967–2,034	
Diabetes								
diagnosed/glucose ≥7 mmol/L	290	2,001	1,888–2,114	0.1668	297	1,863	1,764–1,962	0.0094
fasting glucose <7 mmol/L	2,155	2,086	2,046–2,126		2,685	2,002	1,971–2,034	
Blood pressure								
≥140/90 mm Hg/medication	1,249	2,048	1,993–2,103	0.2821	1,292	1,906	1,854–1,957	0.0002
<140/90 mm Hg	1,271	2,093	2,038–2,147		1,807	2,045	2,002–2,087	
Self-assessment of health status								
very good, good	1,733	2,093	2,047–2,139	0.2876	2,019	2,038	2,000–2,076	<0.0001
average	662	2,019	1,942–2,095		916	1,928	1,870–1,986	
bad, very bad	101	2,064	1,877–2,251		148	1,692	1,552–1,832	

[1] Differences in the size of groups derive from the lack of data for some people; CVD – cardiovascular disease; CI – confidence interval.

Table 3. Prevalence of arterial hypertension by quartiles of dietary total antioxidant potential (DTAP) and dietary polyphenol intake (DPI)

Parameters	Quartile 1	Quartile 2	Quartile 3	Quartile 4	p-value
			Men		
DTAP [mmol/day] mean ±SD range	 5.22 ±1.75 0.47–7.70	 9.43 ±1.02 7.71–11.15	 13.16 ±1.20 11.16–15.38	 21.67 ±8.52 15.39–95.37	
Arterial hypertension [%][1]	50.15	51.56	50.98	46.24	0.1489
DPI [mg/day] mean ±SD range	 1,033 ±285 174–1,409	 1,694 ±158 1,410–1,956	 2,252 ±173 1,957–2,559	 3,305 ±800 2,560–9,047	
Arterial hypertension [%][1]	49.64	50.91	51.91	46.42	0.1511
			Women		
DTAP [mmol/day] mean ±SD range	 5.52 ±1.77 0.32–7.91	 9.72 ±1.00 7.94–11.35	 13.14 ±1.11 11.35–15.19	 20.68 ±9.07 15.20–191.82	
Arterial hypertension [%][1]	45.17	42.88	41.11	38.12	0.0073
DPI [mg/day] mean ±SD range	 1,035 ±273 140–1,414	 1,665 ±138 1,415–1,903	 2,156 ±155 1,904–2,441	 3,093 ±703 2,442–8,793	
Arterial hypertension [%][1]	45.37	43.68	39.40	38.82	0.0030

[1] Adjusted for age, BMI, smoking and physical activity; BMI – body mass index; SD – standard deviation.

Table 4. Multivariate odds ratio (OR) and 95% confidence intervals (95% CI) for arterial hypertension by total dietary total antioxidant potential (DTAP) (per 1 mmol/day) and dietary polyphenol intake (DPI) (per 100 mg/day)

Variables	Men			Women		
	OR	95% CI	p-value	OR	95% CI	p-value
DTAP unadjusted adjusted[1]	 0.989 0.987	 0.979–0.999 0.976–0.998	 0.0480 0.0248	 0.977 0.982	 0.966–0.988 0.970–0.995	 <0.0001 0.0051
DPI unadjusted adjusted[1]	 0.992 0.989	 0.983–0.999 0.981–0.998	 0.0474 0.0194	 0.976 0.978	 0.967–0.985 0.969–0.988	 <0.0001 <0.0001

[1] Adjusted for age, body mass index (BMI), smoking and physical activity.

The results indicate that the mean total antioxidant potential in the diet of the adult Polish population was 12.36 mmol/day in the group of men and 12.27 mmol/day in the group of women, whereas the polyphenol content amounted to 2,069 mg/day and 1,989 mg/day, respectively. However, the comparison of our results with the levels of DTAP and DPI in other populations is very difficult due to, first of all, the use of various methods to determine these substances. The antioxidant potential can be measured, e.g., according to the FRAP or oxygen radical absorbance capacity (ORAC) method. The polyphenols exist as aglycones (the free form) or glycosides (occurring as compounds with sugars, most commonly with glucose).

Since the recommended level of DTAP and DPI has not been established, it is difficult to assess whether the intake of bioactive components of adult residents of Poland meets recommendations.

There are very few studies, particularly conducted in Polish centers, the results of which can be directly compared to our findings. The available data obtained with the ORAC method indicates that DTAP was found at the level of 8,300–10,000 µmolTE/day among the population of Wrocław, Poland.[11,14] Similar results were noted in the European Prospective Investigation into Cancer and Nutrition (EPIC) project, in which DTAP in the Spanish and Greek population was in the range of 11,000–12,000 µmolTE/day.[8,9] In women living in Sweden, DTAP amounted to 12,127 µmolTE/day.[7] All these values were consistent with the recommendations of Priori et al.,[28] who were the only investigators to assess that DTAP has to be at the level of 3,000–5,000 µmolTE/day to ensure the proper antioxidant capacity of tissues and blood.

In the male population of Sweden, DTAP determined with the FRAP method was approx. 22 mmol/day, and was higher by over 60% than in the Polish population.[29]

The mean estimates of the intake of polyphenols (approx. 2,000 mg/person/day) were comparable to those reported from Kraków, Poland (1,757 mg),[15] but higher than in Finland (863 mg),[13] Japan (1,492 mg),[12] France (1,193 mg),[30] and Spain (820 mg).[10]

However, irrespective of the consumption volume, dietary sources of DTAP and DPI differed between the respective countries. The intake of antioxidants in the Polish

Table 5. Contributions of food categories to dietary total antioxidant potential (DTAP) in persons with and without arterial hypertension (AH)

Men			
Food categories	with AH (N = 1,249)	without AH (N = 1,271)	p-value
Beverages	6.52 mmol/day (54.0%): coffee (27.8%); tea (22.7%); alcohol (1.6%)	6.90 mmol/day (54.5%): coffee (30.9%); tea (20.1%); alcohol (1.4%)	0.1271
Vegetables	2.20 mmol/day (18.2%): potato (7.1%); beetroot (3.0%); cabbage (2.2%); tomato (1.2%); broccoli and cauliflower (1.1%)	2.25 mmol/day (17.8%): potato (6.6%); beetroot (3.6%); cabbage (2.2%); tomato (1.1%); broccoli and cauliflower (0.9%)	0.9603
Fruit	1.85 mmol/day (15.3%): apples (4.8%); strawberries (2.1%); grapes (1.7%); plums (1.4%); citrus fruits (0.8%); cherries (0.8%)	1.55 mmol/day (12.2%): apples (4.0%); strawberries (1.3%); grapes. (1.1%); plums (0.9%); citrus fruits (0.7%); cherries (0.8%)	0.0050
Cereals	0.56 mmol/day (4.6%): mixed bread (1.9%); wheat bread (0.9%); rye bread (0.9%)	0.61 mmol/day (4.6%): mixed bread (1.9%); wheat bread (1.0%); rye bread (0.7%)	0.0002
Nuts and seeds	0.32 mmol/day (2.7%)	0.60 mmol/day (4.8%)	0.0295
Chocolate and cocoa	0.29 mmol/day (2.4%)	0.38 mmol/day (3.0%)	0.0002
Women			
Food categories	with AH (N = 1,292)	without AH (N = 1,807)	p-value
Beverages	6.49 mmol/day (55.8%): coffee (32.2%); tea (22.0%); alcohol (0.2%)	7.38 mmol/day (58.2%): coffee (36.4%); tea (19.4%); alcohol (0.3%)	0.0001
Vegetables	1.75 mmol/day (15.0%): potato (5.2%); beetroot (2.4%); cabbage (1.9%); tomato (1.2%); broccoli and cauliflower (1.1%)	1.82 mmol/day (14.4%): potato (4.6%). beetroot (2.8%). cabbage (1.8%). tomato (1.0%). broccoli and cauliflower (1.2%)	0.4879
Fruit	2.12 mmol/day (18.2%): apples (4.9%); strawberries (2.8%); grapes. (2.2%); plums (1.6%); citrus fruits (1.0%)	1.98 mmol/day (15.6%): apples (4.5%); strawberries (2.2%); grapes. (1.7%); plums (1.1%); citrus fruits (1.1%)	0.9210
Cereals	0.40 mmol/day (3.4%): mixed bread (1.0%); wheat bread (0.7%); rye bread (0.7%)	0.43 mmol/day (3.4%): mixed bread (0.9%); wheat bread (0.7%); rye bread (0.7%)	0.0001
Nuts and seeds	0.39 mmol/day (3.3%)	0.42 mmol/day (3.3%)	0.1207
Chocolate and cocoa	0.24 mmol/day (2.1%)	0.36 mmol/day (2.8%)	0.0001

Table 6. Contributions of food categories to dietary polyphenol intake (DPI) in persons with and without arterial hypertension (AH)

Men			
Food categories	with AH (N = 1,249)	without AH (N = 1,271)	p-value
Beverages	818.0 mg/day (40.2%): coffee (18.8%); tea (18.2%); alcohol (1.2%)	860.0 mg/day (40.8%): coffee (22.3%); tea (16.1%); alcohol (1.0%)	0.2013
Vegetables	288.2 mg/day (14.2%): potato (6.7%); cabbage (1.5%); tomato (1.6%)	293.2 mg/day (13.9%): potato (6.3%); cabbage (1.5%); tomato (1.4%)	0.5790
Fruit	409.0 mg/day (20.1%): apples (10.2%); plums (2.4%); strawberries (1.3%); bananas (1.2%); currant (0.9%); grapes (0.9%)	359.5 mg/day (17.1%): apples (8.6%); plums (1.5%); strawberries (0.8%); bananas (1.7%); currant (0.6%); grapes (0.6%)	0.0010
Cereals	382.0 mg/day (18.8%): mixed bread (8.4%); wheat bread (3.9%); rye bread (3.7%)	415.8 mg/day (19.7%): mixed bread (8.5%); wheat bread (4.4%); rye bread (3.1%)	0.003
Nuts and seeds	16.0 mg/day (0.8%)	28.8 mg/day (1.4%)	0.0287
Chocolate and cocoa	56.0 mg/day (2.7%)	74.5 mg/day (3.5%)	0.0002
Women			
Food categories	with AH (N = 1,292)	without AH (N = 1,807)	p-value
Beverages	813.7 mg/day (43.1%): coffee (23.9%); tea (18.1%); alcohol (0.1%)	917.9 mg/day (44.6%): coffee (27.0%). tea (16.0%); alcohol (0.2%)	0.0001
Vegetables	234.7 mg/day (12.4%): potato (5.1%); cabbage (1.2%); tomato (1.6%)	242.0 mg/day (11.8%): potato (4.5%). cabbage (1.3%); tomato (1.4%)	0.6405
Fruit	456.8 mg/day (24.2%): apples (10.8%); plums (2.8%); strawberries (1.7%); bananas (1.3%); currant (1.2%); grapes (1.2%); peaches (1.7%)	440.6 mg/day (21.4%): apples (9.9%); plums (1.9%); strawberries (1.4%); bananas (2.0%); currant (2.0%); grapes (0.9%); peaches (0.9%)	0.8030
Cereals	261.3 mg/day (13.8%): mixed bread (4.7%); wheat bread (3.2%); rye bread (3.1%)	285.0 mg/day (13.9%): mixed bread (4.1%); wheat bread (3.1%); rye bread (3.0%)	0.0010
Nuts and seeds	19.7 mg/day (1.0%)	22.3 mg/day (1.1%)	0.1193
Chocolate and cocoa	47.3 mg/day (2.5%)	75.4 mg/day (3.7%)	0.0001

population, noted both in the current research and previously,[14,15,31] as well as in Japan[12] was related mainly to the consumption of coffee and tea, and then vegetables and fruit, whereas in Finland it was related to the intake of coffee and cereal products,[13] in Spain to coffee, fruit and olive oil,[10] and in Sweden and Greece to vegetables and fruit.[7,9] These results indicate a difference in the structure of dietary sources of DTAP and DPI between people with and without AH. Respondents with AH showed lower consumption of coffee, alcohol, cereal products, chocolate, and cacao, and therefore of fewer bioactive substances derived from those products. Men with AH also consumed more fruit and fewer nuts and seeds. However, the cross-sectional character of the WOBASZ II does not allow for any cause-and-effect conclusions and it is therefore unknown whether their diet underwent modification due to the disease or the people with AH had these dietary habits earlier.

There has been a growing interest in the potential involvement of reactive oxygen forms in the search for AH causes. However, the metabolic mechanisms underlying this relationship still remain insufficiently explained, despite numerous studies. Obviously, the imbalance between free oxygen radicals and antioxidant factors (also from food) contributes to endothelial damage and enhances inflammatory reactions, which have been recently reported to be responsible for AH.[32]

Observational and experimental studies confirm that diets with high antioxidant potential and high polyphenol content contribute to AH reduction.[5,18] However, most of these projects assessed these correlations only at the level of the respective products rich in polyphenols (e.g., cacao, fruit and vegetables, tea, olive oil, etc.),[1] and only few took into consideration total dietary antioxidant potential and total polyphenol intake.

The current results seem to prove a slight but independent relationship between the dietary antioxidants studied and AH among adult Polish residents. Even less advanced statistical analyses showed lower mean values of DTAP and DPI in women with AH than in those without this condition. A significant reduction was also noted in the involvement of women with AH along with the increased DTAP and DPI quartile, even after adjustment for confounding variables. The tendencies were similar in men, although statistically insignificant.

However, more advanced analyses revealed that with DTAP increased by 1 mmol/day or DPI by 100 mg/day, the odds of AH in both sexes decreased by approx. 1–2%, even after correcting for confounding variables.

Our data is comparable to the results obtained in few studies which took into consideration total antioxidant activity and total dietary polyphenol intake. However, it should be added that in some of them the levels of biomarkers excreted with urine were referred to as the variables reflecting their dietary intake.

For instance, in São Paulo, Brazil, an inverse relation was observed between total polyphenol content and AH, but also with regard to the 2nd quartile, OR = 0.36 (CI = 0.19–0.69). Also, significant and linear correlations were noted between certain classes of polyphenols, such as tyrosols, alkylphenols, lignans, and stilbenes, which unfortunately were not evaluated in our study.[16] However, in the PREvencion con DIeta MEDiterranea (PREDIMED) study it was estimated that in individuals with high risk of cardiovascular diseases, the risk of AH in the highest quartile of urinary polyphenols was 0.64 (CI = 0.45–0.92), as compared to the lowest quartile, after eliminating other factors. Also, the values of SBP and DBP were inversely correlated with polyphenol excretion.[19] Clinical-control examinations were performed as part of the same project. In some individuals, the diet was enriched with polyphenols by adding olive oil or nuts. After a year, in individuals with dietary intervention, a significant increase was observed in urinary polyphenols and serum nitric oxide, which was associated with a decrease in SBP and DBP.[33]

It should be emphasized that coffee is the main source of DTAP and DPI in the Polish population (including in individuals with AH). Coffee provides not only antioxidants but also caffeine, which has been reported to be linked with AH, vascular resistance and endothelial dysfunction.[34] On the other hand, as indicated by meta-analysis, in individuals with AH, caffeine increases arterial blood pressure for only 3 h, and no relationship has been confirmed between long-term coffee drinking and elevated AH or increased risk of CVD in AH patients.[35] However, a study involving Kraków residents revealed that the risk of AH was lower in individuals declaring moderate consumption of coffee (3–4 cups/daily), and that only higher coffee intake did not protect against AH.[36]

Considerable quantities of the bioactive substances analyzed in the current study were also obtained from tea. According to the available data, tea reduces arterial blood pressure.[17,37] Unfortunately, the data was obtained from studies performed on a very small number of patients in a short period of time, which does not warrant conclusions regarding the long-term advantages of drinking large amounts of tea.[17]

Considering the inconclusive data on the effect of coffee and tea on AH, it seems that the consumption of fruit and vegetables as the source of DTAP and DPI would be more beneficial for the Polish population.

Some respondents involved in the WOBASZ II took dietary supplements, an additional source of antioxidant potential, which were not taken into consideration in the analysis. However, the estimated involvement of study participants enriching their diet with vitamins and minerals was 12.3% and 15.7%, respectively, in the group with and without AH, and was not statistically differentiated (unpublished data). Therefore, it seems that the supplementation could not significantly modify the relationship between DTAP, DPI and AH.

The advantages of the presented study include:

– results based on a representative sample of the adult

Polish population, in a large number, with the use of standardized methods;
– assessment of individual dietary habits, recommended for the determination of the relationship between nutrition and health in epidemiological studies;
– measurement of the antioxidant potential and polyphenols in reconstituted food samples typical of the Polish market, taking into account culinary processing;
– the use of databases obtained from other countries generates errors due to the lack of regional dishes and because bioactive substances are determined in products from other climate and soil zones. However, culinary processes differently affect both the antioxidant potential and polyphenol content.

Limitations of the study

The limitations of the current study are as follows:
– not very high responsiveness of the respondents in the WOBASZ II study is typical of other currently performed European epidemiological studies. This problem was discussed in previous WOBASZ-related publications.[21,38] Additionally, statistical analyses were performed, confirming the similarity of distribution of people in age groups throughout the Polish population and in the study sample, which indicates the representativeness of the WOBASZ II study;
– arterial blood pressure was taken 3 times, but only during 1 visit;
– single assessment of dietary habits by means of 24-hour-recall is acceptable in large epidemiological studies, but its repetition could likely reduce the inter-individual variation of nutrition.

Conclusions

The intake of food with high antioxidant potential and rich in polyphenols was associated, slightly but independently of other factors, with a lower chance of hypertension in the adult Polish population. Higher DTAP (by 1 mmol/day) or higher DPI (by 100 mg/day) had reduced the odds of AH by approx. 1–2%, even after correcting for confounding variables.

Coffee and tea were the basic dietary sources of the antioxidants studied, irrespective of sex and AH. Taking into consideration the inconclusive data concerning the effects of these beverages on AH, vegetables and fruit should be recommended as a more beneficial source of DTAP and DPI for the Polish population.

The results of the project can help formulate recommendations concerning polyphenol content and antioxidant potential of a daily food ration.

References

1. Sharma R. Polyphenols in health and disease. Practice and mechanisms of benefits. In: Watson RR, Preedy VR, Zibadi S. eds. *Polyphenols in Human Health and Disease.* Tokyo, Japan: Elsevier; 2014:757–778.
2. Medina-Remón A, Tresserra-Rimbau A, Valderas-Martinez P, Estruch R, Lamuela-Raventos RM. Polyphenol consumption and blood pressure. In: Watson RR, Preedy VR, Zibadi S. eds. *Polyphenols in Human Health and Disease.* Tokyo, Japan: Elsevier; 2014:971–987.
3. Pandey KB, Rizvi SI. Plant polyphenols as dietary antioxidants in human health and disease. *Oxid Med Cell Longev.* 2009;2(5):270–278.
4. Manach C, Mazur A, Scalbert A. Polyphenols and prevention of cardiovascular diseases. *Curr Opin Lipidol.* 2005;16(1):77–84.
5. Andriantsitohaina R, Auger C, Chataigneau T, et al. Molecular mechanisms of the cardiovascular protective effects of polyphenols. *Br J Nutr.* 2012;108(9):1532–1549.
6. Chong MF, Macdonald R, Lovegrove JA. Fruit polyphenols and CVD risk: A review of human intervention studies. *Br J Nutr.* 2010;104 (Suppl 3):S28–39.
7. Rautiainen S, Serafini M, Morgenstern R, Prior RL, Wolk A. The validity and reproducibility of food-frequency questionnaire-based total antioxidant capacity estimates in Swedish women. *Am J Clin Nutr.* 2008;87(5):1247–1253.
8. Agudo A, Cabrera L, Amiano P, et al. Fruit and vegetable intakes, dietary antioxidant nutrients, and total mortality in Spanish adults: Findings from the Spanish cohort of the European Prospective Investigation into Cancer and Nutrition (EPIC-Spain). *Am J Clin Nutr.* 2007; 85(6):1634–1642.
9. Dilis V, Trichopoulou A. Antioxidant intakes and food sources in Greek adults. *J Nutr.* 2010;140(7):1274–1279.
10. Tresserra-Rimbau A, Medina-Remón A, Pérez-Jiménez J, et al. Dietary intake and major food sources of polyphenols in a Spanish population at high cardiovascular risk: The PREDIMED study. *Nutr Metab Cardiovasc Dis*. 2013;23(10):953–959.
11. Ilow R, Regulska-Ilow B, Misiewicz D, Różańska D, Kowalisko A, Biernat J. Całkowity potencjał antyoksydacyjny wybranych produktów spożywanych przez 50-letnich mieszkańców Wrocławia w 2008 roku. *Bromat Chem Toksykol.* 2012;45(3):989–994.
12. Taguchi C, Fukushima Y, Kishimoto Y, et al. Estimated dietary polyphenol intake and major food and beverage sources among elderly Japanese. *Nutrients* 2015:7(12):10269–10281.
13. Ovaskainen ML, Törrönen R, Koponen JM, et al. Dietary intake and major food sources of polyphenols in Finnish adults. *J Nutr.* 2008; 138(3):562–566.
14. Ilow R, Regulska-Ilow B, Różańska D, Tangermann S, Grajeta H. Oszacowanie całkowitego potencjału antyoksydacyjnego wybranych produktów spożywanych przez studentów Akademii Medycznej we Wrocławiu w latach 2005–2007. *Bromat Chem Toksykol.* 2012;45(3): 995–1000.
15. Grosso G, Stepaniak U, Topór-Mądry R, Szafraniec K, Pająk A. Estimated dietary intake and major food sources of polyphenols in the Polish arm of the HAPIEE study. *Nutrition* 2014;30(11–12):1398–1403.
16. Miranda AM, Steluti J, Fisberg RM, Marchioni DM. Association between polyphenol intake and hypertension in adults and older adults: A population-based study in Brazil. *PLoS One* 2016;11(10):e0165791.
17. Hügel HM, Jackson N, May B, Zhang AL, Xue CC. Polyphenol protection and treatment of hypertension. *Phytomedicine* 2016;23(2):220–231.
18. Medina-Remón A, Estruch R, Tresserra-Rimbau A Vallverdú-Queralt A, Lamuela-Raventos RM. The effect of polyphenol consumption on blood pressure. *Mini Rev Med Chem.* 2013;13(8):1137–1149.
19. Medina-Remón A, Zamora-Ros R, Rotchés-Ribalta M, et al; PREDIMED Study Investigators. Total polyphenol excretion and blood pressure in subjects at high cardiovascular risk. *Nutr Metab Cardiovasc Dis*. 2011;21(5):323–331.
20. Niklas A, Flotyńska A, Puch-Walczak A, et al. Prevalence, awareness, treatment and control of hypertension in the adult Polish population – Multi-center National Population Health Examination Surveys – WOBASZ studies. *Arch Med Sci.* 2018;14(5):951–961.
21. Drygas W, Niklas AA, Piwońska A, et al. Multi-center National Population Health Examination Survey (WOBASZ II study): Assumptions, methods and implementation. *Kardiol Pol.* 2016;74(7):681–690.

22. Różańska D, Regulska-Ilow B, Ilow R. Wpływ wybranych procesów kulinarnych na potencjał antyoksydacyjny i zawartość polifenoli w żywności. *Probl Hig Epidemiol.* 2014;95:215–222.
23. Benzie IF, Strain JJ. The ferric reducing ability of plasma (FRAP) as a measure of "antioxidant power": The FRAP assay. *Anal Biochem.* 1996;239(1):70–76.
24. Singleton VL, Rossi JA. Colorimetry of total phenolics with phosphomolybdic–phosphotungstic acid reagents. *Amer J Enol Viticult.* 1965; 16:144–158.
25. Carlsen MH, Halvorsen BL, Holte K, et al. The total antioxidant content of more than 3100 foods, beverages, spices, herbs and supplements used worldwide. *Nutr J.* 2010;9(3):1–11.
26. Neveu V, Perez-Jiménez J, Vos F, et al. Phenol-Explorer: An online comprehensive database on polyphenol contents in foods. *Database (Oxford).* 2010; bap024: doi:10.1093/database/bap024
27. Zujko ME, Witkowska AM, Górska M, Wilk J, Krętowski A. Reduced intake of dietary antioxidants can impair antioxidant status in type 2 diabetes patients. *Pol Arch Med Wewn.* 2014;124(11):599–607.
28. Priori RL, Cao JA, Shukitt-Hale B. Can foods forestall aging? Some with high antioxidant activity appear to aid memory. *AgResearch Magazine.* 1999;47:15–17. https://agresearchmag.ars.usda.gov/1999/feb/aging
29. Russnes KM, Möller E, Wilson KM, et al. Total antioxidant intake and prostate cancer in the Cancer of the Prostate in Sweden (CAPS) study: A case control study. *BMC Cancer.* 2016;16:438.
30. Perez-Jimenez J, Fezeu L, Touvier M, et al. Dietary intake of 337 polyphenols in French adults. *Am J Clin Nutr.* 2011;93(6):1220–1228.
31. Zujko ME, Witkowska AM, Waśkiewicz A, Mirończuk-Chodakowska I. Dietary antioxidant and flavonoid intakes are reduced in the elderly. *Oxid Med Cell Longev.* 2015;2015:843173.
32. Beg M, Sharma V, Akhtar N, Guta A, Mohd J. Role of antioxidants in hypertension. *JIACM.* 2011;12(2):122–127.
33. Medina-Remón A, Tresserra-Rimbau A, Pons A, et al; PREDIMED Study Investigators. Effects of total dietary polyphenols on plasma nitric oxide and blood pressure in a high cardiovascular risk cohort. The PREDIMED randomized trial. *Nutr Metab Cardiovasc Dis.* 2015; 25(1):60–67.
34. Di Castelnuovo A, Giuseppe R, Iacoviello L, Gaetano G. Consumption of cocoa, tea and coffee and risk of cardiovascular disease. *Eur J Intern Med.* 2012;23(1):15–25.
35. Mesas AE, Leon-Muñoz LM, Rodriguez-Artalejo F, Lopez-Garcia E. The effect of coffee on blood pressure and cardiovascular disease in hypertensive individuals: A systematic review and meta-analysis. *Am J Clin Nutr.* 2011;94(4):1113–1126.
36. Grosso G, Stepaniak U, Polak M, et al. Coffee consumption and risk of hypertension in the Polish arm of the HAPIEE cohort study. *Eur J Clin Nutr.* 2016;70(1):109–115.
37. Turek I, Kozińska J, Drygas W. Zielona herbata jako czynnik protekcyjny w profilaktyce i leczeniu wybranych chorób serca i naczyń. *Kardiol Pol.* 2012;70(8):848–852.
38. Pająk A, Szafraniec K, Polak M, et al. Changes in the prevalence, treatment, and control of hypercholesterolemia and other dyslipidemias over 10 years in Poland: The WOBASZ study. *Pol Arch Med Wewn.* 2016; 126(9):642–652.

Evaluation of changes in enamel thickness after orthodontic treatment depending on the force applied to remove orthodontic brackets: OCT analysis and universal testing machine

Monika Elżbieta Machoy[1,2,A–F], Julia Seeliger[2,A–D,F], Liliana Szyszka-Sommerfeld[1,B,E,F], Robert Koprowski[3,C,F], Tomasz Gedrange[2,A,E,F], Krzysztof Woźniak[1,A,E,F]

[1] Division of Orthodontics, Pomeranian Medical University, Szczecin, Poland
[2] Division of Orthodontics, Technische Universität Dresden, Germany
[3] Department of Biomedical Computer Systems, Faculty of Computer Science and Materials Science, Institute of Computer Science, University of Silesia, Katowice, Poland

A – research concept and design; B – collection and/or assembly of data; C – data analysis and interpretation; D – writing the article; E – critical revision of the article; F – final approval of the article

Advances in Clinical and Experimental Medicine, ISSN 1899–5276 (print), ISSN 2451–2680 (online) *Adv Clin Exp Med*. 2019;28(6):807–813

Address for correspondence
Monika Elżbieta Machoy
E-mail: m.machoy@gmail.com

Funding sources
None declared

Conflict of interest
None declared

Received on April 30, 2018
Reviewed on May 5, 2019
Accepted on August 9, 2018

Published online on March 19, 2019

Abstract

Background. Adhesive materials used in orthodontics have contributed to the broadening of treatment options with fixed braces. The adhesive materials physically and chemically bond to the enamel surface and orthodontic bracket base, which, apart from offering advantages, also entails the risk of enamel damage when removing these materials from the tissue surface after the treatment is complete.

Objectives. The objective of this study was to assess how the bond strength of adhesive materials affects enamel thickness after removing brackets and whether the type of bonding system affects the amount of adhesive strength of the discussed materials.

Material and methods. The tests were carried out on 2 groups of 40 bovine teeth in each group. In the 1st group, the classical orthophosphoric acid and the Transbond Plus self-etching primer (SEP) were used. In the 2nd group, the Transbond XT SEP was applied. In both groups, Transbond XT Light Cure Adhesive was used. The same metal orthodontic brackets were attached to the enamel surface. Optical Coherence Tomography (OCT) scans were made before and after removing brackets, which enabled tissue thickness measurements. The bond strength was evaluated using a universal testing machine. Parametric tests were performed on all obtained variables. Student's t-tests for independent samples and analysis of correlation with Pearson's r were carried out.

Results. The bond strength between the orthodontic bracket and enamel is statistically significantly different in the 1st group and the 2nd group, and is higher in the 2nd group.

Conclusions. There are no significant differences in enamel thickness depending on the bonding system type and there is no correlation between the enamel thickness and the bond strength of orthodontic brackets to the enamel.

Key words: orthodontics, adhesives, enamel, optical coherence tomography, shear bond strength

Cite as
Machoy ME, Seeliger J, Szyszka-Sommerfeld L, Koprowski R, Gedrange T, Woźniak K. Evaluation of changes in enamel thickness after orthodontic treatment depending on the force applied to remove orthodontic brackets. OCT analysis and universal testing machine. *Adv Clin Exp Med.* 2019;28(6): 807–813. doi:10.17219/acem/94141

DOI
10.17219/acem/94141

Introduction

The use of adhesive force in orthodontics may seem problematic due to the requirements specific to the field for which it is intended. When used in orthodontics, it should meet 2 requirements: be strong enough to support orthodontic brackets during the entire treatment, as well as resist the forces of chewing and tension caused by arches and the action and interference of patients. It should also be delicate enough to avoid enamel damage when removing brackets.[1] This strength is due to the fact that the bonding material sticks to the irregularities of the enamel surface and the base of the attached element. These irregularities result from using etching techniques. The enamel pellicle is removed and the enamel hydroxyapatites and a small amount of the inter-prism substance are dissolved, which results in the formation of micropores with a depth from 5 μm to 50 μm.[2] A 37% orthophosphoric acid solution is used for etching to condition enamel prior to the application of a composite material. The technique is based on the etching agent, adhesive system and composite material. To minimize the stages of attaching brackets, 3 separate elements were combined into 2, having the properties of an etching agent and bonding system.[3–5] Self-etching primers (SEP), due to the presence of an acidic primer, make it possible to exclude the use of an etchant agent.[6] Electron microscope studies showed a similar enamel etching pattern of self-etching and classical systems.[7] Self-etching primers exhibits a more classical etching pattern,[8–10] while maintaining optimal bond strength.[11] The adhesive strength of the self-etching system to the orthodontic brackets is from 20 MPa to 30 MPa,[11] i.e., it shows a range similar to that of classical acid etching.[12] The tests showed that the adhesive penetration range is smaller when using the self-etching system than normal etching. However, this is not a disadvantage, because the bigger the resin hooks in enamel, the greater the risk of its damage when removing brackets.[13] The forces generated during bracket removal can depend on many factors: etching method, type of bonding system, orthodontic material, polymerization methods, and type and architecture of the bracket base.[14,15] An increase in adhesive strength increases the risk of enamel damage.[16] The tests presented in the article were carried out to check how bond strength affects enamel thickness after removing orthodontic brackets and whether the bonding system type affects the bond strength value.

Material and methods

Preparing the teeth for the experiment

The study was carried out in vitro on a group of 80 bovine teeth. The teeth were observed and selected in order to eliminate teeth with caries, cracks, hypomineralized enamel, or any other defects. The teeth were divided into 2 subgroups of 40 teeth each. The procedure of enamel etching was performed under laboratory conditions. In the 1st subgroup, the classical method of enamel etching and the V generation bonding system (Transbond SEP Plus; 3M Unitek, Monrovia, USA) were used. In the 2nd subgroup, the VII generation (self-etching) bonding system (Transbond XT; 3M Unitek) was used. All procedures were performed by the same operator. Prior to the treatment, each tooth surface was cleaned and prepared with the Air-Flow® method (Clinpro Prophy Powder; 3M Espe AG, Seefeld, Germany), sprayed with water and dried with an air syringe for 15 s. For fastening orthodontic brackets, an orthodontic composite material Transbond XT Light Cure Adhesive (3M Unitek) was used. In the 1st group, the vestibular surface of the tooth was etched for 30 s with a 37% solution of phosphoric acid Blue-Etch (Cerkamed, Stalowa Wola, Poland), rinsed with distilled water for 15 s and dried using compressed air. The adhesive system Transbond SEP Plus was rubbed with an applicator into the etched enamel surface for 15 s; then, the surface was dried under a gentle stream of air for 3 s and cured with a halogen lamp with light intensity of 750 mW/cm^2 for 20 s. The orthodontic composite material Transbond XT Light Cure Adhesive was applied to the bracket surface. The bracket was pressed against the enamel surface with commonly used tweezers. The orthodontic bracket was placed in the middle of the mesial–distal axis of the tooth, moving its center 3.5 mm away from the edge of the occlusal surface. The distance was measured using an orthodontic positioner. After proper placement of the bracket, the material was subjected to polymerization with a halogen lamp for 40 s.

In the 2nd group, the self-etching adhesive system (Transbond XT) was used. The SEP, when applied to the tooth surface using an applicator, was left for 10 s, and then the excess was removed with an air stream for 5 s. After this time, the system was polymerized with a halogen lamp with light intensity of 750 mW/cm^2 for 20 s. The orthodontic composite material Transbond XT Light Cure Adhesive was applied to the surface of the bracket. The orthodontic bracket was placed onto the tooth surface using the method described above.

Analysis of the shear bond strength using a universal testing machine

In order to insert a tooth in the appliance of the universal testing machine, a block in which the tooth had been embedded with an exposition of its labial surface was required. A silicone mold with cuboid shaped notches was produced (Fig. 1). One tooth was placed on a stick of wax and fixed into the notch with the labial surface upturned. The notch was filled up with autopolymerizable self-curing resin (SilaPress; Siladent Dr. Böhme & Schöps GmbH, Goslar, Germany). Due to the objective of this study, evaluating the differences in the initial shear bond strength (SBS), no thermocycling or other aging procedures were

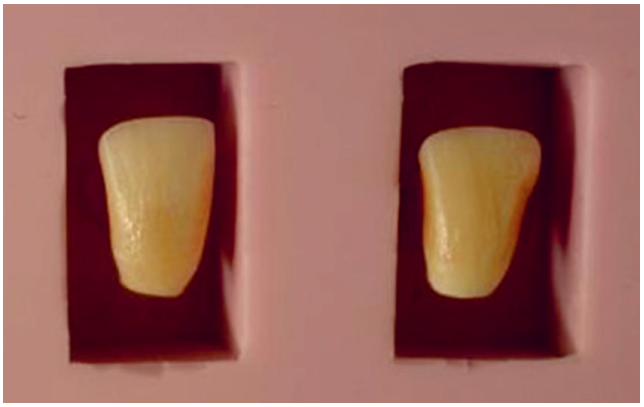

Fig. 1. Silicone mold used to create test blocks

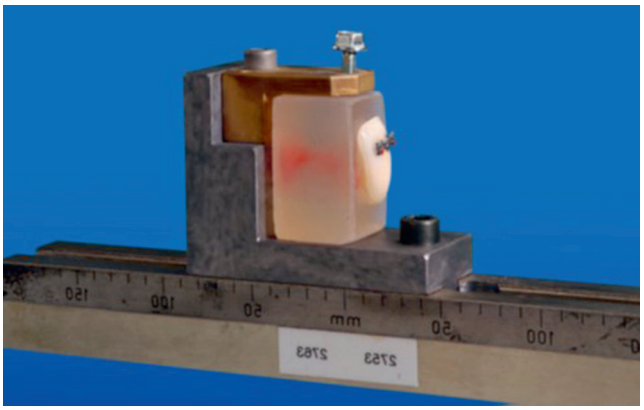

Fig. 2. Test block in the universal testing machine

accomplished. During the whole time, the teeth were stored in saline solution, with the addition of sodium azide (50 mg/L), until the time of the measurements. For measurements of the debonding force, the specimens were positioned in the universal testing machine (TIRAtest-2720, TIRA GmbH, Schalkau, Germany). The shear force was applied with a stainless steel rod parallel to the long axis of the tooth (Fig. 2, 3). A crosshead speed of 0.5 mm/min was chosen. The SBS was recorded by dividing the numerical value (N) of shear force by the base area (mm^2) of the bracket and converted to MPa in order to compare the measurements with those recorded in the literature.

Analysis of enamel thickness using optical coherence tomography

After the evaluation of SBS, the enamel was processed with the use of a micromotor mounted to a dental unit with a speed of 40,000 revolutions/min, water cooling and pressure force of 1.0 N. The force was measured on a test stand consisting of scales, on which the processed tooth was placed. The procedure of cleaning the enamel was considered to be finished on the basis of the naked-eye examination and by touching with the stylet 23 in the dental unit light. The assessment criterion was the smoothness

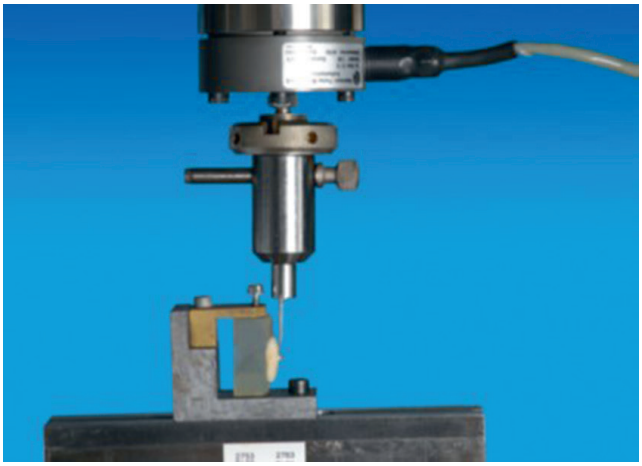

Fig. 3. Steel rod applying the shear force to the bracket from the occlusal surface

Fig. 4. Topcon 3D OCT-2000 used in the experiment

of the tooth surface and the absence of the composite material residues. The area of the test teeth was imaged with a 3D optical coherence tomography (OCT) camera (Topcon, Oakland, USA; Fig. 4) 2 times: imaging of the tooth surface before installing orthodontic brackets and after mechanical processing.

Each time, 2D scans were performed allowing for a clear illustration of the enamel damage in a vertical plane. The procedure made it possible to show the entire surface of the tissue and perform the subsequent comparative analysis of changes in its structure. It was possible to obtain accurate scans of the surface and enamel structure of teeth with due repeatability during 3 examinations, owing to the matrix described above. The matrix allowed for repeatable tooth

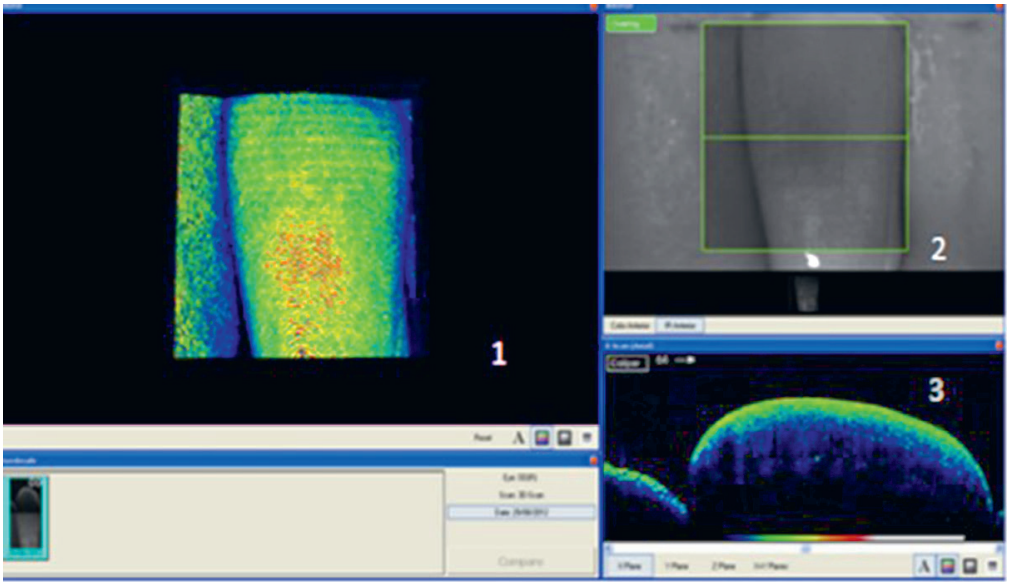

Fig. 5. Image on a computer screen after a tooth scan. 1) 3D image of the tooth surface. 2) A digital image of the picture taken using a coupled digital camera with a resolution of 16.2 Mpix. 3) An axial scan of the enamel tissue

positioning in the frontal, sagittal and horizontal planes relative to the optical axis of the OCT. The obtained scans were subjected to an expert IT analysis. Image pre-processing involved automatic reading of the order of OCT images from the source file with the extension *.fds, allowing for the development of matrices of individual images. Figure 5 shows the pictures and scans obtained using the tomography device. The IT analysis was described and published.[17]

Statistical analysis

IBM SPSS Statistics v. 24 software (IBM Corp., Armonk, USA) was used for statistical analysis. The basic descriptive statistics were calculated and the Kolmogorov–Smirnov test was performed to examine the normality of the distribution of 2 measured variables on a quantitative scale. Parametric tests were performed on all variables. Student's t-tests for independent samples and analysis of correlation with Pearson's r were carried out. The threshold $\alpha = 0.05$ was adopted as the level of significance.

In the first step, the basic descriptive statistics were calculated and the Kolmogorov–Smirnov test was performed, examining the normality of the distribution. In the course of the analysis, it was shown that the shape of enamel thickness distribution deviates significantly from the normal distribution. In turn, the distribution of bond strength is consistent with the normal distribution. The compared groups are of equal size and in the case of enamel thickness, the variances are homogeneous and the skewness of this variable does not exceed the absolute value equal to 1. Therefore, analysis based on parametric tests was performed. The truthfulness of the obtained results in the Student's t-test was verified with the logarythmisation of the enamel thickness value and a simultaneous analysis was carried out on the transformed variable. The described results of basic descriptive statistics are presented in Table 1.

Results

The effect of the adhesive system on enamel thickness and bond strength

Comparisons of 2 groups were made using Student's t-test for independent samples. The obtained results, presented in Table 2, show that only bond strength is statistically

Table 1. Basic descriptive statistics and the result of the Kolmogorov–Smirnov test

V generation adhesive system	M	Me	SD	Sk	Kurt	Min	Max	K-S	p
Bond strength	14.33	14.35	1.22	0.23	−0.87	12.20	16.90	0.11	0.200
Enamel thickness	101.00	105.07	74.90	0.74	0.07	7.48	291.15	0.14	0.036
Enamel thickness (log)	4.25	4.65	0.98	−0.65	−0.52	2.01	5.67	0.19	0.001
VII generation adhesive system	M	Me	SD	Sk	Kurt	Min	Max	K-S	p
Bond strength	16.97	16.90	0.85	0.30	0.47	14.90	19.00	0.14	0.060
Enamel thickness	81.74	60.81	67.37	0.99	−0.02	4.92	256.37	0.18	0.002
Enamel thickness (log)	4.03	4.11	0.93	−0.32	−0.39	1.59	5.55	0.09	0.200

M – mean; Me – median; SD – standard deviation; Min – minimum; Max – maximum; Sk – skewness; Kurt – kurtosis; K-S – result of the Kolmogorov–Smirnov test; p – significance of the distribution normality test.

Table 2. Effect of the bonding system generation on bond strength and enamel thickness

Variables	V generation bonding system (n = 40)		VII generation bonding system (n = 40)		T	p	95% CI		Cohen's d
	M	SD	M	SD			LL	UL	
Bond strength	14.33	1.22	16.97	0.85	–11.20	<0.001	–3.11	–2.17	2.50
Enamel thickness	101.00	74.90	81.74	67.37	1.21	0.230	–12.45	50.98	0.27
Enamel thickness (log)	4.25	0.98	4.03	0.93	1.01	0.316	–0.21	0.64	0.23

n – number of observations; M – mean; SD – standard deviation; t – Student's t-test results; p – significance; 95% CI – 95% confidence interval for the difference between means; LL – lower limit of the CI; UL – upper limit of the CI.

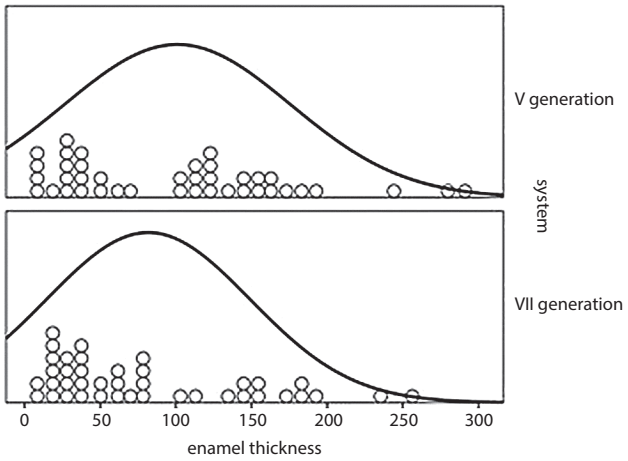

Fig. 6. Distribution of enamel thickness in the V and VII generation system groups

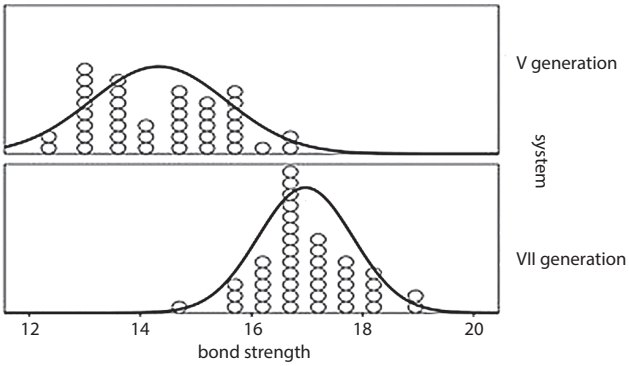

Fig. 7. Distribution of bond strength in the V and VII generation system groups

significantly differentiated between the 2 compared groups. The mean bond strength in the V generation system group was 14.33 MPa, whereas in the VII generation system group it was 16.97 MPa. The VII generation adhesive system is characterized by statistically significantly higher bond strength compared to the V generation system. In the case of enamel thickness, no significant differences are observed, both in the case of non-transformed and logged variables. The mean value of enamel thickness in the V generation system group was 101.00 µm and in the VII generation system group – 81.74 µm. The compared mean values together with the Student's t-test results are presented in Table 2. Figures 6 and 7 present the distribution of enamel thickness and bond strength in the V and VII generation system groups.

Correlation between enamel thickness and bond strength

A correlation analysis was performed in the 2 compared groups to check if enamel thickness correlates with bond strength. All correlation coefficients presented in Table 3 turned out to be statistically insignificant. Therefore, there are no grounds for rejecting the null hypothesis and concluding that bond strength affects enamel thickness. This result was obtained for both the V and VII generation bonding systems.

Table 3. Correlation between bond strength and enamel thickness

Bonding system	Bond strength	Significance	Significance
V generation bonding system	enamel thickness	Pearson's r	0.118
		p-value	0.467
	enamel thickness (log)	Pearson's r	0.072
		p-value	0.657
VII generation bonding system	enamel thickness	Pearson's r	–0.172
		p-value	0.288
	enamel thickness (log)	Pearson's r	–0.130
		p-value	0.424

Discussion

In the presented experiment, the Transbond XT was used in both test groups. It has been used in many studies,[18–21] so the results can be comparable. The bonding material Transbond SEP Plus has also been proven to be one of the best bonds used in orthodontics. The Transbond products are one of the few (next to the Clearfil SE) materials that show an acceptable stress behavior under the thermocycling conditions, which can mimic the in vivo conditions.[20] Also, the risk of debonding-induced enamel defects is related to the bracket system used.[22] Therefore, only 1 bracket system has been used which was also used in earlier studies to get comparable results.[23]

The use of a conventional conditioning system requires an etching agent, which is based on 37% phosphoric acid.

The SEP include phosphoric acid esters with an unknown, but probably lower concentration. The mode of etching and priming of the 2 bonding systems is different. In our research, the effect of the enamel etching method on its thickness after the completed treatment was evaluated. The studies evaluated the entire tissue subjected to etching, measuring the thickness of the cross-section from the inside to the outer border of the tissue, so it was possible to measure all the layers obtained with OCT imaging, which after their combination reflected the entire enamel cross-section. The mean enamel thickness after the completed treatment when using the classical etching method was 101.00 μm and in the VII generation system group – 81.74 μm. However, the differences found were not statistically significant. The results show that enamel thickness after the treatment and its possible damage does not depend in any way on the bonding system type. The other authors' studies suggest a smaller effect of the self-etching system on the enamel, and our experiment leads to the conclusion that the effect of both systems on enamel is similar. The difference in results in this respect is due to the fact that the methodology of compared studies differs. Our own research focused on the quantitative evaluation of enamel, whereas previously presented experiments of other authors such as Retief,[24] Arakawa et al.,[25] Asmussen,[26] and Voss and Charbeneau[27] assessed enamel qualitatively. They measured the amount of dissociated calcium and the depth of penetration of resin hooks. Therefore, it can be concluded that the results of the compared tests are not contradictory, as they measure different enamel features. The use of an etching agent does not reduce enamel thickness due to the lack of abrasive abilities. The etching method can only indirectly affect the final tissue thickness by significantly weakening its structure, which increases the enamel sensitivity to the operator's actions during the removal of brackets and cleaning process. The assessment of the full thickness of the tissue has been difficult so far, which is why there are not many publications that can be referred to when discussing our own results.

The next examined aspect was the bond strength of orthodontic brackets depending on the applied bonding system. In the reported results, the median SBS of the classical enamel etching method was 14.33 MPa, while in the VII generation system group it was 16.97 MPa. According to Reynolds,[28] the minimum SBS of any adhesive for clinical use should lay between 5.88 MPa and 7.84 MPa. The mean values of all tested primers–adhesive combination or systems showed suitable SBS values, far exceeding the minimum value. Retief[29] reported the incidence of enamel fractures in specimens with in vitro bond strength values of 9.7 MPa. Even though the enamel can often withstand greater forces as indicated in the debonding force level reported, it is desirable to follow the instructions for debonding as recommended by the manufacturer to avoid enamel damage.[30] In our results, the SBS in both groups was higher but the presented method was performed in vitro and the in vivo situation can be different. Limited access and poor direct sight may be a problem in the posterior teeth. According to Heravi et al.,[31] the SBS was below the clinically accepted values in most experimental groups. When light curing from the same side of the bracket is not possible, doubling the curing time and increasing the light intensity during trans-illumination are recommended for achieving acceptable bond strengths. Adhesion loss in the oral cavity can also be caused by thermal fluctuations and repetitive mechanical loads, fluid absorption, and biodegradation.[32–35] Also, there was no correlation between SBS and enamel thickness. Many independent studies describe the features of self-etching systems, which include low aggressiveness in relation to the enamel. This causes significantly smaller, irreversible changes in the tissue compared to classical etching, and affects the production of shorter resin hooks. However, self-etching systems generate sufficient bond strength for the clinical procedure and fewer bonding errors in the enamel-bonding system phase than the classical etching method.[36,37]

Conclusions

The bond strength between the orthodontic bracket and enamel is statistically significantly different in the group of classical enamel etching method and the self-etching system group, and is higher in the 2nd group. There are no significant differences in enamel thickness depending on the bonding system type. No correlation has been found between enamel thickness and bond strength of orthodontic brackets to enamel.

References

1. Powers JM, Messersmith ML. Enamel etching and bond strength. In: Brantley WA, Eliades T, eds. *Orthodontic Materials: Scientific and Clinical Aspects*. Stuttgart, Germany: Georg Thieme Verlag; 2001:105–122.
2. Øgaard B, Bishara SE, Duschner H. Enamel effects during bonding–debonding and treatment with fixed appliances. In: Graber TM, Eliades T, Athanasiou AE, eds. *Risk Management in Orthodontics: Experts' Guide to Malpractice*. Batavia, IL: Quintessence Publishing Co.; 2004:19–46.
3. Tay FR, Pashley DH. Aggressiveness of contemporary self-etching systems. Depth of penetration beyond dentin smear layers. *Dent Mat*. 2001;17(4):296–308.
4. Attar N, Taner TU, Tülümen E, Korkmaz Y. Shear bond strength of orthodontic brackets bonded using conventional vs one- and two step self-etching/adhesive systems. *Angle Orthod*. 2007;77(3):518–523.
5. Shinya M, Shinya A, Lassila LV, et al. Treated enamel surface patterns associated with five orthodontic adhesive systems: Surface morphology and shear bond strength. *Dent Mat J*. 2008;27(1):1–6.
6. Nishida K, Yamauchi J, Wada T, Hosoda H. Development of a new bonding system. *J Dent Res*. 1993;72:137.
7. Friedl KH, Oberlander H, Schmalz G, et al. Bond strength of composite resins using a new one-step adhesive system. *J Dent Res*. 2000;79:33–36.
8. Hosein I, Sherriff M, Ireland AJ. Enamel loss during bonding, debonding, and cleanup with use of a self-etching primer. *Am J Orthod Dentofacial Orthop*. 2004;126(6):717–724.

9. Horiuchi S, Kaneko K, Mori H, et al. Enamel bonding of self-etching and phosphoric acid-etching orthodontic adhesives in simulated clinical conditions: Debonding force and enamel surface. *Dent Mat J*. 2009;28(4):419–425.
10. Cal-Neto JP, Miguel JA. Scanning electron microscopy evaluation of the bonding mechanism of a self-etching primer on enamel. *Angle Orthod*. 2006;76(1):132–136.
11. Miyazaki M, Hirohata N, Takagaki K, et al. Influence of self-etching primer drying time on enamel bond strength of resin composites. *J Dent*. 1999;27(3):203–207.
12. Dorminey JC, Dunn WJ, Taloumis LJ. Shear bond strength of orthodontic brackets bonded with a modified 1-step etchant-and-primer technique. *Am J Orthod Dentofacial Orthop*. 2003;124(4):410–413.
13. Bishara SE, Von Wald L, Laffoon JF, et al. Effect of a self-etch primer/adhesive on the shear bond strength of orthodontic brackets. *Am J Orthod Dentofacial Orthop*. 2001;119(6):621–624.
14. Ireland AJ, Hosein I, Sherriff M. Enamel loss at bond-up, debond and clean-up following the use of a conventional light-cured composite and a resin-modified glass polyalkenoate cement. *Europ J Orthod*. 2005;27(4):413–419.
15. Ozcan M, Finnema K, Ybema A. Evaluation of failure characteristics and bond strength after ceramic and polycarbonate bracket debonding. *Europ J Orthod*. 2008;30(2):176–182.
16. Ostman-Andersson E, Marcusson A, Hörstedt P. Comparative SEM studies of the enamel surface appearance following the use of glass ionomer cement and a diacrylate resin for bracket bonding. *Swed Dent J*. 1993;17(4):139–146.
17. Koprowski R, Machoy M, Woźniak K, Wróbel Z. Automatic method of analysis of OCT images in the assessment of the tooth enamel surface after orthodontic treatment with fixed braces. *Biomed Eng Online*. 2014;13:48.
18. Boruziniat A, Khazaei Y, Motaghi S, Moghaddas M. Evaluation of bond strength of orthodontic brackets without enamel etching. *J Clin Exp Dent*. 2015;7(4):519–523.
19. Brauchli L, Zeller M, Wichelhaus A. Shear bond strengths of seven self-etching primers after thermo-cycling. *J Orof Orthop*. 2011;72(5):371–380.
20. Hellak A, Rusdea P, Schauseil M, Stein S. Enamel shear bond strength of two orthodontic self-etching bonding systems compared to Transbond™ XT. *J Orof Orthop*. 2016;77(6):391–399.
21. Menini A, Cozzani M, Sfondrini MF, Scribante A, Cozzani P, Gandini P. A 15-month evaluation of bond failures of orthodontic brackets bonded with direct versus indirect bonding technique: A clinical trial. *Prog Orthod*. 2014;15(1):1–6.
22. Zielinski V, Reimann S, Jager A, Bourauel C. Comparison of shear bond strength of plastic and ceramic brackets. *J Orof Orthop*. 2014;75(5):345–357.
23. Richter C, Jost-Brinkmann PG. Shear bond strength of different adhesives tested in accordance with DIN 13990-1/-2 and using various methods of enamel conditioning. *J Orof Orthop*. 2015;76(2):175–187.
24. Retief DH. Effect of conditioning the enamel with phosphoric acid. *J Dent Res*. 1973;52(2):333–341.
25. Arakawa Y, Takahashi Y, Sebata M. The effect of acid etching on the cervical region of the buccal surface the human premolar, with special reference to direct bonding techniques. *Am J Orthod*. 1979;76(2):201–208.
26. Asmussen E. Penetration of restorative resins into acid etched enamel. II. Dissolution of entrapped air in restorative resin monomers. *Acta Odont Scand*. 1977;35(4):183–191.
27. Voss JE, Charbeneau GT. A scanning electron microscope comparison of three methods of bonding resin to enamel rod ends and longitudinally cut enamel. *J Am Dent Assoc*. 1979;98(3):384–389.
28. Reynolds IR. A review of direct orthodontic bonding. *Brit J Orthod*. 1985;2:171–178.
29. Retief DH. Failure at the dental adhesive-etched enamel interface. *J Oral Rehabil*. 1974;1(3):265–284.
30. Mundstock KS, Sadowsky PL, Lacefield W, Bae S. An in vitro evaluation of a metal reinforced orthodontic ceramic bracket. *Am J Orthod Dentof Orthop*. 1999;116(6):635–641.
31. Heravi F, Moazzami SM, Ghaffari N, Jalayer J, Bozorgnia Y. Evaluation of shear bond strength of orthodontic brackets using trans-illumination technique with different curing profiles of LED light-curing unit in posterior teeth. *Prog Orthod*. 2013;14:49.
32. Gwinnett AJ, Yu S. Effect of long-term water storage on dentin bonding. *Am J Dent*. 1995;8(2):109–111.
33. Kitsako Y, Burrow MF, Nikaido T, Tagami J. The influence of storage solution on dentin bond durability of resin cement. *J Dent*. 2000;16(1):1–6.
34. Murray SD, Hobson RS. Comparison of in vivo and in vitro shear bond strength. *Am J Orthod Dentof Orthop*. 2003;123(1):2–9.
35. Iijima M, Ito S, Yuasa T, Muguruma T, Saito T, Mizoguchi I. Bond strength comparison and scanning electron microscopic evaluation of three orthodontic bonding systems. *J Dent Mat*. 2008;27(3):392–399.
36. de Oliveira CH, da Silva AM, Briso AL, Briso AL, Sundfeld ML. Resin tag length of one-step and self-etching adhesives bonded to unground enamel. *Bull Tokyo Dent Coll*. 2005;46(3):43–49.
37. Bishara SE, Oonsombat C, Soliman MM, Warren JJ, Laffoon JF, Ajlouni R. Comparison of bonding time and shear bond strength between a conventional and a new integrated bonding system. *Angle Orthod*. 2005;75(2):237–242.

A comparison of the remineralizing potential of dental restorative materials by analyzing their fluoride release profiles

Alicja Porenczuk[1,A–D], Bartłomiej Jankiewicz[2,A,D,E], Magdalena Naurecka[3,B,C], Bartosz Bartosewicz[2,A,B], Bartosz Sierakowski[3,B,C], Dariusz Gozdowski[4,C], Jerzy Kostecki[5,B], Barbara Nasiłowska[3,B], Agnieszka Mielczarek[1,A,E,F]

[1] Restorative Dentistry Department, Warsaw Medical University, Poland
[2] Institute of Optoelectronics, Military University of Technology, Warszawa, Poland
[3] Biomedical Engineering Center, Institute of Optoelectronics, Military University of Technology, Warszawa, Poland
[4] Faculty of Agriculture and Biology, Department of Experimental Design and Bioinformatics, Warsaw University of Life Sciences, Poland
[5] Electron Microscopy Laboratory, Institute of Optoelectronics, Military University of Technology, Warszawa, Poland

A – research concept and design; B – collection and/or assembly of data; C – data analysis and interpretation;
D – writing the article; E – critical revision of the article; F – final approval of the article

Advances in Clinical and Experimental Medicine, ISSN 1899–5276 (print), ISSN 2451–2680 (online) *Adv Clin Exp Med*. 2019;28(6):815–823

Address for correspondence
Alicja Porenczuk
E-mail: alicja.porenczuk@gmail.com

Funding sources
The study was supported by grant No. WUM 1S18/PM2/17 from Warsaw Medical University, Poland.

Conflict of interest
None declared

Acknowledgements
The authors would like to express their gratitude to Miron Kaliszewski and Maksymilian Włodarski (Institute of Optoelectronics, Military University of Technology, Warszawa, Poland) for constructing the 3D forms used in the study.

Received on March 8, 2018
Reviewed on May 3, 2018
Accepted on August 9, 2018

Published online on February 8, 2019

Cite as
Porenczuk A, Jankiewicz B, Naurecka M, et al. A comparison of the remineralizing potential of dental restorative materials by analyzing their fluoride release profiles. *Adv Clin Exp Med*. 2019;28(6):815–823. doi:10.17219/acem/94140

DOI
10.17219/acem/94140

Abstract

Background. The accessibility of the remineralizing ions in teeth's environment is essential for their incorporation into caries-affected dentin. Novel bioglass-reinforced materials capable of releasing fluoride, calcium and phosphates may be particularly useful in the tissue remineralization process. A novel restorative material, ACTIVA BioActive-Restorative (Pulpdent Corp., Watertown, USA), is a hydrophilic resin-modified glass-ionomer cement (RMGIC) enriched with bioglass particles and fortified with a patented rubberized polymer resin. Its application in restorative dentistry may be significant, promoting remineralization of carious lesions.

Objectives. The aim of the study was to compare the fluoride ion release profiles from a bioglass-reinforced RMGIC, a conventional glass-ionomer cement (GIC) and a nanohybrid restorative polymer resin.

Material and methods. The quantity of fluoride ions released from ACTIVA, Ketac Molar Quick Aplicap and Tetric EvoCeram was assessed using a fluoride-specific electrode. The surface characteristics of the pre- and post-experimental specimens were studied using a scanning electron microscope (SEM) and confocal microscope. An X-ray powder diffraction (XRD) analysis was additionally used to examine the chemical compositions of the dental materials.

Results. The greatest quantity of fluoride ions was freed from the GIC specimens (20.698–54.118 ppm), followed by the bioglass-reinforced RMGIC (from 1.236 to 15.552 ppm) and nanohybrid polymer resin (0.370–1.148 ppm). The pre-experimental specimens of the bioglass-reinforced RMGIC were porous, while the post-experimental specimens were smoother with visible micro-cracks. The XRD analysis of the bioglass particles confirmed that the material was composed mainly of fluoride (27.70 mass%), silicon (15.62 mass%), aluminum (5.91 mass%), and calcium (5.40 mass%).

Conclusions. The fluoride ion release profile of ACTIVA was lower than the GIC Keta Molar Quick Aplicap, but significantly higher than the nanohybrid restorative polymer resin Tetric EvoCeram.

Key words: fluoride, scanning electron microscopy, bioactive glass, resin-modified glass-ionomer cement, confocal microscopy

The principle underlying minimally invasive dentistry is the introduction of clinical procedures that contribute to the restoration of carious tissues. The remineralization process entails incorporating fluoride, calcium and phosphate ions into demineralized tissues. In deep cavities which are in need of endodontic treatment, partially demineralized dentin may remain at the bottom of the cavity as long as it is hermetically sealed off from the outer environment with bioactive restorative materials (biomaterials). Bioactivity, according to Hench, is the capacity of the dental material to join with living tissue without causing any adverse effects.[1] After placement in the cavity, the process of "bioactive fixation" occurs, in which the biomaterial interacts chemically with the constituents of the tissue, creating a homogenous mass.[2] The most important feature in the remineralizing potential of a biomaterial is its ability to release fluoride ions. In an ionized form, fluoride can easily be exchanged with the hydroxyl ions in hydroxyapatite, leading to the formation of the fluorohydroxyapatite crystal (FHA; general chemical structure $Ca_5(PO_4)_3OH_{1-x}F_x$). The FHA, being resistant to acid demineralization promoted by caries-associated bacteria, is chemically more stable than other hydroxyapatite forms.[3] Moreover, it acts as a reservoir for fluoride ions, releasing them when the pH in the surrounding environment falls below 4.5.[3] The FHA thus protects dental tissues from further acidic degradation. Biomaterials include glass-ionomer cements (GICs) and their derivatives, such as resin-modified glass ionomer cements (RMGICs) and bioglass restoratives – a novelty in restorative dentistry – made from SiO_2-CaO-Na_2O-P_2O_5 components. Stress-bearing cavities would normally be restored with resin-based polymer materials. Although they may contain fluoride in the form of the radiopaque filler ytterbium trifluoride (YbF_3), its release seems insufficient for remineralization.[4] Glass-ionomer cements and their derivatives should therefore be applied in all situations where tissue repair is required.[5] They owe their ability to release ions to their silicate filler content, which continuously releases and recharges fluoride, and to their structural inner porosity, which allows water to flow through the material, leading to the dissolution of the filler. However, biological features of GICs may impair their physical properties, making them brittle and necessitating their replacement.[4] The development of RMGICs was a response to an urgent need for GICs with enhanced mechanical properties. They contain the same filler as GICs, a water-soluble matrix formed by poly(acrylic acid) and organic monomers, such as 2-hydroxyethyl methacrylate (HEMA), taken from polymer resins.[6] Their hydrophilic character, provided by HEMA, improves the water uptake and the dissolution of the filler, along with the release of the desired fluoride ions.[7] Straightforward as this may seem, the level of the fluoride ions liberated from RMGICs is less than GICs, which may be presumed a result of the HEMA altering the acid-base reaction and leading to the formation of a weaker gel network.[5,6] Nevertheless, RMGICs have sufficient physical endurance to be used as a restorative material in deep cavities, and as an alternative to polymer resins.

Recently, continuing progress in the development of dental materials and the search for more efficient biomaterials has led to the incorporation of SiO_2-CaO-Na_2O-P_2O_5 bioglass particles in the polymer matrix. The mechanism of bioglass dissolution is facilitated by the breakup of the Si-O-Si bonds in the silicate network in an aqueous environment, which permits the rapid release of fluoride, calcium and silicon.[5] Hydroxyl ions are also released, leading to the alkalization of the environment as well as eradication of the bacteria.[8] The structure of a bioglass restorative may determine its bioactivity, as its inner porosity facilitates water flow through the material and the dissolution of the bioglass.[9] Although the hydrophilic nature of this material is attributable to HEMA, the amount of bioglass added should be carefully judged. According to Khvostenko et al., approx. 15 weight percentage (wt%) is adequate to obtain the desired properties.[10]

The recently introduced ACTIVA BioActive-Restorative (Pulpdent Corp., Watertown, USA) is a hydrophilic RMGIC enriched with bioglass and fortified with a patented rubberized polymer resin. The material contains both bioglass particles and polyacid components of RMGICs. The material does not contain bis-GMA, bisphenol A (BPA) or BPA derivatives, and is therefore considered more biocompatible than other resin-based materials. According to the manufacturer, the triple setting mode of this material includes the acid-base neutralization reaction of GICs, self-cure and light-cure of the matrix. Recent studies have shown its ability to release remineralizing ions without adverse effects on its physical durability.[11] However, its exact chemical composition and structure have not been disclosed by the manufacturer.

Objectives

The aim of the study was to compare the fluoride ion release profiles of a bioglass-reinforced RMGIC, a conventional GIC and a nanohybrid restorative polymer resin. The null hypothesis stated that the bioglass-reinforced RMGIC releases quantities of fluoride ions comparable to the GIC.

Material and methods

Material

The characteristics of the dental materials used in the study, according to the data provided by the manufacturers, are presented in Table 1. Sodium fluoride (NaF) was obtained from POCH S.A. (Gliwice, Poland) and TISAB I from Hydromet S.C. (Gliwice, Poland). Deionized (DI) water (0.05 µS/cm at 25°C; Hydrolab, Dziewięć Włók, Poland) was used throughout the study.

Table 1. Specifications of dental materials used in the study, according to the data provided by the manufacturers

Material (short name, shade)	Type	Composition	Setting mode	Lot number
ACTIVA BioActive-Restorative (AB, shade A2)	bioglass-reinforced glass-ionomer restorative cement	blend of diurethane and methacrylates with modified polyacrylic acid (44.6%); reactive glass filler (21.8 wt%); inorganic filler (56 wt%), patented rubberized resin (Embrace), water	light-cure and self-cure; curing time 20 s; chemical setting (reaction of neutralization)	151217
Ketac Molar Quick Aplicap (KM)	glass-ionomer restorative cement	Powder: inorganic filler (calcium (Ca), aluminum (Al), lanthanum (La), silicon (Si), fluorosilicate glass (73–74 wt%)); pigments. Liquid: polycarboxylic acid, tartaric acid, water	chemical setting (reaction of neutralization)	570386
Tetric EvoCeram (TE, shade A2)	nanohybrid composite restorative material	dimethacrylates: *bis*-GMA; UDMA (19.7 wt%); inorganic filler (size 40–3,000 nm, barium glass and ytterbium trifluoride (62.5 wt%), mixed oxide, prepolymer (19.7 wt%))	light-cure; curing time 10 s	U49869

wt% – weight percent; *bis*-GMA – bisphenol A glycidyl dimethacrylate; UDMA – urethane dimethacrylate.

Methods

Specimen preparation

Fifteen disc-shaped specimens of each of the 3 dental materials were prepared, 5 per group. The materials were applied to Z-ABS poly(acrylonitrile-co-butadiene-co-styrene) 3D molds (Zortrax S.A., Olsztyn, Poland) and printed using an M200 printer (Zortrax S.A.). Each mold had an internal diameter of 8 mm, height of 3 mm and total surface area of 175.85 mm.^{2} The 3D form was placed on a glass slab and, after application of the material, another glass slab was positioned over it and moderately hand-pressed in order to level up the specimen surface. Light-setting restoratives were cured using a Radii Plus diode polymerization lamp (SDI Ltd., Bayswater, Australia; light intensity 1500 mW/cm^2). The capsulated Ketac Molar Quick Aplicap (KM; 3M ESPE Dental Products, St. Paul, USA) was mechanically mixed in a Silamat Plus mixing unit (Ivoclar Vivadent, Schaan, Liechtenstein), transferred to the molds with a dedicated applier, covered with a glass slab, and left to harden (Fig. 1). After setting, the glass slabs were carefully removed and the specimens were freed from the forms with a 3D reverse form. In order to remove debris from their surfaces, the specimens were polished with silicone carbide paper of varying grits (320, 600, 800, and 1200), acid-etched for 60 s with 38% phosphoric acid (Blue Etch; Cerkamed, Stalowa Wola, Poland), rinsed with water, and blow-dried with air. Immediately after preparation and at the end of the study, the specimens were weighed on a calibrated analytical weight (Mettler AT 200, Mettler-Toledo, Columbus, USA).

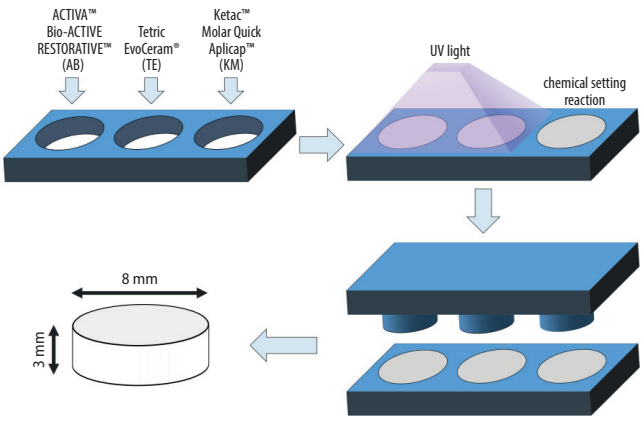

Fig. 1. Schematic illustration of specimens preparation using the 3D forms

The fluoride release test

The specimens were incubated (37°C, 14 days) in polypropylene vials containing 4 mL of deionized (DI) water. As high temperatures can speed up ion movement in a solution and thus give false results,[12] the specimens were removed from the incubator approx. 30 min before each read-out and left to cool in order to produce similar temperature conditions (average read-out temperature: 21.387°C). The quantity of released fluoride ions (ppm) was measured in DI water with a fluoride-specific electrode (model IJ-F; Ionode Pty Ltd., Tennyson, Australia) coupled with a digital ion analyzer (model CX-601; Elmetron, Zabrze, Poland). The electrode was calibrated daily with a series of standard solutions (50 µM/L NaF (949.9 ppb) and 500 µM/L NaF (9.499 ppm)), and was washed with fresh DI water and dried with absorbent paper after each analysis. To maintain constant ionic strength, as well as to decomplex the fluoride ions and adjust the pH of the solution, the same volumes of analyzed DI water and TISAB I were mixed (2:2 mL; 1:1 ratio). During the read-outs, the specimens were removed from the vials, rinsed with fresh DI water, dried with absorbent paper, and transferred to new DI water solutions. The DI water measurements for fluoride ion content were carried out daily on the first 7 days and on day 14. The read-out schedule covered days 1–8 and day 14. No read-outs were carried out between days 8 and 13. The positive controls were Tetric EvoCeram (TE) (Ivoclar Vivadent) and Ketac Molar Quick Aplicap (KM). ACTIVA BioActive-Restorative (AB) served as the experimental group, while the negative control was pure DI water.

The microscopic analyses

As the manufacturers' data on the composition of the dental materials chemical is restricted, the authors wanted to provide the characteristics of the structure and composition of both the pre- and post-experimental specimens using scanning electron microscopes (SEM) (SEM/EDX with an energy-dispersive detector (model 1430 VP with XFlash 4010; Leo Electron Microscopy Ltd., Cambridge, UK), VEGA-II SBU (model VG4300780PL; TESCAN, Brno, Czech Republic), Quanta 3D FEG (model 250 with a large-field low-vacuum detector and low-vacuum secondary electron detectors; FEI Europe, Eindhoven, the Netherlands) and X-ray diffraction (XRD) (Philips XPert with X'Celerator scientific detector, Panalytical B.V.; Almelo, the Netherlands; measurement conditions: CuKα radiation at 40 kV and 30 mA, 25–120° range, 90 s timing and 0.0167° step size). An Imager.Z2m confocal microscope with LSM700 laser system (Carl Zeiss Microscopy GmbH, Jena, Germany; measurement conditions: EC Epiplan 20×/0.6 DIC lens (Carl Zeiss Microscopy GmbH), laser wavelength = 405 nm, power of laser 2%, scanning speed 5, reading frame 2048 × 2048, 16-bit color depth) was also used to present the surfaces of the specimens. Each surface was evaluated at 3 different points, and each measured point was averaged from 2 scans. The assessed PSa (the primary profile's arithmetic mean deviation of all surface heights) index values were averaged using the formula:

$$PSa = \frac{1}{N_x * N_y} \sum_{i=1}^{N_x} * \sum_{j=1}^{N_y} * [z(x_i, y_j) - PSc]$$

where:
N_x, N_y – the number of pixels in X- or Y- direction;
z – the depth of inequalities on the surface; and
PSc – the mean height of the elements on the surface.

Statistical analysis

The statistical analysis was performed using SPSS v. 10.0 for Windows (SPSS Inc., Chicago, USA). The compatibility of the distribution of quantitative variables with normal distribution was checked with the W Shapiro-Wilk test. An analysis of variance (ANOVA) and Scheffé post-hoc test were used to analyze correlations of the variables. In all the tests $p < 0.05$ was considered statistically significant.

Results

At the end of the study, the mean weight of the AB specimens was lower by 0.76%, while the KM specimens manifested an average weight loss of 3.44%. A mean weight gain of 0.22% was observed for the TE specimens.

Fluoride release test

A comparison of the daily mean values of the released fluoride ions from all the tested materials is presented in Fig. 2. The highest quantity of fluoride ions was freed from the KM specimens on days 1–4 (20.698–54.118 ppm; $p < 0.05$), followed by AB, with the highest value noted on day 1 (15.552 ppm; $p < 0.05$). Throughout the observation period, the level of released fluoride ions in the TE specimens (0.370–1.148 ppm) and the control specimens

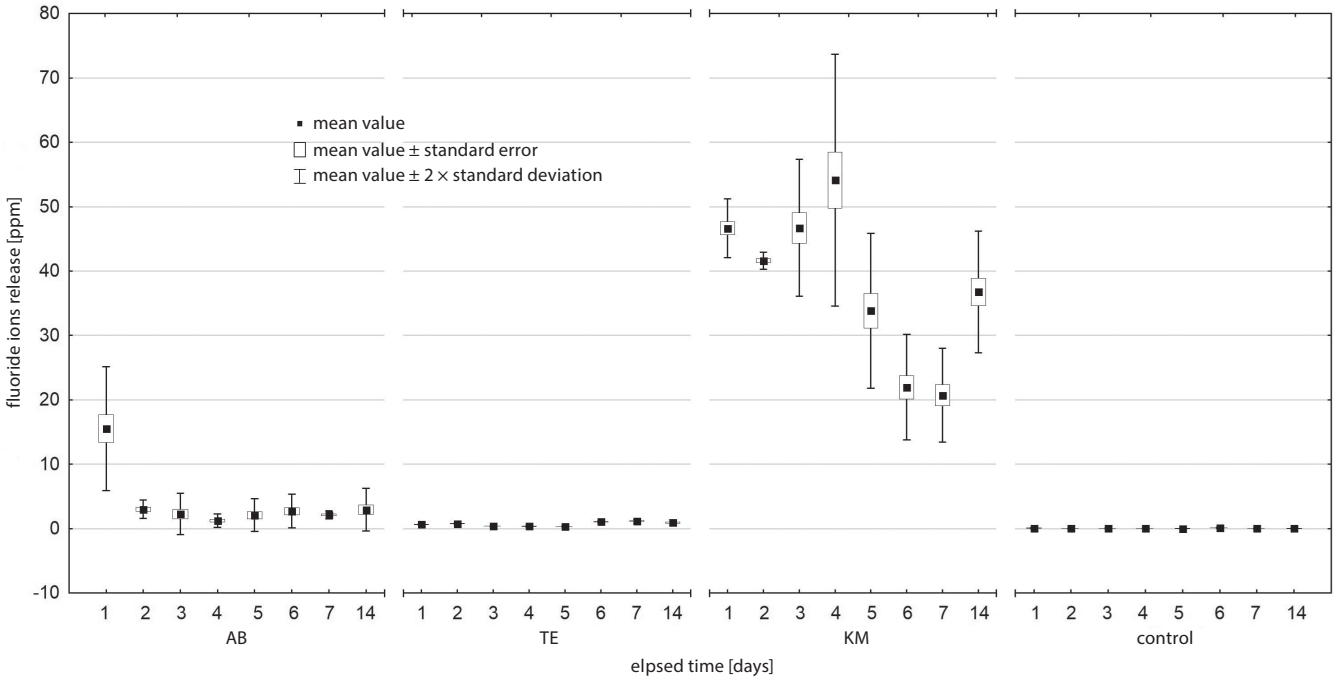

Fig. 2. Daily mean values of the released fluoride ions from dental materials (AB, TE, KM) and the control (C)

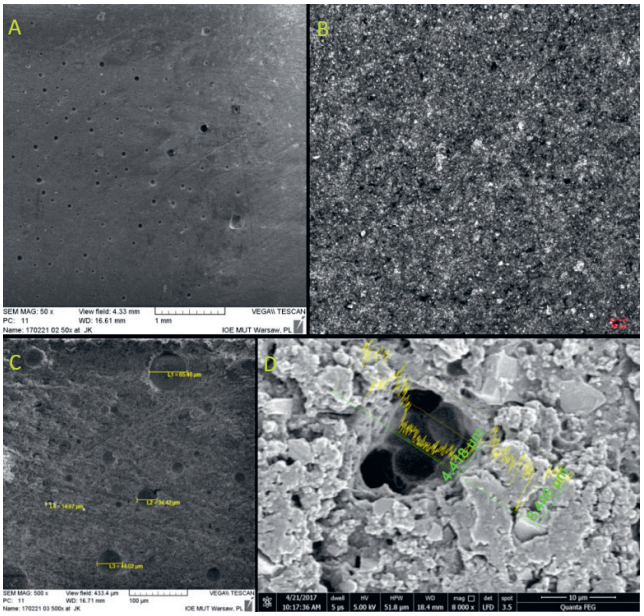

Fig. 3. Images of the pre-experimental AB specimens (A): SEM image of the surface view with visible porosity (VEGA-II SBU; magnification ×50); (B) general surface view in confocal microscope, visible pores and roughness of the specimen; (C) SEM image of various in sizes pores in the material (VEGA-II SBU; magnification ×500); (D) SEM high-magnification inset of the pore (Quanta 3D FEG/LVSED; magnification ×8000)

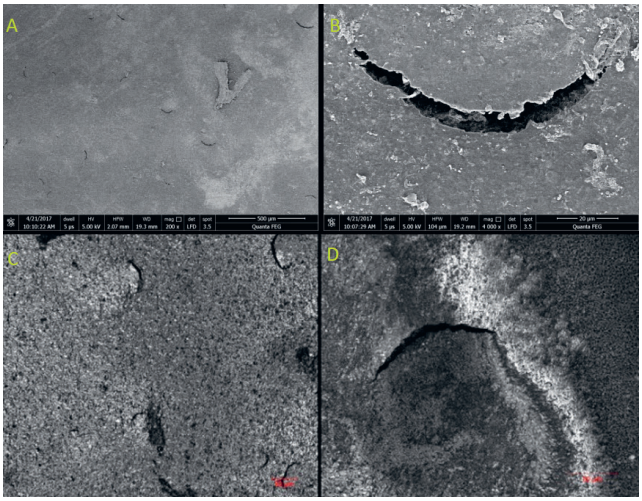

Fig. 4. Images of the post-experimental AB specimens: (A) SEM image of the surface view with visible cracks (Quanta 3D FEG/LFD; magnification ×200); (B) SEM high-magnification inset of the crack (Quanta 3D FEG/LFD; magnification ×4000); (C) general surface view in confocal microscope, visible cracks and smoothness of the specimen; (D) high-magnification inset of the crack in confocal microscope

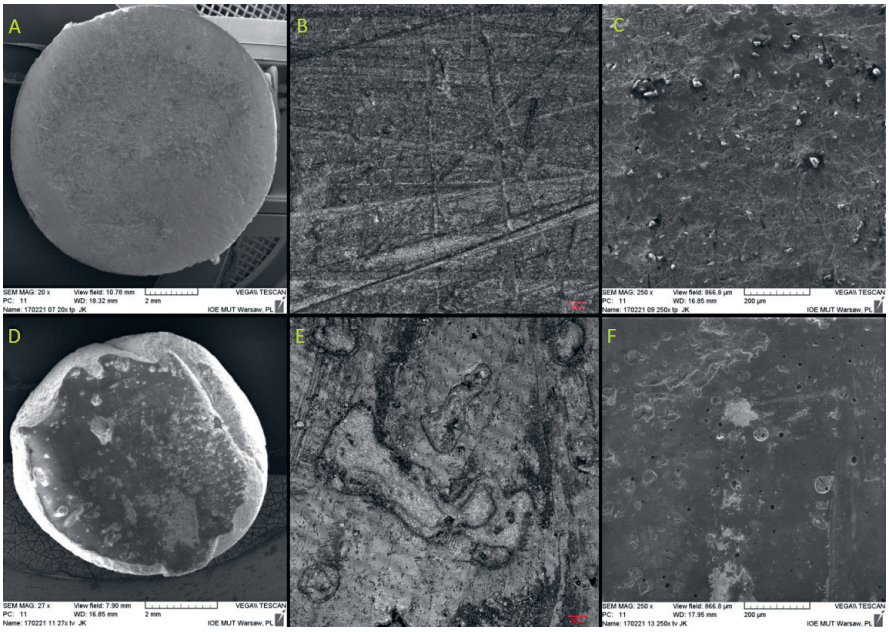

Fig. 5. Images of the TE specimens: pre-experimental (A) SEM image of the surface view (VEGA-II SBU; magnification ×20); (B) surface view in confocal microscope; (C) distribution of filler particles in the material (VEGA-II SBU; magnification ×500); post-experimental (D) general surface view with visible delamination and asperities (VEGA-II SBU; magnification ×27); (E) high-magnification view of delaminated surface in confocal microscope; (F) pores and cracks on the specimen's surface (VEGA-II SBU; magnification ×250)

(0.008–0.122 ppm) were lower than in the other groups. Compared to TE, AB released more fluoride ions on days 1 and 2 ($p < 0.05$), with no further significance. Compared to KM, AB released significantly fewer fluoride ions ($p < 0.05$) starting from day 2.

The microscopic analyses

The pre-experimental surfaces of AB specimens were non-homogeneously studded with pores of various sizes (Fig. 3), while the post-experimental specimens were significantly smoother (PSa index; $p = 0.04$), with fewer pores and multiple comma-like micro-cracks (Fig. 4). Compared to the corresponding TE and KM specimens, the pre-experimental AB specimens were significantly smoother (PSa index; $p < 0.001$). In addition, the AB specimens were significantly smoother than the TE specimens at the end of the study (PSa index; $p = 0.029$).

The pre-experimental TE specimens were quite smooth and homogenous (Fig. 5 A–C), while at the end they were delaminated, with visible pores and asperities (PSa index; $p = 0.027$; Fig. 5 D–F).

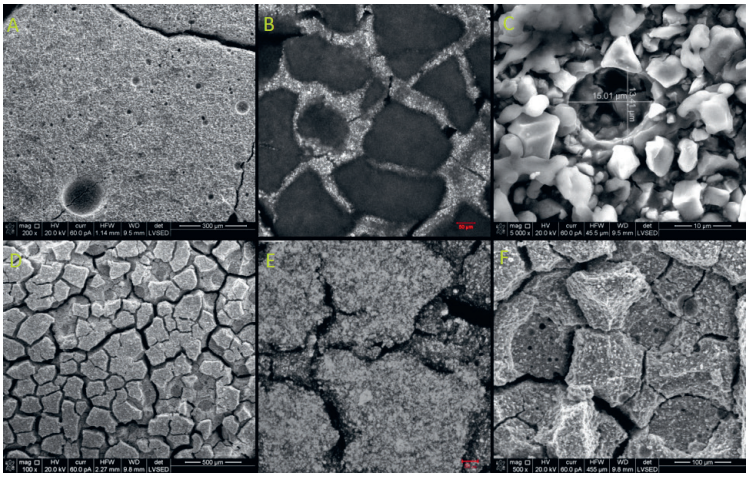

Fig. 6. Images of the KM specimens: pre-experimental (A) SEM image of the surface, visible porosity of the material (Quanta 3D FEG/LVSED; magnification ×200); (B) high-magnification surface view in confocal microscope, visible glass filler in matrix; (C) high-magnification SEM image of the material's inner porosity (Quanta 3D FEG/LVSED; magnification ×5000); post-experimental (D) surface view of the cracked specimen (VEGA-II SBU; magnification ×100); (E) high-magnification view of the cracked surface in confocal microscope; (F) pores and cracks on the specimen's surface (Quanta 3D FEG/LVSED; magnification ×500)

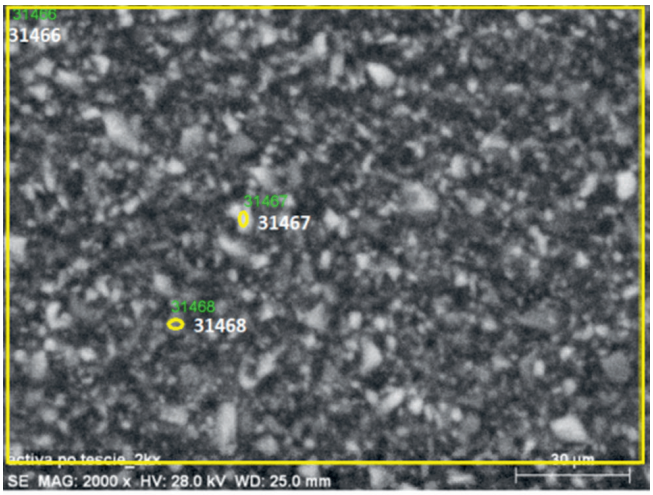

31463 Date:8/28/2017 12:33:13 PM HV:28.0kV Puls th.:11.03kcps
31464 Date:8/28/2017 12:34:08 PM HV:28.0kV Puls th.:14.01kcps
31465 Date:8/28/2017 12:34:49 PM HV:28.0kV Puls th.:12.35kcps

Mass percent (%)

Spectrum	C	O	F	Na	Al	Si	P	S	Ca	Ba
31463	10.50	25.81	24.64	1.01	5.01	17.34	0.79	0.19	3.84	10.85
31464	6.80	31.24	27.99	0.76	3.71	13.65	0.23	0.08	1.10	14.42
31465	5.21	19.84	30.45	1.17	9.02	15.86	1.56	0.14	11.26	5.49
Mean value:	7.50	25.63	27.70	0.98	5.91	15.62	0.86	0.14	5.40	10.26
Sigma:	2.72	5.70	2.91	0.20	2.77	1.86	0.67	0.05	5.26	4.50
Sigma mean:	1.57	3.29	1.68	0.12	1.60	1.07	0.39	0.03	3.03	2.60

Fig. 7. General composition of AB specimens (SEM/EDS). Area 31465 depicting the main elements building the bioglass. Area 31464 indicating the presence of the inorganic filler

The pre-experimental KM specimens were porous, with irregularly shaped filler particles submerged in the matrix (Fig. 6 A–C). After testing, the specimens were less porous and heavily cracked, exposing their inner structure (Fig. 6 D–F).

The X-ray powder diffraction analysis

The general composition of the pre- and post-experimental specimens was assessed using SEM/EDS and XRD analyses. The AB specimens comprised mainly of fluoride (27.70 mass%), silicon (15.62 mass%), aluminum (5.91 mass%), and calcium (5.40 mass%). The largest percentage share of the main elements composing the bioglass were found in area 31465, while area 31464 may depict the inorganic filler due to a high share of silicon and barium (Fig. 7). The post-experimental AB specimens showed a loss in fluoride (22.19 mass%) and natrium (0.89 mass%). The XRD analysis indicated the presence of calcium fluoride and silicon in all the AB specimens (Fig. 8).

The pre-experimental TE specimens were comprised mainly of fluoride (28.65 mass%), ytterbium (16.61 mass%), silicon (16.28 mass%), and zircon (2.19 mass%), whereas the post-experimental specimens showed a loss of fluoride (26.78 mass%) and ytterbium (16.45 mass%). The XRD analysis showed the presence of calcium, silicon and silicon ytterbium in all the TE specimens (Fig. 9).

The primary constituents of the pre-experimental KM specimens were fluoride (41.55 mass%), lanthanum (11.83 mass%), calcium (7.33 mass%), aluminum (8.24 mass%), and silicon (6.66 mass%). A loss of fluoride (41.55 mass%), aluminum (6.92 mass%) and silicon (6.07 mass%) was noted in the post-experimental specimens. The XRD analysis confirmed the presence of calcium and lanthanum oxide in the KM specimens (Fig. 10).

Discussion

The release of fluoride ions from GICs takes place during their maturation and is diffusion-controlled, meaning that it declines in a linear fashion, reaching a plateau within 10–20 days.[13] Mazzoui et al. proved that GICs release most of their fluoride content during the first 7 days (12–30 ppm), with a burst effect occurring in the first 24 h.[14] Our study results showed that the KM specimens

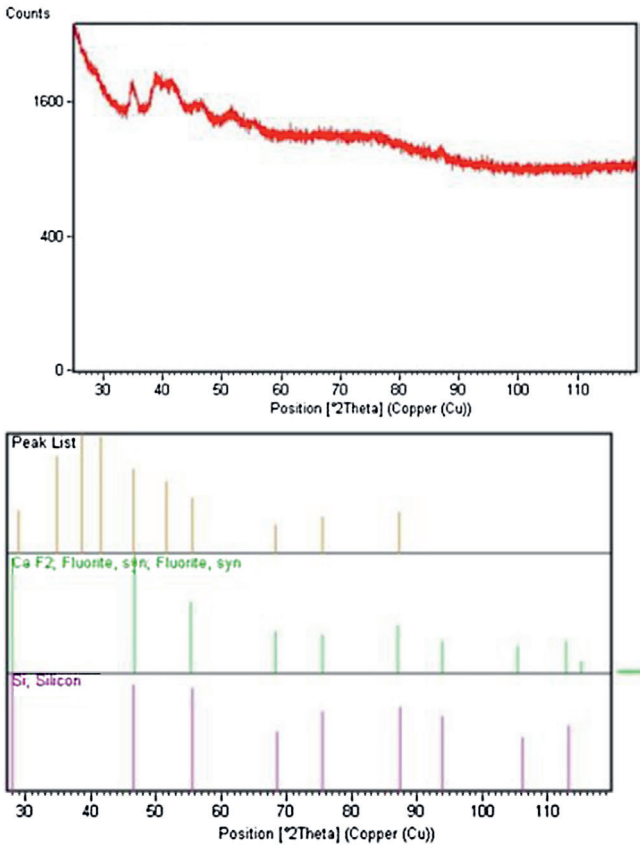

Fig. 8. Composition of AB specimens in XRD analysis

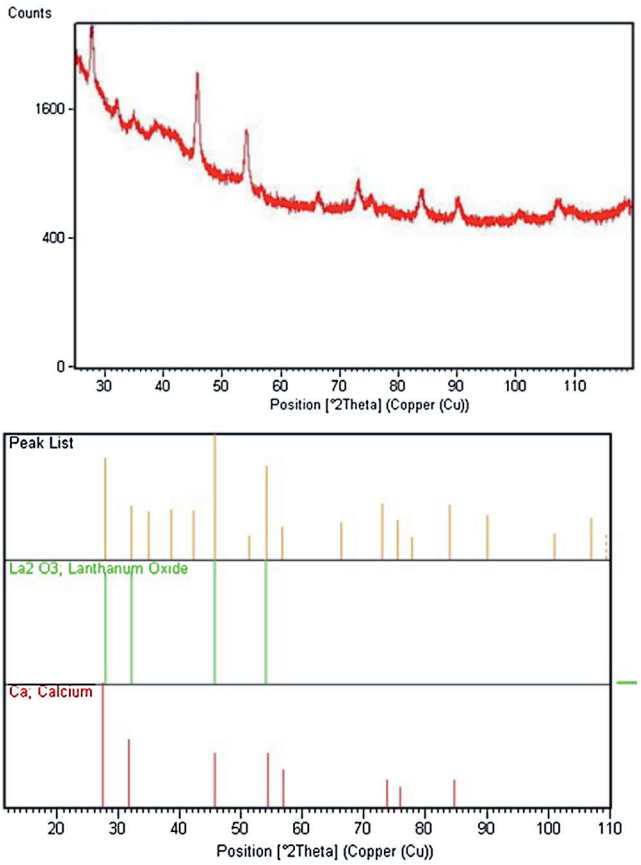

Fig. 10. Composition of KM specimens in XRD analysis

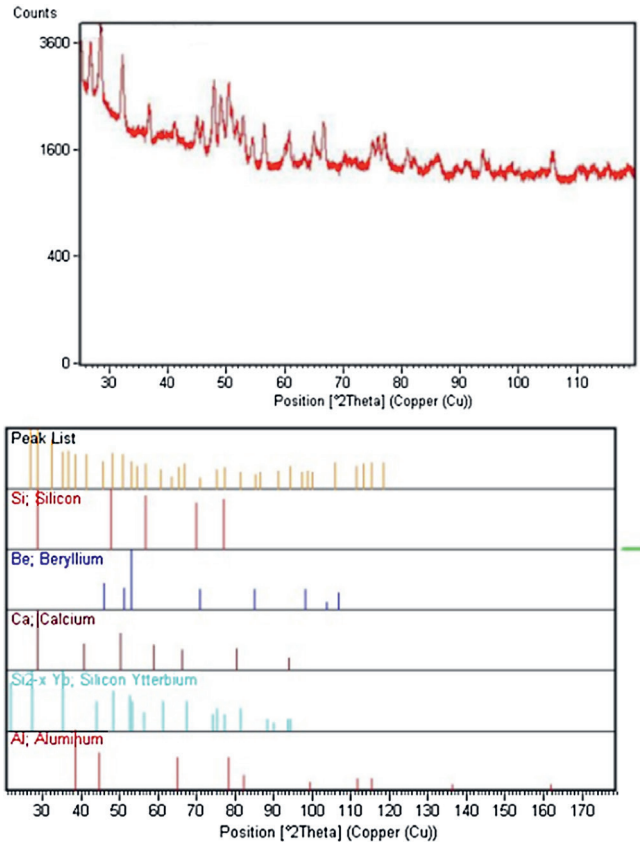

Fig. 9. Composition of TE specimens in XRD analysis

released most of their fluoride ions in the first 4 days (20.698–54.118 ppm), which is compatible with the results reported by Mazzoui et al. Another study indicated that the burst effect of KM was quite low (1.22 ±0.30 ppm)[15] and much lesser than what we observed, possibly due to differences in the measurement conditions and the specimen sizes.

Bioglass dissolution is determined by Si-O-Si bond breakage, which causes a rapid increase in the concentration of fluoride ions between days 0 and 3, followed by a decline.[16,17] This suggests that the chemical composition of bioglass has a tremendous impact on its release profile. For instance, Davis et al. demonstrated that long-lasting fluoride release was significantly higher for composites containing bioglass particles rich in silicon.[18] In a study undertaken by Mneimne et al., bioglass particles rich in phosphate or fluoride were capable of inducing apatite growth faster and at a lower pH.[19] As the exact composition and structure of AB has not been disclosed by the manufacturer, it may be difficult or even impossible to compare its features to other biomaterials. It has been reported that the average daily release of fluoride ions from RMGICs is quite high (4–65 ppm) on the 1st day, declining to approx. 1–2 ppm after 1 week.[13,16,20] Kishore et al. stated that RMGICs were more efficient in their ability to release than GICs (6.7 ±0.158 ppm vs 2.9 ±0.158 ppm),[16]

whereas Kucukyilmaz et al. and Rama Rao et al. stated they were significantly less efficient.[5,20] In our study, the bioglass-reinforced RMGIC (AB) obtained the highest level of freed fluoride ions on the 1st day (15.5 ppm), which later decreased to a continuous plateau of 1.2–3.0 ppm. Compared to KM, its release profile was significantly lower. On this basis, our null hypothesis had to be rejected. Apart from obvious differences in the chemical composition of the 2 materials, we believe that this result may also depend on the storage media, as dental materials kept in DI water show lower ionic flow compared to the pH-cycling method.[4] The pH values of the solutions used may also have had an impact on the ion release.[21] Garoushi et al., who also analyzed AB in similar conditions to those in this study, observed that it released significantly fewer fluoride ions compared to other RMGICs.[22] They also pointed out a tendency for this material to liberate the most ions in the first 24 h (approx. 1.5 ppm), followed by stabilization at a lower level, which is in agreement with our results. Similar conclusions were provided by May and Donly, who found that AB released significantly less fluoride than another RMGIC (Vitremer) throughout their observation period (31 days).[23] Contrary to both Garoushi et al. and May and Donly, we obtained a higher level of released fluoride after 24 h (15.552 ppm vs 1.5 ppm[23] vs 1.920 ppm[23]), which may be due to different read-out equipment and study conditions. Gandolfi et al. support the idea that the presence of hydrophilic resins, such as HEMA or triethylene glycol dimethacrylate (TEGDMA), could lead to hydrolytic disintegration of bioglass particles. Weight reduction of their experimental composites was attributed to the release of calcium and hydroxyl ions.[8] Our study supports their conclusions, as we observed a 0.76% average mass reduction in the AB specimens. Most of the polymer resins released extremely low or even no fluoride ions (less than 0.02–2 ppm within 30–60 days),[13] which was confirmed in this study (TE; ~1.0 ppm).

The SEM/EDS and XRD analyses helped to define only the primary composition of the pre- and post-experimental specimens, as their chemical structure proved to be complex. Despite numerous trials and methodologies, determination of the exact compositions could not be satisfactorily concluded. The SEM analysis showed the presence of pores in the pre-experimental AB specimens, which resemble the inner structure of GICs and may allow water flow through the material. Fewer pores, multiple cracks and delamination of the post-experimental specimens suggested that the material had decomposed in DI water. Even though all the tested materials were kept in a moist and warm environment, their disintegration modes clearly differed from one another. Polymer resins are susceptible to premature failure due to the formation of cracks, micro-cracks and delaminations, which develop in response to various stimuli. Moisture plays an important role in their fatigue, as they are prone to water uptake. Moreover, thermal stress occurs in response to temperature fluctuations throughout the time they are in the oral cavity, even without additional mechanical loading.[24] The development of thermal stress may also depend on the matrix reinforcement and any inhomogeneity within their structure. For instance, resin composites reinforced with glass microspheres were subject to accelerated degradation.[25] The absorbed water, along with temperature changes, may contribute to hygrothermal failure, in which the structure of the polymer is affected by the formation of internal stress leading to further cracking.[24] As a result, we expected the post-experimental TE specimens to be cracked, non-homogeneous and delaminated. Presumably, the presence of the comma-like micro-cracks in the post-experimental AB specimens may also be a result of hygrothermal failure developing within the bioglass-reinforced porous structure of RMGIC.

Conclusions

Within the limitations of this in vitro study, it may be concluded that the fluoride ion release profile of the novel restorative material ACTIVA BioActive-Restorative was lower than the GIC Ketac Molar Quick Aplicap, but significantly higher than that of the nanohybrid restorative polymer resin Tetric EvoCeram.

References

1. Hench LL, Splinter RJ, Allen WC, Greenlee TK. Bonding mechanisms at the interface of ceramic prosthetic materials. *J Biomed Mater Res*. 1971;5(6):117–141.
2. Mousavinasab SM, Khoroushi M, Keshani F, Hashemi S. Flexural strength and morphological characteristics of resin-modified glass-ionomer cement containing bioactive glass. *J Contemp Dent Pract*. 2011;12(1):41–46.
3. ten Cate JM. Contemporary perspective on the use of fluoride products in caries prevention. *Brit Dent J*. 2013;214(3):161–167.
4. Garcez RM, Buzalaf MAR, de Araújo PA. Fluoride release of six restorative materials in water and pH-cycling solutions. *J Appl Oral Sci*. 2007;15(5):406–411.
5. Kucukyilmaz E, Savas S, Kavrik F, Yasa B, Botsali MS. Fluoride release/recharging ability and bond strength of glass ionomer cements to sound and caries-affected dentin. *Niger J Clin Pract*. 2017;20(2):226–234.
6. Nicholson JW, Czarnecka B. The biocompatibility of resin-modified glass-ionomer cements for dentistry. *Dent Mater*. 2008;24(12):1702–1708.
7. Van Landuyt KL, Snauwaert J, Peumans M, De Munck J, Lambrechts P, Van Meerbeek B. The role of HEMA in one-step self-etch adhesives. *Dent Mater*. 2008;24(10):1412–1419.
8. Gandolfi MG, Taddei P, Siboni F, Modena E, De Stefano ED, Prati C. Biomimetic remineralization of human dentin using promising innovative calcium-silicate hybrid "smart" materials. *Dent Mater*. 2011;27(11):1055–1069.
9. McCabe JF, Yan Z, Al Naimi OT, Mahmoud G, Rolland SL. Smart materials in dentistry: Future prospects. *Dent Mater J*. 2009;28(1):37–43.
10. Khvostenko D, Hilton TJ, Ferracane JL, Mitchell JC, Kruzic JJ. Bioactive glass fillers reduce bacterial penetration into marginal gaps for composite restorations. *Dent Mater*. 2016;32(1):73–81.
11. Pameijer CH, Garcia-Godoy F, Morrow BR, Jefferies SR. Flexural strength and flexural fatigue properties of resin-modified glass ionomers. *J Clin Dent*. 2015;26(1):23–27.
12. Yan Z, Sidhu SK, Mahmoud GA, Carrick TE, McCabe JF. Effects of temperature on the fluoride release and recharging ability of glass ionomers. *Oper Dent*. 2007;32(2):138–143.

13. Wiegand A, Buchalla W, Attin T. Review on fluoride-releasing restorative materials: Fluoride release and uptake characteristics, antibacterial activity and influence on caries formation. *Dent Mater*. 2007;23(3):343–362.
14. Mazzaoui SA, Burrow MF, Tyas MJ. Fluoride release from glass ionomer cements and resin composites coated with a dentin adhesive. *Dent Mater.* 2000;16(3):166–171.
15. Basso GR, Della Bona Á, Gobbi DL, Cecchetti D. Fluoride release from restorative materials. *Braz Dent J*. 2011;22(5):355–358.
16. Kishore G, Sai-Sankar AJ, Pratap-Gowd M, Sridhar M, Pranitha K, Sai-Krishna VS. Comparative evaluation of fluoride releasing ability of various restorative materials after the application of surface coating agents: An in vitro study. *J Clin Diagn Res*. 2016;10(12):ZC38–ZC41.
17. Shah FA, Brauer DS, Hill RG, Hing KA. Apatite formation of bioactive glasses is enhanced by low additions of fluoride but delayed in the presence of serum proteins. *Mater Lett*. 2015;153:143–147.
18. Davis HB, Gwinner F, Mitchell JC, Ferracane JL. Ion release from, and fluoride recharge of a composite with a fluoride-containing bioactive glass. *Dent Mater*. 2014;30(10):1187–1194.
19. Mneimne M, Hill RG, Bushby AJ, Brauer DS. High phosphate content significantly increases apatite formation of fluoride-containing bioactive glasses. *Acta Biomater.* 2011;7(4):1827–1834.
20. Rama Rao SB, Patri G, Agnihotri Y, Balagopal S. Fluoride and restorative materials. *Int J Contemp Dent*. 2011;2(3):159–164.
21. Fúcio SB, De Paula AB, Sardi JC, Duque C, Correr-Sobrinho L, Puppin-Rontani RM. *Streptococcus mutans* biofilm influences on the antimicrobial properties of glass ionomer cements. *Braz Dent J*. 2016;27(6):681–687.
22. Garoushi S, Vallittu PK, Lassila L. Characterization of fluoride releasing restorative dental materials. *Dent Mater J.* 2018;37(2):293–300.
23. May E, Donly KJ. Fluoride release and re-release from a bioactive restorative material. *Am J Dent*. 2017;30(6):305–308.
24. Awaja F, Zhang S, Tripathi M, Nikiforov A, Pugno N. Cracks, microcracks and fracture in polymer structures: Formation, detection, autonomic repair. *Prog Mater Sci*. 2016;83:536–573.
25. Awaja F, Arhatari B, Wiesauer K, Leiss E, Stifter D. An investigation of the accelerated thermal degradation of different epoxy resin composites using X-ray microcomputed tomography and optical coherence tomography. *Polym Degrad Stab*. 2009;94(10):1814–1824.

Arabic language skin-related stigmatization instruments: Translation and validation process

Dimitre Dimitrov[1,A,B,D,F], Łukasz Matusiak[2,C,E,F], Andrea Evers[3,E,F], Mohammad Jafferany[4,E,F], Jacek Szepietowski[2,A,C,E,F]

[1] Presidential Medical Wing, Al Mafraq and Sheikh Khalifa Medical City, Abu Dhabi, UAE
[2] Department of Dermatology, Venereology and Allergology, Wroclaw Medical University, Poland
[3] Department of Health, Medical and Neuropsychology, Leiden University, the Netherlands
[4] Department of Psychiatry and Behavioral Science, Central Michigan University, Saginaw, USA

A – research concept and design; B – collection and/or assembly of data; C – data analysis and interpretation; D – writing the article; E – critical revision of the article; F – final approval of the article

Advances in Clinical and Experimental Medicine, ISSN 1899–5276 (print), ISSN 2451–2680 (online) *Adv Clin Exp Med*. 2019;28(6):825–832

Address for correspondence
Jacek Szepietowski
E-mail: jacek.szepietowski@umed.wroc.pl

Funding sources
None declared

Conflict of interest
None declared

Received on September 4, 2018
Reviewed on November 11, 2018
Accepted on January 3, 2019

Published online on February 9, 2019

Abstract

Background. Skin diseases are frequently the reason for social rejection. Therefore, the assessment of stigmatization level in patients suffering from dermatoses plays a crucial role in providing proper health service.

Objectives. The aim of this study was to create and validate Arabic language versions of stigmatization instruments – the 6-item Stigmatization Scale and the Feelings of Stigmatization Questionnaire.

Material and methods. Development of the Arabic language versions was done with international standards of forward-back translations. The validation was performed on 39 psoriatic individuals. The group included 11 females and 28 males. The subjects were asked to fill out both questionnaires: the 6-item Stigmatization Scale and the Feelings of Stigmatization Questionnaire (Arabic language versions) at the time of examination and 7 days after enrollment for reassessment to evaluate test-retest reliability. During the first visit the patients additionally filled out an already existing Arabic version of Dermatology Life Quality Index (DLQI), which was used as a reference questionnaire.

Results. The results concerning the integrity of instruments were very good, and the Cronbach's α coefficient for both scales was 0.89. The reproducibility level assessed with interclass correlation coefficient (ICC) stood at 0.91 for the 6-item Stigmatization Scale and 0.92 for the Feelings of Stigmatization Questionnaire. There was a strong correlation between total score of the 6-item Stigmatization Scale and DLQI. Significant negative moderate correlation was documented between the Feelings of Stigmatization Questionnaire and DLQI. Moreover, both stigmatization instruments correlated significantly with each other.

Conclusions. The developed Arabic language versions of the abovementioned stigmatization instruments can be successfully used in daily clinical practice as well as in clinical research.

Key words: quality of life, stigmatization, skin, 6-item Stigmatization Scale, Feelings of Stigmatization Questionnaire

Cite as
Dimitrov D, Matusiak Ł, Evers A. Arabic language skin-related stigmatization instruments: Translation and validation process. *Adv Clin Exp Med*. 2019;28(6):825–832. doi:10.17219/acem/102617

DOI
10.17219/acem/102617

Introduction

Medical dictionaries define stigmatization as an assignment of negative perceptions to an individual because of a perceived difference from the population at large. This may occur on the basis of physical appearance (including race or sex), of mental or physical illness, or of various other qualities.[1] The medical field recognizes a number of health problems, the sufferers of which are stigmatized, and certain skin diseases are among them. Along with the stigma faced by the individual, associative stigma can impact the family and friends of that person.[2–4]

Skin conditions are frequently the reason of social rejection and might result in a negative influence on the personal and social life of patients. Skin plays an important role in establishing interpersonal relationships, and thus cutaneous disorders, which have significant impact on physical appearance, influence other people's attitudes.[5] Visible skin changes may arouse fear, disgust, aversion, or even intolerance, and other people may be afraid of the possible contagious character of the disease. Having in mind the great impact of the stigmatization process on one's life, measuring its level is necessary to provide proper service to the patients. This underlines the importance of proper stigmatization assessment in patients suffering from various dermatoses. Numerous instruments for assessing the stigmatization experience exist in the form of questionnaires. Our previous search in the English literature found 14 instruments used by different researchers for different skin conditions and we classified them into 2 main groups: dermatology-specific and disease-specific stigmatization instruments.[6] Psoriasis appeared to be most commonly studied dermatologic condition where stigmatization has been assessed.[7] To the best of our knowledge, there is no single skin-related stigmatization instrument available in the Arabic language. Therefore, the aim the current study was to create and validate the Arabic language version of 2 commonly used questionnaires to assess stigmatization in all dermatology patients (6-item Stigmatization Scale[8]) and especially in psoriatic individuals (Feelings of Stigmatization Questionnaire[9]).

Methods

The study was conducted in the Department of Dermatology of Sheikh Khalifa Medical City (SKMC), General Hospital in Abu Dhabi, UAE, and supervised by experts from the Wroclaw Medical University, Poland. The approvals from The Institutional Review Board/Research Ethics Committee (IRB/REC) of SKMC(REC-29.01.2017 [RS-473]) and Ethical Committee of Wroclaw Medical University (KB-604/2016) were obtained prior to commencement of any study procedure.

Translation

The translation of the questionnaires was a multi-stage process based on a reverse translation and involved several independent translators. At the first stage the original questionnaires (English language ones) were given to 2 independent translators: consultant dermatologist and consultant psychiatrist. They translated them from English into Arabic (Version 1 and Version 2). The results were compared, slight differences were found and a bilingual expert helped with the editing (Version 3). After that, Version 3 was given to a 3rd translator (consultant dermatologist) who was not familiar with the original questionnaires. He performed a reverse translation from the already translated Arabic version into English. The back translation of a 6-item Stigmatization Scale was sent to Prof. Dr. Andrea Evers, who created the original questionnaire, for her comments. Prof. Dr. Mohammad Jafferany from Association for Psychoneurocutaneous Medicine of North America (APMNA) served as a consultant of the back translation of Feelings of Stigmatization Questionnaire. Some minor differences were found, discussed and corrected accordingly. The final versions (Version 4) of the Arabic language of both questionnaires were approved based on comments by dermatology experts and linguistic consultations. The aim of the translation was not only to render it in grammaticaly correct Arabic language, but to make the questions understandable for people outside the medical field. All translators mentioned above were of Arabic origin, fluent in both Arabic and English with long experience in the medical field (dermatologist or psychiatrist). Version 4, treated as a final one, was used for the validation process.

Validation

Validation was based on 39 Arabic psoriatic patients. The group included 11 females and 28 males. The mean age of the patients was assessed as 36.3 ±12.2 years. The current mean psoriasis intensity evaluated with Psoriasis Area and Severity Index (PASI) was 3.6 ±5.2 points (range 0–24.5 points).

Patients were asked to fill both questionnaires: 6-item Stigmatization Scale and Feelings of Stigmatization Questionnaire (Arabic language versions) at the time of examination and 7 days after enrollment for reassessment to evaluate test-retest reliability. During the first visit the patients additionally filled already existing Arabic version of Dermatology Life Quality Index (DLQI), which was used as a reference questionnaire. The DLQI was selected as it was the first questionnaire to assess quality of life in dermatologic patients and is currently the most commonly used instrument among dermatologic subjects. Moreover, DLQI is available in various validated language versions.

Statistical analyses were performed using STATISTICA v. 12 software (StatSoft Inc., Tulsa, USA). Internal

consistency was evaluated with Cronbach's α coefficent. Coefficient scores above 0.7 indicate high internal consistency. Correlations of individual components and the total score of the questionnaires were calculated with Spearman's rank correlation test. Spearman's correlation coefficient (ρ) was interpretered as follows: ρ = 0–0.1 – no correlation; ρ = 0.11–0.29 – weak correlation; ρ = 0.3–0.49 – moderate correlation; ρ = 0.5–0.69 – strong correlation, and ρ > 0.7 – very strong correlation.[10]

Differences between 1st and 2nd assessment were verified with Wilcoxon signed-rank test. Interclass correlation coefficient (ICC) was used to assess test-retest reliability. ICC <0.4 indicated poor reliability, ICC >0.4 or/and ICC <0.75 – fair to high reliability, and ICC ≥0.75 – excellent reliability.[11]

The correlation between both stigmatization questionnaires and DLQI was calculated also with Spearman's rank correlation test. The p-values for all statistical analyses were considered significant if $p < 0.05$.

Results

Internal consistency

The evaluation of internal consistency showed that the different items of both questionnaires are interrelated with one another. Cronbach's α coefficient for 6-item Stigmatization Scale was calculated as 0.89 and for Feelings of Stigmatization Questionnaire was also 0.89. The results described above indicated a strong internal consistency of Arabic language versions of both studied instruments.

Convergent validity

All single questions of the 6-item Stigmatization Scale significantly strongly correlated with the total score of the questionnaire (Table 1). Most questions included in Feelings of Stigmatization Questionnaire correlated with the total score as well (Table 2). Twenty out of 33 questions revealed a strong and very strong significant correlation with the total score. Of note, 7 questions (i.e., Q9, Q20, Q22, Q29, Q31, Q34, and Q40) exhibited no significant correlation with the total score. Based on the overall analysis, one may conclude that 6-item Stigmatization Scale demonstrated very good convergent validity; the convergent validity of Feelings of Stigmatization Questionnaire may also be considered as satisfactory.

Test-retest comparison

The reproducibility of both instruments was high. The ICC between scores obtained at the 1st and 2nd visit were 0.91 and 0.92 for 6-item Stigmatization Scale and Feelings of Stigmatization Questionnaire, respectively.

Table 1. Correlation of each item (Q) score with total score of 6-item Stigmatization Questionnaire

Correlations	N	ρ	p-value
Q1 and total score	39	0.79	<0.0001
Q2 and total score	39	0.80	<0.0001
Q3 and total score	39	0.71	<0.0001
Q4 and total score	39	0.79	<0.0001
Q5 and total score	39	0.66	<0.0001
Q6 and total score	39	0.55	<0.001

Table 2. Correlation of each item (Q) score with total score of Feelings of Stigmatization Questionnaire

Correlations	N	ρ	p-value
Q1 and total score	39	0.53	<0.001
Q2 and total score	39	0.78	<0.0001
Q3 and total score	39	0.59	<0.0001
Q4 and total score	39	0.73	<0.0001
Q5 and total score	39	0.70	<0.0001
Q6 and total score	39	0.57	<0.01
Q7 and total score	39	0.72	<0.0001
Q8 and total score	39	0.76	<0.0001
Q9 and total score	39	0.14	0.39
Q10 and total score	39	0.67	<0.0001
Q11 and total score	39	0.39	0.01
Q12 and total score	39	0.35	0.03
Q13 and total score	39	0.53	<0.001
Q14 and total score	39	0.46	0.003
Q15 and total score	39	0.72	<0.0001
Q16 and total score	39	–0.24	0.13
Q17 and total score	39	–0.31	0.05
Q18 and total score	39	0.54	<0.001
Q19 and total score	39	0.62	<0.0001
Q20 and total score	39	0.43	0.007
Q21 and total score	39	0.55	<0.001
Q22 and total score	39	0.71	<0.0001
Q23 and total score	39	–0.13	0.41
Q24 and total score	39	0.72	<0.0001
Q25 and total score	39	–0.11	0.48
Q26 and total score	39	0.63	<0.0001
Q27 and total score	39	0.08	0.63
Q28 and total score	39	0.63	<0.0001
Q29 and total score	39	0.47	0.002
Q30 and total score	39	0.73	<0.0001
Q31 and total score	39	0.49	0.002
Q32 and total score	39	0.74	<0.0001
Q33 and total score	39	–0.11	0.49

There were no significant differences between separate questions and the total scores in conducted assessments for both scales (Table 3, 4).

Table 3. Reproducibility of results obtained with 6-item Stigmatization Scale

Questions	1st assessment [points]	2nd assessment [points]	p-value
Q1	0.69 ±0.83	0.62 ±0.81	0.53
Q2	1.0 ±0.92	0.87 ±0.83	0.27
Q3	0.74 ±0.85	0.69 ±0.73	0.61
Q4	1.18 ±0.94	1.18 ±0.94	0.85
Q5	0.46 ±0.82	0.44 ±0.75	0.78
Q6	0.62 ±0.85	0.64 ±0.78	0.81
Total score	4.69 ±4.16	4.36 ±3.82	0.32

Table 4. Reproducibility of results obtained with Feelings of Stigmatization Questionnaire

Questions	1st assessment [points]	2nd assessment [points]	p-value
Q1	3.41 ±1.60	3.67 ±1.53	0.14
Q2	3.56 ±1.82	3.59 ±1.74	0.86
Q3	3.90 ±1.73	3.79 ±1.24	0.52
Q4	3.41 ±1.60	3.44 ±1.43	0.98
Q5	3.10 ±1.64	3.23 ±1.61	0.50
Q6	3.90 ±1.47	3.72 ±1.36	0.32
Q7	3.13 ±1.75	3.46 ±1.50	0.10
Q8	2.56 ±1.89	3.00 ±1.78	0.09
Q9	2.18 ±1.60	2.15 ±1.74	0.90
Q10	3.41 ±1.79	3.36 ±1.58	0.85
Q11	3.05 ±1.62	2.77 ±1.66	0.49
Q12	2.90 ±1.85	2.85 ±1.83	0.74
Q13	3.38 ±1.43	3.38 ±1.39	0.90
Q14	3.62 ±1.39	3.67 ±1.46	0.82
Q15	2.49 ±1.65	2.87 ±1.64	0.18
Q16	2.54 ±1.79	2.51 ±1.67	0.88
Q17	2.49 ±1.78	2.28 ±1.72	0.32
Q18	3.51 ±1.55	3.18 ±1. 57	0.24
Q19	4.03 ±1.27	3.79 ±1.13	0.09
Q20	2.26 ±1.67	2.10 ±1.39	0.38
Q21	2.18 ±1.65	2.00 ±1.43	0.50
Q22	3.31 ±1.58	3.10 ±1.59	0.23
Q23	2.97 ±1.66	2.62 ±1.79	0.25
Q24	3.33 ±1.56	3.36 ±1.48	0.86
Q25	1.90 ±1.60	2.33 ±1.30	0.05
Q26	3.05 ±1.49	3.10 ±1.50	0.80
Q27	0.49 ±1.10	0.64 ±1.11	0.33
Q28	3.21 ±1.54	3.10 ±1.50	0.54
Q29	3.08 ±1.36	2.95 ±1.41	0.94
Q30	3.62 ±1.44	3.54 ±1.45	0.84
Q31	2.82 ±1.97	3.28 ±1.72	0.10
Q32	3.85 ±1.41	3.90 ±1.12	0.78
Q33	0.95 ±1.38	1.13 ±1.47	0.57
Total score	97.59 ±24.53	98.05 ±26.88	0.83

Correlation with Dermatology Life Quality Index

There was a strong correlation between the total score of 6-item Stigmatization Scale and DLQI ($\rho = 0.54$, $p < 0.001$) (Fig. 1a). A significant negative moderate correlation was documented between the Feelings of Stigmatization Questionnaire and DLQI ($\rho = -0.49$, $p = 0.001$) (Fig. 1b). This illustrates that both newly created Arabic versions of stigmatization instruments showed highly satisfactory correlations with the quality of life assessment. Moreover, both stigmatization instruments correlated significantly with each other ($\rho = -0.42$, $p = 0.007$) (Fig. 2).

Access to instruments

All above results clearly suggest that the Arabic versions of the 6–item Stigmatization Scale and Feelings of Stigmatization Questionnaire fulfilled the criteria for high standard instruments and may be used in clinical practice. They are presented as Appendixes 1, 2 and are available in the electronic version on request directly from Dr. Dimitre Dimitrov (chibi90@yahoo.com).

Discussion

Arabs inhabit the 22 Arab states within the Arab League but can also be found in the global diaspora.[12] They have their own customs, language, art, literature, music, media, cuisine, society, etc.[13]

The enormous emotional burden of patient with skin diseases is well recognized. In fact, the visibility of skin lesions plays an important role in this burden and that was indicated in numerous publications including our previous research.[7] The attitude to individuals with skin diseases can vary widely in different countries and cultures and in certain areas; the fear of stigmatization due to skin disorders can be devastating.[2,4] As mentioned above, our previous research found that psoriasis is the most common skin disease, where the stigmatization experience was studied.[7] We performed an extensive search online in the available English-language literature and could not find any reports about stigmatization experience in dermatological patients among the Arabic population. Most of the research about stigmatization in the medical field in Arabic countries was related to mental health.[14,15] We previously clearly confirmed that the visibility of the skin lesions is a key factor for stigmatization experience and, as we have already emphasized, proper stigmatization assessment in dermatological patients would contribute to the entire, complete understanding of their suffering and would facilitate the holistic therapeutic approach.[6] Therefore, the creation of Arabic-language instruments to assess skin-related stigmatization level was crucial for daily clinical practice and for the future research in this field.

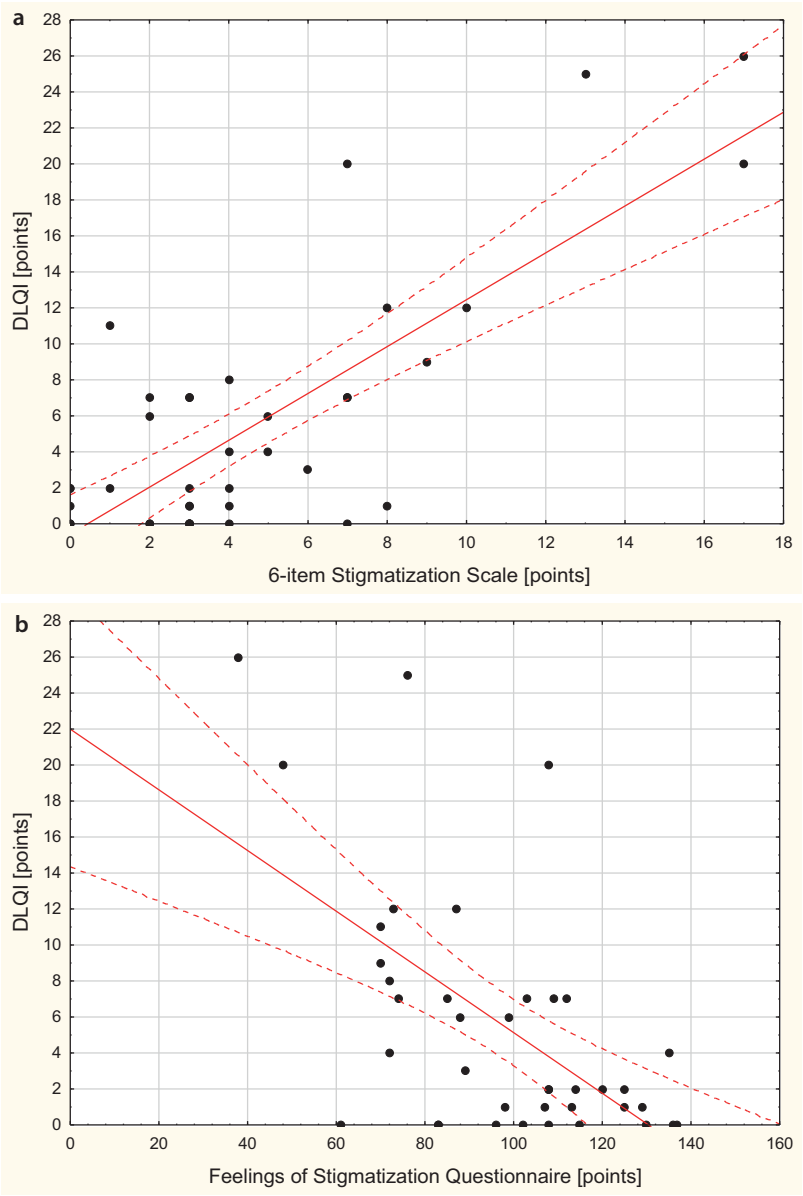

Fig. 1. Correlation between Arabic versions of stigmatization instruments (6-item Stigmatization Scale (a), Feelings of Stigmatization questionnaire (b)) and Dermatology Life Quality Index (DLQI)

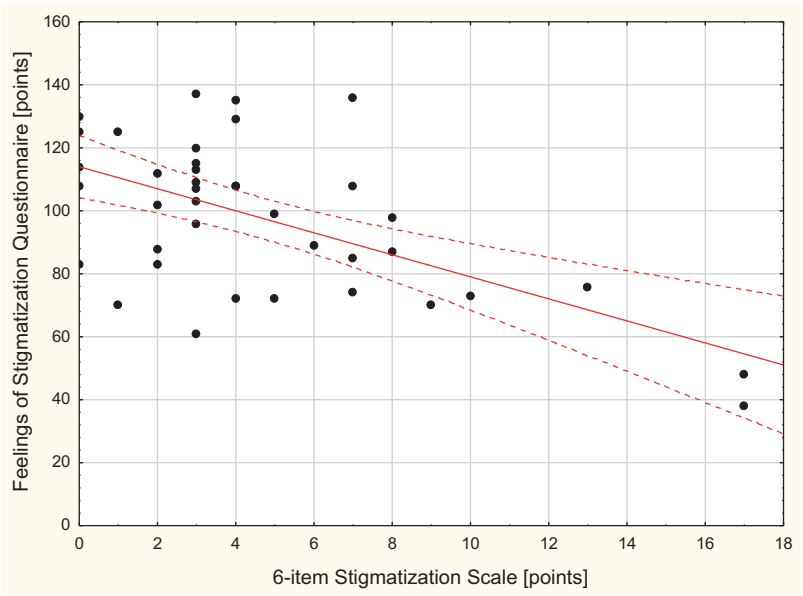

Fig. 2. Correlation between Arabic versions of 6-item Stigmatization Scale and Feelings of Stigmatization Questionnaire

Our current results showed better internal consistency of Arabic versions of both instruments in comparison with, for instance, the results of validated Polish language versions, where the Cronbach's α coefficient for the 6-item Stigmatization Scale was calculated as 0.84 and for the Feelings of Stigmatization Questionnaire as 0.86.[16] Both Arabic versions showed 0.89 Cronbach's α coefficient. The ICC between scores obtained at 1st and 2nd visit were also higher: The results obtained in the Polish language versions were 0.82 and 0.73 for the 6-item Stigmatization Scale and Feelings of Stigmatization Questionnaire, respectively. The Arabic version showed ICC of 0.91 for the 6-item Stigmatization Scale and of 0.92 for the Feelings of Stigmatization Questionnaire. These results were obtained after enrolling the majority of patients with mild disease. We are aware of the fact that this could be considered as a limitation of the study. Another example in regard to the above-mentioned parameters is the Polish-language version of the Family Dermatology Life Quality Index (FDLQI). The authors found that Cronbach's α coefficient was 0.84 and reproducibility level, established with ICC, was calculated at 0.69.[17] All the data presented above clearly suggests a high international standard of the Arabic-language versions of both the 6-item Stigmatization Scale and the Feeling of Stigmatization Questionnaire. We believe that the availability of those questionnaires in the Arabic language will contribute to the service provided to dermatology patients and will stimulate further research on the stigmatization in patients of Arabic origin suffering from various dermatoses.

References

1. Miller-Keane BF. *Encyclopedia and Dictionary of Medicine, Nursing, and Allied Health*. 7th ed. Philadelphia, PA: Saunders; 2003:1676.
2. Ibekwe PU, Ogunbiyi AO, Ogun OG, George AO. Social stigmatization of two sisters with lamellar ichthyosis in Ibadan, Nigeria. *Int J Dermatol*. 2012;51(1):67–68.
3. Masnari O, Landolt MA, Roessler J, et al. Self- and parent-perceived stigmatisation in children and adolescents with congenital or acquired facial differences. *J Plast Reconstr Aesthet Surg*. 2012; 65(12):1664–1670.
4. Kassi M, Kassi M, Afghan AK, Rehman R, Kasi PM. Marring leishmaniasis: The stigmatization and the impact of cutaneous leishmaniasis in Pakistan and Afghanistan. *PLoS Negl Trop Dis*. 2008;2(10):e259.
5. Lawrence JW, Rosenberg L, Rimmer RB, Thombs BD, Fauerbach JA. Perceived stigmatization and social comfort: Validating the constructs and their measurement among pediatric burn survivors. *Rehabil Psychol*. 2010;55(4):360–371.
6. Dimitrov D, Szepietowski JC. Instruments to assess stigmatization in dermatology. *Postepy Hig Med Dosw (Online)*. 2017;71:901–905.
7. Dimitrov D, Szepietowski JC. Stigmatization in dermatology with a special focus on psoriatic patients. *Postepy Hig Med Dosw (Online)*. 2017;71:1115–1122.
8. Lu Y, Duller P, van der Valk PGM, Evers AWM. Helplessness as predictor of perceived stigmatization in patients with psoriasis and atopic dermatitis. *Dermatol Psychosom*. 2003;4:146–150.
9. Ginsburg IH, Link BG. Feelings of stigmatization in patients with psoriasis. *J Am Acad Dermatol*. 1989;20(1):53–63.
10. Finlay AY, Khan GK. Dermatology Life Quality Index (DLQI): A simple practical measure for routine clinical use. *Clin Exp Dermatol*. 1994; 19(3):210–216.
11. Zaki R, Bulgiba A, Nordin N, Ismail NA. Systematic review of statistical methods used to test for reliability of medical instruments measuring continuous variables. *Iran J Basic Med Sci*. 2013;16(6):803–807.
12. Frishkopf M. *Music and Media in the Arab World*. Cairo, Egypt: The American University of Cairo Press; 2010.
13. El-Shamy HM. *Folk Traditions of Arab World: A Guide of Motif Classification*. Bloomington, IN: Indiana University Press; 1995.
14. Dardas LA, Simmons LA. The stigma of mental illness in Arab families: A concept analysis. *J Psychiatr Ment Health Nurs*. 2015;22(9):668–679.
15. Zolezzi M, Alamri M, Shaar S, Rainkie D. Stigma associated with mental illness and its treatment in the Arab culture: A systematic review. *Int J Soc Psych*. 2018;64(6):597–609. doi:10.1177/0020764018789200
16. Hrehorów E, Szepietowski J, Reich A, Evers AW, Ginsburg IH. Instruments for stigmatization evaluation in patients suffering from psoriasis: Polish language versions. *Dermatol Klin*. 2006;8:253–258.
17. Marciniak J, Reich A, Szepietowski J. The Family Dermatology Life Quality Index – formulation and validation of the Polish version. *Forum Dermatologicum*. 2016;2:24–28.

Appendix 1. Arabic Version of 6 items Stigmatization Scale

النسخة العربية لاستبيان العناصر الست لوصمة المرض

السؤال	دائما	غالبا جدا	احيانا	مطلقا
1- أشعر بعدم جاذبيتي لدى الأخرين بسبب مرضي الجلدي				
2- اعتقد ان كثير من الناس يطيلون النظر إلى مرضي الجلدي				
3- يشعر الاخرين بعدم الراحة عند لمسي بسبب مرضي الجلدي				
4- يعتقد الناس ان مرضي الجلدي هو مرض معدي				
5- يتجنبني الناس بسبب مرضي الجلدي				
6- احيانا يعلق بعض الاشخاص تعليقات مزعجة عن مرضي الجلدي				

Appendix 2. Arabic Version of Feelings of Stigmatization Questionnaire

النسخة العربية لاستبيان الشعور بوصمة المرض

		اوافق بشدة	اوافق	غير متأكد و لكن قد اوافق	غير متأكد و لكن لا اوافق	لا اوافق	لا اوافق بشدة
1	احيانا اتجنب اللقاءات الإجتماعية بسبب الصدفية						
2	طلبت من الاشخاص المقربين لي الاحتفاظ سرا بحقيقة اصابتي بالصدفية						
3	يعتقد الكثير من الناس ان الصدفية علامة لضعف الشخصية						
4	كثيرا ما اعتقد ان الناس يعتبرون ان مرضى الصدفية اشخاصا غير نظيفين						
5	اصابتي بمرض الصدفية تجعلني اشعر اني مختلف عن الاخرين						
6	بعض الأحيان أعتقد أن أفراد أسرتي يشعرون أنني أضعف منهم بسبب اصابتي بالصدفية (الّتي لم تصبهم)						
7	اذا شعرت بأن رب العمل قد يكون متحيزا ضد احد بسبب الصدفية , فسوف لا اتقدم بطلب لهذه الوظيفة						
8	عندما تشتد الاعراض الجلدية للصدفية لدي استحي ان اقوم باي علاقة حميمية						
9	اذا أصيب أحد أبنائي بالصدفية أعتقد أنه أو أنها قد يعيش \قد تعيش بنفس جودة الحياة كما لو لم يصب بها.						
10	اعمل ما في وسعي حتى لا يعلم افراد عائلتي الذين لا يشاركوني نفس السكن عن اصابتي بالصدفية						
11	لا يؤثر في اذا اعطاني احد افراد عائلتي المكنسة الكهربائية لازالة القشر المتساقط من جلدي بسبب الصدفية						
12	نادرا ما اشعر بضرورة اخفاء حقيقة اصابتي بالصدفية						
13	عندما يعلم الاخرين باصابتك بالصدفية يبدأون في البحث عن خلل في شخصيتك						
14	ان مرضى الصدفية قد يعاملون كمرضى الجذام						
15	عند زيادة حدة حالة الصدفية اشعر بعدم جذابيتي و اني غير مرغوب جسديا و جنسيا						
16	لم اشعر مطلقا بالحرج او الخجل بسبب اصابتي بالصدفية						
17	اذا اصيب احد اطفالي بالصدفية , فسوف لا اشعر بالذنب						
18	من المحتمل ان يقوم صاحب العمل بتمرير الوظيفة لاحد اخر اذا عرف بان الشخص لديه تاريخ مرضي للاصابة بالصدفية						
19	لا يرغب الناس في صداقتي عندما يعرفون باصابتي بالصدفية						
20	اعتقد ان كثيرا من الاشخاص المقربين لي لم يلاحظوا اني اعاني من الصدفية						
21	يعتقد كثير من المصابين بالصدفية انهم اصبحوا " نظيفين" عندما تتحسن الصدفية						

Appendix 2. Arabic Version of Feelings of Stigmatization Questionnaire – cont.

النسخة العربية لاستبيان الشعور بوصمة المرض

		اوافق بشدة	اوافق	غير متأكد و لكن قد اوافق	غير متأكد و لكن لا اوافق	لا اوافق	لا اوافق بشدة
22	شعرت بالايذاء مما قاله لي الناس بسبب اصابتي بالصدفية						
23	عند تعرفي بشخص ما, فأنني اخبره عن اصابتي بالصدفية						
24	يشعرني بعض الناس كما لو كانت الصدفية نتيجة لارتكابي خطأ ما						
25	يعتقد معظم الناس أن مريض الصدفية مستقر عاطفيا كأي شخص عادي						
26	في بعض الاحيان اشعر بعدم نظافتي كما لو كان هناك شيء اعمق من اصابتي بالصدفية						
27	عندما تتحسن الصدفية بعد العلاج المكثف , اشعر بالرضا عن نفسي						
28	يتجنبني كثير من الناس و يبتعدون عني خوفا من ان الاعراض الجلدية للصدفية قد تكون معدية						
29	يعتقد كثير من المصابين بالصدفية انهم غير نظيفين نتيجة إستخدام كثير من الدهانات و الادوية الموضعية						
30	احيانا اشعر اني منبوذ بسبب اصابتي بالصدفية						
31	اذا لاحظ احد الطفح الجلدي لدي و سألني عنه , لا ابلغه انه بسبب الصدفية						
32	بسبب اصابتي بالصدفية لن اتقدم لطلب وظيفة او اتدرب لوظيفة تستدعي التعامل مع الجمهور						
33	اذااصيب احد ابنائي بالصدفية , فأنني اعتقد انه يمكنه تطوير امكاناته كما لو لم يكن لديه صدفية						

Circulating and circular RNAs and the need for rationalization and synthesis of the research spiral

Pavel Dvorak[1,3,D–F], Sarah Leupen[2,D–F], Pavel Soucek[3,D–F]

[1] Department of Biology, Faculty of Medicine in Pilsen, Charles University, Czech Republic
[2] Department of Biological Sciences, University of Maryland, Baltimore, USA
[3] Biomedical Center, Faculty of Medicine in Pilsen, Charles University, Czech Republic

A – research concept and design; B – collection and/or assembly of data; C – data analysis and interpretation;
D – writing the article; E – critical revision of the article; F – final approval of the article

Advances in Clinical and Experimental Medicine, ISSN 1899–5276 (print), ISSN 2451–2680 (online) *Adv Clin Exp Med*. 2019;28(6):833–838

Address for correspondence
Pavel Dvorak
E-mail: Pavel.Dvorak@lfp.cuni.cz

Funding sources
This work was supported with the National Sustainability Program I (NPU I) provided by the Ministry of Education, Youth and Sports of the Czech Republic (project No. LO1503); and Charles University Research Center program UNCE/MED/006 "University Center of Clinical and Experimental Liver Surgery".

Conflict of interest
None declared

Received on November 11, 2017
Reviewed on February 28, 2018
Accepted on August 9, 2018

Published online on March 6, 2019

Abstract

In this essay, we aim to draw a short comparison between 2 important research topics – circular and circulating RNAs – and show how they are connected. The findings described here in the field of circular RNAs, which are still quite obscured by the rapidly expanding body of knowledge in biology, have added another dimension to our view of the process of gene expression, which is formed by a more complex network of molecule interactions than we previously thought. The term "circulating RNAs" refers to a broad spectrum of RNA fragments originating from different sources, such as physiologically dying cells, sites of inflammation or cancer cells, and fragments floating in human liquid tissues together with other elements. Fragments of nucleic acids circulating in blood are emerging as promising biomarkers in different medical conditions. Interestingly, circular RNAs have been found to be present in human blood and form a fraction of circulating RNAs. In addition to updating readers on these fast-developing areas of biology, we also stress the need for the study of complex networks of molecule interactions as whole structures (in unison with the thoughts of systems biology), as opposed to the trend toward searching for individual key player molecules. Fundamentally, we want to add to the rationalization and synthesis of new research findings in the scientific literature, because this direction is important not only for students, teachers and researchers, but also for the general population.

Key words: synthesis, circular RNA, circulating RNA, complex networks, systems biology

Cite as
Dvorak P, Leupen S, Soucek P. Circulating and circular RNAs and the need for rationalization and synthesis of the research spiral. *Adv Clin Exp Med*. 2019;28(6):833–838. doi:10.17219/acem/94148

DOI
10.17219/acem/94148

Introduction

The discovery of the unexpected amount and roles of circular RNA molecules in human cells is a recent example of how new research findings can be concealed in the stream of the rapidly expanding body of scientific knowledge in biology. Although articles focusing on the theme of circular RNAs have been spreading round the world for about 5 years, information about this phenomenon is still quite unknown among non-specialists, and could even be confused with the topic of circulating RNAs, another widely researched topic with a similar name. The findings in the field of circular RNAs described in this article have added another dimension to our view of the process of gene expression. Similarly, the recent advances in the field of circulating nucleic acids and their clinical applications are very surprising.

It will probably take some more time for these discoveries to be suitably incorporated into university curricula, so we hope that this article can "fill in the gap" at this time. Although part of our goal is to help readers understand the distinctions between these topics in biological research, as well as the importance of each topic, we also aim to demonstrate some connections between them. Additionally, we wish to stress the need for the study of these highly complex networks of molecule interactions as whole structures in opposition to the recently prevalent search for individual key player molecules. Broadly, we want to promote the rationalization and synthesis of new research findings in the scientific literature in general, which is important not only for students, teachers and researchers, but also for the general population. Notably, we are aware that the whole theme of circulating cells and molecules, derived from different sources of tissues and cells, in human peripheral blood is much broader than discussed here, and we leave untouched several broad topics such as circulating nucleosomes and circulating tumor cells.

Circular RNAs

The view that the dominant RNA isoforms produced from eukaryotic genes were unstable variants of messenger RNA (mRNA) has considerably changed after the discovery of the high number of circular RNAs (circRNAs) widely present in human cells.[1–3] Circular RNAs have broadened the spectrum of long non-coding RNAs (lncRNAs), which were arbitrarily defined as having more than 200 nucleotides. LncRNAs may be standalone transcription units, or they may be transcribed from enhancers, promoters or introns of other genes; from pseudogenes; or antisense to other genes with varying degrees of overlap. Some members of lncRNAs have been shown to affect regulation of gene expression at the transcriptional as well as at post-transcriptional level.[4,5] Generally, the 3' and 5' ends of circRNAs are covalently linked during the process named "backsplicing" or "head-to-tail splicing", an alternative splicing of precursor mRNAs (pre-mRNAs) in which a downstream splice donor is joined to an upstream splice acceptor (in the reverse orientation to linear splicing; demonstrated in Fig. 1).[6,7]

Well-known genes from several species such as the mouse sex determining region of Chr Y (*Sry*), rat sex hormone binding globulin (*Shbg*), monkey solute carrier family 8 member A1 (*SLC8A1*, also known as *Ncx1*) or human ETS proto-oncogene 1, transcription factor (*ETS1*) and cytochrome P450 family 2 subfamily C member 18 (*CYP2C18*) were associated with the first reported examples of spliced circRNAs. However, these "strange" molecules were soon

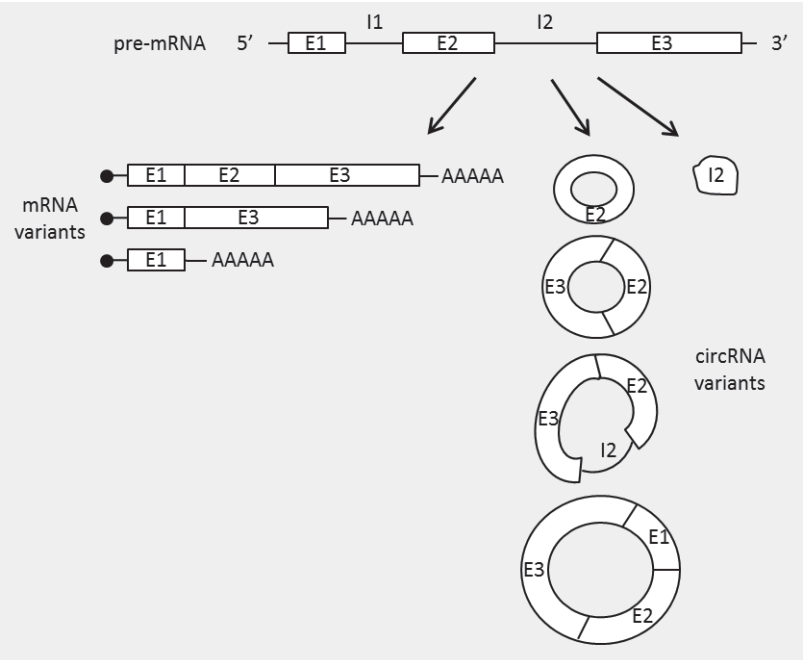

Fig. 1. Biogenesis of circular RNAs. Splicing variants of mRNA are generated in the process of canonical (linear) splicing, and circular RNA (circRNA) variants originate through the process called backsplicing or from intronic transcripts

E – exon; I – intron.

found to be unexpectedly more widespread, following a steep increase of information about these molecules coming from next-generation sequencing studies, which attempted to find genomic rearrangements in cancer samples.[6] The general key findings of several subsequent studies were that circRNAs were localized to the cytoplasm, expressed in high amounts in thousands of human genes, exhibited cell type-specific expression, demonstrated conservation between mouse and human, and were remarkably stable, most likely due to their circular structure.[1–3,8] A great diversity of circRNA isoforms can be generated from a single genomic locus and can consist of 1 or more exons and even contain unspliced intronic sequences.[6,7] Furthermore, circRNAs derived from antisense, 5' or 3' untranslated or intergenic genomic regions were reported.

What do we know about the functional significance of these molecules? To date, several studies have shown that circRNAs can be involved in RNA interference pathways, suggesting that the more stable circRNAs compete with messenger RNAs (mRNAs) for microRNA (miRNA) binding in the cytoplasm and consequently interfere in gene regulation. One of the most studied examples is human ciRS-7 (also known as CDR1as), which is transcribed in the antisense orientation from the cerebellum degeneration-related antigen 1 (*CDR1*) gene. Its overexpression acts as a miR-7 sponge, arresting this miRNA and therefore elevating the level of its targets. MiR-7 is known to regulate, among others, epidermal growth factor receptor (*EGFR*) expression. The EGFR is a cell surface protein (tyrosine kinase) that binds to epidermal growth factors and controls cell growth and proliferation. Mutations in the *EGFR* gene have been associated with the development of several types of cancers, especially lung cancer. In a similar manner, mouse *Sry* circRNA harbors 16 putative target sites for miR-138 and its ability to diminish the silencing activity of this miRNA has been observed in several studies.[3,9–11] In humans, miR-138 can interact with several transcripts related to cholangiocarcinoma, colorectal, ovarian and lung cancer, and also hematopoietic tumors such as lymphocytic leukemia.[9]

Furthermore, the power of circRNAs to act as sponges for other molecules has been extended to proteins (e.g., DNA-/RNA-binding proteins), thus establishing a more general phenomenon. With regard to this aspect, the circRNA that is derived from the *mbl* locus in *Drosophila* (circMbl) harbors binding sites for the MBL protein itself.[7,12] Interestingly, MBL is able to induce circMbl production. Generation of this circRNA consequently renders the pre-mRNA non-productive, limiting further production of MBL protein. CircMbl tethers and decoys MBL, which prevents further generation of circMbl and instead reactivates productive *mbl* mRNA production. Therefore, circMbl seems to be an intricate entity of an MBL autoregulatory circuit. Furthermore, circMbl also encompasses highly conserved miRNA binding sites and therefore circMbl could in fact have multi-faceted roles in the *Drosophila* brain. [7,12]

Different from most circRNAs, circRNAs with intron sequences are usually resident in the nucleus, which is similar to the observations of the nuclear restriction of linear RNAs containing retained introns. It has been reported that nuclear circRNAs can bind to the eukaryotic RNA polymerase II to regulate gene transcription.[13] For instance, ciankrd52, which originates from the 2nd intron region of the ankyrin repeat domain 52 (*ANKRD52*) gene, can interact with the elongating polymerase II complex and accumulates at transcription sites, which promotes transcription of its parental gene *ANKRD52*. Two other nuclear circRNAs, circ EIF3J and circ PAIP2, which contain one potential U1 snRNA-binding site in their retained introns, interact with the U1 snRNP and promote the transcription of their parental genes, *EIF3J* and *PAIP2*, suggesting that nuclear circRNAs, U1 snRNP, and polymerase II might interact with each other at promoter regions.[13]

CircRNAs that harbor binding sites for enzymes and their substrates are likely to function as scaffolds facilitating co-localization and reaction kinetics. This is perhaps best exemplified by circFOXO3, which is highly expressed in non-cancer cells and associated with cell proliferation, apoptosis and cell cycle. CircFOXO3 regulates the cell cycle by combining with CDK2 and CDKN1A (previously p21), which hinders the combination between CDK2 and cyclin E. Meanwhile, circFOXO3 decreases TP53 (p53) expression and increases FOXO3 (Foxo3) expression, which contributes to cell apoptosis and inhibition of proliferation.[14,15]

CircBase (circbase.org), one of the several freely available databases where public data sets of circRNAs can be accessed, downloaded and browsed within the genomic context, lists tens of thousands of circRNAs discovered in many different human cells.[16] As well as being an informational resource, the site provides custom scripts in Python that can locate circRNA sequences in any RNA sequence data, so researchers and students can use this site not just to learn more about circRNAs but also to discover new ones.

Recently, circRNAs were located not just inside cells, but also in the bloodstream. Using RNA sequencing of clinical samples, Memczak et al. found around 2,400 circRNA candidates expressed in human whole blood and, moreover, observed that the overall circRNA expression level in blood is unexpectedly similar to that of neuronal tissues, where circRNAs are highly abundant.[17] Thus, some circular RNAs are also circulating RNAs. This leads us directly to our 2nd theme – circulating RNAs and their potential for liquid biopsy.

Circulating RNAs and liquid biopsy

The presence of cell-free DNA (cfDNA) in human peripheral blood is a well-established phenomenon, first reported by Mandel and Metais in 1948.[18] Fragments of DNA

(double-stranded, mostly approx. 150 bp in length) are shed into the bloodstream from dying cells during cellular turnover or other forms of cell death; alternatively, they can be actively secreted from cells in association with membrane-derived vesicles or conjugated with lipid-protein complexes (both mechanisms are also valid in the case of tumor cells). Researchers working in this field proposed the possibility of non-invasive testing for blood-based cfDNA in different clinical circumstances and, especially in cases of prenatal (e.g., non-invasive prenatal testing – NIPT) and cancer (e.g., detection of *EGFR* mutations from the plasma of lung cancer patients) testing, this approach has achieved considerable success.[19–21]

In a manner similar to cfDNA, fragments of RNAs are released into the blood by several microvesicle-dependent or microvesicle-independent mechanisms. Although cell-free RNA (cfRNA) is generally even less stable in blood circulation than cfDNA, research has shown that different kinds of vesicles (exosomes, microvesicles or apoptotic bodies) can sequester fragments of mRNA, short and long non-coding RNAs as well as other biomolecules. A large variety of cell types can release extracellular vesicles and it was discovered that miRNA within circulating exosomes can be biologically active at distant sites.[22]

During carcinogenesis, this process of encapsulation can result in the formation of so-called tumor-educated platelets (TEPs).[21] Tumor-educated platelets have emerged as important players in different tumor-related processes including invasion and establishment of distant metastasis. Alternatively, cfRNA can be conjugated with RNA-binding proteins such as Argonaut 1 and 2.

Thus, a so-called "liquid biopsy" could provide a promising alternative or complement to tissue biopsy, which is usually performed on tissue taken from the primary tumor, if it is accessible. Furthermore, tissue biopsy is limited in that it reflects the molecular composition of only a small fraction of tumor cells at the time of sample-taking. Progress in technology, specifically the advent of massively parallel sequencing (next-generation sequencing – NGS), has provided unprecedented opportunities to investigate cell-free nucleic acids in a genome-wide fashion and at single-base resolution with the possibility to detect the wider intra-patient tumor heterogeneity.[23] Moreover, cell-free nucleic-acid-based profiling of cancer patients offers a number of critical advantages for essentially real-time monitoring of tumor response to therapy in cancer patients. Krug et al. investigated whether using a combined isolation of exosomal RNA and cfDNA could improve blood-based liquid biopsy for *EGFR* mutation detection in non-small-cell lung cancer (NSCLC) patients.[24] They concluded that combining exosomal RNA and ctDNA increased the sensitivity for *EGFR* mutation detection in plasma, with the largest improvement seen in the subgroup of M0/M1a disease patients known to have low levels of ctDNA, and posed challenges for mutation detection on ctDNA alone.

Challenges in detecting circular RNAs and circulating transcriptome

We can stress several issues among the challenges for circRNA detection in RNA sequencing data. Firstly, variations in preparation protocols alter the amount of circRNA in a library depending on the RNA purification method, size selection and oligo(dT) vs random priming. Secondly, there are several known sources of artefacts from common RNA-sequencing protocols, e.g., reverse transcriptase can join 2 distinct RNA molecules in a non-canonical order, particularly when the 2 RNAs contain a common sequence; 2 distinct cDNAs may be ligated together in non-canonical order during adaptor ligation; reverse transcriptase can displace cDNA from the template, generating a single cDNA that contains multiple copies of a circRNA. Thirdly, a convolution of homology and sequencing errors can lead to false alignments to a backsplice junction.[25]

It should be noted that the vast majority of research in the circulating transcriptome field are single-centered retrospective studies and that the cohorts typically used are insufficiently powered. As a consequence, there are many non-overlapping and even contradictory reports relating to the circulating transcriptome. These differences are primarily because of biological and technical variation between studies such as the starting material used in experiments (e.g., purification of cells, cell types, control populations used), technological platforms (e.g., microarray, quantitative real-time polymerase chain reaction (qRT-PCR), next-generation sequencing), and differing statistical methodologies used. Such confounding factors are especially problematic for studies of the circulating transcriptome which are characterized by low-quality and low-quantity RNA.[26,27]

At present, the low amount and high degradation rate of tumor-derived cfRNAs (with the exception of miRNAs and circRNAs) together with a high admixture of their physiological counterparts, derived from non-neoplastic cells, still pose major challenges for the development of sensitive and robust detection methods, which would be highly valuable in routine oncology practice. Importantly, due to their increased stability relative to other RNA fragments in the open blood environment and also their tissue specificity, circulating miRNAs have captured the attention of many researchers and are now being extensively studied as attractive new biomarkers across different medical fields.[26,27] Circular RNAs (circRNAs) have also been shown to be more stable than their linear counterparts,[28] and after the discovery that circular RNAs can also circulate in the human bloodstream they quickly joined miRNAs at the top of biomarker research.[11] For example, as human brain tissue is mostly inaccessible in patients with neurological disorders, peripheral blood presents a primary source of tissue for biomarker-based diagnostics.

Rationalization and synthesis of new research findings

It has become clear that the wide spectrum of non-coding RNAs can interact with each other and regulate the amount of coding RNAs and, in combination with transcription factors and other regulative elements, form a highly complex network of molecule interactions that results in time- and site-specific gene expression (shown in a simplified form in Fig. 2). Similarly, complex networks have also been revealed in other physiological processes such as metabolic and signaling pathways. Because the evolution of complex networks of interactions seems to be a natural tendency, many other examples on a cellular level are likely to be uncovered.

The increasing amount of information about the individual components of the complex networks of molecule interactions, coming from high-throughput "-omics" techniques, allows us to raise questions which would fit into the field covered by systems biology.[29–31] Examples of such questions are as follows: "Can we characterize the complex network of molecule interactions as a whole structure without just summarizing the characteristics of its individual components?"; "Does this higher level of network characteristics show some patterns which are shared by other complex networks consisting of different compounds?"; "Can some kind of classification of complex networks be defined based on such patterns?"; "Can normal and pathological states of complex networks be distinguished according to such patterns?"; "Can we foresee how a change in a component would change the behavior of the whole complex network?"; "How many individual components of a complex network need to be disrupted before an impact on the whole structure can be detected?"; "Would a treatment strategy taking into account system biology results be more successful than a strategy focusing only on a key component of the complex network?".

Researchers try to find answers to such questions through the development of different network diagrams and computational and mathematical models. It is a rapidly developing area of biology research, however, it could be challenging to find the reasonable level of these models which would be comprehensible for a broader biology-educated community or even broader population. Open source software platforms and databases such as STRING (https://string-db.org/) and Cytoscape (http://www.cytoscape.org/) may be employed for visualizing complex networks and integrating these with biological data of different kinds.

Conclusions and perspectives

The discoveries that circRNAs are abundantly expressed in human cells and are involved in gene expression regulation through regulatory elements such as miRNAs and RNA-binding proteins have significantly broadened our view of the whole process of gene expression. These molecules have emerged as attractive targets for primary as well as applied research and a lot of their characteristics were revealed.[11,32] However, although the initiation of eukaryotic translation relies on the cap structure in the 5' end of mRNA, protein-coding circRNAs, circZNF609

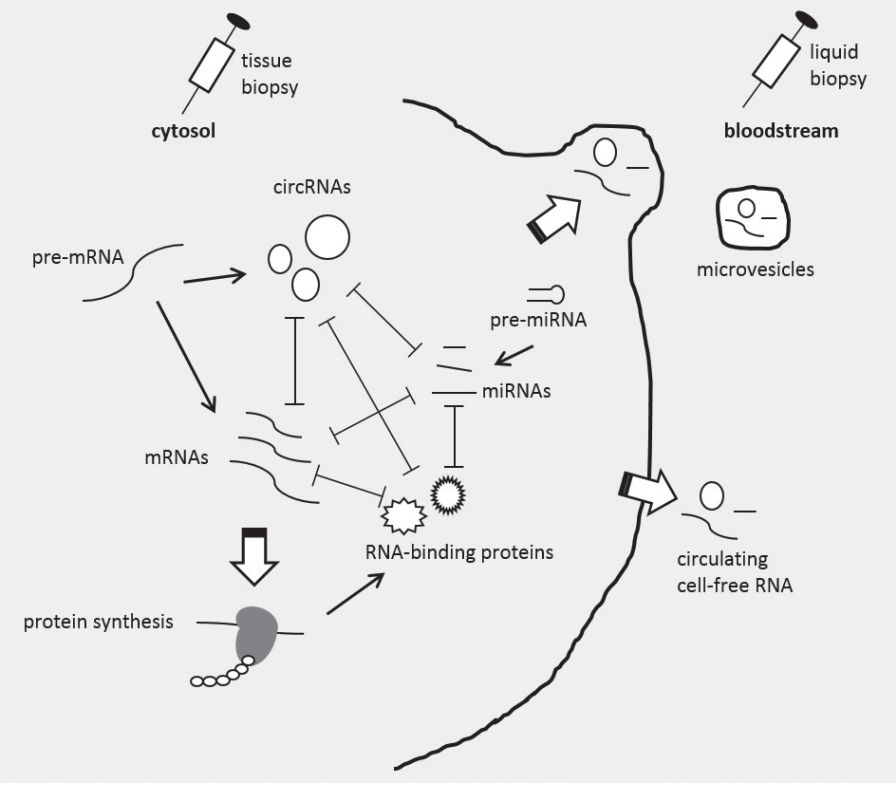

Fig. 2. Tissue vs liquid biopsy in the context of the complex network of molecule interactions involved in protein synthesis regulation

in human muscle cells and circMbl in fruit fly head have been described very recently and have opened a completely new field within this topic.[33,34]

RNA fragments originating from different sources are floating in human liquid tissues and are called circulating RNAs; if not encapsulated, they are degraded in a short period of time. Interestingly, circRNAs have been found to circulate in human blood and form a fraction of circulating RNAs. Because circRNAs are reasonably stable, many research teams have started to evaluate them as prospective biomarkers.[32,35] These recent findings have created an intersection between the 2 otherwise different topics – circular and circulating RNAs.

One of the main goals of current cancer research is to find the key players on the molecular level and through their modification open the possibility of reliable interventions in clinical situations. However, in the context of complex networks of molecule interactions, it is questionable if this approach alone will lead to useful solutions. Research should also focus on these complex networks of molecular interactions as whole structures, e.g., by looking for characteristic expression profiles across different types of molecules and examining how these profiles differ in physiological and pathophysiological states. We would like to encourage this type of research as well as education focused on the rationalization and synthesis of new research findings and their comparison in the context of other highly complex subsystems present in living organisms.

References

1. Jeck W, Sorrentino J, Wang K, et al. Circular RNAs are abundant, conserved, and associated with ALU repeats. *RNA*. 2012;19(2):141–157. doi:10.1261/rna.035667.112
2. Salzman J, Gawad C, Wang P, Lacayo N, Brown P. Circular RNAs are the predominant transcript isoform from hundreds of human genes in diverse cell types. *PLoS One*. 2012;7(2):e30733. doi:10.1371/journal.pone.0030733
3. Memczak S, Jens M, Elefsinioti A, et al. Circular RNAs are a large class of animal RNAs with regulatory potency. *Nature*. 2013;495(7441):333–338. doi:10.1038/nature11928
4. Fatica A, Bozzoni I. Long non-coding RNAs: New players in cell differentiation and development. *Nat Rev Genet*. 2013;15(1):7–21. doi:10.1038/nrg3606
5. Kung J, Colognori D, Lee J. Long noncoding RNAs: Past, present, and future. *Genetics*. 2013;193(3):651–669. doi:10.1534/genetics.112.146704
6. Barrett S, Salzman J. Circular RNAs: Analysis, expression and potential functions. *Development*. 2016;143(11):1838–1847. doi:10.1242/dev.128074
7. Ebbesen K, Kjems J, Hansen T. Circular RNAs: Identification, biogenesis and function. *Biochim Biophys Acta*. 2016;1859(1):163–168. doi:10.1016/j.bbagrm.2015.07.007
8. Salzman J, Chen R, Olsen M, Wang P, Brown P. Cell-type specific features of circular RNA expression. *PLoS Genet*. 2013;9(9):e1003777. doi:10.1371/journal.pgen.1003777
9. Kulcheski F, Christoff A, Margis R. Circular RNAs are miRNA sponges and can be used as a new class of biomarker. *J Biotechnol*. 2016;238:42–51. doi:10.1016/j.jbiotec.2016.09.011
10. Hansen T, Jensen T, Clausen B, et al. Natural RNA circles function as efficient microRNA sponges. *Nature*. 2013;495(7441):384–388. doi:10.1038/nature11993
11. Huang S, Yang B, Chen B, et al. The emerging role of circular RNAs in transcriptome regulation. *Genomics*. 2017;109(5–6):401–407. doi:10.1016/j.ygeno.2017.06.005
12. Ashwal-Fluss R, Meyer M, Pamudurti N, et al. circRNA biogenesis competes with pre-mRNA splicing. *Mol Cell*. 2014;56(1):55–66. doi:10.1016/j.molcel.2014.08.019
13. Huang G, Li S, Yang N, Zou Y, Zheng D, Xiao T. Recent progress in circular RNAs in human cancers. *Cancer Lett*. 2017;404:8–18. doi:10.1016/j.canlet.2017.07.002
14. Kristensen L, Hansen T, Venø M, Kjems J. Circular RNAs in cancer: Opportunities and challenges in the field. *Oncogene*. 2017;37(5):555–565. doi:10.1038/onc.2017.361
15. Zhang H, Jiang L, Sun D, Hou J, Ji Z. CircRNA: A novel type of biomarker for cancer. *Breast Cancer*. 2017;25(1):1–7. doi:10.1007/s12282-017-0793-9
16. Glažar P, Papavasileiou P, Rajewsky N. circBase: A database for circular RNAs. *RNA*. 2014;20(11):1666–1670. doi:10.1261/rna.043687.113
17. Memczak S, Papavasileiou P, Peters O, Rajewsky N. Identification and characterization of circular RNAs as a new class of putative biomarkers in human blood. *PLoS One*. 2015;10(10):e0141214. doi:10.1371/journal.pone.0141214
18. Mandel P, Metais P. Les acides nucléiques du plasma sanguin chez l'homme. *C R Seances Soc Biol Fil*. 1948;142(3–4):241–243.
19. Vermeesch J, Voet T, Devriendt K. Prenatal and pre-implantation genetic diagnosis. *Nat Rev Genet*. 2016;17(10):643–656. doi:10.1038/nrg.2016.97
20. Volik S, Alcaide M, Morin R, Collins C. Cell-free DNA (cfDNA): Clinical significance and utility in cancer shaped by emerging technologies. *Mol Cancer Res*. 2016;14(10):898–908. doi:10.1158/1541-7786.mcr-16-0044
21. Sorber L, Zwaenepoel K, Deschoolmeester V, et al. Circulating cell-free nucleic acids and platelets as a liquid biopsy in the provision of personalized therapy for lung cancer patients. *Lung Cancer*. 2017;107:100–107. doi:10.1016/j.lungcan.2016.04.026
22. Falcon-Perez J, Royo F. Circulating RNA: Looking at the liver through a frosted glass. *Biomarkers*. 2015;20(6–7):339–354. doi:10.3109/1354750x.2015.1101785
23. Jiang P, Lo Y. The long and short of circulating cell-free DNA and the ins and outs of molecular diagnostics. *Trends Genet*. 2016;32(6):360–371. doi:10.1016/j.tig.2016.03.009
24. Krug A, Enderle D, Karlovich C, et al. Improved EGFR mutation detection using combined exosomal RNA and circulating tumor DNA in NSCLC patient plasma. *Ann Oncol*. 2018;29(3):700–706. doi:10.1093/annonc/mdx765
25. Szabo L, Salzman J. Detecting circular RNAs: Bioinformatic and experimental challenges. *Nat Rev Genet*. 2016;17(11):679–692. doi:10.1038/nrg.2016.114
26. Fernandez-Mercado M, Manterola L, Larrea E, et al. The circulating transcriptome as a source of non-invasive cancer biomarkers: Concepts and controversies of non-coding and coding RNA in body fluids. *J Cell Mol Med*. 2015;19(10):2307–2323. doi:10.1111/jcmm.12625
27. Tiberio P, Callari M, Angeloni V, Daidone M, Appierto V. Challenges in using circulating miRNAs as cancer biomarkers. *Biomed Res Int*. 2015;2015:1–10. doi:10.1155/2015/731479
28. Enuka Y, Lauriola M, Feldman M, Sas-Chen A, Ulitsky I, Yarden Y. Circular RNAs are long-lived and display only minimal early alterations in response to a growth factor. *Nucleic Acids Res*. 2015;44(3):1370–1383. doi:10.1093/nar/gkv1367
29. Breitling R. What is systems biology? *Front Physiol*. 2010;1:9. doi:10.3389/fphys.2010.00009
30. Kitano H. Systems biology: A brief overview. *Science*. 2002;295(5560):1662–1664. doi:10.1126/science.1069492
31. Yurkovich J, Palsson B. Quantitative-omic data empowers bottom-up systems biology. *Curr Opin Biotechnol*. 2018;51:130–136. doi:10.1016/j.copbio.2018.01.009
32. Li M, Ding W, Sun T, et al. Biogenesis of circular RNAs and their roles in cardiovascular development and pathology. *FEBS J*. 2018;285(2):220–232. doi:10.1111/febs.14191
33. Legnini I, Di Timoteo G, Rossi F, et al. Circ-ZNF609 is a circular RNA that can be translated and functions in myogenesis. *Mol Cell*. 2017;66(1):22–37.e9. doi:10.1016/j.molcel.2017.02.017
34. Pamudurti N, Bartok O, Jens M, et al. Translation of circRNAs. *Mol Cell*. 2017;66(1):9–21.e7. doi:10.1016/j.molcel.2017.02.021
35. Zhang H, Jiang L, Sun D, Hou J, Ji Z. CircRNA: A novel type of biomarker for cancer. *Breast Cancer*. 2018;25(1):1–7. doi:10.1007/s12282-017-0793-9

Current facts constituting an understanding of the nature of adenomyosis

Veronika Aleksandrovych[1,A–F], Paweł Basta[2,B,C,E,F], Krzysztof Gil[1,A,D–F]

[1] Department of Pathophysiology, Jagiellonian University Medical College, Kraków, Poland
[2] Department of Gynecology and Oncology, Jagiellonian University Medical College, Kraków, Poland

A – research concept and design; B – collection and/or assembly of data; C – data analysis and interpretation;
D – writing the article; E – critical revision of the article; F – final approval of the article

Advances in Clinical and Experimental Medicine, ISSN 1899–5276 (print), ISSN 2451–2680 (online) *Adv Clin Exp Med*. 2019;28(6):839–846

Address for correspondence
Veronika Aleksandrovych
E-mail: v.aleksandrovych@doctoral.uj.edu.pl

Funding sources
None declared

Conflict of interest
None declared

Received on September 4, 2017
Reviewed on October 16, 2017
Accepted on October 25, 2017

Published online on August 7, 2018

Abstract

Adenomyosis seems to be the most widespread coexistent pathology included under the umbrella of common benign disorders of the human uterus. The incidence of adenomyosis is under discussion since different imaging criteria are used. In the majority of cases, prevalence is determined among women with uterine fibroids and endometriosis or severe gynecological symptoms. This common benign pathology is asymptomatic in 1/3 of cases. Up to 50% of women with infertility are affected by adenomyosis. It seems to be an important risk factor for spontaneous pre-term delivery and pre-term premature rupture of the membranes. Nowadays, the etiology of adenomyosis is still unclear and requires deeper investigation. This review summarizes the aspects of prevalence, co-existence, risk factors, classification, mechanisms of pathogenesis, genes and immunological features, main histological features, animal models, and clinical manifestation of adenomyosis. It might facilitate understanding of the independent nature of such a dual enigma as adenomyosis.

Key words: infertility, adenomyosis, myometrium, metaplasia, endometrial junctional zone

Cite as
Aleksandrovych V, Basta P, Gil K. Current facts constituting an understanding of the nature of adenomyosis. *Adv Clin Exp Med*. 2019;28(6):839–846. doi:10.17219/acem/79176

DOI
10.17219/acem/79176

Introduction

Adenomyosis is a benign condition of the uterus characterized by the presence of ectopic endometrial glands and stroma below the endometrial-myometrial junction (at a depth of at least 2.5 mm below the basal layer of the endometrium).[1,2] The focuses of endometrial glands and stroma in the myometrium are typically surrounded by its hyperplastic tissue.[3] Lymphatic and vascular channels carry out penetration of normal myometrium.[4,5] The level of endometrial invasion into a myometrium has been the issue of heated debate.[6] The majority of cases are observed in multiparous premenopausal women. Likelihood estimation of diagnosis demands obligatory histological analyses, which are commonly provided after hysterectomy. By far, the majority of adenomyosis cases are detected in autopsy and coexist with endometriosis and uterine fibroids, which explain a wide range of distribution (from 5% to 70%) according to literature data.[4,7]

Historical notes

A Bohemian physician and pathologist, Carl von Rokitansky, first described adenomyoma as a focal core of endometrial glands and stroma surrounded by smooth muscle cells in 1860. He referred to it as "cystosarcoma adenoids uterinum" with a neoplastic nature.[8–12] Surprisingly, Knapp, an expert in the history of medicine, in 1999 claimed that the 1st who described a similar condition (later named adeno- or endometriosis) was Daniel Schrön from Germany in 1690 in the work "Disputatio Inauguralis Medica de Ulceribus Uteri". Moreover, some of pathological descriptions made between the 17th and 18th centuries are similar to the modern classification of endometriosis or adenomyosis. Knapp challenged the primacy in describing the pathology in his Letter to Editor of Fertility and Sterility, which was published. Unfortunately, his request remained unanswered due to the author's sudden death within a few months after publication.[12]

The name adenomyoma was coined around the end of the 19th century. In 1896, both Cullen and Von Recklinghausen described the condition, followed by Pick and Rolly in 1897.[11] In addition, Cullen provided the 1st ever classification of adenomyomas, while its pathogenetic nature was depicted by Meyer in 1903. He emphasized that it is a variant of "epithelial invasion of inflammatory infiltrated tissue" and affects 2 kinds of epithelium: dystopic and orthotopic (embryonic and mature). The origin of dystopic nature was also supported by Orloff, who described it in 1895 as "glandular spaces under the serosa covering uterine myomata", and focused on developing from "embryonic cells".[10–12]

Until the 1920s, adenomyosis and endometriosis were considered to be a part of the same entity.[13] In 1925, Frankl depicted and named the invasion of mucosal tissue in the myometrium as "adenomyosis uteri", thereby singling out adenomyosis among adenomyomas.[10–12]

Finally, in 1972, Bird proposed the modern explanation of adenomyosis. He described that adenomyosis is a non-malignant endometrial invasion into the myometrium and leads to macroscopic changes of uterus size. Under a microscope, hypertrophy and hyperplasia of the myometrium are observed with penetration of the endometrium inside (glands and stroma). Nowadays, this gynecological disease is characterized by the invasion of endometrial components more than 2.5 mm below the endo-myometrial junction in the microscope's low-power field.[2,9,12]

Prevalence and co-existence of adenomyosis

The incidence of adenomyosis is unclear and debatable due to the use of a variety of criteria.[12] Numerous publications have shown that the prevalence of adenomyosis widely varies (from 5–8% to 40–70% of all uterine specimens), with a mean of 20–25%.[4,7,8] The same statistical data was present after histological analysis of postoperative material. Based on a literature review, prevalence of adenomyosis ranges from a high of 61.5% to a low of 8.8%, with a peak among women between 35 and 50 years of age.[7,14]

The diagnosis of adenomyosis can be time-consuming and challenging, based on lucky histological observation of the material. Interestingly, the rate of detection depends on the quantity and quality of samples observed and can vary from 31% to 62% in the same uterus.[9]

Current studies demonstrate that about 4/5 of cases with adenomyosis coexist with uterine fibroids and endometriosis.[5,15] According to statistical data, approx. every 5th removed uterus with leiomyomata has a focus of adenomyosis, while up to 55% of adenomyosis samples reveal developing uterine fibroids. Kitawaki proved these conclusions with his own analysis of data presented of the coexistence of both pathologies: adenomyosis with leiomyomata in 35–55% of cases, while leiomyomata with adenomyosis in 64%. At the same time, Kitawaki noted that adenomyosis is associated with endometriosis too: adenomyosis with endometriosis in 70% of cases, while "vice versa" only in 6–20% of all cases.[7]

It is important to note that diseases such as polyps of the endometrium, typical and atypical endometrial hyperplasia and endometrial carcinoma often coexist with adenomyosis, compared to their separate detection.[7] On the other hand, no study has demonstrated the natural transformation of adenomyosis to adenocarcinoma.[16]

Risk factors

It is important to consider that adenomyosis often coexists with other gynecological disorders and is revealed by histological examination. As it appears from these

features, suggested risk factors could not be clearly evaluated and most of them were received after retrospective studies.

Adenomyosis is common for women in the 5th decade of life but it has also been revealed in patients in the postmenopausal period after chemotherapy of breast cancer with tamoxifen.[9,17] Increasing age up to menopause has long been considered a risk factor.[18]

Multiparity is associated with adenomyosis. This might be explained by a mechanism of trophoblast invasion into the myometrium during pregnancy.[9,19] Romanek et al. proved by analysis that the relative risk of adenomyosis was almost 2 times lower among nulliparous women in comparison with multiparous.[19,20] Different studies have presented controversial data regarding abdominal delivery and further risk of pathology development; the role of cesarean sections also remains unclear.[19]

Undoubtedly, sex hormones have a great impact on adenomyosis.[21] It has been demonstrated that estrogen receptors are always present in adenomyosis tissue, however, their quantity was reduced compared to a corresponding normal myometrium.[7] Progesterone and androgen receptors were also found in adenomyotic tissue. Some authors have noted a balance between the amount of both steroids in healthy and adenomyotic tissue, while others have demonstrated a slightly higher density of progesterone receptors when compared to estrogen. It is important to note that ectopic as well as eutopic endometrium reflect all cyclic changes.[22]

Several studies have revealed that smoking can also be a risk factor of adenomyosis. Shrestha showed that the risk of adenomyosis is higher in smokers, especially in those who smoked for more than 10 years.[20] On the other hand, Taran et al. noted that smokers appear less likely to have adenomyosis and this might be explained by declining estrogen levels in the blood, which is common for smokers.[7,9]

Panganamamula et al. focused attention on previous surgery on endometrium, proved the first hypothesis that endometrial resection's involvement in pathogenesis of adenomysosis, made by Coltate and Smith in 1991.[23] The data rendering a strict direct link between adenomyosis and uterine trauma is still inconsistent. As often as not, in the literature, such traumatic conditions as spontaneous abortion, dilation, curettage, and endometrial ablation are discussed.[23] Levgur et al. noticed that the instrumental curettage of the uterus could be a risk factor only in the case of abortion, whereas in the nonpregnant uterus it did not impact subsequent development of adenomyosis.[4,23,24] If it is not expelled, a pregnancy could be a crucial point in the expansion of adenomyosis. One argument in favor of this is the fact that, despite about 20% of nulliparous women presenting with adenomyosis, a higher percentage of women after any term of pregnancy are affected by the disease.[7]

Some studies have shown that production of prolactin by the endometrium, myometrium and even in leiomyomas could stimulate a mitogenic activity in smooth muscle cells through its receptors. This may suggest a link between adenomyosis and depression with a common pathogenic factor.[9]

Classification

Adenomyosis has 2 types: diffuse and focal, which is also named "adenomyoma" in the literature. In comparison with the anterior and lateral sides of the uterus, the posterior wall is affected more often.[6,12]

Bird et al. in 1972 divided the depth of invasion into 3 grades. The 1st grade is characterized by the existence of adenomyosis within 1 low-power field below the basal endometrium. The 2nd grade is represented by deeper penetration, to the mid-myometrium, while the 3rd grade penetrates beyond the mid-myometrium. His team assessed the extent (density) of glandular involvement of the myometrium as follows: "slight" – a few (1–3) adenomyotic glands per low-power field; "moderate" – several (4–9) and "marked" – many (10 or more).[6]

Definition of endomyometrial junctional zone

The endomyometrial junctional zone (JZ) is a distinct, hormonally sensitive part of the endomyometrial interface that was first visualized more than 20 years ago by magnetic resonance imaging (MRI).[3,10] However, the realization that the inner portion of the human myometrium constitutes a separate entity within the uterine musculature is more than a century old. Brosens et al. referred to Werth and Grusdew, who called it the "archimyometrium" in 1898.[25]

The JZ is not the outer myometrium.[12] They have different origins: the JZ originates from the Müllerian ductus and the outer myometrium from the mesenchyme. As endometrium, the JZ expresses steroid hormone receptors, has a cycle-dependent type of growth and is involved in implantation and deep placentation. Also, normal uterine peristaltic activity originates from the JZ. This zone has been cited in literature as the archimyometrium, stratum basale, inner myometrium, junctional zone myometrium, endometrio–myometrial interface, transitional zone, and sub-endometrial myometrium. Ultrasound and MRI detect this zone in human uteri. Commonly, the thickness of the JZ is 5 mm or less, whereas it has a tendency to grow with age. Physiologically, JZ could be up to 0.8 cm among women without adenomyosis and 1.1 cm among those affected, respectively.[26,27]

The changing of JZ size and characteristics (>12 mm, hemorrhagic high-signal myometrial spots) is a poor prognostic for adenomyosis and has a strong correlation with prognosis.[25,28] It has been called the gold standard in revealing adenomyosis. Bergeron et al. hypothesized that a disturbance of JZ may be involved by triggering an "invasive" factor.[5]

Pathogenesis

The etiology of adenomyosis is still uncertain. Some theories equally explain the possible pathogenesis of the disorder while at the same time complementing each other. They focus on local invasion, cellular proliferation and angiogenesis.

This pathological condition originates from the deep basal layer of the endometrium as a result of its invagination in the myometrium, possibly due to loss of tissue cohesion. Tissue affected by adenomyosis is characterized by higher expression of estradiol receptors (ER) compared to typical endometrium, combined with expression of the apoptosis-suppressing gene product – B cell lymphoma/leukemia-2 (Bcl-2) protein. Enhancement of Bcl-2 expression is involved in the pathogenesis of uterine adenomyosis.[5,29–31]

From another point of view, the basalis invaginates into the myometrium along the lymphatic vessels. This was proved by pathological examination of postsurgical samples – adenomyotic focuses were found within intra-myometrial lymphatics. As the endometrial and myometrial tissues originate from the Müllerian ducts, adenomyosis can be the result of metaplasia from de novo ectopic intramyometrial endometrial tissue. This was defined as the 3rd theory of the pathogenesis of adenomyosis.[5]

It should be noted that myofibroblasts express some extracellular matrix proteins and definitely take part in the development of pathological focuses. The invasion of endometrial tissue inside the myometrium leads to its hypertrophy as a consequent response.[28] Mast cells in the endometrial tissue are located in close vicinity to smooth muscle cells and impact its differentiation and development by secreting nerve growth factor (NGF), preadipocyte factor-1 (Pref-1) and insulin-like growth factor-2. It is important to note that NGF is involved in the mechanism of pain and might reflect the severity of the process, which can be useful from the clinical point of view. Preadipocyte factor-1 could be a possible protective factor for further differentiation of cells. Koike et al. concluded that the mast cell might preserve the balance in an affected uterus.[28] Zhao et al. observed the expression levels of caveolin 1 (CAV1) in adenomyosis-affected tissue and showed that focuses of adenomyosis have a low level of CAV1 expression, which could be associated with adenomyosis-related dysmenorrhea.[32] The latest data provided by An et al. depicted that macrophages have an impact on epithelial–mesenchymal transition (EMT)-like processes, and thereby could be effector cells in that disease.[33]

Currently, the interest of researchers is focused on abnormal angiogenesis in JZ, which might be involved in the pathogenesis of adenomyosis. Moreover, abnormal vascularization is common for half of the patients: vascular distribution is generally irregular and vessels are thick, dilated, and/or reticular.[13] Vascular endothelial growth factor (VEGF), fibroblast growth factor (FGF)-1, FGF-2, thrombospondin 1 (TSP-1), and platelet-derived growth factor (PDGF) are potent angiogenic factors.[28]

In general, adenomyosis is characterized by overexpression of VEGF and hypoxia-inducible factor 1-alpha (HIF1-alpha), increasing the number of small vessels. Kang et al. observed 2 alleles of VEGF genes (22578A and 21154A) and concluded that they might be protective factors of adenomyosis.[13,34] Tokyol et al. emphasized that the quantity and intensity of cyclo-oxygenase (COX-2) expression in the endometrium was growing during both phases of the cycle in patients with adenomyosis in comparison to healthy controls.[35] Another characteristic feature of the pathology is the prevalence of defective myometrial spiral artery remodeling associated with alteration.[36]

In adenomyosis-induced animal models, the insulin growth factor-II (IGF-II) mRNA was found to be markedly downregulated compared to normal endometrium, as observed by a global gene transcription profiling analysis. Levy et al. proved this with the same tendency of IGF-II expression.[21] Despite that, its expression in uterine fibroid has the opposite character and this likely indicates different molecular and pathogenic backgrounds of uterine fibroid and adenomyosis. However, the expression of IGF-II can stimulate abnormal myometrial growth in patients with adenomyosis, explaining the frequent coexistence of both pathologies.

Histological features

Adenomyosis is identified in 20–30% of all uteri removed at surgery, where it causes globular and cystic enlargement of the myometrium, with some cysts filled with extravasated, often hemolyzed red blood cells and siderophages.[5] However, in specimens larger than 280 g it is much less common.[4] Microscopically, populations of spindle cells include smooth muscle cells and components of adenomyotic lesions, and make contact with the adenomyotic stroma.[28] On gross examination, the myometrium contains small, soft, red areas, some of which are cystic. Microscopic examination of these lesions reveals glands lined by mildly proliferative to inactive endometrium and surrounded by endometrial stroma. Secretory changes are rare, except during pregnancy and in patients treated with progestins. Myometrial changing (hyperplasia and hypertrophy) could lead to enlarging of the uterus.[19] Over time, the uterus may also be enlarged from cyclic bleeding into adenomyotic foci. Varying degrees of glandular hyperplasia may be seen, and occasionally hyperplastic surface endometrium extends into the foci of adenomyosis.[37]

Pathological foci are usually seen at a depth of at least 2 mm in the myometrium on more than 1 microscopic field at ×10 magnification of the JZ. This is useful and important for the uterus during pregnancy and postmenopause. Glands and stroma in adenomyosis are usually in the proliferative phase, whereas they may contain secretory to menstrual transformations. The stromal fibroblasts are

histologically different from myocytes.[5] During differential histological analysis, it is important to pay attention to the features of adenomyoma (different from adenomyosis): usually circumscribed, nodular aggregate of smooth muscle, endometrial glands and (usually) endometrial stroma.[5]

Genes and immunity of adenomyosis

Genetic factors can explain the nature of a variety of diseases, and adenomyosis is no exception. Wang et al. has not revealed any chromosomal aberrations during examination of 25 cases of adenomyosis by comparative genomic hybridization.[7] Mutations in k-ras and p53 are common in adenomyosis.[5] Kitawaki has mentioned that Goumenou et al. observed 31 cases of adenomyosis and revealed the incidence of loss of heterozygosity on 2p22.3-p16.1, 3p24.2-p22 and 9p21 chromosomal regions as 19.4%, 9.7% and 6.5%, respectively.[7] Human leukocyte antigen-DR (HLA-DR) expression is significantly higher in stromal cells compared to glandular cells in adenomyosis tissue. This might be involved in the immune reactions which occur in adenomyosis.[38]

Goumenou et al. observed the expression of p16, retinoblastoma (pRb) and cyclin D1 oncoproteins in patients with adenomyosis. Loss of expression of either pRb or p16, or the overexpression of cyclin D1, could lead to tissue growth. His team showed that for endometrial tissue in patients with adenomyosis during the 1st phase of the cycle, high expression of p16 was and low of pRb is common, whereas for endometrioma this balance was reversed. He concluded that the prevalence of p16 expression was common for adenomyosis in comparison with endometriomas. This clarified the differences in pathogenic mechanisms during both widespread gynecological pathologies.[39]

Fibroblast growth factor 2 (FBG2) is located on chromosome 4q26–27. It can upregulate the expression of VEGF and synergistically act with VEGF in stimulating new vessel formation. Kang et al. demonstrated that the FGF2 754C/G polymorphism is correlated with increased risk of adenomyosis among Chinese women.[28,34,40]

For identification of endometrial stromal cells among the myometrium in adenomyotic foci, immunohistochemical staining for CD10 is used, while it cannot distinguish such pathological conditions as myometrial invasion and carcinoma of endometrium from those involving adenomyosis (in situ). The cells close to the neoplasm also express this marker.[5]

Vimentin expression is lower in adenomyosis in comparison with eutopic endometrium, while expression of α-smooth muscle actin and desmin is consistent.[28]

Interleukin-10 (IL-10) is an important immunomodulatory cytokine produced by many cell populations. It is one of the major anti-inflammatory cytokines and plays important role in several chronic inflammatory diseases and cancers. Wang et al. demonstrated that patients with adenomyosis have elevated expression of IL-10 in eutopic and ectopic endometrium (in the secretory phase), which could play a significant role in the pathogenesis of this disease by altering the immune system.[41] Later, Qin et al. observed the expression of interleukin-10 receptor 1 (IL-10R1) and interleukin-10 receptor 2 (IL-10R2) in adenomyosis. They showed that expression of IL-10R1 and IL-10R2 was higher in adenomyotic samples in comparison with eutopic endometrium of women with adenomyosis or in normal endometrium. They suggested that IL-10 receptors have a possible connection to the immunotolerance and/or anti-inflammatory process during adenomyosis.[42]

Leukemia inhibitory factor (LIF) is a pleiotropic cytokine of the interleukin-6 family, produced by the endometrium during the implantation window. Xiao et al. found significantly lower LIF immunolabeling intensity in women with adenomyosis in comparison to fertile women. The dysregulation of both LIF mRNA and protein in the endometrium during the implantation window suggests that adenomyosis may be associated with impaired implantation.[43,44] Garavaglia et al. noted an overxpression of the human leukocyte antigens (HLA) of class II and an increase of complement components C3 or C4 in adenomyosis.[13,31]

Model systems

Nowadays, different animal models are widely used for the observation and re-creation of adenomyosis, while for endometriosis only humans and non-human primates are used.[45] Usually, as the object of experimental models for adenomyosis, non-human primates, horses, dogs, cats, rabbits, and laboratory rodents are used.[28] This pathology occurs naturally in non-human primates, notably Macaca mulata. Several mouse strains also develop adenomyosis spontaneously and it can be found in a small percentage of adult animals.[17,46] Moreover, spontaneous development of adenomyosis with a prevalence of ~80% by 12 months of age was revealed in CD-1 mice.[42] Adenomyosis has also been induced in mice by hormonal manipulation such as by the implantation of a single anterior pituitary gland into the uterine lumen.[17] Other experiments were focused on the administration of tamoxifen and further development of adenomyosis in mice. Far fewer studies on adenomyosis have been performed in rats than in mice. Rabbit is a convenient animal model because pathology can spontaneously manifest and its prevalence can be enhanced by estrogen administration during a period of 1–2 years.[45]

Symptoms

Adenomyosis does not present pathognomonic clinical symptoms.[6,13] About 1/3 of women with adenomyosis do not have any symptoms.[4,5,12] The most frequent symptoms

are common with other gynecological disorders: menorrhagia, dysmenorrhea, metrorrhagia, dyspareunia, and chronic, erratic or constant pelvic pain. Symptoms of heavy/abnormal bleeding are thought to be positively associated with the depth of penetration of adenomyosis into the myometrium.[25,47–49] Dysmenorrhea is correlated with the prevalence of adenomyotic glands.[6]

Diagnosis

In general, symptomatology does not allow detection of adenomyosis in time. The diagnosis can include vaginal examination, transvaginal sonography (TVS) and MRI.[18] Unfortunately, diagnostic hysteroscopy does not make it possible to discover pathognomonic signs in such cases.[12] On pelvic examination, the uterus may be enlarged, soft and mildly tender, especially if a patient is examined premenstrually. Ultrasonography is helpful to observe the size and shape of the uterus (a globular or asymmetrical uterus, myometrial cysts), localization of heterogeneous myometrium and of focal abnormal echotexture. Three-dimensional reconstruction of the uterine anatomy in the coronal plane provides new and unrivaled views of the JZ.[3] Sometimes, the adenomyosis may be confined to a part of the myometrium in the form of a well-circumscribed lump, which is called adenomyoma. This is in contrast to the uterine myoma, which does not present a well-defined capsule.[15]

Although pelvic ultrasound is a widely accepted imaging modality, the reported sensitivity for the trans-abdominal approach is only 32–63% with a corresponding specificity of 95–97%.[50] Improvement may be achieved with a transvaginal approach. Hysterosalpingography may be of help, while diverticula extending into the myometrium are present. Magnetic resonance imaging allows observation of the inner myometrium and detection of its thickness

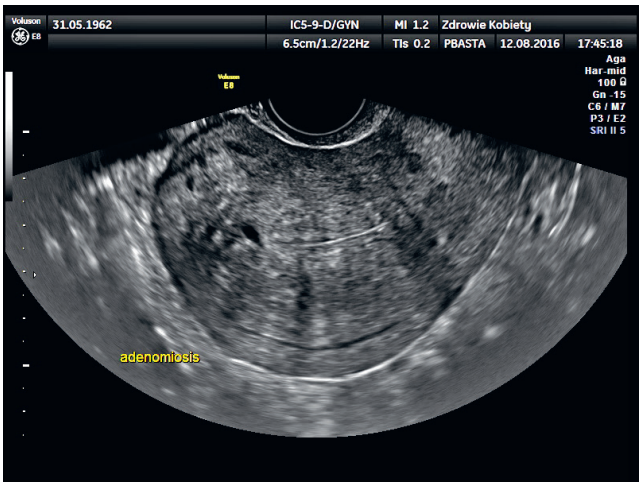

Fig. 1. Transvaginal ultrasound B-mode scan. Sagittal view. Typical changes within the uterus for adenomyosis: enlarged vascular spaces within the inner layer of myometrium and small myometrial cysts (subendometrial cysts – specific sign)

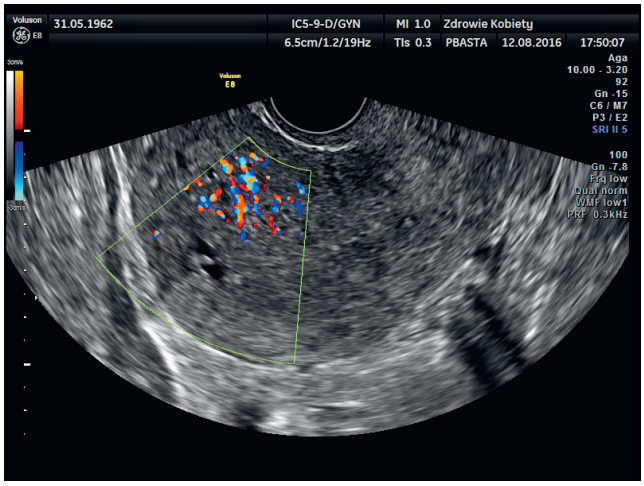

Fig. 2. Transvaginal ultrasound color Doppler scan. Sagittal view. Increased vascularity within myometrium is demonstrated, which is one of the ultrasound adenomyosis features

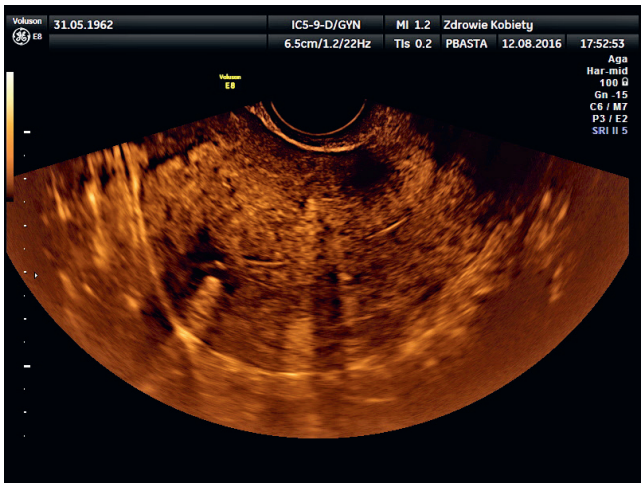

Fig. 3. Transvaginal ultrasound B-mode scan (amber filter). Sagittal view. Typical for adenomyosis changes within the uterus: sub-endometrial echogenic linear striations and acoustic shadowing as a result of ultrasound beam diffraction by irregular structure of myometrium – endometrial tissue causes a hyperplastic reaction ("Venetian blind" appearance)

and nature of changes, which is considered the hallmark of adenomyosis.[12]

Undoubtedly, the histological examination of a few postsurgical uterine transmural sections (from body and fundus) provide the final diagnosis.[5] Only histological examination can reveal the existence of ectopic glands in the endometrium (the "adeno" component), different from those received by different imaging techniques, which in the majority observe the organization of smooth muscle (the "myosis" component).[10]

Treatment

The primary indication for treatment is the presence of symptoms that negatively affect woman's daily life. Conservative treatment of pain with nonsteroidal

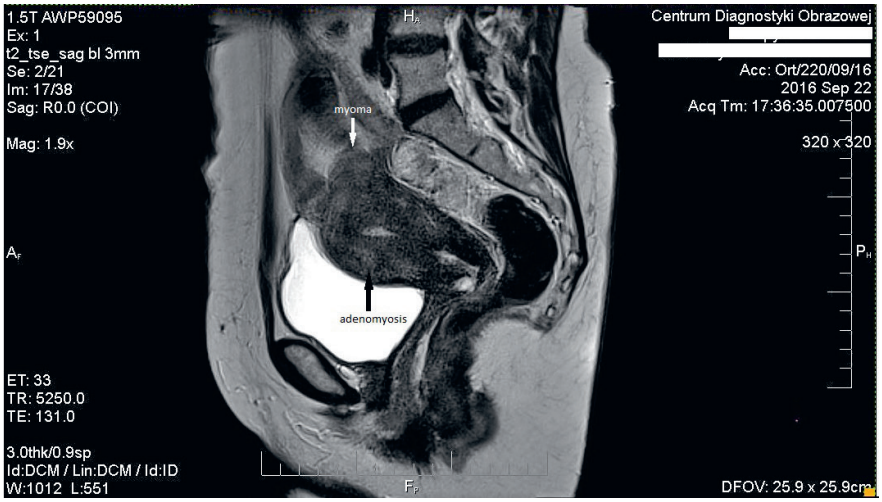

Fig. 4. Contrast-enhanced pelvic magnetic resonance imaging (MRI) of the same patient. T2-weighted image in sagittal section. Magnetic resonance imaging view corresponds with diffuse adenomyosis – high T2 signal regions on the anterior wall of the uterus, representing cystic changes

anti-inflammatory drugs (NSAIDs) and hormonal control of excessive cyclic bleeding maintain the first line of management. Oral progesterone, contraceptive pills, hormonal patches or rings, or levonorgestrel intrauterine device (IUD) can effectively control symptoms. When conservative management is not efficient or contraindicated, surgical manipulations (endometrial ablation/resection, myometrial excision/reduction, myometrial electrocoagulation, uterine artery ligation) are used for the treatment of symptoms. However, these methods are not very effective.[9] For superficial adenomyosis, using endoscopic endometrial ablation is preferred.[5,51] The coexistence of uterine fibroids and adenomyosis in 1 patient could complicate the diagnosis as the have a similarity in symptoms. Thus, in both pathologies uterine artery embolization (UAE) is performed.[9] Less than a half of patients after such surgical treatment have regression in 2–3 years.[19] Unfortunately, variants with leiomyomata are still complicated to identify among patients with adenomyosis. The former detailed diagnosis of both pathologies might be helpful before UAE, by reason of poor post-surgical prognosis among women with adenomyosis.[14] If a woman is not a candidate for any medical or surgical conservative management or if that treatment cannot sufficiently control the symptoms, hysterectomy is the final line of treatment.

Outcome

The junctional zone is quite important for the process of human placentation and is characterized by unique vascular plasticity in terms of physiological remodeling of the myometrial spiral arteries in pregnancy. Increasing thickness of JZ, changes in neo-angiogenesis and alterations in this zone, which are common for adenomyosis and endometriosis, may be associated with a shallow type of defective deep placentation.[10–12] As it appears from this statement, both pathologies may form the pathogenic background for negative obstetric outcome (preterm birth, fetal growth retardation and postpartum hemorrhage).[36]

Several studies have proved that women with adenomyosis, revealed before pregnancy, had significantly increased risk of preterm delivery, preterm premature rupture of membranes, fetal malpresentation and cesarean delivery. Hypothetically, this could be connected with the enlargement of adenomyotic focuses during pregnancy and further its association with inflammatory consequences.[52–54] Adenomyosis is connected with impaired implantation, destroying the uterine cavity's receptivity, accompanied by lower expression of the adhesion molecules necessary for embryo implantation (integrin β-3 and osteopontin). These factors make it possible to evaluate patients with adenomyosis as a target group for in vitro fertilization (IVF) treatment.[39,55]

Neoplastic transformation of adenomyosis is rare: only a few case reports of adenocarcinomas have been published. Koike et al. analyzed all the available data and presented in their review, to date, 44 cases that have been documented.[28]

References

1. Kido A, Fujimoto K, Matsubara N, Kataoka M, Konishi I, Togashi K. A layer of decreased apparent diffusion coefficient at the endometrial-myometrial junction in uterine adenomyosis. *Magn Reson Med Sci.* 2015;15(2):220–226.
2. Zhou C, Zhang T, Liu F, et al. The differential expression of mRNAs and long noncoding RNAs between ectopic and eutopic endometria provides new insights into adenomyosis. *Mol Biosyst.* 2016;12(2):362–370.
3. Exacoustos C, Brienza L, Di Giovanni A, et al. Adenomyosis: Three-dimensional sonographic findings of the junctional zone and correlation with histology. *Ultrasound Obstet Gynecol.* 2011;37(4):471–479.
4. Levgur M, Abadi MA, Tucker A. Adenomyosis: Symptoms, histology, and pregnancy terminations. *Obstet Gynecol.* 2000;95(5):688–691.
5. Bergeron C, Amant F, Ferenczy A. Pathology and physiopathology of adenomyosis. *Best Pract Res Clin Obstet Gynaecol.* 2006;20(4):511–521.
6. Peric H, Fraser IS. The symptomatology of adenomyosis. *Best Pract Res Clin Obstet Gynaecol.* 2006;20(4):547–555.
7. Kitawaki J. Adenomyosis: The pathophysiology of an oestrogen-dependent disease. *Best Pract Res Clin Obstet Gynaecol.* 2006;20(4):493–502.
8. Graziano A, Lo Monte G, Piva I. Diagnostic findings in adenomyosis: A pictorial review on the major concerns. *Eur Rev Med Pharmacol Sci.* 2015;19(7):1146–1154.

9. Taran FA, Stewart EA, Brucker S. Adenomyosis: Epidemiology, risk factors, clinical phenotype and surgical and interventional alternatives to hysterectomy. *Geburtshilfe Frauenheilkd*. 2013;73(9):924–931.
10. Benagiano G, Brosens I. History of adenomyosis. *Best Pract Res Clin Obstet Gynaecol.* 2006;20(4):449–463.
11. Benagiano G, Brosens I, Lippi D. The history of endometriosis. *Gynecol Obstet Invest.* 2014;78(1):1–9.
12. Benagiano G, Brosens I, et al. Glob. libr. women's med., (ISSN: 1756-2228) 2010. doi: 10.3843/GLOWM.10460
13. Di Donato N, Montanari G, Benfenati A, et al. Prevalence of adenomyosis in women undergoing surgery for endometriosis. *Eur J Obstet Gynecol Reprod Biol.* 2014;181:289–293.
14. Woźniakowska E, Milart P, Paszkowski T. Embolizacja tętnic macicznych – zagadnienia kliniczne. *Ginekol Pol.* 2013;84:1051–1054.
15. Aleksandrovych V, Bereza T, Sajewicz M, Walocha JA, Gil K. Uterine fibroid: Common features of widespread tumor (Review article). *Folia Med Cracov.* 2015;55(1):61–75.
16. Verit FF, Yucel O. Endometriosis, leiomyoma and adenomyosis: The risk of gynecologic malignancy. *Asian Pac J Cancer Prev.* 2013;14(10): 5589–5597.
17. Parrott E, Butterworth M, Green A, White IN, Greaves P. Adenomyosis: A result of disordered stromal differentiation. *Am J Pathol*. 2001;159(2): 623–630.
18. Naftalin J, Hoo W, Pateman K, Mavrelos D, Holland T, Jurkovic D. How common is adenomyosis? A prospective study of prevalence using transvaginal ultrasound in a gynaecology clinic. *Hum Reprod*. 2012;27 (12):3432–3439.
19. Romanek K, Bartuzi A, Bogusiewicz M, Rechberger T. Risk factors for adenomyosis in patients with symptomatic uterine leiomyomas. *Ginekol Pol.* 2010;8:678–680.
20. Shrestha A. Risk factors for adenomyosis. *J Nepal Health Res Counc.* 2012;10(22):229–233.
21. Levy M, Mittal K, Chiriboga L, Zhang X, Yee H, Wei JJ. Differential expression of selected gene products in uterine leiomyomata and adenomyosis. *Fertil Steril.* 2007;88(1):220–223.
22. Shen M, Liu X, Zhang H. Transforming growth factor β1 signaling coincides with epithelial–mesenchymal transition and fibroblast-to–myofibroblast transdifferentiation in the development of adenomyosis in mice. *Hum Reprod*. 2016;31(2):355–369.
23. Panganamamula UR, Harmanli OH, Isik-Akbay EF, Grotegut CA, Dandolu V, Gaughan JP. Is prior uterine surgery a risk factor for adenomyosis? *Obstet Gynecol*. 2004;104(5 Pt 1):1034–1038.
24. Curtis KM, Hillis SD, Marchbanks PA, Peterson HB. Disruption of the endometrial–myometrial border during pregnancy as a risk factor for adenomyosis. *Am J Obstet Gynecol.* 2002;187(3):543–544.
25. Brosens I, Derwig I, Brosens J, Fusi L, Benagiano G, Pijnenborg R. The enigmatic uterine junctional zone: The missing link between reproductive disorders and major obstetrical disorders? *Hum Reprod.* 2010;25(3):569–574.
26. Hauth EA, Jaeger HJ, Libera H, Lange S, Forsting M. MR imaging of the uterus and cervix in healthy women: determination of normal values. *Eur Radiol.* 2007;17(3):734–742.
27. Tian T, Zhang GF, Zhang H, Liu H. Intravoxel incoherent motion diffusion-weighted imaging in differentiating uterine fibroid from focal adenomyosis: Initial results. *Springerplus.* 2016;5:9.
28. Koike N, Tsunemi T, Uekuri C, et al. Pathogenesis and malignant transformation of adenomyosis (Review). *Oncol Rep*. 2013;29(3):861–867.
29. Russell P, Brennan B. Aberrant bcl-2 modulated apoptosis of the endometrium. *Pathology.* 2005;37:387–389.
30. Zhang L, Li J, Li M. Expression of bcl-2 protein in adenomyosis [in Chinese]. *Zhonghua Fu Chan Ke Za Zhi.* 2000;35(9):533–535.
31. Garavaglia E, Audrey S, Annalisa I. Adenomyosis and its impact on women fertility. *Iran J Reprod Med.* 2015;13(6):327–336.
32. Zhao L, Zhou S, Zou L, Zhao X. The expression and functionality of stromal caveolin 1 in human adenomyosis. *Hum Reprod.* 2013;28(5): 1324–1338.
33. An M, Li D, Yuan M, Li Q, Zhang L, Wang G. Interaction of macrophages and endometrial cells induces epithelial–mesenchymal transition-like processes in adenomyosis. *Biol Reprod.* 2017;96(1):46–57.
34. Kang S, Li SZ, Wang N, et al. Association between genetic polymorphisms in fibroblast growth factor (FGF)1 and FGF2 and risk of endometriosis and adenomyosis in Chinese women. *Hum Reprod.* 2010;25(7):1806–1811.
35. Tokyol C, Aktepe F, Dilek FH, Sahin O, Arioz DT. Expression of cyclooxygenase-2 and matrix metalloproteinase-2 in adenomyosis and endometrial polyps and its correlation with angiogenesis. *Int J Gynecol Pathol.* 2009;28:148–156.
36. Brosens I, Pijnenborg R, Benagiano G. Defective myometrial spiral artery remodelling as a cause of major obstetrical syndromes in endometriosis and adenomyosis. *Placenta.* 2013;34(2):100–105.
37. Rubin E, Farber JL. *Pathology.* 2nd ed. Philadelphia, PA: Lippincott; 1988.
38. Koumantakis EE, Panayiotides JG, Goumenou AG, et al. Different HLA-DR expression in endometriotic and adenomyotic lesions: Correlation with transvaginal ultrasonography findings. *Arch Gynecol Obstet*. 2010;281:851–856.
39. Goumenou AG, Matalliotakis IM, Tzardi M, Fragouli IG, Mahutte NG, Arici A. p16, retinoblastoma (pRb), and cyclin D1 protein expression in human endometriotic and adenomyotic lesions. *Fertil Steril.* 2006;85(Suppl 1):1204–1207.
40. Kang S, Zhao J, Liu Q, Zhou R, Wang N, Li Y. Vascular endothelial growth factor gene polymorphisms are associated with the risk of developing adenomyosis. *Environ Mol Mutagen.* 2009;50:361–366.
41. Wang F, Li H, Yang Z, Du X, Cui M, Wen Z. Expression of interleukin-10 in patients with adenomyosis. *Fertil Steril.* 2009;91(5):1681–1685.
42. Qin X, Zhang H, Wang F, Xue J, Wen Z. Expression and possible role of interleukin-10 receptors in patients with adenomyosis. *Eur J Obstet Gynecol Reprod Biol*. 2010;161(2):194–198.
43. Xiao Y, Sun X, Yang X, et al. Leukemia inhibitory factor is dysregulated in the endometrium and uterine flushing fluid of patients with adenomyosis during implantation window. *Fertil Steril.* 2010;94(1): 85–89.
44. Tremellen KP, Russell P. The distribution of immune cells and macrophages in the endometrium of women with recurrent reproductive failure. II: Adenomyosis and macrophages. *J Reprod Immunol.* 2012;93(1):58–63.
45. Greaves P, White IN. Experimental adenomyosis. *Best Pract Res Clin Obstet Gynaecol.* 2006;20(4):503–510.
46. Chen Y, Zhu B, Zhang H, et al. Epigallocatechin-3-gallate reduces myometrial infiltration, uterine hyperactivity, and stress levels and alleviates generalized hyperalgesia in mice induced with adenomyosis. *Reprod Sci.* 2013;20(12):1478–1491.
47. Ates S, Ozcan P, Aydin S. Differences in clinical characteristics for the determination of adenomyosis coexisting with leiomyomas. *J Obstet Gynaecol Res*. 2016;42(3):307–312.
48. Weiss G, Maseelall P, Schott LL. Adenomyosis a variant, not a disease? Evidence from hysterectomized menopausal women in the Study of Women's Health across the Nation (SWAN). *Fertil Steril.* 2009;91(1): 201–206.
49. Goluda M, Ujec M, Gabryś M, Kmieciak K. *Adenomioza*. Wrocław, Poland: Wydawnictwo Cornetis; 2003.
50. Weerakkody Y, Gaillard F, et al. Adenomyosis of the uterus. https://radiopaedia.org/articles/adenomyosis-of-the-uterus. Accessed on January 12, 2017.
51. Scarperi S, Pontrelli G, Campana C. Laparoscopic radiofrequency thermal ablation for uterine adenomyosis. *JSLS*. 2015;19(4): pii:e2015.00071. doi: 10.4293/JSLS.2015.00071
52. Kim SC, Lee NK, Yun KY, Joo JK, Suh DS, Kim KH. A rapidly growing adenomyosis associated with preterm delivery and postpartum abscess formation. *Taiwan J Obstet Gynecol.* 2016;55(4):620–622.
53. Mochimaru A, Aoki S, Oba MS, Kurasawa K, Takahashi T, Hirahara F. Adverse pregnancy outcomes associated with adenomyosis with uterine enlargement. *J Obstet Gynaecol Res*. 2015;41(4):529–533.
54. Juang CM, Chou P, Yen MS, Twu NF, Horng HC, Hsu WL. Adenomyosis and risk of preterm delivery. *BJOG.* 2007;114(2):165–169.
55. Harada T, Khine YM, Kaponis A, Nikellis T, Decalvas G, Taniguchi F. The impact of adenomyosis on women's fertility. *Obstet Gynecol Surv.* 2016;71(9):557–568.

The role of compression therapy in the treatment of venous leg ulcers

Paulina Mościcka[1,2,A–D,F], Maria T. Szewczyk[1,2,A–C,E,F], Justyna Cwajda-Białasik[1,2,A–C,E,F], Arkadiusz Jawień[3,A–C,E,F]

[1] Department of Surgical Nursing and Treatment of Chronic Wounds, Department of Health Sciences, Collegium Medicum in Bydgoszcz, Nicolaus Copernicus University in Toruń, Poland
[2] Department of Vascular Surgery and Angiology, Antoni Jurasz University Hospital No. 1 in Bydgoszcz, Collegium Medicum in Bydgoszcz, Nicolaus Copernicus University in Toruń, Poland
[3] Department of Vascular Surgery and Angiology, Antoni Jurasz University Hospital No. 1, Collegium Medicum in Bydgoszcz, Nicolaus Copernicus University in Toruń, Poland

A – research concept and design; B – collection and/or assembly of data; C – data analysis and interpretation; D – writing the article; E – critical revision of the article; F – final approval of the article

Advances in Clinical and Experimental Medicine, ISSN 1899–5276 (print), ISSN 2451–2680 (online) *Adv Clin Exp Med*. 2019;28(6):847–852

Address for correspondence
Paulina Mościcka
E-mail: moscicka76@op.pl

Funding sources
None declared

Conflict of interest
None declared

Received on July 2, 2016
Reviewed on August 14, 2016
Accepted on October 20, 2017

Published online on August 7, 2018

Abstract

Epidemiological data regarding venous leg ulcers, specifically low healing rates and frequent recurrences (occurring in 20–70% of the cases), seems surprising regarding recent progress in the management of this complication. The aim of this review is to present the current state of knowledge on venous leg ulcer management, especially compression therapy. Treatment of venous ulcers should be comprehensive and well-organized, based on modern standards and up-to-date, and should involve elaborated treatment strategies. A thorough diagnostic process followed by adequate treatment may result in marked improvement of the outcomes, with up to 67% healing rate at 12 weeks and up to 81% within 24 weeks. Continuation of therapeutic activities after the ulceration has been healed is reflected by a marked decrease in the recurrence rates, down to 16% whenever the patient is actively involved in the therapeutic process. Furthermore, early diagnosis and appropriate causal treatment may prevent progression of the illness.

Key words: venous ulcers, compression therapy, recurrent ulcers

Cite as
Mościcka P, Szewczyk MT, Cwajda-Białasik J, Jawień A. The role of compression therapy in the treatment of venous leg ulcers. *Adv Clin Exp Med*. 2019;28(6):847–852. doi:10.17219/acem/78768

DOI
10.17219/acem/78768

Introduction

Crural venous ulcers constitute a serious health, social and economic problem. A multicenter study on the epidemiology of venous diseases carried out in Poland demonstrated that 1.26% of patients suffer from venous ulceration and another more than 2% have recovered from this condition.[1] Approximately 80% of lower extremity ulceration cases are a consequence of chronic venous insufficiency (CVI).[2,3] Healing of venous ulcers is complex and lasts from a few weeks to several years. Treatment should include multidirectional and interdisciplinary activities aimed at decreasing/reduction of venous hypertension.[4,5] Compression therapy is the gold standard in the treatment of crural venous ulcers, as it reduces vein diameter and stimulates venous drainage.[6,7] In line with current recommendations, continuation of causal treatment and sustaining physiological blood pressure values are recommended after the ulcers have healed completely.[3,7] Conservative treatment, without compression therapy and venous hypertension control, is associated with high risk for recurrent ulceration.[8,9] Epidemiological data implies that recurrence may occur in 26–70% of the patients.[10–12]

Improper venous outflow results from a dysfunction of 1 or, more often, a few causative mechanisms of venous circulation: valve efficiency, vein patency, vessel wall tension, and muscle pump performance.[13,14] Valve insufficiency causes the blood to recede in a peripheral direction after a momentary movement upwards during muscle performance. This takes place during the diastolic phase, when valve closure is the only mechanism preventing the blood from flowing backwards. The presence of non-adapted valves is the cause of primary deep vein failure. On the other hand, past thrombotic process is most frequently responsible for the secondary damage of valves.[4,15]

Another potential cause of disorders in venous outflow is the closure of deep vein lumen, which results in a complete and/or partial obstruction in the deep venous system. The only way of venous return are superficial veins that become dilated and overloaded due to an enhanced perfusion. Venous dilation may result in valve insufficiency, development of varicose veins in the superficial system and reverse flow in perforating veins. At the same time, deep vein thrombosis results in recanalization which leads to the damage and dysfunction of the vascular wall and valves.[15] The changes of the vascular wall lead to dilation of the vein, which, as a result, causes valve cusps to move away from each other. This results in venous reflux and venous hypertension, and eventually leads to varicose vein development.[13]

Disorders in venous blood outflow may be also associated with muscle pump dysfunction. The most likely reason of the latter is muscle atrophy (for example, due to arthritis or physical inactivity), which reduces the compression force necessary to overcome gravity, stimulate the flow and prevent long-term blood retention.[16]

The occurrence of 1 and often a few of the dysfunctions leads to reflux and retention of blood in 1, 2 or 3 venous systems and, as a consequence, to the pathological increase in hydrostatic pressure to more than 90 mm Hg, i.e., so-called venous hypertension. This is particularly evident in the area of the distal perforating veins that connect these 2 systems. As a result, the most severe skin lesions develop in the area of the medial malleolus.[14,17]

Clinical manifestation of chronic venous insufficiency

Clinical manifestation, along with the degree of development of chronic venous disorders (CVD), more advanced changes in the form of CVI and ulceration, is presented by CEAP classification (C – clinical, E – etiology, A – anatomic, P – pathophysiologic). The clinical picture of CVI comprises the occurrence of varicose veins, edema, atrophic skin lesions, and subjective afflictions such as pain, muscle cramps, paresthesia, and itchiness, in the advanced form of venous ulcers. It depends on the kind of pathology occurring in the venous system, the pace of the changes, hemodynamic disorders, duration of the illness, and also on subjective sensations reported by the patient.[18]

A varicose vein is defined as a vein which has changed its shape, course or elongation. In the initial stage, only cosmetic effects are visible in the form of telangiectasia – the dilation of intradermal veins to 1 mm, and in reticular veins – as an intradermal dilations to 4 mm, which can be a sign of the early stage of venous insufficiency. These effects can occur individually or create clusters in the form of "a sprawling shrub". They can be located in any place, e.g., on the side of a thigh, in the popliteal fossa or in the area of the medial malleolus, where their radial composition is referred to as corona phlebectaticaica.[4,18–20] Larger varicose veins emerge most frequently (90%) from inflows or trunks of the great saphenous vein; cases of varicose veins of small saphenous vein are less visible (5%).[18,19]

Edema occurs in about 50% of patients with CVI. It is a clinical sign of an increased volume of extravascular extracellular fluid, the presence of which can be confirmed if, after pressing the skin with a thumb for 10 s, an imprint is visible.[21] In the initial phase, edema recedes after a nights' sleep, but increases during daytime proportionately to physical exertion and the time spent in a sitting or standing position or under the influence of high temperature.[22] After a couple of years, protrusions appear in the area of the edema.[22] Atrophic skin lesions are, apart from edema and developing varicose veins, the earliest signs of venous hypertension. The characteristic area where they occur is located above the ankles, most frequently on the shin medial surface.[4,23,24] The clinical picture of these lesions is diverse: from skin discoloration and inflammation to hard-to-heal ulcers. The 1st symptom of skin lesions is intensified hemosiderosis.[3,18,24] Color changes, the

so-called skin lesions, are accompanied by changes in the thickness of the skin and subcutaneous tissue. The skin becomes thin, less elastic, hard, and dry. Such skin condition on the shins is defined as lipodermatosclerosis.[18,24] In the case of regular skin discolorations, areas of microcirculatory vessel atrophy can occur, called Milian's white atrophy (atrophie blanche), which are characterized by the presence of white, very delicate and thin skin with visible peripheral vessels.[3] In the next stage, fibrosis causes accretion of the fibrous ring above the ankles, and the skin becomes more vulnerable to infections and local allergic reactions.[2,18]

In about 1% of the patients, ulceration appears within the area of the skin lesions. It can emerge due to superficial, deep and perforating vein insufficiency, any 2 or all of them simultaneously.[3,18,25] Similarly to skin lesions, ulceration is most frequently located in the area of the medial malleolus, i.e., in the area which is the most vulnerable to the influence of venous hypertension.[3,26] Ulceration can emerge as a result of, e.g., injury, skin irritation or scratching of the skin due to itchiness.

The clinical symptoms of CVI are diverse and to a large extent depend on the subjective attitude of the patient, stage of disease development, environmental and cultural conditions, as well as the patient's personality, and her/his psychosocial needs. Among the reported symptoms, there are: discomfort caused by the cosmetic defect, sensation of heaviness and/or fullness, and distension of lower limbs (especially in a sitting position). Skin itchiness, prickling, paresthesia, a burning sensation and muscle cramps are also reported by the patients. In the advanced form of the disease, symptoms are even more acute and, additionally, severe pain occurs, especially in the case of venous ulceration.[2,4,18,27] People with a long history of ulceration or with frequently recurrent ulceration suffer from various forms of depression of diverse intensity.[4,27–30]

Venous ulcers: Clinical aspects

Venous ulceration is the most frequent cause of chronic wounds located within the lower limbs. Active and healed ulcerations occur in 0.3 up to ca. 3% of the adult population. Ulcers occur twice as often in women (especially in their 40s) as in men, who are affected by the problem 10 years later, on average. The highest morbidity occurs between the age of 50 and 80.[1] According to the CEAP classification, venous ulceration is defined as a deficiency of full-thickness skin, usually in the area of the ankles, which has no tendency of idiopathic healing and is maintained by venous disorders.[31] It is most frequently (74%) located in the area of the medial malleolus, but it can also occupy other surfaces.[4] The small, shallow wound can reach even enormous size, encircling the entire shin. Ulceration is usually of oval shape with a flat bottom covered with necrotic tissue, fibrin clusters and, if there is an infection, also with pus.[2,4] If a proper healing process takes place, the ulceration has flat irregular edges, and in wounds which have been present for years, a thick, shaft-shaped edge may be present.[2,32] The skin surrounding the ulceration also looks different, as it gets thicker and dry.[33]

Venous ulceration treatment, apart from invasive treatment which is introduced with patients with no contraindications to a surgical procedure, includes numerous elements of conservative therapy. The basic aim of this treatment is the improvement of conditions of the local circulation, and reintroduction of proper nutrition and oxygenation of tissues.[34–36] It requires undertaking actions connected with compression therapy, i.e., limitation of the influence of venous hypertension, limitation of the processes of inflammation and wound infections, as well as many comprehensive actions, such as venous system diagnostics (Duplex scan, ankle-brachial index), causative therapy – compression therapy, topical treatment, physiotherapeutic procedures (sequential pneumatic massage/manual massage – edema reduction), physical activity, prophylaxis, limb care and hygiene, educating the patient, using analgesic, phlebotropic and rheologically active drugs, weight reduction, supplementing of deficiencies, and high-protein diet.[4,36,37]

Compression therapy in the treatment of venous leg ulcers

Compression therapy is the gold standard in the treatment of venous ulcers. It involves application of gradual, external and layer pressure with the highest pressure in the area of ankle and the lowest pressure under the knee, using special bandages or ready-to-use layered compression bandage systems. Proper systematic application of compression therapy reverses the pathological changes of the venous system, i.e., "venous hypertension", which are the cause of ulceration, and improves ulceration healing conditions.[3,7,36,38] The narrowing of the vessel lumen leads to a decrease of the volume of venous blood in a limb and speeds up its flow. It also reduces the painfulness of ulceration and edema. There is also an improvement in the activity of the calf's muscle pump, condition of the skin and subcutaneous tissue.[39,40] Among the methods used in compression therapy in venous ulceration treatments, we can distinguish: short-stretch bandages, elastic bandages, compression stockings and other knitwear products, as well as devices generating dynamic compression/intermittent pneumatic compression.[3,4] The most suitable compression material in the treatment of active ulceration are short-stretch bandages put on in a 2- or multi-layer system.[7,41] However, in the case of small-area ulceration, ready-to-use compression products are the most suitable solution. The opinion of experts on the matter of compression therapy is unequivocal and says that in venous ulceration treatment, the recommended pressure in the ankle area is 40 mm Hg and 17–20 mm Hg under the knee.[3,7,36]

Effective and safe compression therapy depends on the correct application, which involves the proper theoretical and practical preparation of specialist nurses. Compression therapy should not be performed by unqualified people.

Local treatment of venous leg ulcers

Venous ulcer care involves optimization of the microenvironment of the wound's background and includes only actions reflecting the physiological course of healing. The TIME strategy to a great extent contributes to the stimulation of natural healing mechanisms and includes the following elements of ulceration debridement: T – tissue debridement, I – infection and inflammation control, M – moisture balance, and E – epidermization stimulation.[3,7]

In accordance with the TIME strategy recommended by scientific societies, wound debridement involves all the procedures performed within the wound connected with deterging, as well as eliminating the exudate, damage and contamination occurring within the wound bed (e.g., foreign bodies, dirt, sand, or splinters), bacteria and other germs, tissues that are necrotic and have limited blood supply, and pus.[42–44] There are various methods of ulceration debridement, e.g., surgical, enzymatic, autolytic, mechanical, the use of biosurgical methods, negative pressure, and ultrasound.[3,7,44]

Preventing recurrence of venous leg ulcers

The healing of the ulceration does not mean the pathology in the venous circulation system is cured. The main risk factor of ulceration recurrence is the continuous influence of venous hypertension, which is most frequently caused by CVI and post-thrombotic syndrome. Recurrence risk factors are most often divided into local and general.[5,10,40]

Local factors include: 1. no compression therapy after the healing of the ulceration – insufficient knowledge and neglect on the part of medical staff; 2. lack of cooperation of the patient during the compression therapy, e.g., a low level of knowledge and motivation of the patient, confidence in the ineffectiveness of compression in the prevention of recurrence, treating the healing as a complete recovery, confidence about other causes of recurrence, difficulties in putting on and the inconvenience connected with wearing compression stockings, and lack of cooperation on the part of the patient's family/caregiver; 3. lack of systematic application of compression therapy; 4. decrease in tolerability of compression therapy (improper degree of compression), and 5. orthopedic disorders: numbness of ankle joint, improperly fitted shoes, etc.

Systemic factors influencing the risk of ulceration recurrence include obesity, arterial hypertension, improper nutrition (including protein-energy deficit), lack of proper exercise stimulating ankle joint mobility, increasing venous return, smoking, alcoholism, post-thrombotic syndrome, and others.[8–10,33,45–47]

After the healing of ulceration, the monitoring of the patient and the constant maintenance of low pressure values are required. That is why compression therapy is recommended after the healing of ulceration.[48] Educating the patients and their family is an important part of the therapy and prophylaxis. It is the kind of action that aims at changing the role of the patient from a passive task performer to a partner, who will consciously and actively take part in the healing process. Customized and systematic education enables the patient to understand the core of the problem, which is a condition for good cooperation between the patients and the therapeutic team. This can be the basis of the effective healing process.[39,49–51]

Conclusions

Compression therapy is the gold standard in the treatment of venous ulcers and results in the highest healing rates. It involves employing external and layered pressure, using special bandages, ready-to-use layered compression bandage systems, and, in the case of small ulceration which does not weep, compression stockings.[3,7,36,52,53] A systematic literature review shows that every form of properly employed compression favorably influences the process of venous ulceration healing, and it is difficult to determine which method is the most effective.[25,34,54] In the research carried out by Szewczyk among 112 people suffering from venous ulcers, the healing dynamics of ulceration treated with 2- and 4-layer compression system was comparable.[4] In another study conducted in an ulceration treatment clinic on a group of 46 patients with venous ulcers, the authors demonstrated a similar effectiveness of the 2- and 4-layer system as well as compression stockings.[55] In yet another study, a group of 134 patients with wounds of venous etiology was randomly divided into 2 groups.[41] In one group, individually selected compression stockings were used, and in the other group, short-stretch bandages were applied to compare their effectiveness. In the group where stocking were used, the rate of healing and the time of healing were higher. On the other hand, another study, which included 200 patients with ulceration of venous etiology, compared the effectiveness of 4-layer compression therapy and elastic bandages.[56] The final analysis demonstrated that 4-layer compression was more effective. Customized compression and pressure degree significantly improve the conditions existing in venous circulation and microcirculation, if applied constantly.

In the majority of cases of venous ulcers, conservative treatment in line with the standards brings good results if the care is based on systematic interdisciplinary actions. If the care is occasional, the ulceration lasts longer and the

rate of recurrence is high. The most important predictors include the duration of ulceration and its initial area. It has been proved that ulcerations characterized by short duration (<6 months) and small initial area (<5 cm^2) have the highest (95%) chance of healing within a period shorter than 24 weeks. It takes much more time for developed and extensive ulcers to heal.[4,32,57,58]

The care of a patient with CVI does not end with the healing of the ulceration. In order to maintain skin continuity, actions are required to be undertaken by both the patient and the therapeutic team. No or insufficient participation of one of the parties may lead to another ulceration. Epidemiological studies show high rates of recurrence which are about 26–70%.[12,32,57,58] According to the study data, about 26% of ulcers recur within the 1st 12 months after the therapy is over.[26] Regularly controlled and constantly monitored patients can significantly extend the period of remission, or even avoid ulceration recurrence.[59] It is thought in the scientific community that the most effective method of prevention is the continuation of compression therapy. Although there are still no high-quality studies comparing recurrence rates depending on application/no application of compression, experts unequivocally emphasize the high effectiveness of compression therapy in both the treatment of ulcers and the prevention of recurrence.[3,7,60–62]

To summarize, systematic application of properly customized compression therapy in the form of special bandages or ready-to-use compression products remains the gold standard in the conservative treatment of venous leg ulcers. Compression therapy is recommended in order to prevent recurrence as well as emergence of recurring ulceration in the case of a healed ulceration.[3,7]

References

1. Jawień A, Grzela T, Ochwat A. Prevalence of chronic venous insufficiency in men and women in Poland: Multicentre cross-sectional study in 40,095 patients. *Phlebology.* 2003;18(3):110–122.
2. Negus D, Coleridge Smith P. Diagnostyka różnicowa owrzodzeń podudzi. In: Negus D, Coleridge Smith P, Bergan J, eds. *Owrzodzenia Podudzi – Diagnostyka i Leczenie*. Bielsko Biała, Poland: Alfa Medica Press; 2006:90–105.
3. Szewczyk M, Jawień A, Andruszkiewicz A, et al. Zalecenia specjalistycznej opieki nad chorym z owrzodzeniem żylnym goleni. *Pielęg Chir Angiol.* 2007;3:95–138.
4. Szewczyk MT. *Ocena Dynamiki Procesu Gojenia Owrzodzeń Żylnych z Zastosowaniem Kompresjoterapii i Holistycznego Modelu Opieki Pielęgniarskiej.* Bydgoszcz, Poland: Wydawnictwo Naukowe Uniwersytetu Mikołaja Kopernika; 2006.
5. Szewczyk MT. Wybrane aspekty opieki nad chorym z owrzodzeniem żylnym. In: Jawień A, Szewczyk MT, eds. *Kliniczne i Pielęgnacyjne Aspekty Opieki nad Chorym z Owrzodzeniem Żylnym Goleni.* Poznań, Poland: Wydawnictwo Medyczne Termedia; 2008:125–131.
6. Szewczyk MT, Jawień A. Kompresjoterapia jako podstawowy element leczenia owrzodzeń żylnych. *Leczenie Ran.* 2004:1:1–4.
7. Jawień A, Szewczyk M, Kaszuba A, et al. Wytyczne grupy ekspertów w sprawie gojenia owrzodzeń żylnych goleni. *Leczenie Ran.* 2011;8: 59–80.
8. Jawień A, Szewczyk MT. Profilaktyka trzeciorzędowa w zapobieganiu nawrotowym owrzodzeniom żylnym goleni. *Prz Flebol.* 2005;13(6): 223–268.
9. Szewczyk MT, Cwajda-Bialasik J, Jawień A. Prevention of recurrent venous ulceration. *Postepy Dermatol Alergol.* 2012;29(4):308–312.
10. Gohel MS, Taylor M, Earnshaw JJ, Heather BP, Poskitt KR, Whyman MR. Risk factors for delayed healing and recurrence of chronic venous leg ulcers: An analysis of 1324 legs. *Eur J Vasc Endovasc Surg.* 2005;29(1): 74–77.
11. Nelson EA, Harper DR, Prescott RJ, Gibson B, Brown D, Ruckley CV. Prevention of recurrence of venous ulceration: Randomized controlled trial of class 2 and class 3 elastic compression. *J Vasc Surg.* 2006;44(4):803–808.
12. Finlayson K, Edwards H, Courtney M. Factors associated with recurrence of venous leg ulcers: A survey and retrospective chart review. *Int J Nurs Stud.* 2009;46(8):1071–1078.
13. Migdalski A, Ciecierski M, Jawień A. Fizjologia i patofizjologia odpływu żylnego. *Przew Lek.* 2004;8(7):33–35.
14. Szotkiewicz A, Jawień A. Patogeneza owrzodzeń żylnych goleni. In: Jawień A, Szewczyk MT, eds. *Owrzodzenia Żylne Goleni.* Warszawa, Poland: Wydawnictwo Medyczne "Twoje Zdrowie"; 2005:11–19.
15. Zapalski S. Anatomia i fizjologia układu żylnego kończyn dolnych. In: Zapalski S, ed. *Niewydolność Układu Żylnego Kończyn Dolnych.* Gdańsk, Poland: Via Medica; 1999:27–34.
16. Gravereaux EC, Donaldson MC. Niewydolność żylna. In: Adamiec R, ed. *Choroby Naczyń. Podręcznik Towarzyszący do Braunwald's Heart Disease*. Lublin, Poland: Wydawnictwo Czelej; 2008:908–918.
17. Szewczyk MT, Jawień A. Wybrane aspekty zachowawczego leczenia owrzodzeń żylnych. Część I: Kompresjoterapia. *Postepy Dermatol Alergol.* 2005;3:133–140.
18. Ciecierski M. Obraz kliniczny przewlekłej niewydolności żylnej. In: Jawień A, Szewczyk MT, eds. *Owrzodzenia Żylne Goleni.* Warszawa, Poland: Wydawnictwo Medyczne "Twoje Zdrowie"; 2005:51–57.
19. Jawień A, Ciecierski M, Piotrowicz R. Przewlekła niewydolność żylna. *Przew Lek.* 2000;1(3):7–75.
20. Chi YW, Raffetto JD. Venous leg ulceration pathophysiology and evidence-based treatment. *Vasc Med.* 2015;20(2):168–181.
21. Ciecierski M, Grzela T, Miszewski M. Obrzęki kończyn dolnych. In: Jawień A, Szewczyk MT, eds. *Kompresjoterapia*. Poznań, Poland: Wydawnictwo Medyczne Termedia; 2009:29–68.
22. Wiktor M. Patofizjologia. In: Chęciński P, ed. *Obrzęk chłonny*. Poznań, Poland: Wydawnictwo Medyczne Termedia; 2010;27–41.
23. Skórski M. Przewlekła niewydolność żylna. In: Pasierski T, Gaciong Z, Torbicki A, Szmidt J, eds. *Angiologia.* Warszawa, Poland: Wydawnictwo Lekarskie PZWL; 2004:362–368.
24. Szewczyk MT, Jawień A, Cwajda J. Zaburzenia integralności skóry u chorych z przewlekłą niewydolnością żylną. *Postepy Dermatol Alergol.* 2005;3:141–147.
25. Danielsson G, Eklof B, Grandinetti A, Lurie F, Kistner RL. Deep axial reflux, an important contributor to skin changes or ulcer in chronic venous disease. *J Vasc Surg.* 2003;38(6):1336–1341.
26. Nelson EA, Bell-Syer SE. Compression for preventing recurrence of venous ulcers. *Cochrane Database Syst Rev.* 2012;15(8):CD002303.
27. Vandenkerkhof EG, Hopman WM, Carley ME, Kuhnke JL, Harrison MB. Leg ulcer nursing care in the community: A prospective cohort study of the symptom of pain. *BMC Nurs.* 2013;12:1472–6955.
28. Szewczyk M, Jawień A, Hildebrandt Z. Problemy chorych z przewlekłą niewydolnością żylną. Psychospołeczne konsekwencje choroby – część II. *Prz Flebol.* 2005;13(4):99–107.
29. Szewczyk MT, Jawień A, Hildebrandt Z. Subiektywne postrzeganie stanu zdrowia chorych z przewlekłą niewydolnością żylną – część I. *Prz Flebol.* 2005;13(4):175–181.
30. Szewczyk MT, Rogala J, Cwajda J, Ciezniakowska K, Jawień A. Psychological and social problems of patients with chronic venous disease. *Postepy Dermatol Alergol.* 2007;24:207–210.
31. Eklof B, Rutherford RB, Bergan JJ, et al. Revision of the CEAP classification for chronic venous disorders: Consensus statement. *J Vasc Surg.* 2004;40(6):1248–1252.
32. Phillips TJ, Machado F, Trout R, Porter J, Olin J, Falanga V. Prognostic indicators in venous ulcers. *J Am Acad Dermatol.* 2000;43(4):627–630.
33. Heinen MM, Persoon A, van de Kerkhof P, Otero M, van Achterberg T. Ulcer-related problems and health care needs in patients with venous leg ulceration: A descriptive, cross-sectional study. *Int J Nurs Stud.* 2007;44(8):1296–1303.
34. Kramer SA. Compression wraps for venous ulcer healing: A review. *J Vasc Nurs.* 1999;17(4):89–97.
35. Johnson S. Compression hosiery in the prevention and treatment of venous leg ulcers. *J Tissue Viability.* 2002;12(2):72–74.

36. Vin F, Benigni JP. Compression therapy. International Consensus Document Guidelines according to scientific evidence. *Int Angiol.* 2004; 23(4):317–345.
37. O'Meara S, Cullum N, Nelson EA, Dumville JC. Compression for venous leg ulcers. *Cochrane Database Syst Rev.* 2012;14(11):CD000265.
38. Lorimer KR, Harrison MB, Graham ID, Friedberg E, Davies B. Venous leg ulcer care: How evidence-based is nursing practice? *J Wound Ostomy Continence Nurs.* 2003;30(3):132–142.
39. Moffat C, Harper P. *Leg Ulcer.* London, UK: Churchill Livingstone; 1997.
40. Heinen M, Borm G, van der Vleuten C, Evers A, Oostendorp R, van Achterberg T. The lively legs self-management programme increased physical activity and reduced wound days in leg ulcer patients: Results from a randomized controlled trial. *Int J Nurs Stud.* 2012;49(2):151–161.
41. Junger M, Wollina U, Kohnen R, Rabe E. Efficacy and tolerability of an ulcer compression stocking for therapy of chronic venous ulcer compared with a below-knee compression bandage: Results from a prospective, randomized, multicentre trial. *Curr Med Res Opin.* 2004; 20(10):1613–1623.
42. Szewczyk MT, Mościcka P, Hancke E, Cwajda J, Ciezniakowska K, Jawień A. Use of TIME strategy in wound bed debridement: Venous leg ulcer. *Zakażenia.* 2006;6:86–89.
43. Gottrup F, Apelqvist J, Bjarnsholt T, et al. EWMA document: Antimicrobials and non-healing wounds. Evidence, controversies and suggestions. *J Wound Care* 2013;22(5 Suppl):S1–89.
44. Strohal R, Dissemond J, Jordan O'Brien J, et al. EWMA document: Debridement. An updated overview and clarification of the principle role of debridement. *J Wound Care.* 2013;22(1):5.
45. Graham ID, Harrison MB, Shafey M, Keast D. Knowledge and attitudes regarding care of leg ulcers. Survey of family physicians. *Can Fam Physician.* 2003;49:896–902.
46. Flaherty E. The views of patients living with healed venous leg ulcers. *Nurs Stand.* 2005;19(45):82–83.
47. Jawień A, Szewczyk MT. Specjalistyczna opieka medyczna. In: Jawień A, Szewczyk MT, eds. *Owrzodzenia Żylne Goleni.* Warszawa, Poland: Wydawnictwo Medyczne "Twoje Zdrowie"; 2005:166–177.
48. Franks PJ, Oldroyd MI, Dickson D, Sharp EJ, Moffatt CJ. Risk factors for leg ulcer recurrence: A randomized trial of two types of compression stocking. *Age Ageing.* 1995;24(6):490–494.
49. Erickson CA, Lanza DJ, Karp DL, et al. Healing of venous ulcers in an ambulatory care program: The roles of chronic venous insufficiency and patient compliance. *J Vasc Surg.* 1995;22(5):629–636.
50. Edwards LM. Why patients do not comply with compression bandaging. *Br J Nurs.* 2003;12(11 Suppl):S5–6,S8,S10 passim.
51. Brooks J, Ersser SJ, Lloyd A, Ryan TJ. Nurse-led education sets out to improve patient concordance and prevent recurrence of leg ulcers. *J Wound Care.* 2004;13(3):111–116.
52. Anderson I. Compression hosiery to reduce leg ulcer recurrence. *Nurs Times.* 2013;109(6):18–20.
53. Mooij MC, Huisman LC. Chronic leg ulcer: Does a patient always get a correct diagnosis and adequate treatment? *Phlebology.* 2016;31(1 Suppl): 68–73.
54. Anderson I. Optimising concordance with compression hosiery in the community setting. *Br J Community Nurs.* 2015;20(2):67–68.
55. Szewczyk MT, Jawień A, Cierzniakowska K, Cwajda-Bialasik J, Mościcka P. Comparison of the effectiveness of compression stockings and layer compression systems in venous ulceration treatment. *Arch Med Sci.* 2010;6(5):793–799.
56. Enoch S, Williams D, Price P, Harding P. Randomized clinical trial and economic analysis of four-layer compression bandaging for venous ulcers (Br J Surg 2003;90:794–798). *Br J Surg.* 2003;90(10):1307.
57. Margolis DJ, Berlin JA, Strom BL. Which venous leg ulcers will heal with limb compression bandages? *Am J Med.* 2000;109(1):15–19.
58. Szewczyk MT, Jawień A. Kompresjoterapia w leczeniu owrzodzeń żylnych. In: Jawień A, Szewczyk MT, eds. *Kompresjoterapia.* Poznań, Poland: Wydawnictwo Medyczne Termedia; 2009:82–95.
59. Kunimoto BT. Management and prevention of venous leg ulcers: A literature-guided approach. *Ostomy Wound Manage.* 2001;47(6):36–42.
60. Kunimoto B, Cooling M, Gulliver W, Houghton P, Orsted H, Sibbald RG. Best practices for the prevention and treatment of venous leg ulcers. *Ostomy Wound Manage.* 2001;47(6):34–46.
61. Barwell JR, Davies CE, Deacon J, et al. Comparison of surgery and compression with compression alone in chronic venous ulceration (ESCHAR study): Randomized controlled trial. *Lancet.* 2004;363(9424): 1854–1859.
62. Coleridge Smith PD. Diagnostyka anatomiczna – ultrasonografia duplex Doppler. In: Negus D, Coleridge Smith P, Bergan J, eds. *Owrzodzenia Podudzi – Diagnostyka i Leczenie.* Bielsko-Biała, Poland: Alfa Medica Press; 2006:117–125.